# A Statistical Method for One-to-Three-Day Tropical Cyclone Track Prediction

By
Clifford R. Matsumoto

PI: William M. Gray

Department of Atmospheric Science
Colorado State University
Fort Collins, Colorado

NEPRF N00014-83-K-0002
NSF ATM-8214041

Colorado State University

Department of Atmospheric Science

Paper No. 379

# A STATISTICAL METHOD FOR ONE- TO THREE-DAY TROPICAL CYCLONE TRACK PREDICTION

By

Clifford R. Matsumoto

Department of Atmospheric Science

Colorado State University

Fort Collins, Colorado 80523

December, 1984

Department of Atmospheric Science Paper No. 379

## ABSTRACT

The problem of forecasting the movement of tropical cyclones is crucial in many parts of the world. Progress on improving the accuracy of track prediction has been slow to come and the need for further research on statistical-synoptic approaches exists. This newly developed method of forecasting one- to three-day cyclone motion is an improvement over existing forecast schemes for the following reasons: (1) cyclones are stratified based on their positions relative to the 500 mb subtropical ridge to better define the environmental influences on the cyclones; (2) the 72-hour forecast track is segmented into three 24-hour time steps to permit the application of updated persistence and synoptic data relative to each new cyclone position as the 24-hour displacements are stepped forward to the desired forecast projection; and (3) the prognostic synoptic data are introduced only at their valid times and relative to the cyclone position at the valid time such that they are treated like analysis data.

A screening -- multiple regression technique is used to compute the regression coefficients. ''Perfect-prog'' concept is used to introduce prognostic synoptic data as potential predictors. Actual forecast fields are used to test the skill of the new model to be referred to as CSU84.

Comparison with operational forecast techniques on a nearly homogeneous sample, using a persistence-climatology model as a normalizer to indicate relative skill of the models as compared to a no-skill forecast, indicate that CSU84 is six times as skillful as the best operational model in the Atlantic and at least four times as skillful as the best operational model in the northwest Pacific. These very encouraging verification results suggest the potential for significant reduction in foreast position errors and should hasten the testing of the model in an operational environment.

TABLE OF CONTENTS

TABLE OF CONTENTS (Cont'd)

## LIST OF SYMBOLS AND ACRONYMS

| | |
|---|---|
| BPAC | Blended Persistence And Climatology forecast aid for the NW Pacific and North Indian Oceans |
| $C_o$ | the intercept value for the regression equation |
| $C_n$ | the n regression coefficients |
| CLIM | CLIMatology forecast aid for the NW Paific and North Indian Oceans |
| CLIPER | CLImatology and PERsistence forecast system for the Atlantic (Neumann, 1972) |
| COSMOS | Cyclops Objective Steering Model Output Statistics forecast aid at JTWC (Allen, 1984) |
| CYCLOPS | CYCLone Operational Prediction System forecast model for the NW Pacific |
| CY50 | CYclops forecast model that uses 500 mb steering for the NW Pacific and North Indian Ocean |
| DOM | direction of motion |
| $E_c$ | CLIPER forecast error |
| $E_m$ | model forecast error |
| FLAT | forecast latitude |
| FLON | forecast longitude |
| FNOC | Fleet Numerical Oceanography Center, Monterey, CA |
| H | 500 mb geopotential height |
| HOUR | 12 or 24 hours for computing displacement |
| HP | 500 mb height pattern indicator |
| HPAC | Half Persistence And Climatology forecast aid for the NW Pacific and North Indian Ocean |

| | |
|---|---|
| HATTRACK | Hurricane And Typhoon TRACKing forecast aid for the NW Pacific and North Indian Oceans (Renard, 1968) |
| HURRAN | HURRicane ANalog forecast system for the Atlantic (Hope and Neumann, 1970) |
| JTWC | Joint Typhoon Warning Center, Guam |
| $LAT_o$ | current latitude |
| $LAT_p$ | previous latitude either 12 or 24 hours earlier |
| $LON_o$ | current longitude |
| $LON_p$ | previous longitude either 12 or 24 hours earlier |
| m | meter |
| mb | millibar |
| m/s | meter per second |
| MFM | Movable Fine Mesh dynamical model (Hovermale and Livezey, 1977) |
| MOHATT | MOdified HATTrack forecast aid for the NW Pacific and North Indian Ocean (Renard et al., 1973) |
| MOS | Model Output Statistics |
| n | number of predictors for a given regression equation |
| $P_n$ | the n predictor values |
| NCAR | National Center for Atmospheric Research, Boulder, CO |
| NEPRF | Naval Environmental Prediction Research Facility, Monterey, CA |
| NEWLAT | forecast latitude |
| NEWLON | forecast longitude |
| NHC | National Hurricane Center, Miami, FL |
| NHC67 | NHC statistical-synoptic forecast system (Miller, et al., 1968) |
| NHC72 | NHC statistical-synoptic forecast system (Neumann, et al., 1972) |
| NHC73 | NHC statistical-dynamical forecast system (Neumann and Lawrence, 1973) |
| NMC | National Meteorological Center, Washington, D.C. |

| | |
|---|---|
| NTCM | Navy Two-Way Interactive Tropical Cyclone Model for the NW Pacific and North Indian Ocean (Harrison, 1981) |
| OLDLAT | forecast minus 24-hour latitude |
| OLDLON | forecast minus 24-hour longitude |
| OTCM | One-Way Interactive Tropical Cyclone Model for the NW Pacific and North Indian Ocean (Hodur and Burk, 1978) |
| SANBAR | SANders BARotropic model for the Atlantic (Sanders and Burpee, 1968) |
| T | time |
| TYAN | TYphoon ANalog forecast system for the NW Pacific and North Indian Ocean (Jarrell and Somerville, 1970) |
| P | Sea level Pressure |
| SMOS | Simulated Model Output Statistics |
| XLAT | best track latitude |
| XLON | best track longitude |
| XTRP | EXTRaPolation forecast aid for the NW Pacific and North Indian Oceans |
| $\Sigma$ | summation |
| x | multiplication |
| X | east-west displacement |
| Y | north-south displacement |
| S | cyclone speed in m/s |
| $\Psi$ | gradient of geopotential height |
| $\varphi$ | latitude |
| $\Omega$ | angular speed of rotation of the earth |
| $\Delta$ | delta |
| U | east-west component of the geostrophic steering wind/east-west cyclone motion |
| V | north-south component of the geostrophic steering wind north-south cyclone motion |

| | |
|---|---|
| $\Delta H$ | 24-hour change of height |
| $\Delta P$ | 24-hour change of sea level pressure |
| $\Delta\varphi$ | 24-hour change of height gradient |
| % | percent improvement or deterioration of model skill over CLIPER forecast error |

# 1. INTRODUCTION

The problem of forecasting the movement of tropical cyclones, particularly recurvature and landfall, is crucial in many parts of the world. Considerable effort has been expended by the various Meteorological Services of a number of nations on improving the accuracy of track prediction. A historical overview will be presented in Chapter 2.

Although significant progress has been made in developing statistical and dynamical models for forecasting the tracks of tropical cyclones, the forecast errors over the last few years (Fig. 1.1) have shown little improvement. The official forecasts for the NW Pacific issued by the US Joint Typhoon Warning Center (JTWC) on Guam have average forecast position errors on the order of 120, 240, and 360 nautical miles (n mi.) for 24-, 48-, and 72-hour forecasts while those for the North Atlantic issued by the US National Hurricane Center (NHC) in Miami have errors on the order of 120, 250, and 380 n mi.

Attempts to develop more sophisticated numerical models continue in hopes of achieving a breakthrough in track prediction. However, the achievement of this goal does not appear to be close at hand. In addition, in most developing countries, computer facilities are not adequate to apply the more sophisticated dynamical models. Therefore, the need remains for a tropical cyclone forecasting technique requiring only meteorological data from a network of conventional surface and upper-air observing stations as basic input.

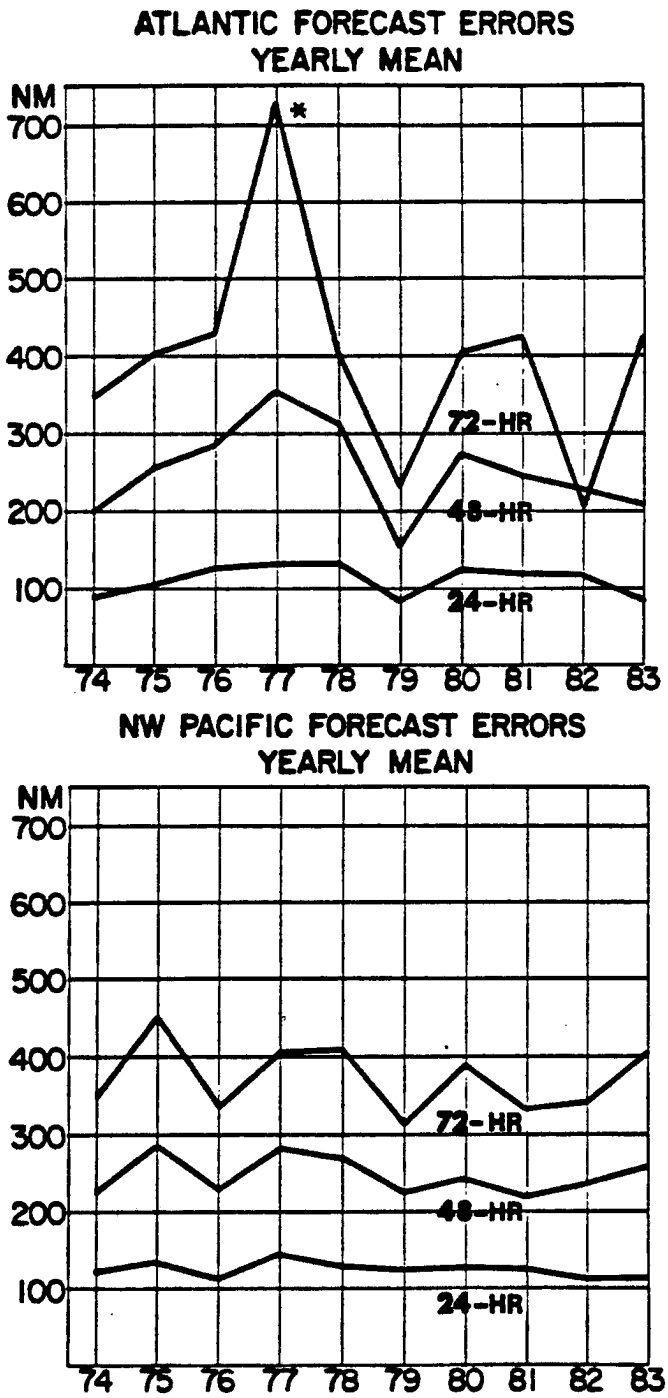


Fig. 1.1. The yearly mean official forecast errors (n mi.) during the period 1974-1983 for the Atlantic and NW Pacific. The yearly fluctuation is much higher in the Atlantic than the NW Pacific due to far fewer cases. In 1977, for example, there were only two cases for verification at 72 hours. The 1974-1982 errors for the Atlantic are from Annual Data and Verification Tabulation while the 1983 errors are from the minutes of the 38th Annual International Hurricane Conference. The errors for the NW Pacific are from the Annual Tropical Cyclone Typhoon Reports, 1974-1983.

The purpose of this research is to apply a new statistical method of introducing synoptic and persistence predictors to develop an improved prediction model that could be used at all operational forecast centers. Such a model would need to be simple so that it could operate without a link to a large computer data base or numerically produced analysis or forecast fields, yet be sophisticated enough to produce accurate forecasts at both the short and longer forecast periods.

The research was also an effort to quantify the results of various earlier work linking tropical cyclone motion to synoptic scale forcings at several vertical levels. Observational studies have shown the importance of surface pressure changes far removed from the cyclone as well as upper tropospheric winds at large distances poleward of the cyclone on indicating future changes in cyclone motion. Specific references to these studies are cited in Chapter 2.

The motivation for this work arose as a result of nearly three years of operational tropical cyclone forecasting by the author during which time the strengths and weaknesses of the myriad of objective techniques in use became obvious. Almost all of these track prediction schemes perform adequately on well-behaved cyclones that follow climatological tracks. However, on those anomalous, difficult cases when the forecaster needs objective guidance the most, the schemes invariably failed. The inherent weaknesses in the design of current operational techniques will be addressed in Chapter 3.

In developing a new statistical forecast model, the method of introducing and applying the various climatological, persistence and synoptic predictors for predicting the future motion of tropical cyclones is patterned after the normal procedure followed by most

forecasters as they subjectively formulate the forecast track.

The innovative approach developed here primarily involves the discretizing of the 72-hour forecast track into three 24-hour time steps and applying updated persistence and synoptic data relative to each new cyclone position as the forecast is stepped forward in 24-hour increments. The perfect-prog method is used to introduce updated synoptic information but only at the valid time of the prognostic data and always relative to the cyclone position at the valid time of the prognostic data. Climatology is incorporated via a stratification scheme based on the position of the cyclone relative to the 500 mb subtropical ridge. Segmenting the 72-hour cyclone motion permits the cyclone category to change after each 24 hours of motion. The three categories relative to the ridge -- south, on, north -- result in three sets of regression equations, with each set comprised of separate equations for the north-south and east-west displacements. A more detailed discussion of the model designs will be presented in Chapter 3.

Chapter 4 will discuss the multiple regression technique required to handle the large number of cases and potential predictors. Correlation coefficient fields between the synoptic predictors and east-west and north-south cyclone motion will be presented along with an examination of the contribution of each of the predictors to the reduction of variance.

Verification of this new statistical prediction model, to be referred to as CSU84, will be presented in Chapter 5. Also presented in this chapter will be sensitivity tests that simulate operational

conditions. This was accomplished by perturbing the "best track"[1] initial positions and by using actual forecast fields produced by a numerical model.

Although CSU84 was initially an attempt to improve track forecasts primarily at the higher latitudes and at the longer forecast periods, the results indicate considerable skill at the lower latitudes and shorter forecast periods as well.

---

(1) The best track positions are the accepted cyclone positions after a post-cyclone analysis.

## 2. BACKGROUND

The movements of tropical cyclones remain one of the most important and difficult forecasting problems in tropical meteorology. Earliest attempts at developing objective forecast schemes hypothesized that tropical cyclones were carried along by the prevailing larger scale environmental flows in which they were embedded like eddies in a river. This concept has come to be known as ''steering''.

Recently, observational studies have demonstrated a highly significant relationship between tropical cyclone motion and synoptic-scale flow (~ 500-1000 km) around the cyclone. The pressure level at which the speed and direction of the surrounding winds (or equivalently the pressure or height gradients across the cyclone) best correlate with those of the cyclone has been referred to as the steering level.

One problem in applying the steering concept has been the selection of the proper level that best correlated with the movement of the cyclone. Although different forecast schemes use different steering levels, it is generally accepted that the mid-tropospheric levels are the best in predicting tropical cyclone movement.

George (1975) found that for NW Pacific cyclones, the composite 500 mb winds averaged between 1-7$^{o}$ latitude radius from the cyclone center had the strongest correlation with the direction of cyclone movement while the 700 mb winds best correlated with the cyclone speed. Gray (1977) presented similar results for Atlantic cyclones. Chan (1982) using composite wind data over an area (5-7$^{o}$ latitude radius from the

cyclone center) outside the strong inner circulation of the cyclone found that the winds at the mid-troposphere (700, 600 and 500 mb) correlated best with both the direction and speed of cyclone movement. More importantly, Chan found that cyclones having different zonal components of motion have different relationships with their 5-7° surrounding flow. Holland (1983) showed that cyclone motion was the result of a nonlinear combination of two processes: 1) an interaction between the cyclone and its basic current (the well-known steering concept), and 2) an interaction with the earth's vorticity field which causes a westward deviation from the pure steering flow. Similar to Chan's findings, Holland discovered that westward moving cyclones were only marginally affected by fluctuations in the basic flow whereas northward and eastward moving cyclones may undergo large motion changes for a similar range of fluctuations.

Attempts to use winds and heights at upper tropospheric levels (e.g., Jordan, 1952; Miller, 1958) have historically not been as successful and have received little use. However, recent findings have supported a good correlation between upper tropospheric winds and cyclone recurvature. Specifically, George and Gray (1977), using 10 years of composited rawinsonde reports, found large-scale differences at the 200 mb level 15° to 20° from the cyclone prior to significant changes in cyclone movement. Their result indicated that the strength of the upper level westerlies northwest and north of the cyclone is strongly related to cyclone recurvature.

Bao and Sadler (1982) also found a strong relationship between the 200 mb winds at and before recurvature along the cyclone's subsequent track and the speed of movement of the cyclone after recurvature.

Gentry (1983) found that when the mean 200 mb winds at about 15° to 20° northwest and north of the cyclone equal or exceed 20 m/s, 80% of the cyclones recurved before traveling as much as 12 degrees of longitude further west.

Weir (1982) developed an operational technique for the NW Pacific using 200 mb winds to assist in forecasting the acceleration of typhoons as they interact with the mid-latitude westerlies.

Apparently, upper tropospheric levels are generally poor steering levels with the exception of recurving cyclones. The reason for this observed peculiarity is perhaps due to the greater 200-500 mb directional shear in the deep tropics. With recurving cyclones, on the other hand, directional shear is much less because in the baroclinic zones of the mid-latitudes, the winds at 200 mb are dynamically linked to the flow at 500 mb. Thus, the 200 mb winds provide an extra degree of predictive information for cyclones interacting with the mid-latitude westerlies.

The surface-pressure map together with 24-hour surface-pressure changes (to eliminate large diurnal effects in the tropics) has been used by tropical cyclone forecast centers since the 1950's. It is still used in conjunction with more sophisticated techniques to better assess the shorter range objective forecasts vis-a-vis the current synoptic situation. In addition, pressure changes outside the cyclone's circulation have been used to indicate future changes in motion. When there are large pressure changes far removed from the cyclone, their effect is to turn the cyclone at right angles to the line connecting the isallobaric center and the cyclone center.

A new prediction model was developed with the intent of objectively assimilating all of these observational links between cyclone motion and the synoptic scale flow. Specifically, all cyclones were stratified relative to the 500 mb subtropical ridge to incorporate the findings of Chan (1982), Xu and Gray (1982), Holland (1983) and others indicating different steering relationships for cyclones having different zonal components of motion and different locations relative to the ridge. Further, 200 mb steering predictors were used 0-20° northwest and north of the cyclone based on the correlation between upper tropospheric winds and recurvature shown by the numerous studies just cited. Five hundred millibar heights and surface pressures and their 24-hour changes were used as predictors to assess the current and recent changes in the synoptic situation at two different levels. The use of 200 mb steering winds provided a third vertical level. Seventy-two hours of cyclone motion were segmented into three 24-hour time steps and forecast fields relative to the cyclone position at the beginning of each time step were used to better define the synoptic flow and its changes affecting the movement of the cyclone as it evolved over a 3-day period.

Based on the steering concept just mentioned, a number of other tropical cyclone track forecasting schemes have been developed to (statistically or dynamically) relate cyclone motion to the surrounding flow field. A review of the basic categories of objective techniques used for predicting tropical cyclone motion and a general summary of the major tropical cyclone track prediction methods developed over the years will now be presented.

There are four basic categories of objective techniques used for predicting tropical cyclone motion:

(1) climatology-persistence
(2) steering flow
(3) statistical
(4) numerical

Appendix A presents the various techniques currently in operational use in the Atlantic and the NW Pacific/North Indian Oceans. A more detailed discussion of these track prediction models can be found in Neumann and Pelissier (1981) for the Atlantic and in the Annual Tropical Cyclone Report prepared by the JTWC for the other ocean basins.

## 2.1 Climatology-Persistence Methods

Climatology-persistence methods rely upon empirical relationships related to the tracks of previous cyclones or the past motion of the current cyclone. These techniques are useful for well-behaved cyclones that move along a climatological track with few changes in direction. Because most cyclones in the deep tropics embedded in the easterlies exhibit this type of motion, climatology-persistence methods perform well for cyclones at low latitudes. But these techniques break down in the westerly wind belt regions.

## 2.2 Steering Flow Method

The steering flow concept views the tropical cyclone as a point vortex moving precisely with the basic environmental or steering current. Observations (Chan, 1982; Holland, 1983) support this concept of the cyclone's response to the environmental flow. The difficulty of operationally applying this concept occurs when the data do not allow for a clear cut definition of the steering current, or when there is vertical shear in the environmental flow which lead to doubt as to the optimum steering level.

## 2.3 Statistical Methods

The statistical approach compares different parameters or combinations of parameters quantitatively to cyclone motion. Multiple regression analysis is employed to develop correlation coefficients and regression equations relating tropical cyclone motion to a series of these parameters.

Statistical models for predicting tropical cyclone motion can be grouped into two broad categories: those models based on analogs and those based on regression equations (Neumann, 1979). The latter, in order of increasing sophistication, can be further categorized as follows:

(a) Those models which use predictors based on climatology and persistence;

(b) Those models which include, but which are not limited to, predictors derived from observed synoptic data;

(c) Those models which include, but which are not limited to predictors (a) and (b), but also include predictors derived from numerically-forecast data.

The models that fall into category (c) are known as statistical/dynamical models while those that fall into categories (a) and (b) have been referred to respectively as simulated analog models and classical or statistical-synoptic models. The following subsections of statistical method are paraphrased from the WMO Report on operational techniques for forecasting tropical cyclone movement (Neumann, 1979).

### 2.3.1 Analog Models

#### 2.3.1.1 The Analog Concept

Analog models derive their success from their ability to identify families of cyclone tracks. Using a series of computer algorithms, a current cyclone is associated with its most likely family, which allows inferences to be made about its future motion. The analog process identifies historical cyclones temporally and spatially similar to the current cyclone. Typical factors are time of year, the cyclone's initial direction of motion and speed, and the position of the analog cyclone relative to the current cyclone. Selected analog tracks are translated to a common origin and combined with persistence to produce the final forecast. Refinements over the years have included analog weighting schemes, use of past as well as current motion and better combinations of climatology and persistence.

#### 2.3.1.2 Historical Development

The first fully operational model for predicting tropical cyclone motion by analog methods was developed by Hope and Neumann (1970) for use by the US National Hurricane Center (NHC) on Atlantic cyclones. The technique, known by the acronym HURRAN (HURRicane ANalog), has been in continuous use at the Center since the beginning of the 1969 hurricane season.

Concurrently and independently, Hodge and McKay (1970) collaborated with the US Navy and developed an analog prediction model for North Pacific typhoons. Their model, known as TYFOON, was revised by Jarrell and Somerville (1970) and became operational at the Joint Typhoon Warning Center, Guam in August 1970.

Following the introduction of HURRAN and TYFOON, and their moderate

success, the analog concept became quite popular. The HURRAN/TYFOON system was adopted and modified for use in the North Indian Ocean, southwest Indian Ocean, northeastern Pacific and in the southwest Pacific and Australian area.

2.3.1.3 Advantages and Disadvantages of the Analog Method

The main advantage of the analog is its simplicity and economy in terms of computer resources. It is quick to run and is one of the first objective guidances available to the forecaster. In addition, the method tends to be reasonably accurate for cyclones in the deep tropics embedded in the easterlies since analog forecasts represent typical or normal cyclone motion and deviations from normal in the tropics are small.

At higher latitudes, however, where cyclones are affected by the westerlies, anomalous situations are much more common and analog forecasts are more unreliable. Neumann and Hope (1972) have found that about one out of three forecast situations in the Atlantic is too anomalous for an analog method to arrive at a reasonable solution.

Another disadvantage of the analog method is the forecast bias introduced when cyclones are prematurely dropped from the historical record due to landfall, extratropical transition or dissipation. In these instances, the forecast is excessively influenced by the remaining cyclone tracks.

2.3.2 Regression Equation Models

2.3.2.1 Historical Development

The first of the statistical systems for tropical cyclone track forecasting was developed by Riehl, et al. (1956). They used the geostrophic wind components computed from the 500 mb heights around the

periphery of the cyclone to represent the vertically integrated steering flow. Miller and Moore (1960) incorporated additional geostrophic wind components for steering at the 700 and 300 mb levels as well as the past movement of the cyclone, as predictors. Arakawa (1964) and Tse (1966) developed a similar method for the NW Pacific as did Kumar and Prasad (1973) for the North Indian Ocean. The Tse method is somewhat unique in that one of five sets of regression equations were used, depending on which one of five easily identifiable 700 mb patterns existed.

All of these methods used a relatively small grid surrounding the cyclone and were only used to forecast 24-hour cyclone motion. However, because of their sensitivity to the initial analysis, all suffered from the subjectivity of uncertain analysis close to the cyclone center.

Veigas, et al. (1959) were the first to apply screening - multiple linear regression methods to the problem of tropical cyclone forecasting. Rather than restrict potential predictors to the cyclone vicinity, Veigas, et al. used a large storm-centered grid to introduce predictors that represented large-scale weather patterns. This method had the advantage of being less sensitive to the analysis near the cyclone.

A major advance in statistical prediction of tropical cyclone motion occurred with the development of the NHC64 system. In this scheme, Miller and Chase (1966) combined the better features of the Veigas, Miller-Moore and Riehl-Haggard methods into a single model. Sea level pressure, 700 mb heights and 500 mb heights, as well as 1000-700 mb thicknesses, 700-500 mb thicknesses, 500 mb height changes, geostrophic wind components at the 1000 mb, 700 mb and 500 mb levels and the past 12-hour movement of the cyclone center, were used as

predictors. Cyclones greater than 34 kts for the period 1945-1961 formed the development set which was divided into two classes - north and south of 27.5°N. A screening-multiple linear regression technique was used to derive four sets of equations -- one set for the 0 to 12 hour north-south and east-west displacements, a second set for the 12 to 24 hour displacements, a third set for the 24 to 36 hour displacements and a fourth set for the 36 to 48 hour displacements. Forecasts for periods greater than 12 hours were prepared by adding forecast displacements for successive periods. A 48 to 72 hour forecast was added to the technique later.

As a result of NHC64's poor performance on an erratic cyclone (Betsy) in 1966, a new statistical model was developed (Miller, et al., 1968). The revised model, known as NHC67, is still in use at the NHC in Miami. The 1945-1961 data base was expounded to include the 1962-1965 hurricane cases and the NHC64 equations were rederived. Additional predictors were screened in developing the NHC67 equations. These additional predictors were the 1000 mb heights (in place of sea level pressure), 1000 and 700 mb 24-hour height changes and the thermal winds computed from the thicknesses. Although equations for the 48 to 72 hour forecast were derived in support of the new operational requirement for 72-hour forecasts, it was felt that these equations were of questionable value.

In order to provide an analog forecast as part of the predictor set for higher echelon prediction models quickly and under any anomalous synoptic condition, Neumann (1972) developed a rather simple regression equation model for the Atlantic area known by the acronym CLIPER (CLImatology and PERsistence). Operational use of this improved analog

model confirmed that climatology and persistence were being better used than by earlier models for cyclones embedded in the easterlies. However, when cyclones recurved out of the tropics, CLIPER and the other analog models were still inferior to the older models such as NHC67 which included environmental flow in the predictor selection process. Accordingly, Neumann, et al. (1972) blended the better features of both approaches into a new model for the Atlantic area known as NHC72.

However, Atlantic cyclones that exhibited anomalous (non-climatological) motion continued to confirm the inherent inability of the purely "classical" models typified by NHC67 and NHC72 to forecast such motion. This led to the development of the so-called statistical/dynamical (as well as the "purely" dynamical) models which are conceptually more capable of properly responding to anomalous synoptic conditions. Such models use the output from a numerical model as one set of predictors for input. Neumann and Lawrence (1973) used selected predictors from the 24-, 36-, and 48-hour prognostic 500 mb geopotential height fields produced by the US National Meteorological Center (NMC) Primitive Equation (PE) model for their statistical/dynamical NHC73 model. A great deal of success was achieved by NHC73, primarily on the longer-range forecasts. Another statistical/dynamical model developed by Nomoto, et al. (1976) is being used by the Japan Meteorological Agency on NW Pacific typhoons in the vicinity of Japan.

The term statistical/dynamical can also be applied to the HATTRACK (Hurricane And Typhoon-TRACKing) (Renard, 1968) and the MOHATT (MOdified HATTrack) (Renard, et al., 1973) techniques used by JTWC on Guam. Instead of regression equations, tropical cyclones are geostrophically

steered in six-hourly time steps using the US Navy's smoothed numerical prognoses at various levels (1000 mb, 850 mb, 700 mb, 500 mb, 400 mb, and 200 mb). The operational forecasts starting at time $T_o$ are based on a forecast cycle starting at time $T_o$ minus 12 hours. This allows for a comparison of the 12-hour forecast from the $T_o$-12 position to the current $T_o$ position. This error, assumed to be a bias, is linearly applied with certain constraints, to the remaining 72-hour forecast track. The operational version of HATTRACK/MOHATT is known by the acronym CYCLOPS (CYCLone Operational Prediction System).

Since 1983, a model output statistic technique known by the acronym COSMOS (Cyclops Objective Steering Model Output Statistics) (Allen, 1984) has been in operational use at JTWC, Guam, to assist the forecaster in interpreting the output from CYCLOPS. COSMOS uses the CYCLOPS forecasts at the 850, 700, and 500 mb levels to produce its own forecast based on a statistical analysis of the past performance of CYCLOPS.

2.3.2.2 Advantages and Disadvantages of the "Classical" Models

Several models in this category are in current operational use at various tropical cyclone forecast centers. These include Arakawa's (1964) and Tse's (1966) models in the NW Pacific; Kumar and Prasad's (1973) model in the North Indian Ocean; and the North Atlantic NHC67 (Miller, et al., 1968) and NHC72 (Neumann, et al., 1972) models. All of these models incorporate predictors obtained from current or recently observed synoptic data to forecast future positions of the cyclone out to as much as 72 hours.

The reduction of variance of such models typically decreases rapidly with increased forecast projection. Predictors are selected

from climatology and persistence as well as from one or more of the current and 24-hour old 1000, 700, and 500 mb height fields. In fact, persistence provides most of the reduction of variance for the shorter-term forecast (Neumann, et al. (1972).

Separate sets of regression equations (stratification) representing different synoptic patterns have been developed for some of these models. Tse's (1966) model stratifies according to five easily identifiable 700 mb patterns. The NHC67 model stratifies according to the cyclone's initial location north or south of 27.5°N with an additional substratification dependent on the cyclone's speed. A stratification based on the cyclone's initial motion is used by the NHC72 model.

Both the NHC67 and the NHC72 (as well as the NHC73) models use predictors from three levels -- 1000, 700, and 500 mb. According to Neumann (1979), tests conducted at the NHC subsequent to the development of these models suggest that better operational performance may be possible by the elimination of the 700 mb data. Data at this level are highly correlated with the 500 mb level and it appears that the models use more predictors than warranted by the sample size.

#### 2.3.2.3 Advantages and Disadvantages of the Statistical-Dynamical Models

At the upper echelon of the statistical models for the prediction of tropical cyclone motion are those models which derive a portion of the variance reduction from predictors taken from the output of a numerical prediction model. Such models also derive a portion of their forecast skill from other sources such as climatology, persistence or current synoptic data.

The use of Model Output Statistics (MOS) is conceptually the most

effective method of introducing numerically forecast data into a statistical prediction model. However, the lack of adequate data sample prevents the direct introduction of a numerical model output into a statistical model. As a result, substitute methods of using the statistical-dynamical approach have been derived. One of these is referred to as the "perfect-prog" approach and a second as the Simulated Model Output Statistics (SMOS). The perfect-prog approach was used in the development of the model described in this paper.

In the perfect-prog method, observed values of a predictor at time $T_o + \Delta T$ are used to derive a statistical relationship between predictor and predictand at the same time $T_o + \Delta T$. In actual practice, however, forecast values of the predictor must be used and, therefore, any forecast error or bias is passed on to the statistical model. This is the principal reason why the predictive skill of statistical-dynamical models developed using the perfect-prog method degrades significantly when used operationally. With the MOS technique, the biases of the numerical model would be statistically corrected and certain inaccuracies recognized.

In the SMOS method, the covariance matrices containing the sums and cross-products of all possible combinations of variable pairs are modified or "contaminated" by introducing an error component similar to that of actual prognostic data. The purpose of the contamination is to partially compensate for the tendency of screening programs to overweight or select too many predictors from the perfect-prog data at the expense of the other potential predictors.

As discussed in Neumann and Lawrence (1973), NHC73 was tested on operational independent data using different sets of regression

equations developed from the perfect-prog and SMOS methods. Both versions performed well at the extended forecast periods. As expected, the perfect-prog equations performed relatively poorly during the first half of the 72-hour forecast period. Predictor over-weighting was assumed to be the probable explanation. The improvement in the perfect-prog forecasts at the extended periods suggested that the variance reducing potential of the numerically forecast data is greater than that provided by the current data at 48 hours and beyond.

The better operational performance of the SMOS equations for the shorter range forecast periods was believed to be the more realistic blend of current and numerically forecast data as a result of the contamination of the perfect-prog predictors.

In Japan, a statistical-dynamical model described by Nomoto, et al. (1976) was also designed around the perfect-prog concept. Its synoptic predictors come only from numerically produced 24-hour 500 mb prognositc geopotential height fields. When additional persistence predictors were included, the model provided 12-, 24-, 36-, and 48-hour forecast positions. With the exception of the HATTRACK/MOHATT version called CYCLOPS, there are no statistical-synoptic schemes of any kind in operational use in the NW Pacific or North Indian Oceans as of this date.

## 2.4 Numerical Method

Numerical models "appear" to provide the best promise for improvement in track forecasting. Dynamical techniques are based on the notion that the motion of the cyclone may be derived from the numerical integration of geophysical equations of motion.

2.4.1 Historical Development

Harrison (1973) developed a simple nested grid model that was applicable to forecasting typhoon motion in the NW Pacific using the primitive equations. This is the original version of the nested two-way interactive tropical cyclone model (NTCM) in operational use at JTWC on Guam (Harrison, 1981). Prior to the development of the operational version of NTCM, a more simple version of the model without the fine grid was adapted for use in 1975. This coarse-mesh ($2^{o}$), three-layer dry model initially possessed boundary conditions which were insulated, free slip walls on the north and south and cyclic on the east and west. Hodur and Burk (1978) modified this "channel" model version of the coarse mesh to include one-way interactive lateral boundaries with large-scale forcing coming from forecast fields from a hemispheric PE model in 12-hour intervals. This modification, along with the adjustment of the initial wind fields near the center based on the difference between the actual and predicted cyclone motion after 6 hours (Shewchuk and Elsberry, 1978), are incorporated in the current operational model known as OTCM. The NTCM and the OTCM are two of the better objective techniques at JTWC providing fairly accurate overall track prediction.

In the Atlantic, the SANBAR barotropic model (Sanders and Burpee, 1968) was developed on the belief that momentum advection is the primary physical mechanism for motion of intense tropical cyclones and that the cyclone is steered by the large-scale environmental flow in which it is embedded. Accordingly, the model uses a deep-layer (1000 - 100 mb) pressure - weighted U and V wind field analysis over the grid domain of the model. In the version of the model used operationally at the NHC, a

technique developed by Pike (1972) is used to modify the wind field near the cyclone to make it conform better to the initial cyclone motion vector. This technique is similar to one developed later by Shewchuk and Elsberry (1978) for use on the OTCM for the NW Pacific.

The baroclinic Movable Fine Mesh (MFM) dynamical model (Hovermale and Livezey, 1977) at the NHC was first tested operationally on Atlantic tropical cyclones during the 1975 season and has been in operational use since 1976. The MFM has far more resolution in the vertical (10 layers) than the NTCM or the OTCM and also includes parameterizations of cumulus convection and the planetary boundary layer. A fine grid of 60 km is used over its entire domain.

The NTCM and OTCM, on the other hand, have only three vertical layers and use a simple analytic heating scheme with no surface friction. The finer scale of the NTCM (41-km fine grid) moves with the cyclone within a coarser channel model with grid spacing of 205 km. Once initialized, the model runs independently of any forecast fields. By contrast, the boundary conditions of both the MFM and OTCM are externally specified by forecast fields from the NMC spectral global model and FNOC global model, respectively.

### 2.4.2 Advantages and Disadvantages of Numerical Models

Since a dynamical model does not depend on the statistical relationships between a current cyclone and historical cyclones, the reliability of the model could be expected to be independent of the details of a cyclone's past behavior. Thus, variations in the future track of a cyclone are explicitly predicted through the equations of motion.

However, due to uncertain initial analyses, principally in and around the cyclone vortex, all dynamical models are noted for poor performance at the shorter forecast period and an overall motion that is too slow. They do demonstrate increased skill for the longer forecast periods beyond 36 hours. This observation has been noted by Fiorino, et al. (1982) for the NTCM and Neumann and Pelissier (1981) for the MFM. In an effort to improve the accuracy at the shorter forecast period, both the OTCM and SANBAR incorporate a biasing technique that forces the initial cyclone motion in the model to match the observed motion of the actual cyclone. A similar bias-corrector technique is envisioned for the NTCM. Thus, the model is no longer independent of the cyclone's past behavior which is touted as one of the numerical model's strong points.

In addition, the NTCM is initialized from the operational FNOC global band tropical analysis fields. Since the analysis contains a mixture of observations, observed climatology and persistence, in data-sparce areas the cyclone track will probably have a significant climatological component.

The disadvantage of the complex and resource costly MFM is that computer resource limitations preclude any more than a 48 hour forecast, and then only under certain high threat conditions. Further, guidance from an MFM run is not available until approximately eight hours after synoptic time. Both the NTCM and OTCM, due to their relative simplicity, are run routinely to 72 hours four times a day on all tropical storms and typhoons. Their quick turnaround puts the model output at the disposal of the forecaster at the same time as he receives guidance from the other objective aids.

## 2.5 The Forecasting Dilemma

The error statistics over the years suggest that no one objective technique performs better than all others on every cyclone. Some schemes work well for some cyclones but poorly on others. This is one of the reasons for the myriad of forecast aids in operational use. An obvious problem of having too many techniques for objective guidance is illustrated in Fig. 2.1 where a typical "shotgun" effect makes it difficult for the forecaster to select the best forecast track. Such a scatter in the forecast track is common when a large directional change, as in recurvature, occurs. Note that the two numerical models (NTCM and OTCM) and COSMOS, which applies MOS technique to the output from a purely steering scheme at three vertical levels, performed superior to the other aids. The superior performance of the dynamical models over the past five years for the NW Pacific and NHC73 for the Atlantic north zone indicates the importance of synoptic data, particularly in a prognostic sense, in any attempt to forecast cyclone motion.

However, the lack of observational data, analysis schemes that disregard certain observational data in favor of climatology, and the imperfect physics involved with PE models lead to inaccurate analysis and prognostic fields. If the forecaster was able to modify these fields when they were obviously in error an improved accuracy in track prediction would likely be obtainable. A statistical-dynamical model such as the one developed and detailed in this paper permits such a man-machine interface.

In addition, the method with which the prognostic data, whether they be perfect-prog, MOS or SMOS, are introduced into the statistical scheme appears to be the key to limiting the amount of degradation all

statistical-dynamical models suffer when they are used operationally with actual forecast fields. An innovative approach to incorporating the prognostic data, as well as persistence and climatology, into a statistical model has been developed here and the results indicate that the problem of operational degradation may have been, to a large extent, solved.

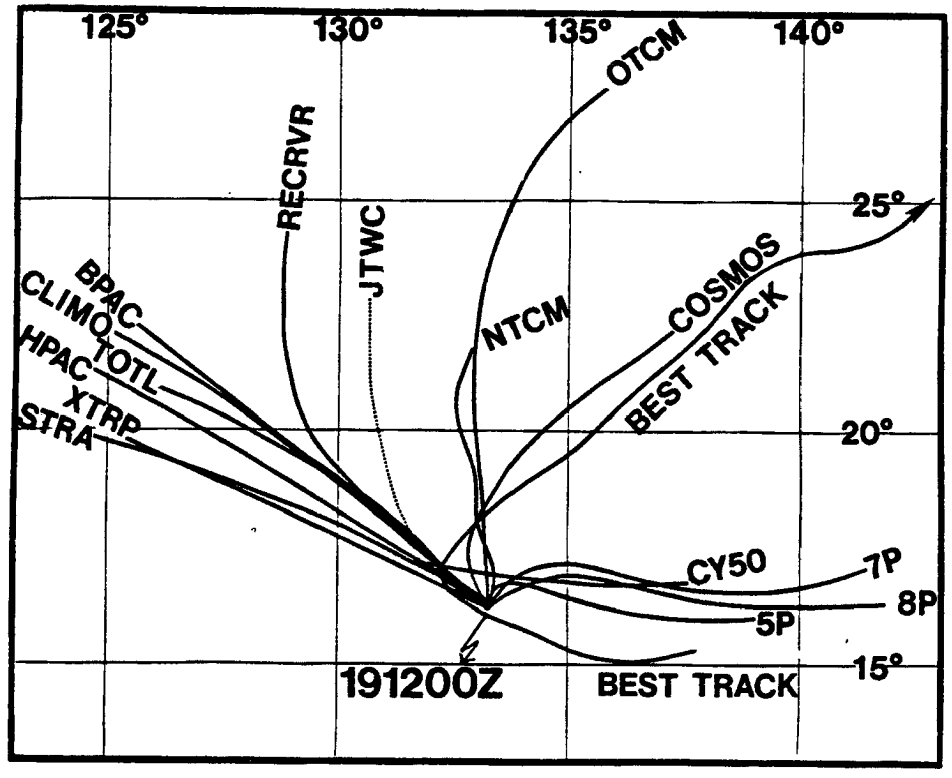


Fig. 2.1. The array of JTWC's objective forecasting techniques available to support the 19 August 1983 1200Z warning for Tropical Storm Dom. Included are the forecast issued at 191200Z and the eventual best track. (From 1983 Annual Tropical Cyclone Report.)

## 3. DEVELOPMENTAL DATA BASE AND METHODOLOGY

Multiple linear regression techniques were used to develop forecast equations for the prediction of the east-west (U) and north-south (V) components of tropical cyclone motion. Predictors used are shown in Fig. 3.1 and include past 12- and 24-hour motion, steering at the 500 mb and 200 mb levels and the current and 24-hour changes of 500 mb geopotential heights and sea level pressures relative to the cyclone position at each of the three forecast times of T=0, T=24 hours, T=48 hours. This key point will be amplified later.

The developmental data were obtained from all tropical cyclone (including tropical depressions) cases between 1946-1981. No cases were omitted because of intensity or geographical limitations. The year 1948 and every third year thereafter were selected to be used as an independent set for testing and were not used in the development of the regression coefficients. Years instead of cases were selected for the independent set because it was felt that this would result in a more representative selection for all three categories relative to the ridge. Enough years were selected for the independent set to provide approximately one-third the number of cases as the dependent set. The best track positions for the Atlantic basin were obtained from the Best Track of The National Hurricane Center while those for the other basins were obtained from the Annual Typhoon/Tropical Cyclone Reports published by the Joint Typhoon Warning Center (JTWC) on Guam. The synoptic data were derived from grid point analyses archived at The National Center

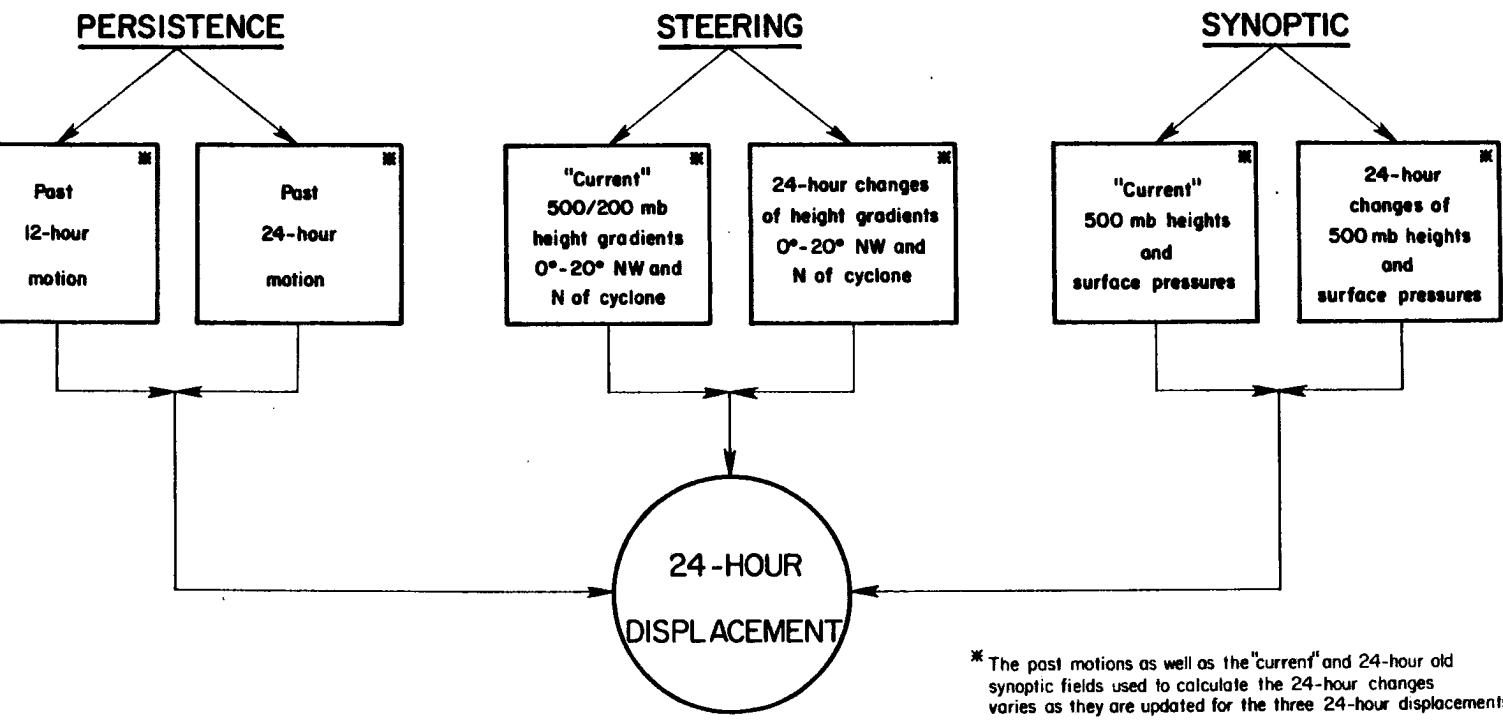


. The three components of predictors used by CSU84.

for Atmospheric Research (NCAR). These grid point data were interpolated onto a $5^{\circ}$ x $5^{\circ}$ grid (Fig. 3.2) with a domain of $-10^{\circ}$ to $+35^{\circ}$ latitude and $\pm 40^{\circ}$ longitude relative to the cyclone center to represent the synoptic forcing. The grid was offset poleward of the cyclone center to limit the number of grid points in the tropics, where the analyses tend to revert to climatology. A similar grid has been previously used by Xu and Gray (1982).

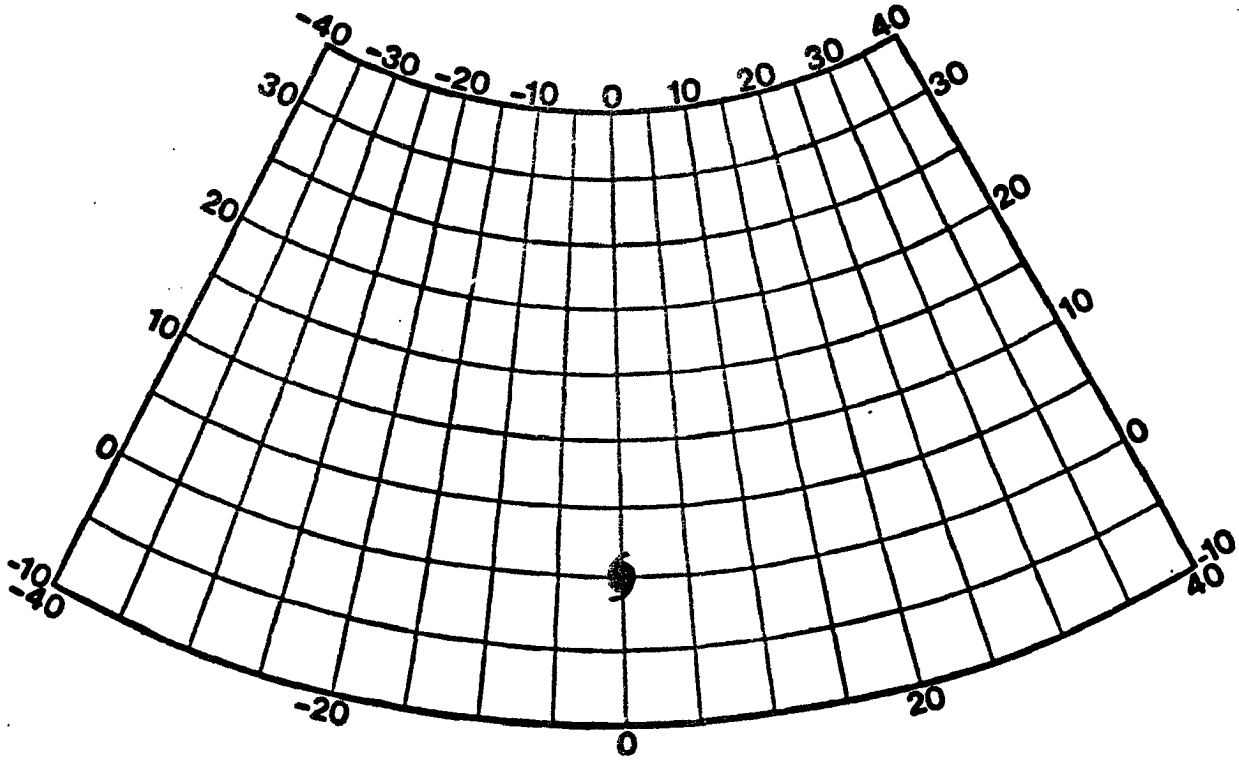


Fig. 3.2. $5^{\circ}x5^{\circ}$ geographical grid with a domain of -10 to + $35^{\circ}$ latitude and $\pm 40^{\circ}$ longitude relative to the cyclone center.

Actual prognostic fields of 500 mb D values and sea level pressures used to verify the model in a simulated operational setting were received from the Fleet Numerical Oceanography Center (FNOC), Monterey, CA, archived on a 63 x 63 hemispheric grid for the period 1968-1981. The 200 mb prognostic heights were not available from the Navy. Thus, testing of the model using actual progs was limited to a version of the

model that did not include 200 mb steering predictors. The lack of 200 mb steering predictors did not present a problem for the NW Pacific since testing of the two versions revealed no significant differences in that ocean basin. However, differences in the Atlantic were sizeable and will be discussed in Chapter 5.

## 3.1 Stratification Scheme

Thirty-six years of tropical cyclone tracks (1946-1981) were subjectively analyzed along with daily 500 mb synoptic charts to select the recurvature point for each cyclone. Based on the recurvature point, every 00Z and 12Z position along with its subsequent 24-hour track segment was placed in one of three categories relative to the 500 mb subtropical ridge. This data base stratification methodology relative to the 500 mb ridge is based on earlier work by Xu and Gray (1982) correlating fast, slow and looping motion with cyclones located north, south or near the subtropical ridge.

The south-of-ridge category is comprised of all cyclones that never recurved and the track segments of those recurving cyclones up to 24 hours prior to the recurvature point. The north-of-ridge category is comprised of all cyclones that existed north of the ridge throughout their lifetime and the track segments of those recurving cyclones beyond 24 hours after the recurvature point. The on-the-ridge category is comprised of the track segments of recurving cyclones between 24 hours before and 24 hours after the recurvature point.

Because of the frequent observation of recurving cyclones in the NW Pacific that exhibit long northward tracks before turning eastward, the criteria for stratifying the cyclone tracks relative to the ridge were modified for the NW Pacific and North Indian Oceans. Instead, the

south-of-ridge category includes those recurving cyclones up to the point where their direction of motion (DOM) became greater than 330°. The north-of-ridge category includes those recurving cyclones beyond the point where their DOM became greater than 30°. The on-the-ridge category is comprised of the track segment of recurving cyclones where the DOM is between 330° and 30°.

In an attempt to better forecast the extreme cases (which statistical methods frequently fail to do), the three categories were further separated into fast and slow motion groups based on the long wave pattern as depicted by the 500 mb height difference at certain longitudes along a chosen latitude. The specific grid points at which the height differences were noted were determined from the composition of fast minus slow cyclones performed by Xu and Gray (1982) as shown in Figs. 3.3 and 3.4 for the Atlantic and NW Pacific. Based on their composition, a quantity to be used for categorizing the speed for the Atlantic cyclones was calculated according to:

| | |
|---|---|
| $H_{15,-40} + H_{15,25} - 2 \times H_{15,-5}$ | for cyclones north of the ridge |
| $H_{10,10} - H_{10,-15} - 20$ | for cyclones on the ridge |
| $2 \times H_{20,5} - H_{20,-25} - H_{20,25}$ | for cyclones south of the ridge |

and for the Pacific:

| | |
|---|---|
| $H_{10,-35} + H_{10,15} - 2 \times H_{10,-5}$ | for cyclones north of the ridge |
| $H_{10,10} - H_{10,-5}$ | for cyclones on the ridge |
| $2 \times H_{15,0} - H_{15,-30} - H_{15,40}$ | for cyclones south of the ridge |

H is the 500 mb height in meters and the subscripts indicate the degrees of latitude and longitude away from the cyclone center where the heights are to be observed. Latitudes are positive poleward of the

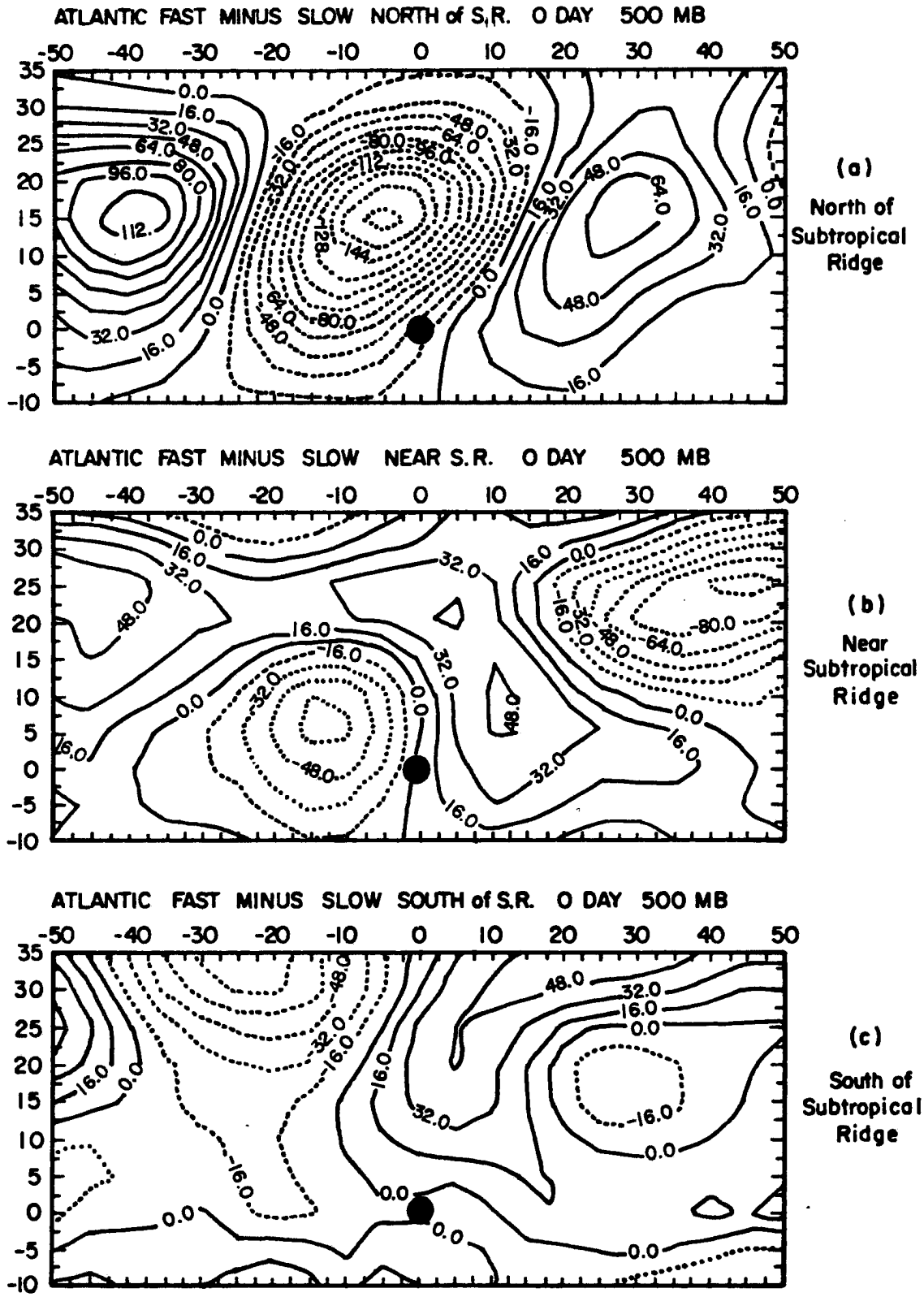


Fig. 3.3. 500 mb composite height differences in meters of fast minus slow cyclones in the Atlantic. The large dot marks the position of the cyclone. (From Xu and Gray, 1982).

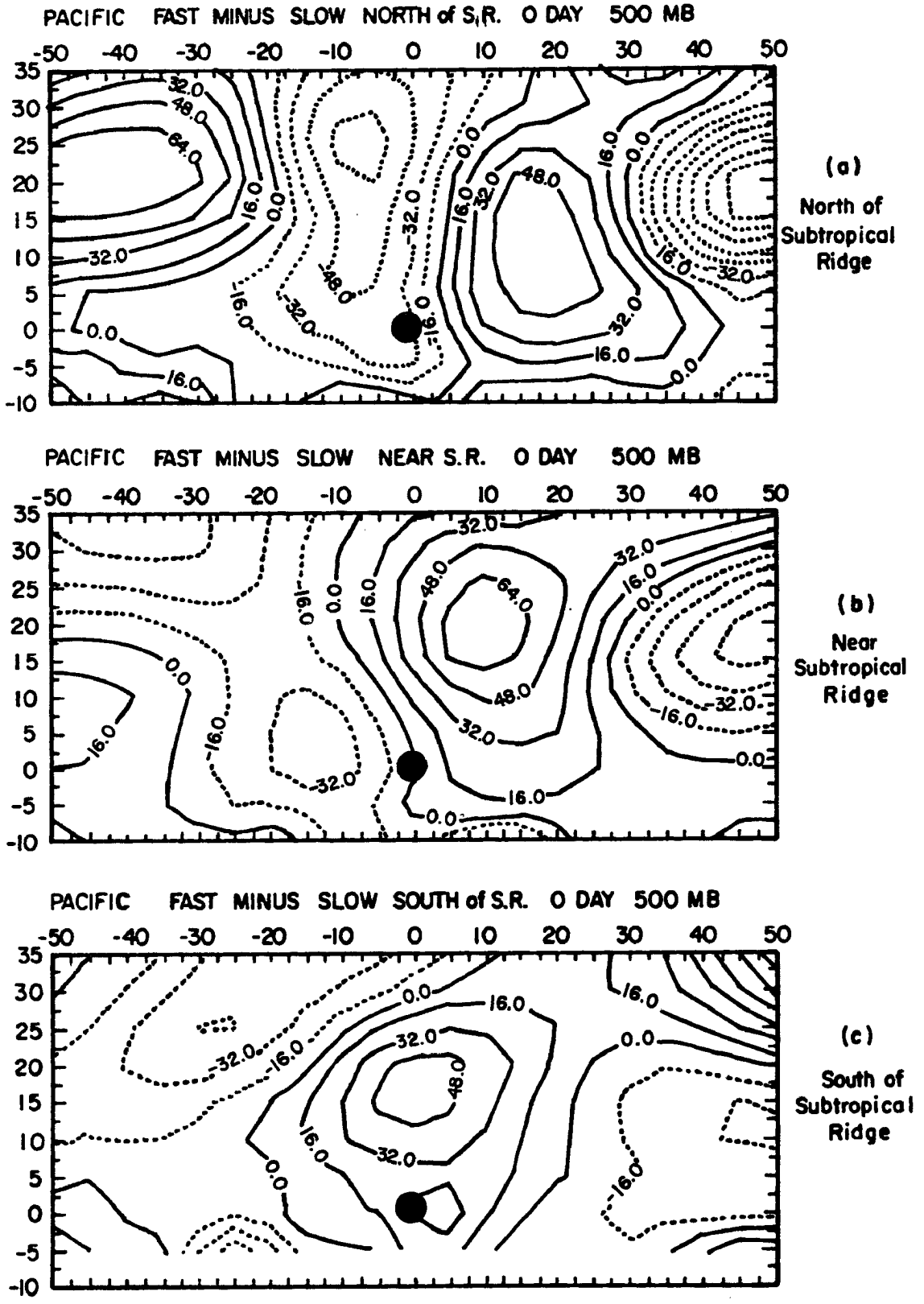


Fig. 3.4. 500 mb composite height differences in meters of fast minus slow cyclones in the Pacific. The large dot marks the position of the cyclone. (From Xu and Gray, 1982).

cyclone and longitudes are positive eastward of the cyclone center.

If the speed stratification parameter was greater than or equal to zero, the long wave pattern was assumed to be favorable for fast motion so the cyclone was placed in the fast category. On the other hand, if the parameter was less than zero, the long wave pattern was assumed to be favorable for slow motion so the cyclone was placed in the slow category. The intent was that this screening would be able to omit the slow moving cyclones (less than 2.5 m/s) from one set of equations and the fast moving cyclones (greater than 7.5 m/s) from the other set of equations.

In a conceptual sense, as illustrated in Figs. 3.5 through 3.7, different 500 mb long wave patterns are associated with fast and slow motion and it was felt that this procedure would result in a crude classification according to synoptic types in a manner similar to the scheme proposed by Tse (1966) for typhoon forecasting in the Pacific. If this theory holds, then certain predictors would be selected in different orders or given different weights for the fast and slow cases.

3.2 24-Hour Time Steps

For extended forecast periods, a likely weakness of a stratification based on the position of the cyclone relative to the ridge is that a tropical cylone's position relative to the ridge may change over a span of three days. Although the initial position of the cyclone may place it south of the ridge, for example, it may be located north of the ridge 48 hours later and the environmental influences affecting its movement over the next 24 hours will certainly differ from those affecting its movement had it remained south of the ridge during the entire 72-hour period.

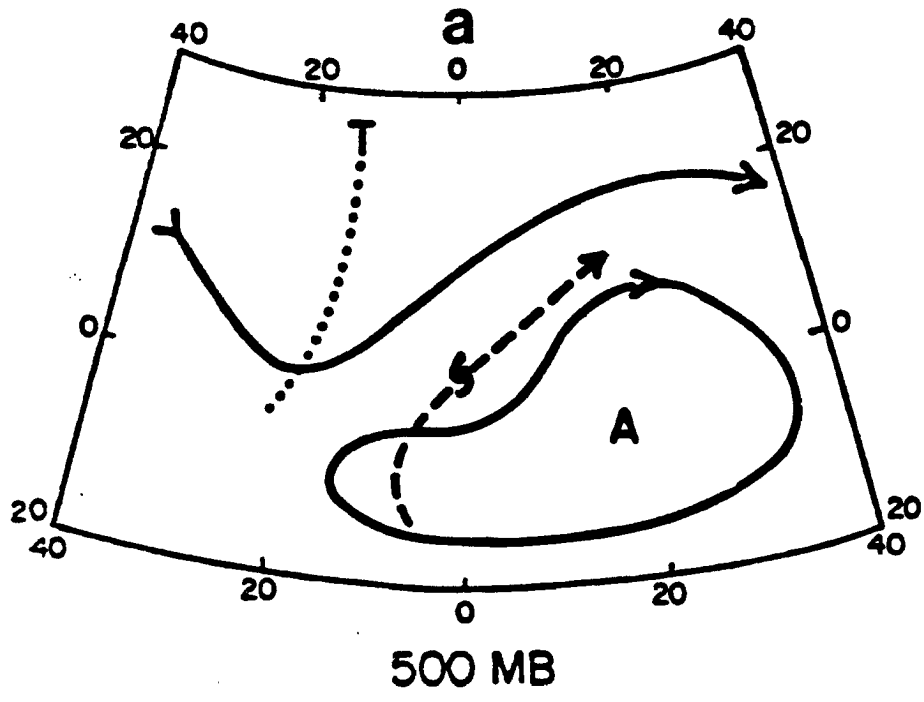


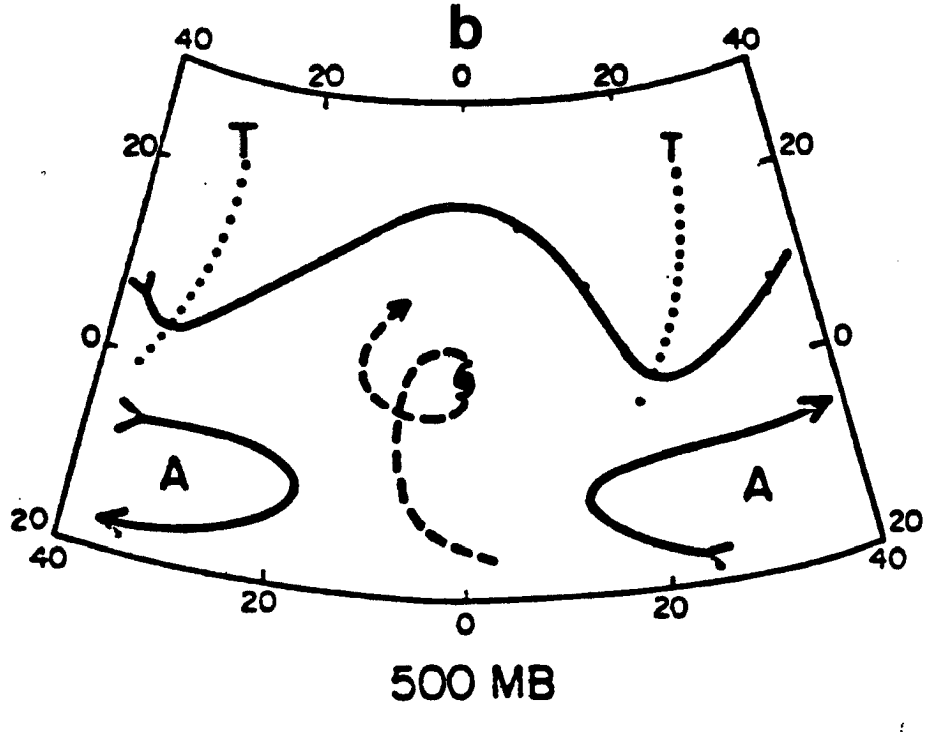


Fig. 3.5. a) Favorable height pattern for fast motion north of the subtropical ridge. b) Typical height pattern for slow motion north of the subtropical ridge. (From Xu and Gray, 1982.)

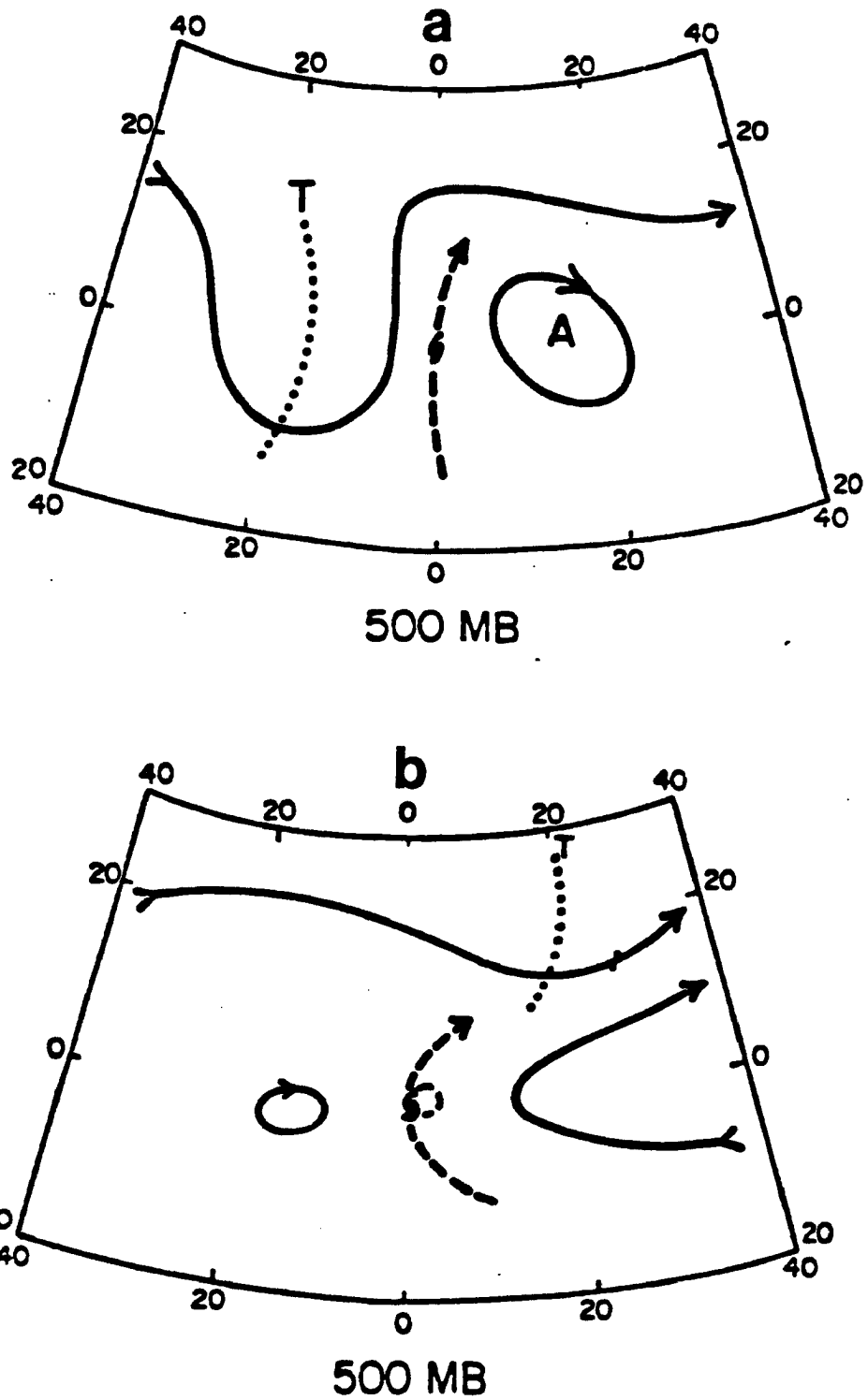


Fig. 3.6. a) Typical height pattern favorable for fast motion on the subtropical ridge. b) Typical height pattern for slow motion on the subtropical ridge. (From Xu and Gray, 1982.)

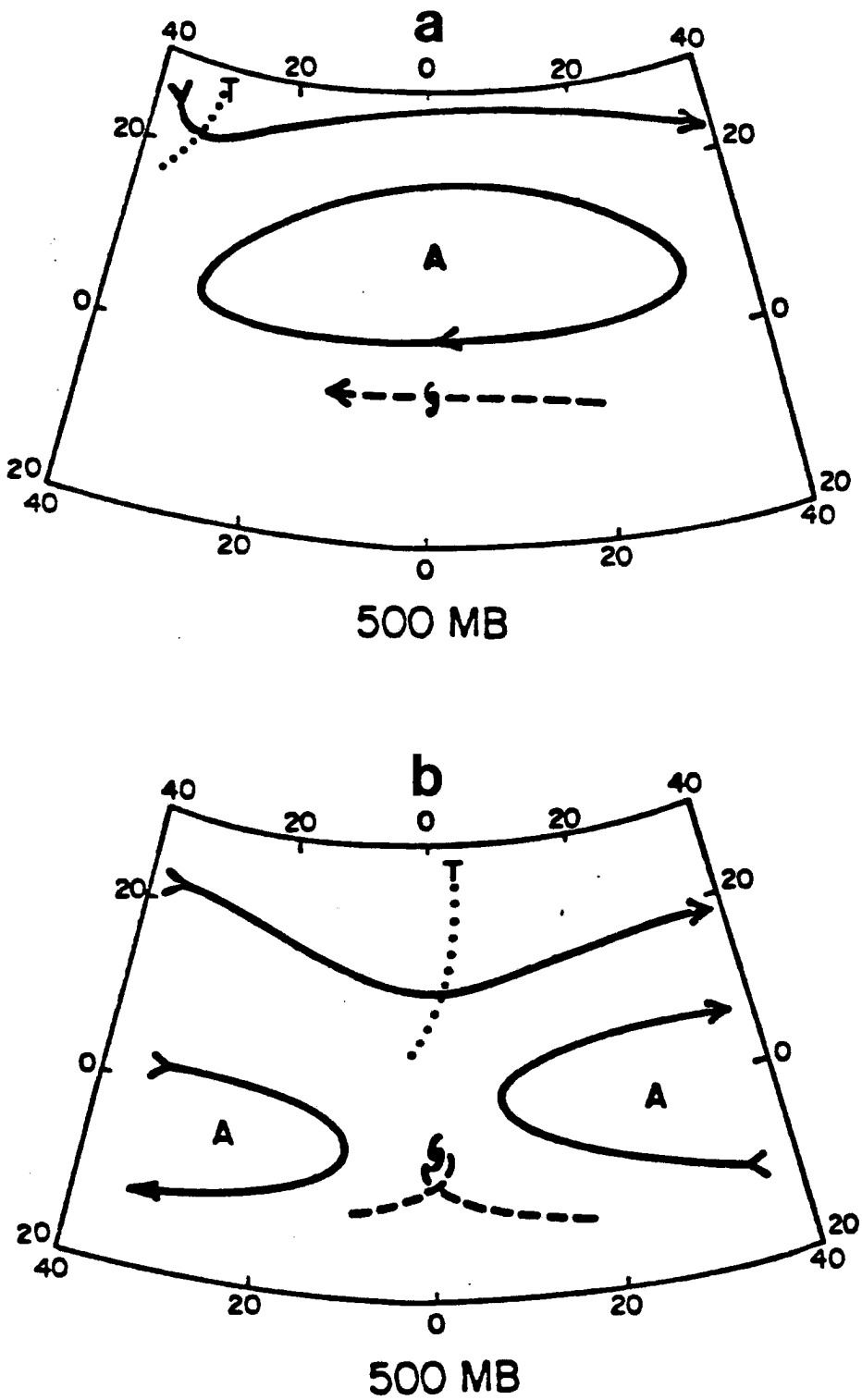


Fig. 3.7. a) Favorable height pattern for fast motion south of the subtropical ridge. b) Typical height pattern for slow motion south of the subtropical ridge. (From Xu and Gray, 1982.)

In order to eliminate the problem of a cyclone in one category moving into a different category during the course of a 72-hour motion, and also to attempt to better describe the environment in which the cyclone was embedded as it changed over the period of 72 hours, the 72-hour period was segmented into three 24-hour periods. The segmenting of 72-hour motion into 3 discrete 24-hourly time steps departs from the traditional statistical approach. There is an important distinction between CSU84 and the other statistical models in forming the developmental set. The other models require 72-hour tracks for each sample case whereas each sample case for CSU84 is composed of a 24-hour track. It is therefore possible to generate a much larger sample to develop the model's regression equations. For the Atlantic, there were 977 cases for the south-of-ridge category, 1034 cases for the north-of-ridge category and 371 cases for the on-the-ridge category. For the NW Pacific, there were 4074 cases south of the ridge, 799 cases north of the ridge and 973 cases on the ridge.

With the discretized steps, CSU84 calculates new past-motion persistence predictors and updates synoptic grid-point data relative to the new cyclone position at the start of each 24-hour forecast. The direction of motion over the previous 24 hours or a subjective analysis of the new position of the cyclone relative to the subtropical ridge is used to determine changeover from one stratification class to another. With the objective method of changing categories for cyclones in the south-of-ridge category, if the motion over the previous 24-hour period indicates a heading between $330^{o}$ and $30^{o}$, that segment is placed in the on-the-ridge category for the formulation of the next 24-hour motion. Similarly, for cyclones in the south-of-ridge or on-the-ridge

categories, if the motion over the previous 24-hour period is between $31^{o}$ and $120^{o}$, that segment is placed in the north-of-ridge category for the formulation of the next 24-hour motion.

The perfect-prog approach is used to provide the new synoptic information in the research mode. The 24- and 48-hour 500 mb height and surface pressure prognostic fields would provide the information to formulate the 48-hour and 72-hour forecast motions, respectively in an operational setting. In other words, the 24-hour prognostic fields would be applied to the 24- to 48-hour motion and the 48-hour prognostic fields to the 48- to 72-hour motion. This is a significant departure from the traditional method of introducing prognostic data. Figure 3.8 is a flowchart depicting the 3-step procedure for arriving at the 24-, 48- and 72-hour forecast positions.

## 3.3 Application of Prognostic Data

The method of applying the prognostic data in CSU84 is unique. Other statistical models that employ prognostic data invariably use several forecast fields (24-, 36-, and 48-hour) for every forecast period, i.e., 0 to 12, 0 to 24, 0 to 36, 0 to 48, 0 to 72. The weakness of such an approach (Neumann, 1975) is that the predictors from the prognostic data fields are given excessive weight over those of the observed data. This ''overweighting'' is understandable when the perfect-prog approach is used to introduce the prognostic data since all the prog data would be "perfect" -- the data come from verifying analysis fields. Thus, it is of no surprise that these models would degrade when actual forecast fields, which are not as accurate as the perfect-prog development data, are used to introduce the synoptic predictors in operational use. This point will be amplified in Chapter 5.

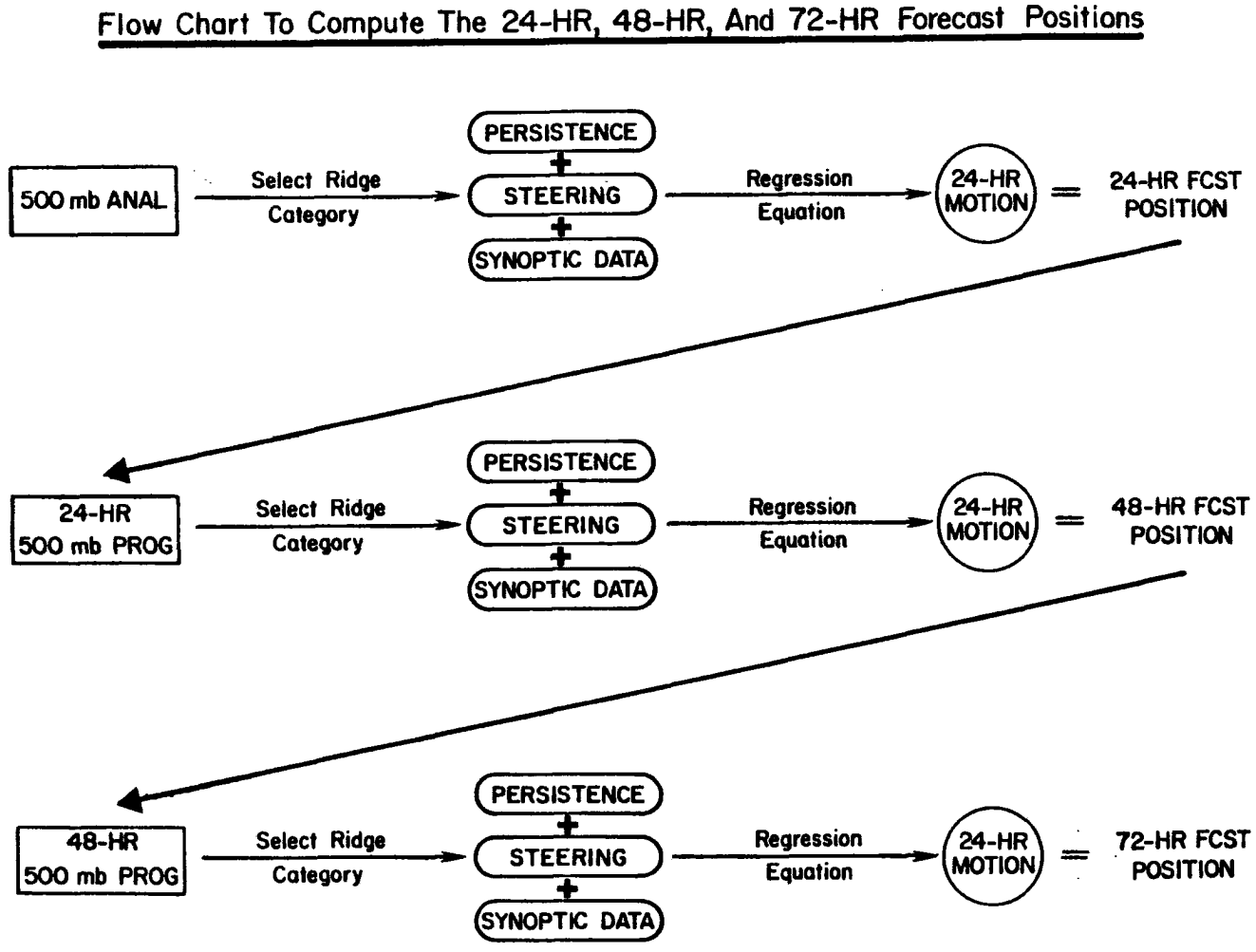


Fig. 3.8. 3-step flow chart depicting the procedure for computing the 24-, 48- and 72-hour forecast positions.

The unique method of applying prognostic data developed in CSU84 minimizes this degradation in two ways. First, by using just the current and 24-hour old analyses to compute the first 24 hours of motion, one has a "solid" 24-hour forecast position on which to build a 48-hour forecast based on prognostic data to arrive at a 72-hour forecast position. Second, the 48-hour forecast position is computed based on a 24-hour motion using the 24-hour forecast fields and the initial analysis fields to provide the tendencies of heights and pressures. Hence, just one forecast field is required to compute the second 24-hour motion and it is only the third and final 24-hour increment that depends on two prog fields (24-hour and 48-hour). It would appear logical to shorten the forecast interval that a scheme relies on as much as possible so that if the prog field is in error, the error in the ensuing forecast position will be kept to a minimum. Further, although one or both of the forecast fields may be in error, the tendencies may still be fairly accurate. Thus, by discretizing the 72-hour cyclone motion into three shorter 24-hour segments, the reliance of the forecast scheme on "perfect" synoptic data to predict a 24-hour motion should not be as unrealistic as the reliance it would have if it was used to predict a 72-hour motion. If this notion holds, then the degradation in skill when using actual prognostic data may not be as drastic. This CSU84 method conceptually appears to be superior to ones that attempt to compute a 24-hour forecast position based on analyses as well as prognostic data and then to recompute 48 and 72 hours of motion always from the initial position using three forecast fields (24-, 36-, and 48-hour), all of which could contain significant errors.

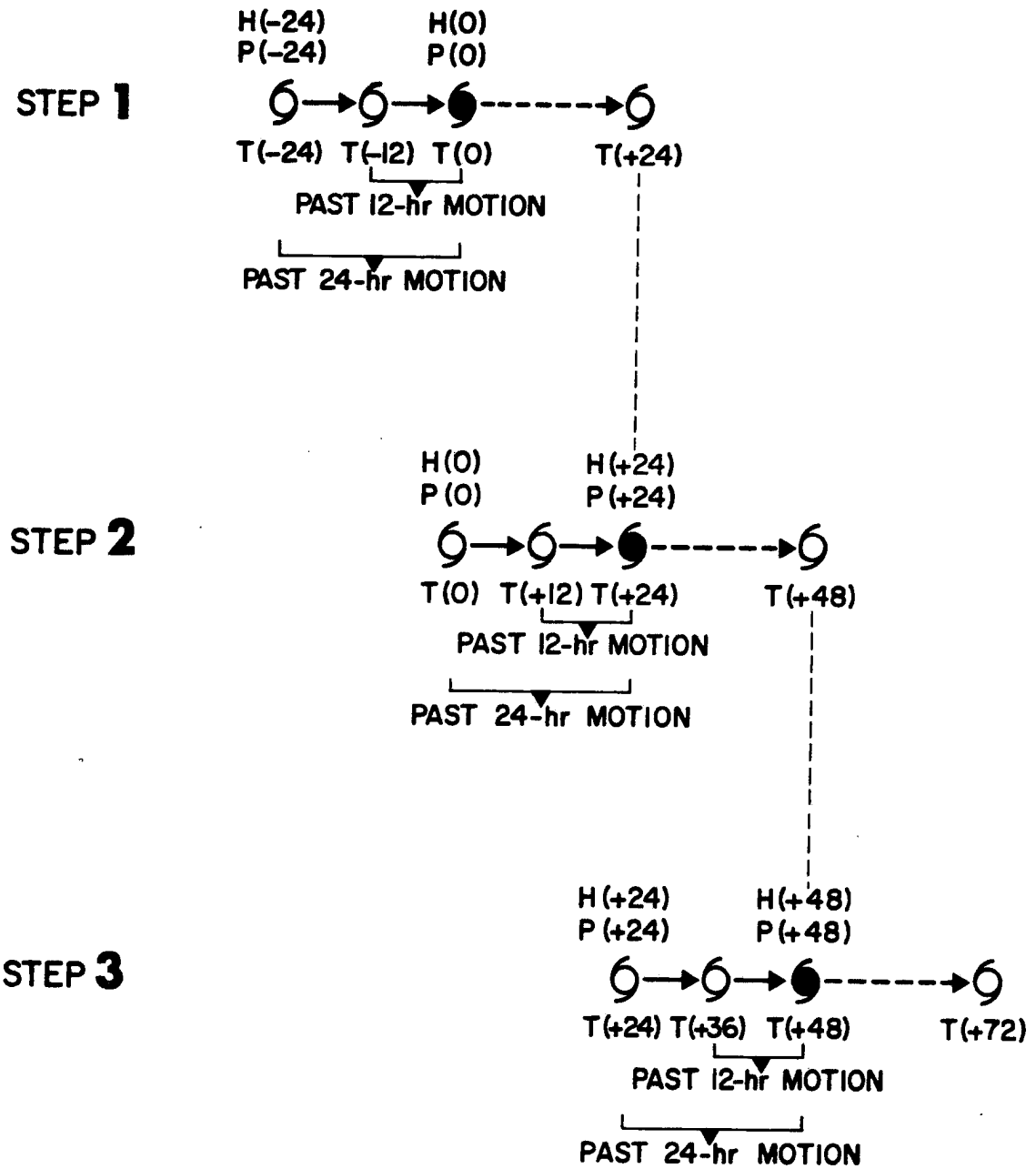


Fig. 3.9. Schematic diagram illustrating how the past motions and synoptic fields used to provide the predictors for a 24-hour displacement change relative to the new position of the cyclone.

A more specific schematic diagram of the three steps needed for a forecast projection of 72 hours is presented in Fig. 3.9. Note that the definition of past motion and current and 24-hour old synoptic data changes as each 24-hour displacement is stepped forward. As a result, the actual values of the selected predictors will change as the forecast positions are projected forward in time. This is because all of the predictors are relative to the position of the cyclone at the time they are applied and because the ridge position category might change. By implication, prognostic data are used as if they were analysis data at their respective valid times.

The cyclone symbols with the darkened circle are the positions from which the three 24-hour displacements are computed. The two cyclone symbols with the open circle to the left of these positions represent the 12- and 24-hour old positions relative to each of the three positions at which each 24-hour forecast is made. The cyclone symbol with the open circle to the right of the darkened circles is the 24-hour displacement. As the 72-hour forecast process is stepped forward in 24-hour increments, each 24-hour displacement position becomes the new position from which to compute the next 24-hour displacement.

The "H" and "P" above the cyclone symbols indicate which 500 mb height and surface pressure fields provide the required synoptic predictors to compute the displacements. With $T_o$ the time at the initial position, H(o) and P(o) corresponds to the current analyses, H(-24) and P(-24) correspond to 24-hour-old analyses, H(+24) and P(+24) correspond to the 24-hour prognoses and H(+48) and P(+48) correspond to the 48-hour prognoses.

# 4. THE REGRESSION EQUATIONS

## 4.1 The Regression Equation

A stagewise-stepwise multiple linear regression procedure proposed by Lund (1971) was adopted to develop the prediction equations. Due to the large number of both sample cases and potential predictors, the normal stepwise regression approach would have been inappropriate since the two covariance arrays containing the sums of squares and cross-products would have exceeded the memory size of the largest available computers. With the procedure suggested by Lund, there is just one relative coefficient matrix instead of two covariance matrices.

The regression equations were obtained using the subroutines available in The International Mathematics and Statistics Libraries (IMSL, 1982) that reside on the NCAR CRAY-1 computer. The method employed was as follows:

(1) Means, standard deviations and correlation coefficients were computed for each predictor

(2) IMSL subroutine BECOVM computed the corrected sum of squares and cross-products

(3) IMSL subroutine RLMUL performed an analysis of variance including the standard deviation of the residuals and the regression coefficient and intercept estimates.

(4) IMSL subroutine RLRES performed a residual analysis on the predictors used in fitting a regression model. The residual from this

fitted model became the new dependent variable (predictand) and steps (1) - (4) repeated 20 times to select the 20 best predictors.

(5) IMSL subroutine RLSEP performed a forward stepwise regression analysis using the 20 predictors selected from the stagewise procedure to compute the regression coefficients. The process that is accomplished by the first four steps has also been referred to as successive elimination. After the removal of each selected predictor, a new residual is calculated with the remaining predictors and that becomes the new predictand with which the remaining predictors are correlated.

4.2 Geographical Inhomogeneity

Northern Hemisphere cyclone tracks exhibit significant regional variations. In the NW Pacific, the near-equatorial monsoon trough is responsible for erratic motion with low latitude cyclones. Further, cyclones in the NW Pacific sometimes travel far poleward before being steered eastward by the westerlies. For the South China Sea region, complicated and conflicting wind flow patterns between the southwest monsoon flow and the continental northeasterlies lead to a strong vertical wind shear and extremely erratic motion is common. In the North Indian Ocean, weak steering currents lead to slow motion. In the Atlantic, cyclones generally track in a west to northwestward direction recurving at higher latitudes. Unlike the Pacific, the ratio of very fast and very slow moving cyclones to the total is high which results in difficult forecast situations.

Regression equations were therefore developed separately for the four geographical regions with slight regional changes. Due to the low annual frequency of cyclones in the North Indian Ocean, it was necessary

to use 500 mb computed geostrophic winds in place of 200 mb computed geostrophic winds since 200 mb data are available only after 1962. This permitted the use of the entire historical best tracks going back to 1946. Additionally, no speed stratification was attempted in the North Indian Ocean to further increase the sample size.

For the South China Sea, because the vertical shear of the steering flow was thought to be of overriding importance in the motion process vis a vis the location of the mid-level subtropical ridge for cyclone motion in this region, these cyclones were not stratified relative to the 500 mb subtropical ridge. Storms in this region were also not stratified by speed both because they tend to move slowly and also in order to obtain as large a sample size as possible. Instead, additional steering levels - 700 mb and 850 mb - were incorporated in an attempt to better depict the steering flow at different vertical levels.

For the NW Pacific, two observed phenomena presented special difficulties in stratification. One was the erratic motion of cyclones embedded in the near-equatorial monsoon trough. The other was the long northward track of cyclones prior to being steered eastward by the upper level westerlies.

In the first instance of anomalous motion, it is obvious that the direction of motion is a poor indicator of future motion. Instead of deleting these monsoon-trough cases, these cyclones were left intact in the developmental data set with the understanding that correlation of motion south of the ridge with synoptic predictors might not be as high as those for the Atlantic cyclones. To handle the long northward trek of cyclones in the NW Pacific, the criteria for the on-the-ridge category was broadened to include all segments that had a direction of

motion between 330° and 30° rather than restricting this category to 24 hours before and after the recurvature point.

4.3 The Potential Predictors

Equations for the east-west and north-south components of cyclone motion were developed by screening over 700 potential predictors. These predictors included the past 12-hour and past 24-hour east-west and north-south motions and grid point synoptic data of "current" and the past 24-hour changes of 500 mb heights and sea level pressures. Recall that all of the predictors are applied relative to a new cyclone position each time a 24-hour motion is computed. Thus, the synoptic grid, and the 12- and 24-hour old cyclone positions needed to calculate the past motions, move with the cyclone.

As a result, the analysis field valid at the initial time $T_o$ is the "current" synoptic field and that field, along with the analysis field valid at $T_o$ minus 24 hours ($T_{-24}$), are used to calculate the 24-hour changes of 500 mb heights and sea level pressures. These two fields are also used to compute the "current" and 24-hour changes of the steering predictors. Once the first 24-hour displacement has been stepped forward, the 24-hour forecast field valid at $T_o$ plus 24 hours ($T_{+24}$) becomes the "current" synoptic field and the analysis field at $T_o$ becomes the 24-hour-old field and all of the grid-point predictors as well as the updated persistence predictors are computed relative to the new cyclone position at $T_{+24}$. When the second 24-hour displacement is stepped forward from the $T_{+24}$ cyclone position, the 48-hour forecast field valid at $T_o$ plus 48 hours ($T_{+48}$) becomes the "current" synoptic field and the forecast field valid at $T_{+24}$ becomes the 24-hour-old field. Then, all of the grid-point predictors as well as the updated

persistence predictors are computed relative to the new cyclone position at $T_{+48}$. Using these updated predictors, the final 24-hour displacement is stepped forward from the $T_{+48}$ cyclone position to determine the 72-hour forecast position. All references to steering winds apply to geostrophic winds which were calculated from the gradients of geopotential heights using the following formula:

For the wind at the cyclone center, the U and V components are computed as:

$$U = ((H_{-10,-10} + H_{-10,-5} + H_{-10,0} + H_{-10,5} + H_{-10,10}) - (H_{10,-10} + H_{10,-5} + H_{10,0} + H_{10,5} + H_{10,10})) / (5\sin\phi)$$

$$V = ((H_{-10,10} + H_{-5,10} + H_{0,10} + H_{5,10} + H_{10,10}) - (H_{-10,-10} + H_{-5,-10} + H_{0,-10} + H_{5,-10} + H_{10,-10})) / (5\sin\phi\cos\phi)$$

For the wind $10^{\circ}$ northwest of the cyclone center, the U and V components are computed as:

$$U = (H_{5,-10} - H_{15,-10}) / \sin\phi$$

$$V = (H_{10,-5} - H_{10,-15}) / (\sin\phi\cos\phi)$$

For the wind $5^{\circ}$ northwest of the cyclone center, the U and V components are computed as:

$$U = (H_{0,-5} - H_{10,-5}) / \sin\phi$$

$$V = (H_{5,0} - H_{5,-10}) / (\sin\phi\cos\phi)$$

For the wind $10^{\circ}$ north of the cyclone center, the U and V components are computed as:

$$U = (H_{5,0} - H_{15,0}) / \sin\phi$$

$$V = (H_{10,5} - H_{10,-5}) / (\sin\phi\cos\phi)$$

For the wind $5^{\circ}$ north of the cyclone center, the U and V components

are computed as:

$U = (H_{0,0} - H_{10,0}) / \sin\phi$

$V = (H_{5,5} - H_{5,-5}) / (\sin\phi\cos\phi)$

For the wind 15° northwest of the cyclone center, the U and V components are computed as:

$U = (H_{10,-15} - H_{20,-15}) / \sin\phi$

$V = (H_{15,-10} - H_{15,-20}) / (\sin\phi\cos\phi)$

For the wind 20° northwest of the cyclone center, the U and V components are computed as:

$U = (H_{15,-20} - H_{25,-20}) / \sin\phi$

$V = (H_{20,-15} - H_{20,-25}) / (\sin\phi\cos\phi)$

For the wind 15° north of the cyclone center, the U and V components are computed as:

$U = (H_{10,0} - H_{20,0}) / \sin\phi$

$V = (H_{15,5} - H_{15,-5}) / (\sin\phi\cos\phi)$

For the wind 20° north of the cyclone center, the U and V components are computed as:

$U = (H_{15,0} - H_{25,0}) / \sin\phi$

$V = (H_{20,5} - H_{20,-5}) / (\sin\phi\cos\phi)$

$H_{i,j}$ is the 500 mb or 200 mb height at grid point i,j where i represents latitude and j represents longitude from the cyclone center. Latitudes are positive to the north and longitudes are positive to the east of the cyclone center. $\varphi$ is the latitude of the grid point at which the steering wind is being computed.

Table 4.1 lists the 732 potential predictors for the Atlantic and NW Pacific. Table 4.2 lists the 728 potential predictors for the North Indian Ocean and Table 4.3 lists the 1364 potential preditors for the South China Sea. The list of 728 potential predictors for the Atlantic and NW Pacific using 500 mb steering instead of 200 mb steering is identical to those listed for the North Indian Ocean. The 500 mb steering wind over the cyclone center is computed for all versions of the model. This is the reason for the difference in the number of predictors between the two versions for the NW Pacific and the Atlantic.

Variations of the model using surface pressure gradients as well as thickness of the surface to 500 mb surfaces were tested. However, the screening program failed to select either category of predictors.

The three categories of predictors used in the CSU84 prediction model were shown in Chapter 3. As explained earlier, the "current" and the 24-hour-old synoptic data are not always the analysis and the 24-hour-old analysis at the initial time for the 24- to 48- and 48- to 72-hour predictions. These fields change as the three 24-hour displacements are stepped forward. In development, a perfect-prog approach was used to introduce analysis data valid at the verifying times. In actual practice, 24- and 48-hour forecast fields would be used at their verifying times.

Importance of Different Predictors. The reduction of variance due to each of the three categories of predictors was examined for Atlantic and Pacific. A few surprising observations are evident from Table 4.4. One was the significant difference in the variance reducing potential of the steering component for the north-of-ridge and on-the-ridge between the Atlantic and NW Pacific.

TABLE 4.1

The 732 potential forecast predictors for the Atlantic and NW Pacific

| | |
|---|---|
| 1-170 | 24-hr 500 mb height changes at the 17 X 10 grid points [$\Delta H$] |
| 171-340 | 500 mb heights at the 17 X 10 grid points [H] |
| 341-510 | 24-hr sea level pressure changes at the 17 X 10 grid points (mb) [$\Delta P$] |
| 511-680 | Sea level pressures at the 17 X 10 grid points (mb) [P] |
| 681-682 | Past 24-hr U and V cyclone motion (km/hr) [$U_{-24}$, $V_{-24}$] |
| 683-684 | Past 12-hr U and V cyclone motion (km/hr) [$U_{-12}$, $V_{-12}$] |
| 685-686 | 500 mb U and V wind components at cyclone center [$\Phi_{500u}$, $\Phi_{500v}$] |
| 687-688 | 24-hr 500 mb U and V wind change at cyclone center [$\Delta\Phi_{500u}$, $\Delta\Phi_{500v}$] |
| 689-690 | 200 mb U and V wind components at cyclone center [$\Phi_{200u}$, $\Phi_{200v}$] |
| 691-692 | 24-hr 200 mb U and V wind change at cyclone center [$\Delta\Phi_{200u}$, $\Delta\Phi_{200v}$] |
| 693-694 | 200 mb U and V wind components 10° northwest of cyclone center [$\Phi_{200NW10u}$, $\Phi_{200NW10v}$] |
| 695-696 | 24-hr 200 mb U and V wind change 10° northwest of cyclone center [$\Delta\Phi_{200NW10u}$, $\Delta\Phi_{200NW10v}$] |
| 697-698 | 200 mb U and V wind components 5° northwest of cyclone center [$\Phi_{200NW5u}$, $\Phi_{200NW5v}$] |
| 699-700 | 24-hr 200 mb U and V wind change 5° northwest of cyclone center [$\Delta\Phi_{200NW5u}$, $\Delta\Phi_{200NW5v}$] |
| 701-702 | 200 mb U and V wind difference between 10° northwest and 5° northwest of cyclone center [$\Phi_{200NW10-5u}$, $\Phi_{200NW10-5v}$] |
| 703-704 | 24-hr 200 mb U and V wind change difference between 10° northwest and 5° northwest of cyclone center [$\Delta\Phi_{200NW10-5u}$, $\Delta\Phi_{200NW10-5v}$] |
| 705-706 | 200 mb U and V wind components 10° north of cyclone center [$\Phi_{200N10u}$, $\Phi_{200N10v}$] |
| 707-708 | 24-hr 200 mb U and V wind change 10° north of cyclone center [$\Delta\Phi_{200N10u}$, $\Delta\Phi_{200N10v}$] |

TABLE 4.1 (cont'd)

| | |
|---|---|
| 709-710 | 200 mb U and V wind components 5° north of cyclone center [$\Phi_{200N5u}$, $\Phi_{200N5v}$] |
| 711-712 | 24-hr 200 mb U and V wind change 5° north of cyclone center [$\Delta\Phi_{200N5u}$, $\Delta\Phi_{200N5v}$] |
| 713-714 | 200 mb U and V wind difference between 10° north and 5° north of cyclone center [$\Phi_{200N10-5u}$, $\Phi_{200N10-5v}$] |
| 715-716 | 24-hr 200 mb U and V wind change difference between 10° north and 5° north of cyclone center [$\Delta\Phi_{200N10-5u}$, $\Delta\Phi_{200N10-5v}$] |
| 717-718 | 200 mb U and V wind components 15° northwest of cyclone center [$\Phi_{200NW15u}$, $\Phi_{200NW15v}$] |
| 719-720 | 24-hr 200 mb U and V wind change 15° northwest of cyclone centers [$\Delta\Phi_{200NW15u}$, $\Delta\Phi_{200NW15v}$] |
| 721-722 | 200 mb U and V wind components 20° northwest of cyclone centers [$\Phi_{200NW20u}$, $\Phi_{200NW20v}$] |
| 723-724 | 24-hr 200 mb U and V wind change 20° northwest of cyclone center [$\Delta\Phi_{200NW20u}$, $\Delta\Phi_{200NW20v}$] |
| 725-726 | 200 mb U and V wind components 15° north of cyclone center [$\Phi_{200N15u}$, $\Phi_{200N15v}$] |
| 727-728 | 24-hr 200 mb U and V wind change 15° north of cyclone center [$\Delta\Phi_{200N15u}$, $\Delta\Phi_{200N15v}$] |
| 729-730 | 200 mb U and V wind components 20° north of cyclone center [$\Phi_{200N20u}$, $\Phi_{200N20v}$] |
| 731-732 | 24-hr 200 mb U and V wind change 20° north of cyclone center [$\Delta\Phi_{200N20u}$, $\Delta\Phi_{200N20v}$] |

TABLE 4.2

The 728 Potential Forecast Predictors For The North Indian Ocean

| | |
|---|---|
| 1-170 | 24-hr 500 mb height change at the (17 X 10) grid points [$\Delta H$] |
| 171-340 | 500 mb heights at the 17 X 10 grid points [H] |
| 341-510 | 24-hr sea level pressure change at the 17 X 10 grid points (mb) [$\Delta P$] |
| 511-680 | Sea level pressures at the 17 X 10 grid points (mb) [P] |
| 681-682 | Past 24-hr U and V cyclone motion (km/hr) [$U_{-24}$, $V_{-24}$] |
| 683-684 | Past 12-hr U and V cyclone motion (km/hr) [$U_{-12}$, $V_{-12}$] |
| 685-686 | 500 mb U and V wind components at cyclone center [$\Phi_{500u}$, $\Phi_{500v}$] |
| 687-688 | 24-hr 500 mb U and V wind change at cyclone center [$\Delta\Phi_{500u}$, $\Delta\Phi_{500v}$] |
| 689-690 | 500 mb U and V wind components 10° northwest of cyclone center [$\Phi_{500NW10u}$, $\Phi_{500NW10v}$] |
| 691-692 | 24-hr 500 mb U and V wind change 10° northwest of cyclone center [$\Delta\Phi_{500NW10u}$, $\Delta\Phi_{500NW10v}$] |
| 693-694 | 500 mb U and V wind components 5° northwest of cyclone center [$\Phi_{500NW5u}$, $\Phi_{500NW5v}$] |
| 695-696 | 24-hr 500 mb U and V wind change 5° northwest of cyclone center [$\Delta\Phi_{500NW5u}$, $\Delta\Phi_{500NW5v}$] |
| 697-698 | 500 mb U and V wind difference between 10° northwest and 5° northwest of cyclone center [$\Phi_{500NW10-5u}$, $\Phi_{500NW10-5v}$] |
| 699-700 | 24-hr 500 mb U and V wind change diffeence between 10° northwest and 5° northwest of cyclone center [$\Delta\Phi_{500NW10-5u}$, $\Delta\Phi_{500NW10-5v}$] |
| 701-702 | 500 mb U and V wind components 10° north of cyclone center [$\Phi_{500N10u}$, $\Phi_{500N10v}$] |
| 703-704 | 24-hr 500 mb U and V wind change 10° north of cyclone center [$\Delta\Phi_{500N10u}$, $\Delta\Phi_{500N10v}$] |
| 705-706 | 500 mb U and V wind components 5° north of cyclone center [$\Phi_{500N5u}$, $\Phi_{500N5v}$] |

TABLE 4.2 (cont'd)

| | |
|---|---|
| 707-708 | 24-hr 500 mb U and V wind change 5° north of cyclone center [$\Delta\Phi_{500N5u}$, $\Delta\Phi_{500N5v}$] |
| 709-710 | 500 mb U and V wind difference between 10° north and 5° north of cyclone center [$\Phi_{500N10-5u}$, $\Phi_{500N10-5v}$] |
| 711-712 | 24-hr 500 mb U and V wind change difference between 10° north and 5° north of cyclone center [$\Delta\Phi_{500N10-5u}$, $\Delta\Phi_{500N10-5v}$] |
| 713-714 | 500 mb U and V wind components 15° northwest of cyclone center [$\Phi_{500NW15u}$, $\Phi_{500NW15v}$] |
| 715-716 | 24-hr 500 mb U and V wind change 15° northwest of cyclone center [$\Delta\Phi_{500NW15u}$, $\Delta\Phi_{500NW15v}$] |
| 717-718 | 500 mb U and V wind components 20° northwest of cyclone center [$\Phi_{500NW20u}$, $\Phi_{500NW20v}$] |
| 719-720 | 24-hr 500 mb U and V wind change 20° northwest of cyclone center [$\Delta\Phi_{500NW20u}$, $\Delta\Phi_{500NW20v}$] |
| 721-722 | 500 mb U and V wind components 15° north of cyclone center [$\Phi_{500N15u}$, $\Phi_{500N15v}$] |
| 723-724 | 24-hr 500 mb U and V wind change 15° north of cyclone center [$\Delta\Phi_{500N15u}$, $\Delta\Phi_{500N15v}$] |
| 725-726 | 500 mb U and V wind components 20° north of cyclone center [$\Phi_{500N20u}$, $\Phi_{500N20v}$] |
| 727-728 | 24-hr 500 mb U and V wind change 20° north of cyclone center [$\Delta\Phi_{500N20u}$, $\Delta\Phi_{500N20v}$] |

TABLE 4.3

The Potential Forecast Predictors For The South China Sea

| | |
|---|---|
| 1-170 | 24-hr 500 mb height changes at the 17 X 10 grid points [ΔH] |
| 171-340 | 500 mb heights at the 17 X 10 grid points [H] |
| 341-510 | 24-hr sea level pressure changes at the 17 X 10 grid points (mb) [ΔP] |
| 511-680 | Sea level pressures at the 17 X 10 grid points (mb) [P] |
| 681-850 | 24-hr 700 mb height changes at the 17 X 10 grid points [ΔH7] |
| 851-1020 | 700 mb heights at the 17 X 10 grid points [H7] |
| 1021-1190 | 24-hr 850 mb height changes at the 17 X 10 grid points [ΔH8] |
| 1191-1360 | 850 mb heights at the 17 X 10 grid points [H8] |
| 1361-1362 | Past 24-hr U and V cyclone motion (km/hr) [$U_{-24}$, $V_{-24}$] |
| 1363-1364 | Past 12-hr U and V cyclone motion (km/hr) [$U_{-12}$, $V_{-12}$] |

TABLE 4.4

Percent of variance reduction due to the three categories of predictors (see Fig. 3.7) for the Atlantic and the NW Pacific. Version $CSU84_{500}$ of the model uses 500 mb steering. Version $CSU84_{200}$ uses 200 mb steering.

| Atlantic | | U | | V | |
|---|---|---|---|---|---|
| | | $CSU84_{500}$ | $CSU84_{200}$ | $CSU84_{500}$ | $CSU84_{200}$ |
| North | Persistence | 17 | 63 | 11 | 11 |
| | Steering | 0 | 4 | 52 | 53 |
| | Synoptic | 65 | 16 | 15 | 16 |
| On | Persistence | 9 | 8 | 10 | 10 |
| | Steering | 49 | 53 | 63 | 59 |
| | Synoptic | 26 | 21 | 14 | 12 |
| South | Persistence | 12 | 52 | 46 | 44 |
| | Steering | 48 | 0 | 0 | 0 |
| | Synoptic | 13 | 18 | 23 | 26 |

| NW Pacific | | U | | V | |
|---|---|---|---|---|---|
| | | $CSU84_{500}$ | $CSU84_{200}$ | $CSU84_{500}$ | $CSU84_{200}$ |
| North | Persistence | 47 | 12 | 51 | 52 |
| | Steering | 0 | 49 | 2 | 1 |
| | Synoptic | 28 | 14 | 19 | 22 |
| On | Persistence | 19 | 14 | 36 | 46 |
| | Steering | 9 | 1 | 0 | 1 |
| | Synoptic | 35 | 52 | 35 | 27 |
| South | Persistence | 56 | 51 | 40 | 37 |
| | Steering | 0 | 0 | 0 | 0 |
| | Synoptic | 6 | 9 | 11 | 12 |

For the Atlantic, the variance reduction due to steering was overwhelming for the meridional motion (V) north of the ridge and for both components of motion on the ridge. For the NW Pacific, however, steering contributed little to the reduction of variance, with one exception. Nearly 50% of the variance of zonal motion was explained by 200 mb steering predictors north of the ridge.

A second surprise is the amount of variance reduction due to synoptic predictors as compared to persistence. With the exception of the south-of-ridge category, the synoptic predictors are responsible for as much, if not more, of the variance reduction as is persistence in both ocean basins. This certainly indicates the model's potential for predicting anomalous cyclone motion if an anomaly is present in the analysis or forecast fields.

4.4 Correlation Coefficient Fields

Figures 4.1 through 4.4 present the correlation coefficient fields between the 500 mb geopotential heights/sea level pressures and tropical cyclone motion in the Atlantic north of the ridge prior to the selection and removal of any predictors. Northward and eastward cyclone motions are positive. The correlation coefficient fields for the other two categories relative to the ridge are presented in Appendix B. Correlations between cyclone motion and the synoptic fields are stronger in the Atlantic basin than in any of the other basins.

For the south-of-ridge category the difference in the degree of correlation between the synoptic fields and cyclone motion for the Atlantic as compared to the Pacific is particularly striking. Again, the erratic motion of Pacific cyclones embedded in the monsoonal trough

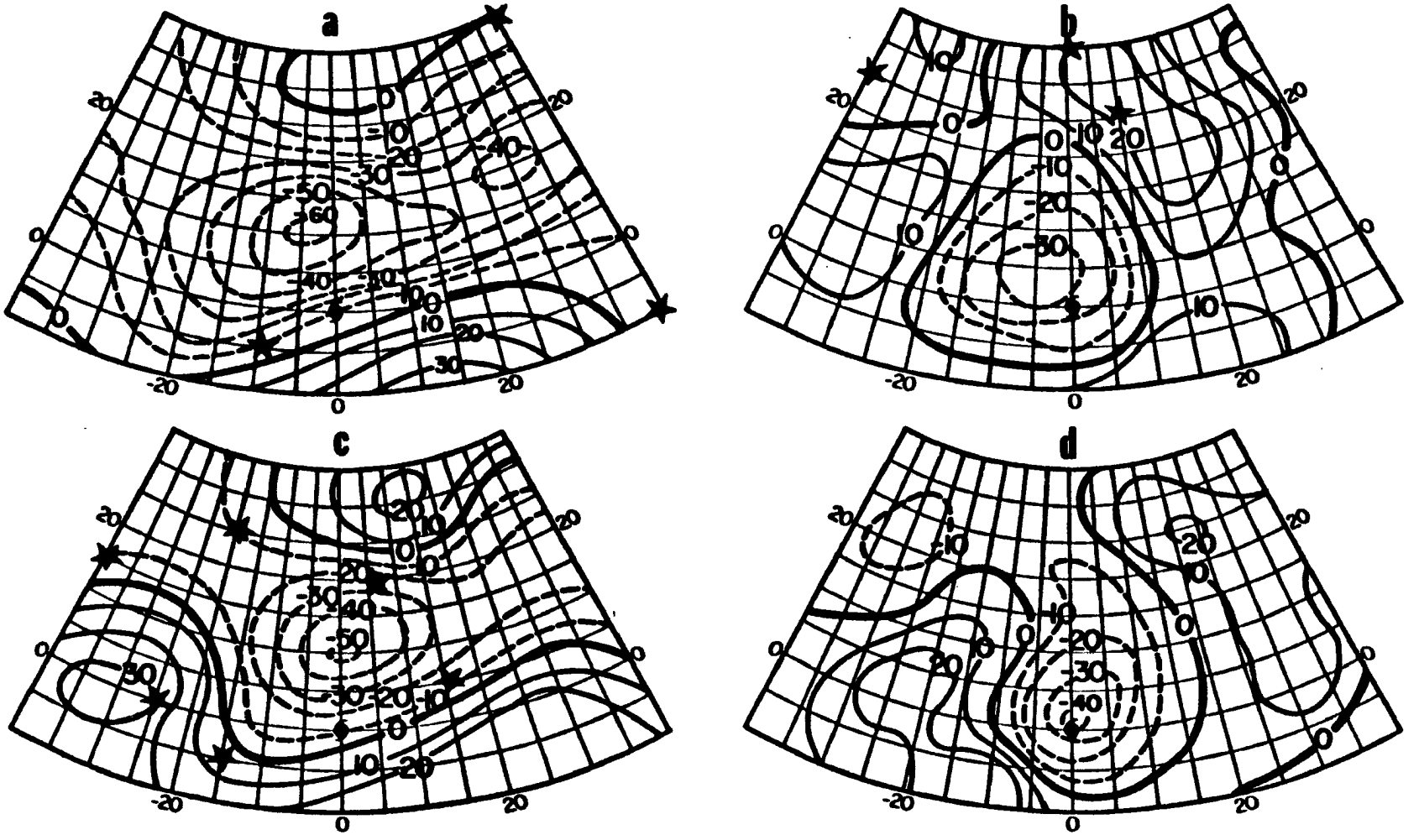


Fig. 4.1. Correlation coefficient fields (x .01) for the Atlantic north-of-ridge fast U motion. The four panels present the correlation between cyclone motion and (a) 500 mb height; (b) 24-hour change of the 500 mb height; (c) sea level pressure; and (d) 24-hour change of sea level pressure. Northward and eastward cyclone motions are positive. The position of the cyclone is denoted by (§) and the stars indicate the gridpoints at which predictors were selected.

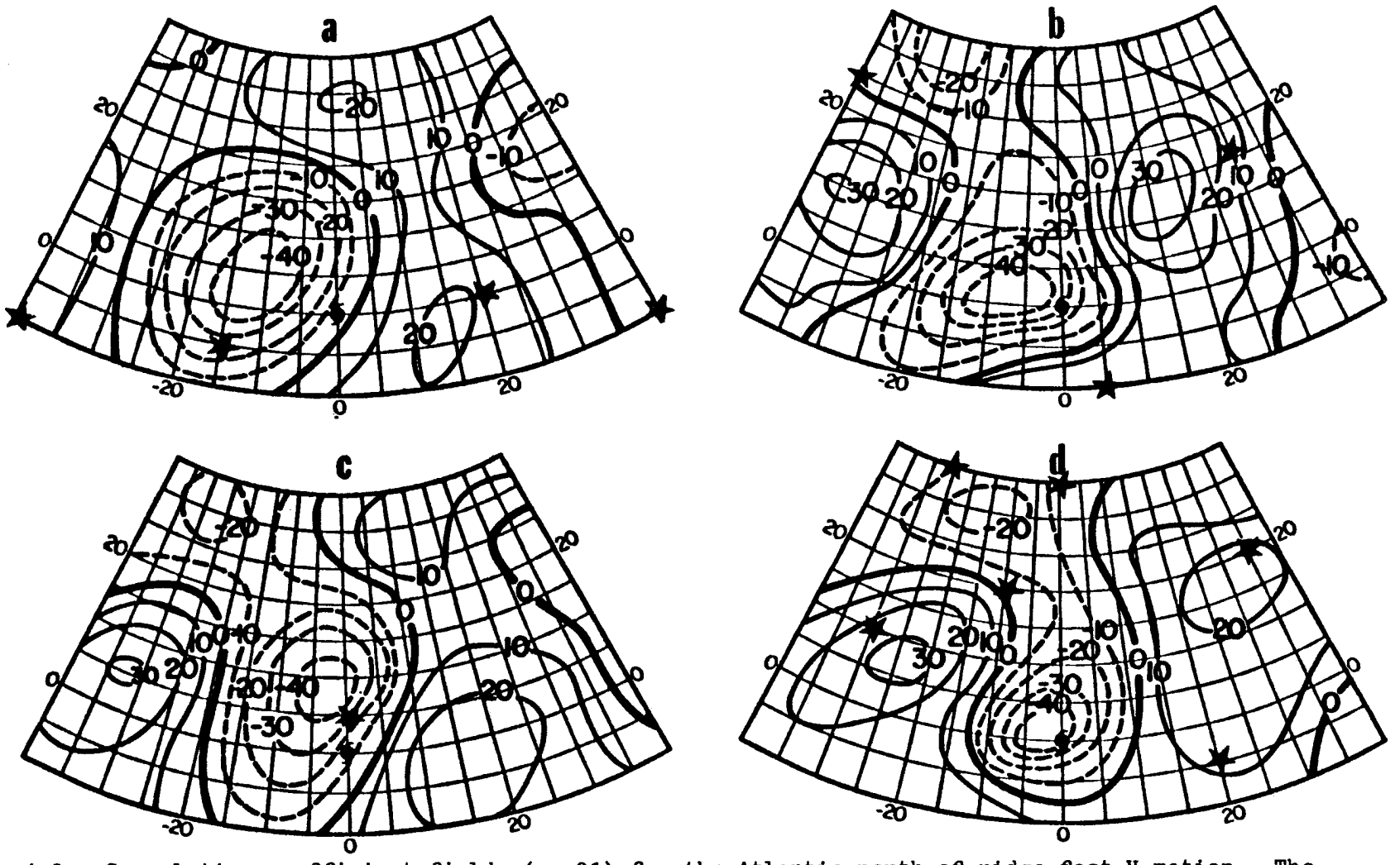


Fig. 4.2. Correlation coefficient fields (x .01) for the Atlantic north-of-ridge fast V motion. The four panels present the correlation between cyclone motion and (a) 500 mb height; (b) 24-hour change of the 500 mb height; (c) sea level pressure; and (d) 24-hour change of sea level pressure. Northward and eastward cyclone motions are positive. The position of the cyclone is denoted by ( ) and the stars indicate the gridpoints at which predictors were selected.

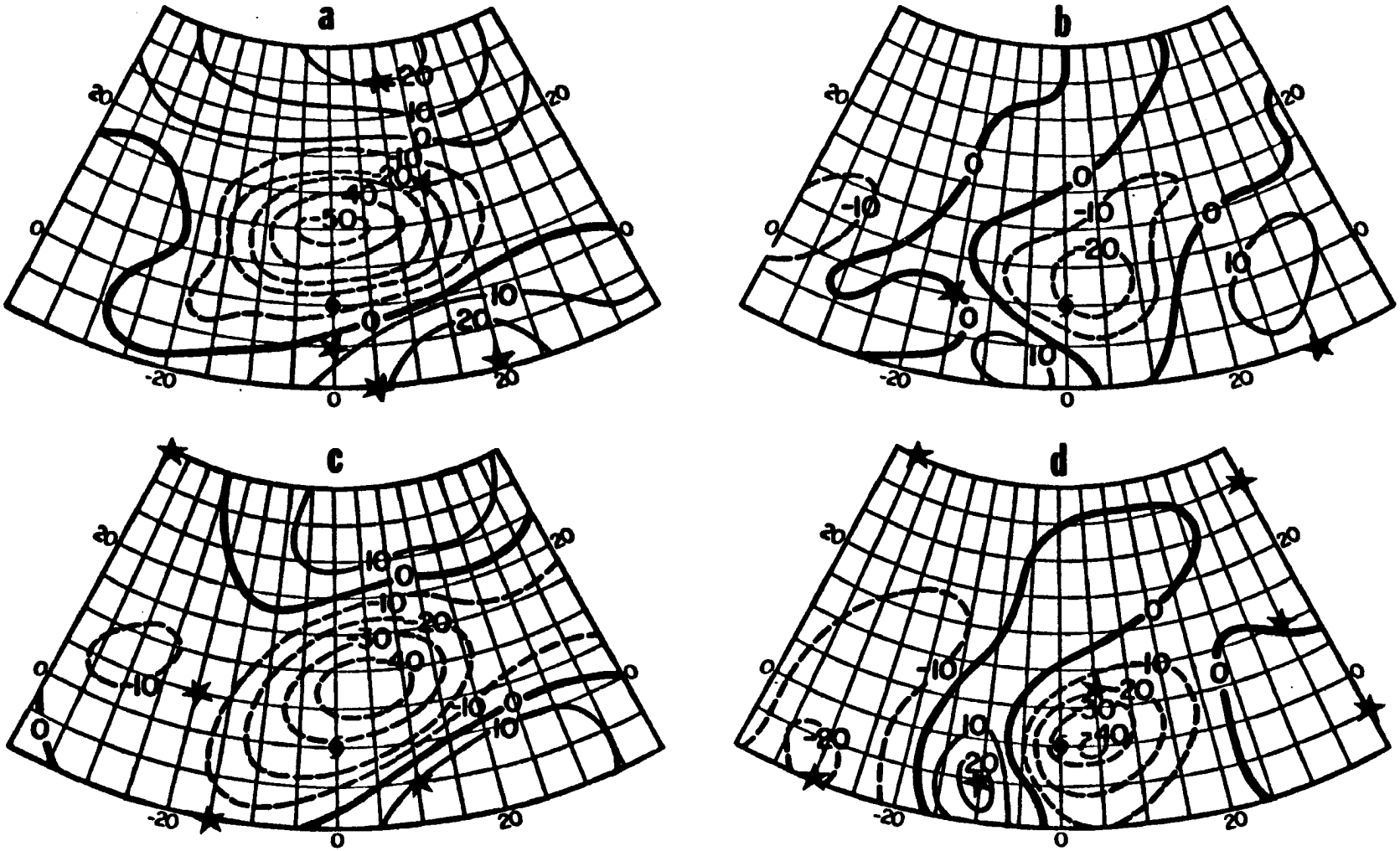


Fig. 4.3. Correlation coefficient fields (x .01) for the Atlantic north-of-ridge slow U motion. The four panels present the correlation between cyclone motion and (a) 500 mb height; (b) 24-hour change of the 500 mb height; (c) sea level pressure; and (d) 24-hour change of sea level pressure. Northward and eastward cyclone motions are positive. The position of the cyclone is denoted by (●) and the stars indicate the gridpoints at which predictors were selected.

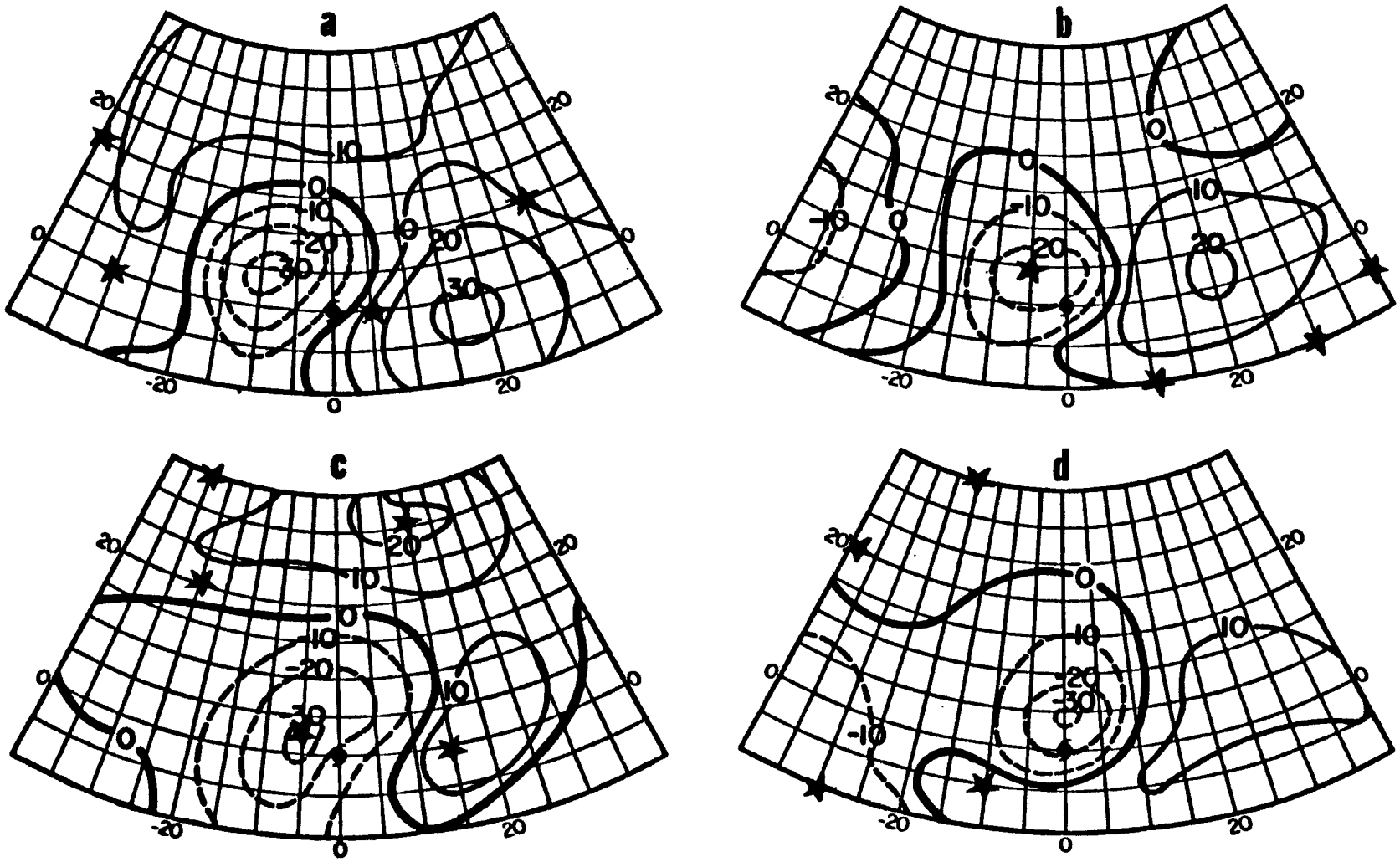


Fig. 4.4. Correlation coefficient fields (x .01) for the Atlantic north-of-ridge slow V motion. The four panels present the correlation between cyclone motion and (a) 500 mb height; (b) 24-hour change of the 500 mb height; (c) sea level pressure; and (d) 24-hour change of sea level pressure. Northward and eastward cyclone motions are positive. The position of the cyclone is denoted by (●) and the stars indicate the gridpoints at which predictors were selected.

appears to account for the poor correlation of cyclone motion with the synoptic fields in the Pacific, especially south of the ridge.

In general, for the south-of-ridge category, above normal heights and pressures to the north are associated with westward motion (Figs. B.5 and B.7, panels a and c), and above normal heights and pressures to the east are associated with northward motion (Figs. B.6 and B.8, panels a and c). The 24-hour change or tendency fields (panels b and d), although weaker, imply the same correlation.

For the north-of-ridge category, there is again nothing unexpected in the figures. Eastward motion is associated with falling heights and pressures to the north (Figs. 4.1 and 4.3) and northward motion is associated with falling heights and pressures to the north and west (Figs. 4.2 and 4.4). The correlations are more concentrated with stronger gradients of correlation than for the south-of-ridge categories.

The ability of the screening process to pick out the subtle differences in the longitudinal position of the trough between the fast and slow cases is encouraging. Note that the centers of maximum correlation indicate that for the slow cases, the trough has already passed the cyclone and is located east of the cyclone. Compare the centers of maximum correlation relative to the cyclone for the four panels between Fig. 4.1 and 4.3.

For the on-the-ridge, the correlation fields are slightly more complex. In general, falling heights and pressures to the north and rising heights and pressures to the south are associated with eastward motion (Figs. B.1 and B.3); falling heights and pressures to the

west and rising heights and pressures to the east are associated with northward motion (Figs. B.2 and B.4).

Figures 4.5 through 4.8 present the correlation coefficient fields between the 500 mb geopotential heights/sea level pressures and tropical cyclone motion in the NW Pacific north of the ridge prior to the selection and removal of any predictors. The correlation coefficient fields for the other two categories relative to the ridge are presented in Appendix C. The relatively weak correlation between the synoptic fields and cyclone motion south of the ridge (Figs. C.5 through C.8) is to be noted. Most of the variance reducing potential comes from the 12-hour past motion. Synoptic information reduces the variance by only an additional 10%. This explains why statistical techniques such as HPAC that use only climatology and persistence perform well in the low latitudes. The surprisingly weak correlation of cyclone motion to synoptic fields in the south-of-ridge category for the NW Pacific can be explained by the presence of the near-equatorial monsoon trough in this part of the globe. When cyclones develop within this trough zone, the cyclones tend to drift erratically due to the lack of significant steering flow until they drift poleward and are picked up by the westerlies.

In general, correlations between cyclone motion and synoptic features are similar to the Atlantic although there are differences. One of the most noticeable differences is the sea level pressure fields for the north-of-ridge category. Unlike the Atlantic, the strong correlation between low pressures to the north and eastward motion is not observed as seen in panel c on Figs. 4.5 and 4.7. Also note the weak correlation between low pressures to the northwest and northward

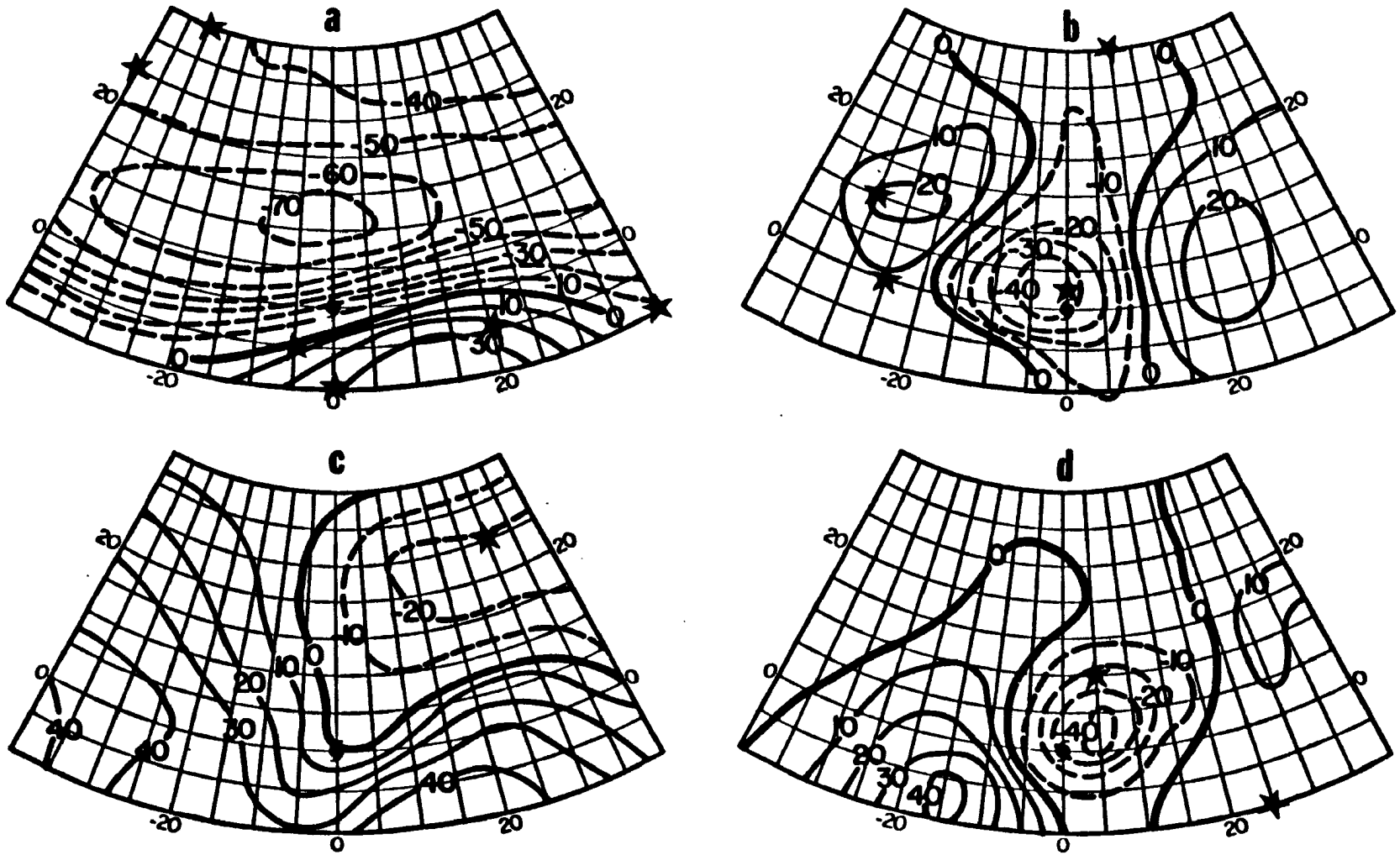


Fig. 4.5. Correlation coefficient fields (x .01) for the NW Pacific north-of-ridge fast U motion. The four panels present the correlation between cyclone motion and (a) 500 mb height; (b) 24-hour change of the 500 mb height; (c) sea level pressure; and (d) 24-hour change of sea level pressure. Northward and eastward cyclone motions are positive. The position of the cyclone is denoted by ( ) and the stars indicate the gridpoints at which predictors were selected.

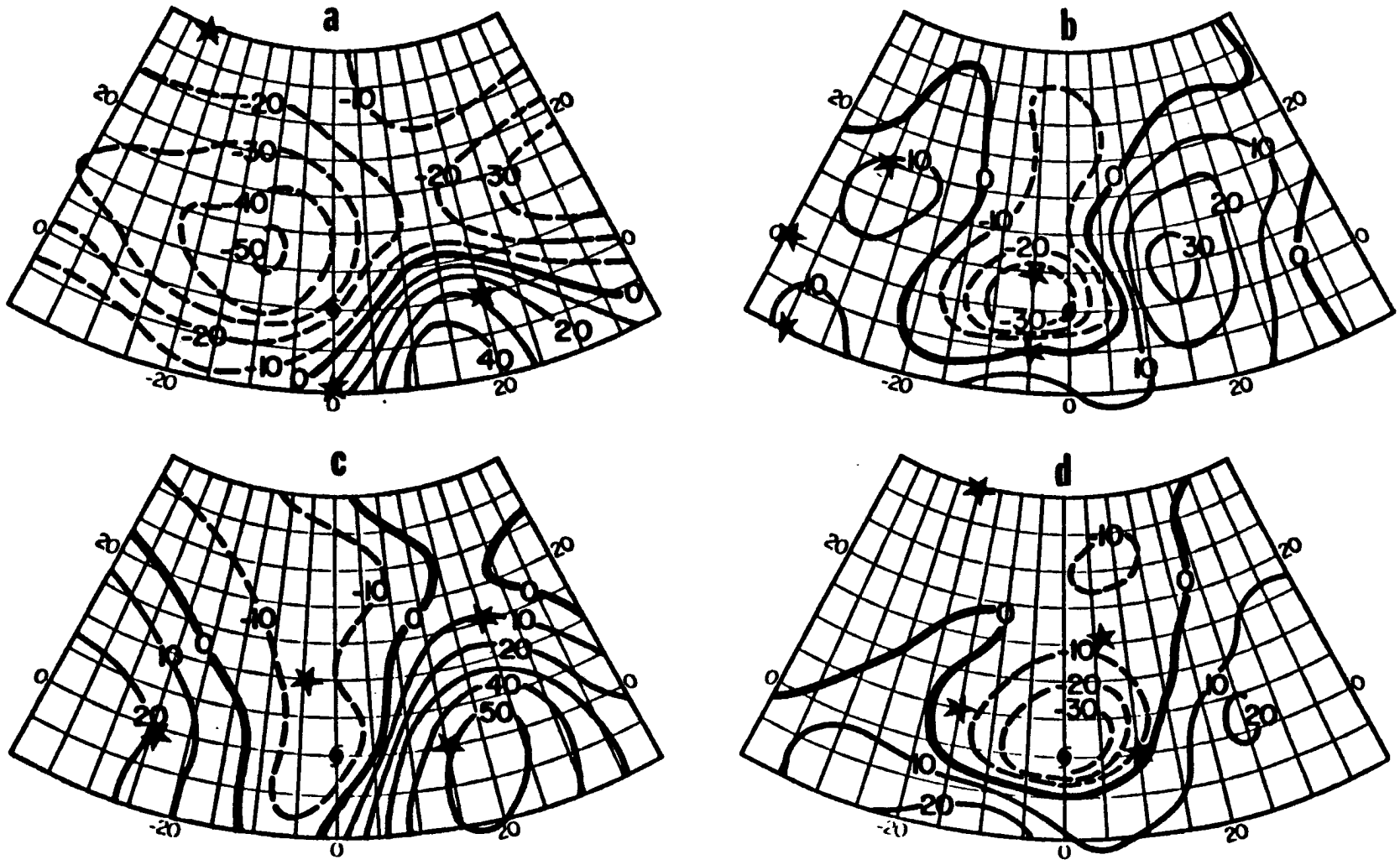


Fig. 4.6. Correlation coefficient fields (x .01) for the NW Pacific north-of-ridge fast V motion. The four panels present the correlation between cyclone motion and (a) 500 mb height; (b) 24-hour change of the 500 mb height; (c) sea level pressure; and (d) 24-hour change of sea level pressure. Northward and eastward cyclone motions are positive. The position of the cyclone is denoted by (§) and the stars indicate the gridpoints at which predictors were selected.

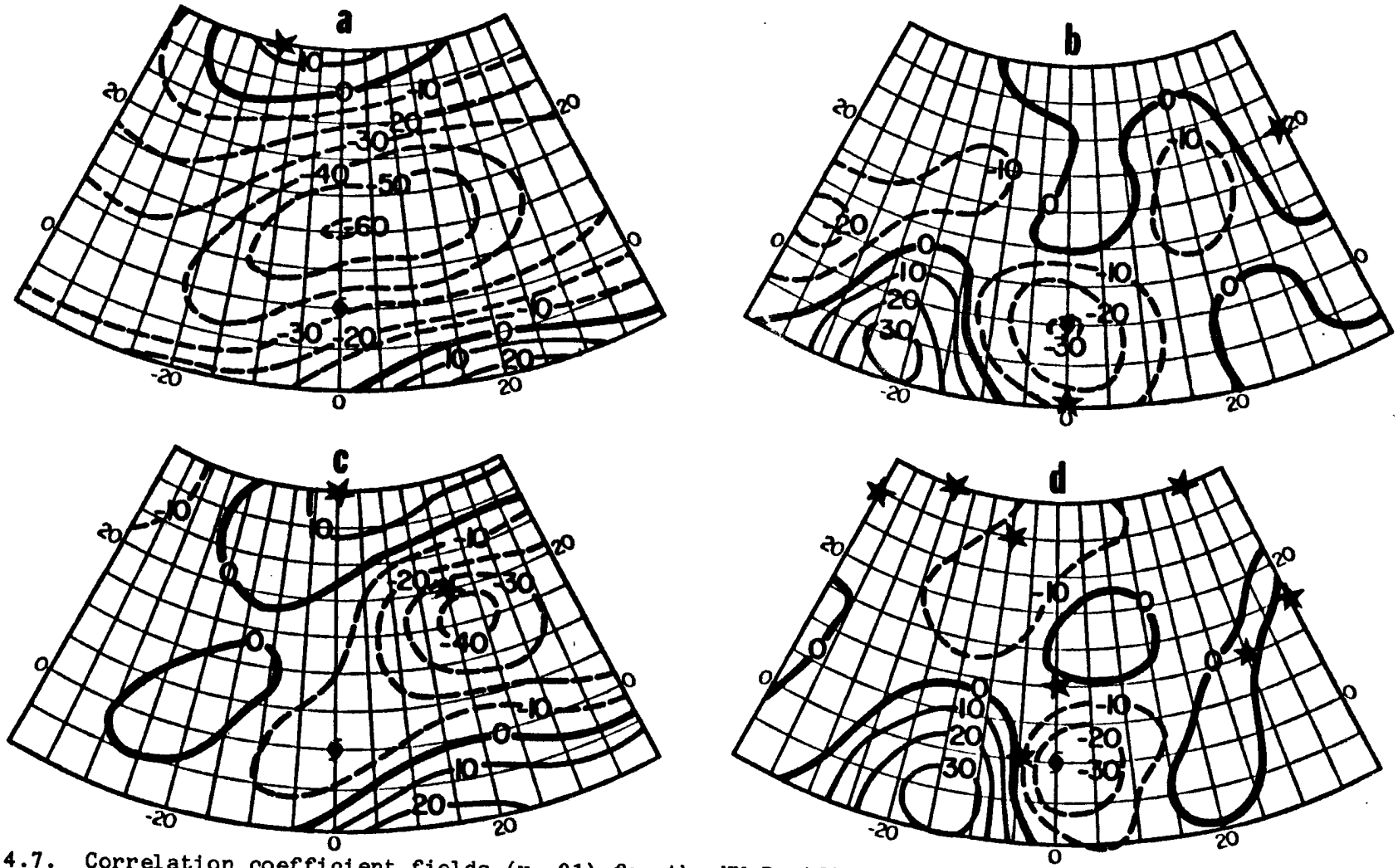


Fig. 4.7. Correlation coefficient fields (x .01) for the NW Pacific north-of-ridge slow U motion. The four panels present the correlation between cyclone motion and (a) 500 mb height; (b) 24-hour change of the 500 mb height; (c) sea level pressure; and (d) 24-hour change of sea level pressure. Northward and eastward cyclone motions are positive. The position of the cyclone is denoted by (ϕ) and the stars indicate the gridpoints at which predictors were selected.

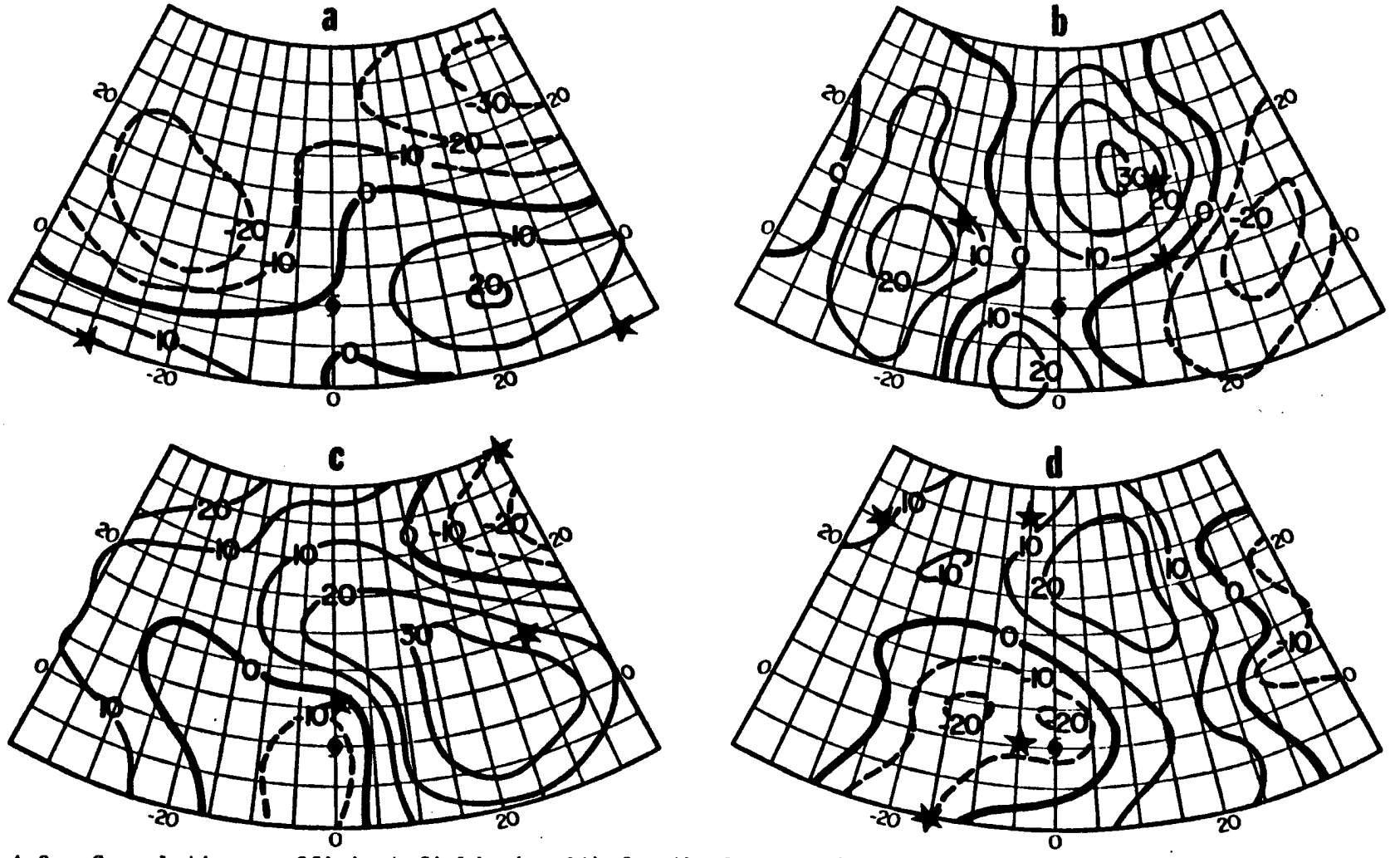


Fig. 4.8. Correlation coefficient fields (x .01) for the NW Pacific north-of-ridge slow V motion. The four panels present the correlation between cyclone motion and (a) 500 mb height; (b) 24-hour change of the 500 mb height; (c) sea level pressure; and (d) 24-hour change of sea level pressure. Northward and eastward cyclone motions are positive. The position of the cyclone is denoted by (●) and the stars indicate the gridpoints at which predictors were selected.

motion. Refer to panel c on Figs. 4.6 and 4.8. The strongest correlation occurs between the 500 mb heights and fast zonal motion for both north-of-ridge (Fig. 4.5 panel a) and on-the-ridge categories (Fig. C.1 panel a). Note that although the center of the strongest negative correlation $10^{o}$ north-northwest of the cyclone center was selected as one of the predictors for fast zonal motion for the on-the-ridge category (Fig. C.1 panel a), the center of the strongest negative correlation $10^{o}$ north of the cyclone center for the north-of-ridge category (Fig. 4.5 panel a) was not selected. The difference in the selection/non-selection is attributable to the order in which the predictors are selected. Recall that the correlation fields shown are the correlation prior to the selection and removal of any predictors. For the on-the-ridge category, the 500 mb height at the center of the strongest correlation was selected first while other predictors such as steering and 24-hour height change were selected first for the north-of-ridge category. When this occurred, the residual that remained tend to be poorly correlated with the original height field.

North Indian Ocean

Figures 4.9 and 4.10 present the fields of correlation between the 500 mb geopotential heights/sea level pressures and tropical cyclone motion in the North Indian Ocean north of the ridge. The correlation fields for the other two categories relative to the ridge are presented in Appendix D. Overall, correlation coefficients are much lower compared to the other ocean basins, particularly south of the subtropical ridge as depicted by Figs. D.3 and D.4. Neither the 500 mb heights nor sea level pressure correlates very strongly with cyclone motion south of the ridge. This tends to explain the rather poor

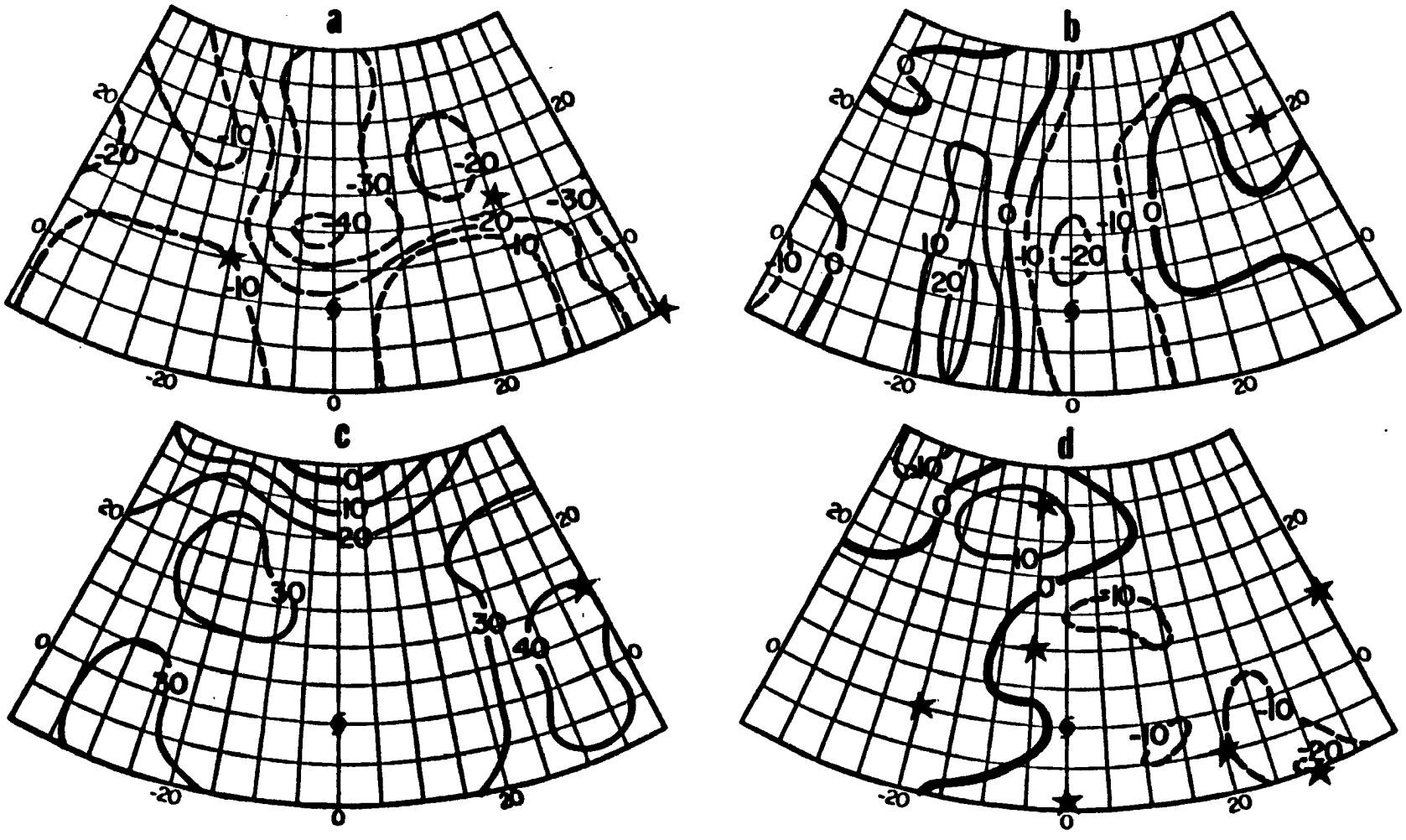


Fig. 4.9. Correlation coefficient fields (x .01) for the North Indian Ocean north-of-ridge U motion. The four panels present the correlation between cyclone motion and (a) 500 mb height; (b) 24-hour change of the 500 mb height; (c) sea level pressure; and (d) 24-hour change of sea level pressure. Northward and eastward cyclone motions are positive. The position of the cyclone is denoted by (●) and the stars indicate the gridpoints at which predictors were selected.

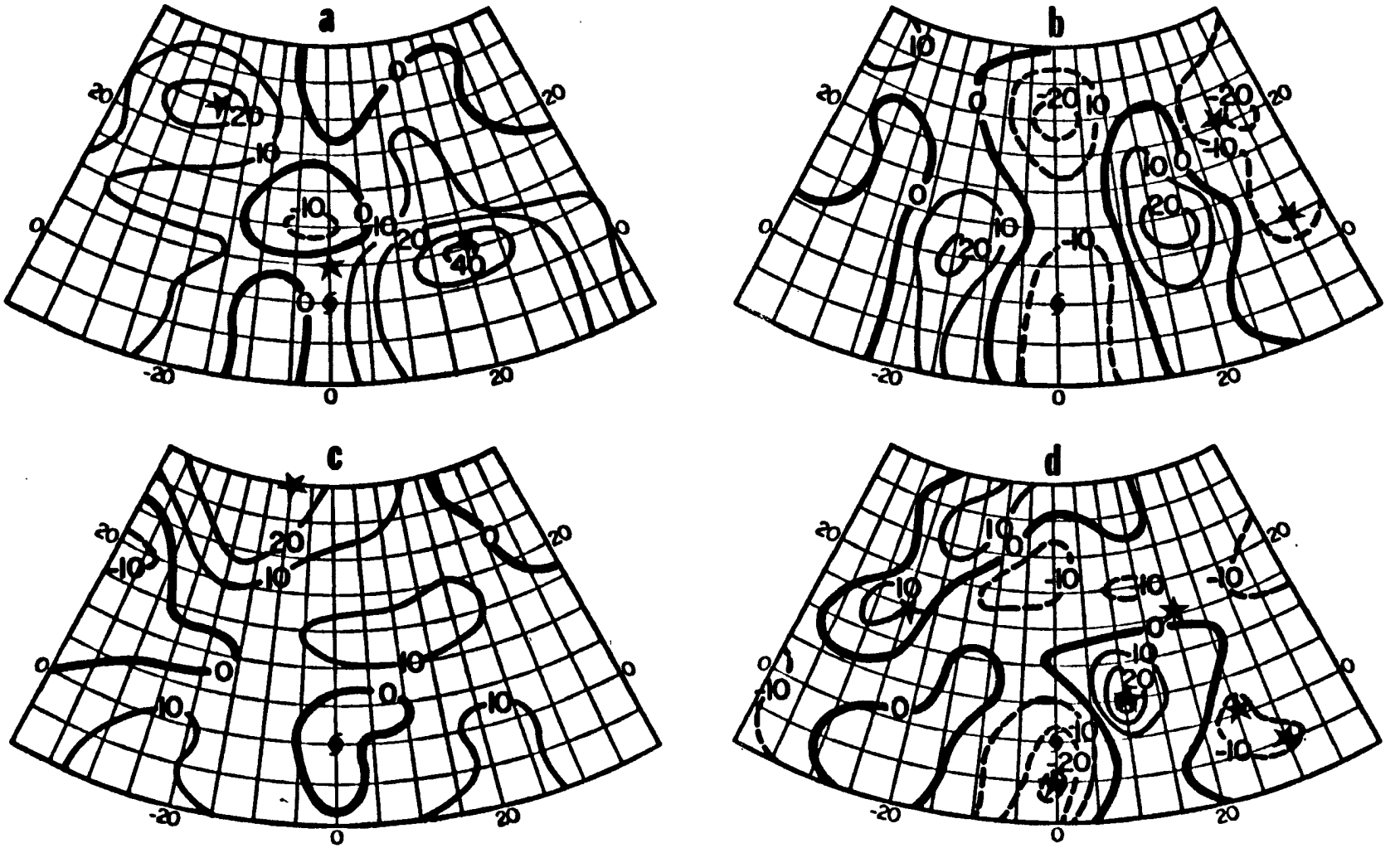


Fig. 4.10. Correlation coefficient fields (x .01) for the North Indian Ocean north-of-ridge V motion. The four panels present the correlation between cyclone motion and (a) 500 mb height; (b) 24-hour change of the 500 mb height; (c) sea level pressure; and (d) 24-hour change of sea level pressure. Northward and eastward cyclone motions are positive. The position of the cyclone is denoted by (§) and the stars indicate the gridpoints at which predictors were selected.

reduction in variance -- only 55% for zonal motion and 47% for meridional motion -- for this category of cyclones. Although the reduction in variance is relatively low, the forecast errors for the cyclones south of the ridge, as will be shown in the next chapter, are surprisingly small for both the dependent and independent set due to the small standard deviation. This is a result of the generally slow movement of these cyclone systems.

Strongest correlation for this ocean basin occurs between the 500 mb heights and zonal and meridional motion north of the ridge (panel a on Figs. 4.9 and 4.10). Again, the reason for the selection of the grid-point nearest the heights $20^{o}$ east-northeast of the cyclone center that exhibited the strongest positive correlation with meridional motion north of the ridge and the non-selection of the grid-point nearest the heights $10^{o}$ north of the cyclone center that exhibited strong negative correlation with zonal motion is due to the order of predictor selection.

In general, grid points near the centers of strongest positive or negative correlation were selected to provide height and pressure information to empirically predict 24-hour cyclone motion. Figure 4.10 shows a good example of the correlation field between 24-hour sea level pressure change and meridional motion north of the ridge. Refer to panel d on Fig. 4.10.

Table 4.5 illustrates the reduction of variance by the various predictors for the North Indian Ocean. Unlike the Atlantic and NW Pacific, steering does not contribute to cyclone motion except for a slight contribution to the zonal motion north of the ridge. Instead, it is the synoptic predictors, primarily the surface pressure tendencies,

TABLE 4.5

Percent of variance reduction by the various predictors for the North Indian Ocean. (X - persistence; H - 500 mb height; ΔH - 24-hour change of 500 mb height; P - surface pressure; ΔP - 24-hour change of surface pressure; S - steering at 500 mb).

| | U | | V | |
|---|---|---|---|---|
| North (237 cases) | X = 31<br>H = 5<br>ΔH = 4<br>P = 6<br>ΔP = 14<br>S = 14 | 42 | X = 18<br>H = 17<br>ΔH = 7<br>P = 4<br>ΔP = 28<br>S = 0 | 56 |
| On (188 cases) | X = 29<br>H = 5<br>ΔH = 6<br>P = 14<br>ΔP = 21<br>S = 5 | 46 | X = 32<br>H = 0<br>ΔH = 9<br>P = 0<br>ΔP = 18<br>S = 6 | 27 |
| South (188 cases) | X = 41<br>H = 7<br>ΔH = 2<br>P = 1<br>ΔP = 5<br>S = 1 | 15 | X = 33<br>H = 5<br>ΔH = 1<br>P = 3<br>ΔP = 4<br>S = 1 | 13 |

that play a significant role. With the exception of the south-of-ridge category, they are dominant. Such a large difference from the NW Pacific explains why an attempt to use regression equations developed for NW Pacific cyclones failed when used for North Indian Ocean cyclones.

The screening process was terminated when a selected predictor contributed less than 1 percent to the reduction in the variance or when a maximum number of 20 predictors had been selected. As will be explained in Chapter 5, speed stratification failed to enhance the predictive skill of the model. As a result, the regression equations presented in this chapter apply to the model versions with no speed stratification. Tables 4.6 through 4.8 list the selected predictors,

the associated coefficients and the reduction of variance for the three stratified categories in the Atlantic. Similar information for the NW Pacific is presented in Tables 4.9 through 4.11. Tables 4.12 through 4.14 apply to the North Indian Ocean and Table 4.15 to the South China Sea.

Note that for all of the ocean basins, the majority of the selected synoptic predictors are located at grid points $15^{\circ}$ or greater from the cyclone center. Many of them are located on the edge of the grid $40^{\circ}$ from the cyclone. It was gratifying to observe that the large-scale circulation features were being incorporated into the model without explicitly forcing out of the regression any grid points near the cyclone.

Further, many and sometimes more, 24-hour past changes of the 500 mb heights and sea level pressure were selected compared to the current heights or pressures. Apparently, by not using prognostic data prior to its valid time, the tendencies of heights and pressures were critical in determining how the current fields would evolve over the next 24 hours.

TABLE 4.6

Predictors, coefficients and reduction of variance for 24-hr U and V motion north-of-ridge for the Atlantic

| | U | | | | V | | | |
|---|---|---|---|---|---|---|---|---|
| | With 200 mb steering | | With 500 mb steering | | With 200 mb steering | | With 500 mb steering | |
| $C_0$ | -6405.097 | | 546.603 | | -3159.411 | | 2463.241 | |
| $C_1$ | .583 | $U_{-12}$ | -.457 | $H_{10,-5}$ | .377 | $\Phi_{500v}$ | .434 | $\Phi_{500v}$ |
| $C_2$ | -4.999 | $P_{10,0}$ | .662 | $U_{-12}$ | .304 | $V_{-12}$ | .365 | $V_{-12}$ |
| $C_3$ | .220 | $\Phi_{200NW5u}$ | .557 | $H_{-10,15}$ | -.170 | $\Delta\Phi_{200N5u}$ | .532 | $H_{-5,-40}$ |
| $C_4$ | 3.103 | $P_{10,-30}$ | -.352 | $\Delta H_{5,-5}$ | -7.026 | $P_{5,0}$ | -.195 | $\Delta\Phi_{500N5u}$ |
| $C_5$ | .133 | $V_{-24}$ | -2.840 | $P_{10,-5}$ | .460 | $H_{-5,-35}$ | -5.107 | $P_{5,0}$ |
| $C_6$ | 2.821 | $\Delta P_{35,-30}$ | .519 | $\Delta H_{-5,-5}$ | -.112 | $\Phi_{200NW10-5u}$ | -.310 | $\Delta H_{-5,-15}$ |
| $C_7$ | .583 | $H_{-10,15}$ | -1.178 | $\Delta P_{30,40}$ | 1.661 | $\Delta P_{20,30}$ | 1.314 | $\Delta P_{20,25}$ |
| $C_8$ | 1.731 | $P_{30,0}$ | 1.313 | $\Delta P_{30,10}$ | 2.433 | $P_{0,15}$ | .578 | $H_{0,15}$ |
| $C_9$ | -.485 | $\Delta P_{5,-5}$ | .707 | $H_{0,-5}$ | 2.693 | $P_{10,-30}$ | 1.999 | $\Delta P_{15,-30}$ |
| $C_{10}$ | -2.112 | $H_{30,40}$ | 7.014 | $\Delta P_{-10,35}$ | -.237 | $\Delta H_{0,-35}$ | -.130 | $\Phi_{500NW10-5u}$ |
| $C_{11}$ | 8.311 | $\Delta P_{-10,35}$ | -1.491 | $\Delta P_{10,35}$ | .417 | $H_{0,15}$ | -.562 | $H_{-10,5}$ |
| $C_{12}$ | -2.144 | $\Delta P_{5,5}$ | -1.632 | $\Delta P_{20,-35}$ | 2.044 | $\Delta P_{10,15}$ | -.166 | $\Delta H_{10,-15}$ |
| $C_{13}$ | .169 | $\Delta H_{10,10}$ | -.561 | $\Delta H_{0,0}$ | -.464 | $\Delta H_{-5,-15}$ | 6.886 | $\Delta P_{-5,-10}$ |
| $C_{14}$ | -3.821 | $\Delta P_{0,20}$ | -.741 | $H_{-10,-10}$ | 5.705 | $\Delta P_{-5,-10}$ | -.080 | $H_{35,-35}$ |
| $C_{15}$ | 2.712 | $P_{0,30}$ | .215 | $\Delta H_{10,15}$ | .097 | $\Delta H_{30,10}$ | -.220 | $\Delta H_{-5,-40}$ |
| $C_{16}$ | .072 | $H_{30,40}$ | 1.971 | $P_{25,-10}$ | -.348 | $\Delta H_{5,-10}$ | -.324 | $\Delta H_{5,0}$ |
| $C_{17}$ | 1.475 | $\Delta P_{25,30}$ | 1.161 | $\Delta P_{35,-30}$ | 3.762 | $\Delta P_{-5,20}$ | .063 | $\Delta\Phi_{500N10v}$ |
| $C_{18}$ | -.117 | $\Delta H_{10,-20}$ | -.074 | $\Phi_{500N20u}$ | -5.302 | $\Delta P_{-10,0}$ | -5.227 | $\Delta P_{-10,0}$ |
| $C_{19}$ | -1.212 | $\Delta P_{25,-30}$ | | | .296 | $\Delta H_{-5,-5}$ | 2.875 | $\Delta P_{0,10}$ |
| $C_{20}$ | 1.629 | $\Delta P_{5,-40}$ | | | -.146 | $\Delta H_{0,40}$ | | |
| Reduction of variance | 84% | | 83% | | 80% | | 78% | |

TABLE 4.7

Predictors, coefficients and reduction of variance for 24-hr U and V motion on-the-ridge for the Atlantic

| U | | | | V | | | |
|---|---|---|---|---|---|---|---|
| With 200 mb steering | | With 500 mb steering | | With 200 mb steering | | With 500 mb steering | |
| $C_0$ | -17982.797 | | -9051.025 | | -5549.292 | | -5865.584 |
| $C_1$ | .308 | $\Phi_{500u}$ | .301 | $\Phi_{500u}$ | .359 | $\Phi_{500v}$ | .443 | $\Phi_{500v}$ |
| $C_2$ | .536 | $H_{0,5}$ | .188 | $V_{-12}$ | .454 | $V_{-12}$ | .369 | $V_{-12}$ |
| $C_3$ | .508 | $U_{-12}$ | .230 | $H_{5,-35}$ | .178 | $\Delta\Phi_{200v}$ | .224 | $\Delta\Phi_{500N5v}$ |
| $C_4$ | -.055 | $\Delta\Phi_{200NW20v}$ | -.186 | $H_{20,-10}$ | 4.351 | $\Delta P_{0,40}$ | 10.424 | $\Delta P_{-10,40}$ |
| $C_5$ | -.938 | $\Delta H_{-10,-20}$ | -1.206 | $\Delta P_{35,-35}$ | -2.210 | $\Delta P_{5,-20}$ | -2.399 | $\Delta P_{10,-20}$ |
| $C_6$ | 9.708 | $P_{-5,25}$ | 4.779 | $P_{0,40}$ | .955 | $H_{-10,-25}$ | .787 | $H_{0,-20}$ |
| $C_7$ | .958 | $\Delta P_{30,30}$ | -1.371 | $\Delta H_{-10,-25}$ | 2.535 | $\Delta P_{15,15}$ | -2.228 | $\Delta P_{30,-20}$ |
| $C_8$ | .249 | $H_{15,-40}$ | .360 | $U_{-12}$ | -.087 | $\Delta P_{15,15}$ | .285 | $\Delta H_{20,10}$ |
| $C_9$ | .087 | $\Phi_{200NW15u}$ | .319 | $H_{0,0}$ | -.240 | $U_{-24}$ | -.235 | $U_{-24}$ |
| $C_{10}$ | 2.444 | $P_{35,-10}$ | 1.980 | $P_{30,-35}$ | -.437 | $\Delta H_{-10,10}$ | 2.479 | $\Delta P_{20,40}$ |
| $C_{11}$ | -.154 | $\Delta H_{15,-35}$ | .128 | $\Delta H_{30,20}$ | 2.460 | $\Delta P_{20,40}$ | -.714 | $\Delta H_{0,-25}$ |
| $C_{12}$ | 2.661 | $\Delta P_{20,5}$ | -2.361 | $\Delta P_{15,-20}$ | .126 | $\Delta H_{30,-40}$ | .153 | $\Delta H_{30,-40}$ |
| $C_{13}$ | 3.834 | $P_{0,-35}$ | .794 | $\Delta H_{5,-25}$ | -1.430 | $\Delta P_{35,-20}$ | -.099 | $\Phi_{500NW20v}$ |
| $C_{14}$ | -2.787 | $P_{10,25}$ | -8.626 | $\Delta P_{-10,-10}$ | -.035 | $\Phi_{200NW20v}$ | -.207 | $\Delta H_{10,35}$ |
| $C_{15}$ | .149 | $\Delta H_{20,20}$ | 5.877 | $\Delta P_{-5,-15}$ | -.515 | $\Delta H_{0,-30}$ | 3.476 | $P_{0,35}$ |
| $C_{16}$ | -3.878 | $\Delta P_{5,20}$ | -.202 | $\Delta H_{5,40}$ | -.372 | $\Delta H_{-10,-10}$ | -.378 | $\Delta H_{0,5}$ |
| $C_{17}$ | -1.689 | $\Delta P_{15,-25}$ | -6.993 | $\Delta P_{5,20}$ | .063 | $\Phi_{200N10-5v}$ | -2.209 | $P_{10,0}$ |
| $C_{18}$ | .096 | $\Delta H_{30,-40}$ | .239 | $\Delta H_{10,20}$ | .261 | $\Delta H_{0,-40}$ | 6.095 | $\Delta P_{-10,20}$ |
| $C_{19}$ | -2.834 | $\Delta P_{10,0}$ | -.067 | $\Delta H_{20,-15}$ | -.045 | $\Phi_{200N10-5u}$ | | |
| $C_{20}$ | 5.173 | $\Delta P_{-5,-15}$ | | | | | | |
| Reduction of variance | 83% | | 84% | | 88% | | 88% | |

TABLE 4.8

Predictors, coefficients and reduction of variance for 24-hr U and V motion south-of-ridge for the Atlantic

| | U | | | | V | | | |
|---|---|---|---|---|---|---|---|---|
| | With 200 mb steering | | With 500 mb steering | | With 200 mb steering | | With 500 mb steering | |
| $C_0$ | 12.750 | | -1090.111 | | -9080.922 | | -3143.237 | |
| $C_1$ | .321 | $U_{-12}$ | .209 | $\Phi_{500u}$ | .469 | $V_{-12}$ | .550 | $V_{-12}$ |
| $C_2$ | -.465 | $H_{15,-5}$ | .341 | $U_{-12}$ | .211 | $H_{15,5}$ | -.570 | $\Delta H_{5,-15}$ |
| $C_3$ | -.376 | $\Delta H_{10,5}$ | -4.807 | $\Delta P_{5,10}$ | -.407 | $\Delta H_{5,-20}$ | .207 | $H_{15,5}$ |
| $C_4$ | 2.603 | $P_{15,-40}$ | .885 | $\Delta P_{35,40}$ | .245 | $H_{-5,30}$ | 9.816 | $\Delta P_{5,15}$ |
| $C_5$ | -2.147 | $\Delta P_{25,30}$ | 2.342 | $P_{10,-35}$ | -1.149 | $\Delta P_{30,-15}$ | .786 | $H_{-10,30}$ |
| $C_6$ | .635 | $P_{35,30}$ | -1.819 | $\Delta P_{25,30}$ | 10.404 | $\Delta P_{5,15}$ | -1.235 | $\Delta P_{30,-15}$ |
| $C_7$ | -.124 | $H_{25,-20}$ | 1.197 | $P_{35,-35}$ | -1.112 | $\Delta P_{-10,10}$ | -9.642 | $\Delta P_{-10,10}$ |
| $C_8$ | .178 | $H_{10,-35}$ | -.430 | $H_{15,-10}$ | -6.875 | $\Delta P_{5,-5}$ | -7.640 | $\Delta P_{5,-5}$ |
| $C_9$ | -.264 | $H_{5,20}$ | -.480 | $\Delta H_{10,5}$ | 2.995 | $P_{15,0}$ | 1.541 | $\Delta P_{20,40}$ |
| $C_{10}$ | .674 | $\Delta H_{-5,10}$ | .144 | $\Delta H_{30,-35}$ | 1.700 | $\Delta P_{20,40}$ | -.701 | $H_{0,-5}$ |
| $C_{11}$ | .717 | $P_{35,-30}$ | -3.586 | $\Delta P_{-5,0}$ | -1.197 | $P_{25,-10}$ | -.252 | $\Delta H_{0,30}$ |
| $C_{12}$ | 2.583 | $P_{15,20}$ | 1.160 | $P_{30,25}$ | -3.636 | $\Delta P_{0,-40}$ | 4.315 | $\Delta P_{0,-25}$ |
| $C_{13}$ | -.476 | $H_{10,5}$ | .253 | $H_{10,-30}$ | 5.374 | $\Delta P_{0,-25}$ | -.080 | $U_{-12}$ |
| $C_{14}$ | -5.704 | $\Delta P_{5,10}$ | -.095 | $H_{25,-40}$ | -.742 | $H_{0,-5}$ | -.660 | $\Delta H_{-5,-35}$ |
| $C_{15}$ | .827 | $H_{35,40}$ | -.666 | $H_{-10,-20}$ | .932 | $H_{-10,10}$ | 2.436 | $P_{15,0}$ |
| $C_{16}$ | | | 6.046 | $\Delta P_{0,-25}$ | .163 | $H_{15,-35}$ | -1.002 | $P_{25,-10}$ |
| $C_{17}$ | | | -.338 | $\Delta H_{10,-25}$ | -1.963 | $P_{15,-25}$ | 6.834 | $\Delta P_{-10,-5}$ |
| $C_{18}$ | | | -.112 | $V_{-12}$ | 3.443 | $P_{0,5}$ | .180 | $\Delta H_{10,-35}$ |
| $C_{19}$ | | | 1.711 | $P_{10,-5}$ | 1.040 | $P_{25,-40}$ | | |
| $C_{20}$ | | | .354 | $\Delta H_{-5,10}$ | -.082 | $\Delta H_{20,-40}$ | | |
| Reduction of variance | 72% | | 73% | | 70% | | 69% | |

TABLE 4.9

Predictors, coefficients and reduction of variance for 24-hr U and V motion north-of-ridge for the NW Pacific.

| | U | | | | V | | | |
|---|---|---|---|---|---|---|---|---|
| | With 200 mb steering | | With 500 mb steering | | With 200 mb steering | | With 500 mb steering | |
| $C_0$ | 2567.649 | | 11215.979 | | -3371.009 | | 108.378 | |
| $C_1$ | .191 | $\Phi_{500u}$ | .430 | $U_{-12}$ | .599 | $V_{-12}$ | 4.427 | $\Delta P_{-5,-35}$ |
| $C_2$ | .484 | $U_{-12}$ | -.345 | $H_{15,0}$ | 2.781 | $P_{15,25}$ | .552 | $V_{-12}$ |
| $C_3$ | -3.952 | $\Delta P_{10,5}$ | .205 | $V_{-12}$ | -.407 | $H_{10,-5}$ | 1.776 | $P_{15,30}$ |
| $C_4$ | .847 | $H_{-5,15}$ | -4.643 | $P_{0,40}$ | .553 | $H_{0,35}$ | -8.952 | $P_{5,0}$ |
| $C_5$ | -5.038 | $P_{0,40}$ | .496 | $\Delta H_{10,-30}$ | -4.198 | $P_{10,-5}$ | 8.643 | $P_{0,15}$ |
| $C_6$ | .448 | $\Delta H_{10,-30}$ | .698 | $H_{-5,10}$ | -.289 | $\Delta H_{20,-15}$ | .118 | $\Delta\Phi_{500v}$ |
| $C_7$ | -.548 | $H_{-10,-30}$ | -2.940 | $\Delta P_{25,-40}$ | -.479 | $\Delta H_{5,-10}$ | .400 | $H_{0,30}$ |
| $C_8$ | -.111 | $\Phi_{200NW20v}$ | -5.845 | $\Delta P_{5,5}$ | 4.766 | $\Delta P_{0,10}$ | -.527 | $H_{5,-5}$ |
| $C_9$ | .224 | $V_{-12}$ | -.145 | $\Delta H_{25,20}$ | -.532 | $H_{-10,0}$ | 5.029 | $P_{-10,40}$ |
| $C_{10}$ | 9.023 | $\Delta P_{-10,25}$ | 4.377 | $\Delta P_{0,15}$ | 10.393 | $P_{-5,20}$ | -1.584 | $\Delta P_{25,-20}$ |
| $C_{11}$ | -2.589 | $\Delta P_{25,-40}$ | -.353 | $H_{-10,-30}$ | -4.958 | $P_{-5,40}$ | .072 | $\Phi_{500N20v}$ |
| $C_{12}$ | -.088 | $\Delta\Phi_{200NW15u}$ | .368 | $H_{0,35}$ | .106 | $\Delta\Phi_{200N15u}$ | .364 | $\Delta H_{5,-25}$ |
| $C_{13}$ | -1.899 | $P_{25,40}$ | -.300 | $H_{10,15}$ | -1.639 | $\Delta P_{20,35}$ | -4.057 | $\Delta P_{5,-15}$ |
| $C_{14}$ | -.198 | $\Phi_{500v}$ | -.757 | $H_{-10,40}$ | -.031 | $\Phi_{200NW10-5u}$ | -.437 | $\Delta H_{0,30}$ |
| $C_{15}$ | 2.770 | $P_{15,-40}$ | 2.004 | $\Delta P_{35,-35}$ | 1.911 | $\Delta P_{25,0}$ | .174 | $\Delta H_{10,40}$ |
| $C_{16}$ | .230 | $\Delta H_{35,-5}$ | -1.495 | $\Delta P_{10,5}$ | -4.530 | $\Delta P_{0,30}$ | .692 | $\Delta H_{-10,35}$ |
| $C_{17}$ | -.068 | $\Phi_{200N20u}$ | -.929 | $P_{25,40}$ | .155 | $\Delta H_{15,40}$ | 5.807 | $\Delta P_{-10,20}$ |
| $C_{18}$ | .222 | $\Delta H_{15,40}$ | .105 | $\Delta H_{15,40}$ | 1.426 | $\Delta P_{30,-40}$ | 4.216 | $P_{-5,0}$ |
| $C_{19}$ | -4.979 | $\Delta P_{0,40}$ | -2.804 | $\Delta P_{10,0}$ | 1.568 | $P_{25,15}$ | -1.535 | $\Delta P_{15,35}$ |
| $C_{20}$ | | | -.072 | $\Phi_{500NW10-5u}$ | -.137 | $\Delta H_{30,-35}$ | .081 | $\Delta\Phi_{500N10-5u}$ |
| Reduction of variance | 76% | | 75% | | 75% | | 73% | |

TABLE 4.10

Predictors, coefficients and reduction of variance for 24-hr U and V motion on-the-ridge for the NW Pacific

| | U | | | | V | | | |
|---|---|---|---|---|---|---|---|---|
| | With 200 mb steering | | With 500 mb steering | | With 200 mb steering | | With 500 mb steering | |
| $C_0$ | -7662.345 | | -3312.594 | | -4706.509 | | -4613.508 | |
| $C_1$ | -.464 | $H_{10,-5}$ | -.597 | $H_{5,-5}$ | .533 | $V_{-12}$ | -.055 | $H_{20,40}$ |
| $C_2$ | .302 | $U_{-12}$ | .319 | $U_{-12}$ | -.897 | $H_{5,-10}$ | .534 | $V_{-12}$ |
| $C_3$ | 4.497 | $P_{-10,0}$ | .198 | $\Phi_{500NW5u}$ | 3.999 | $P_{0,40}$ | -1.025 | $H_{5,-10}$ |
| $C_4$ | -.261 | $H_{10,15}$ | -.130 | $H_{15,25}$ | -8.257 | $\Delta P_{-10,-10}$ | 5.968 | $P_{0,40}$ |
| $C_5$ | -.628 | $\Delta H_{5,-10}$ | -.669 | $\Delta H_{5,-10}$ | 3.491 | $P_{-10,0}$ | -7.715 | $\Delta P_{-10,-10}$ |
| $C_6$ | 1.530 | $\Delta P_{25,-35}$ | .191 | $V_{-24}$ | -1.430 | $\Delta P_{20,-5}$ | -.191 | $\Delta H_{20,-15}$ |
| $C_7$ | 3.031 | $P_{-5,25}$ | 6.560 | $\Delta P_{-10,-30}$ | -.215 | $\Delta H_{15,-25}$ | 3.423 | $P_{-10,-40}$ |
| $C_8$ | 8.773 | $\Delta P_{-10,-30}$ | .401 | $H_{0,40}$ | 4.691 | $\Delta P_{5,15}$ | .092 | $H_{30,15}$ |
| $C_9$ | .349 | $H_{0,40}$ | 5.444 | $P_{-10,-5}$ | -3.971 | $P_{5,-5}$ | -1.182 | $P_{30,10}$ |
| $C_{10}$ | -.892 | $\Delta H_{-10,-10}$ | 1.463 | $\Delta P_{25,-5}$ | .291 | $H_{-10,-40}$ | -.124 | $U_{-24}$ |
| $C_{11}$ | .114 | $\Delta H_{30,-15}$ | -2.644 | $\Delta P_{10,15}$ | -.124 | $U_{-24}$ | -.290 | $\Delta H_{15,-30}$ |
| $C_{12}$ | -2.928 | $\Delta P_{10,20}$ | -.082 | $\Delta H_{20,-5}$ | -.129 | $\Delta H_{30,5}$ | 2.851 | $\Delta P_{5,15}$ |
| $C_{13}$ | 1.920 | $P_{30,25}$ | 1.603 | $\Delta P_{30,-40}$ | 4.703 | $P_{0,20}$ | -.090 | $\Phi_{500N10-5u}$ |
| $C_{14}$ | .183 | $V_{-24}$ | .693 | $P_{35,35}$ | 1.675 | $\Delta P_{15,-40}$ | .374 | $H_{0,10}$ |
| $C_{15}$ | .062 | $\Phi_{200u}$ | -3.718 | $\Delta P_{-10,40}$ | -.120 | $\Delta H_{15,20}$ | -.069 | $\Delta H_{35,35}$ |
| $C_{16}$ | -1.332 | $\Delta P_{35,25}$ | .200 | $\Delta H_{25,-35}$ | -.076 | $\Delta H_{35,30}$ | .180 | $\Delta H_{15,-40}$ |
| $C_{17}$ | -.319 | $H_{0,-35}$ | -.168 | $H_{5,20}$ | .050 | $\Delta\Phi_{200v}$ | -5.257 | $\Delta P_{-10,5}$ |
| $C_{18}$ | .369 | $H_{-5,-10}$ | .092 | $\Delta\Phi_{500N10-5v}$ | -.084 | $\Delta H_{35,-30}$ | 1.068 | $\Delta P_{30,-40}$ |
| $C_{19}$ | -.059 | $\Delta H_{25,35}$ | -.050 | $\Delta H_{30,40}$ | -.035 | $\Delta\Phi_{200N10v}$ | 4.664 | $\Delta P_{0,-15}$ |
| $C_{20}$ | -.091 | $\Delta H_{35,-25}$ | | | -3.980 | $\Delta P_{-10,10}$ | -.229 | $\Delta H_{10,-15}$ |
| Reduction of variance | 67% | | 63% | | 74% | | 72% | |

TABLE 4.11

Predictors, coefficients and reduction of variance for 24-hr U and V motion south-of-ridge for the NW Pacific

| | U | | | | V | | | |
|---|---|---|---|---|---|---|---|---|
| | With 200 mb steering | | With 500 mb steering | | With 200 mb steering | | With 500 mb steering | |
| $C_0$ | 2757.719 | | 3133.007 | | -1500.630 | | -1280.997 | |
| $C_1$ | .594 | $U_{-12}$ | .604 | $U_{-12}$ | .499 | $V_{-12}$ | .506 | $V_{-12}$ |
| $C_2$ | -.476 | $H_{10,-10}$ | -.417 | $H_{10,-10}$ | .218 | $H_{15,5}$ | .257 | $H_{15,5}$ |
| $C_3$ | -.565 | $\Delta H_{5,5}$ | -.508 | $\Delta H_{5,5}$ | .044 | $\Delta\Phi_{500v}$ | 2.465 | $\Delta P_{5,15}$ |
| $C_4$ | -.094 | $V_{-12}$ | -.117 | $V_{-12}$ | -2.534 | $P_{0,-10}$ | -7.410 | $\Delta P_{-10,-10}$ |
| $C_5$ | -2.222 | $\Delta P_{15,10}$ | -1.327 | $\Delta P_{15,10}$ | 1.926 | $\Delta P_{5,10}$ | .348 | $H_{-5,15}$ |
| $C_6$ | 6.602 | $\Delta P_{-10,10}$ | .059 | $H_{35,-20}$ | -5.799 | $\Delta P_{-10,-10}$ | -.302 | $H_{5,-5}$ |
| $C_7$ | 6.913 | $\Delta P_{-10,-35}$ | 5.807 | $\Delta P_{-10,10}$ | -5.745 | $P_{-5,40}$ | .057 | $\Delta H_{35,-35}$ |
| $C_8$ | -2.765 | $P_{0,-20}$ | .245 | $H_{5,-40}$ | -.131 | $H_{10,-30}$ | -.420 | $P_{35,15}$ |
| $C_9$ | .219 | $H_{5,-40}$ | -.437 | $P_{35,30}$ | .131 | $H_{5,20}$ | -.102 | $\Delta H_{15,30}$ |
| $C_{10}$ | -.526 | $\Delta P_{35,30}$ | 6.250 | $\Delta P_{-10,-35}$ | 6.953 | $P_{-10,10}$ | -.179 | $\Delta H_{15,-25}$ |
| $C_{11}$ | -3.323 | $\Delta P_{5,-15}$ | -2.749 | $\Delta P_{5,15}$ | .417 | $H_{-10,40}$ | 4.560 | $P_{-5,10}$ |
| $C_{12}$ | .247 | $\Delta H_{5,20}$ | -2.675 | $P_{5,25}$ | -.169 | $H_{5,0}$ | -1.651 | $P_{10,0}$ |
| $C_{13}$ | 4.195 | $P_{-10,-10}$ | .266 | $\Delta H_{5,20}$ | -.099 | $\Delta P_{20,-25}$ | -2.944 | $P_{-10,40}$ |
| $C_{14}$ | .058 | $\Delta H_{35,-15}$ | -.898 | $\Delta P_{15,30}$ | 1.056 | $\Delta P_{15,20}$ | .247 | $\Delta H_{-5,25}$ |
| $C_{15}$ | .196 | $\Delta H_{5,-25}$ | -.090 | $H_{20,40}$ | 3.356 | $\Delta P_{-5,-30}$ | .150 | $\Delta H_{5,-20}$ |
| $C_{16}$ | -.425 | $H_{-10,10}$ | 1.477 | $P_{15,40}$ | -.543 | $\Delta H_{-10,-10}$ | -.612 | $\Delta H_{-10,-5}$ |
| $C_{17}$ | .084 | $\Delta H_{25,-35}$ | 5.361 | $\Delta P_{-10,-10}$ | .296 | $\Delta H_{-5,5}$ | .323 | $\Delta H_{-5,5}$ |
| $C_{18}$ | -.815 | $\Delta P_{15,30}$ | -.315 | $P_{30,-15}$ | -.074 | $\Delta H_{25,-40}$ | .030 | $U_{-12}$ |
| $C_{19}$ | -.237 | $P_{35,40}$ | -2.094 | $\Delta P_{5,5}$ | .026 | $H_{35,-40}$ | | |
| $C_{20}$ | 3.619 | $\Delta P_{-10,-20}$ | | | | | | |
| Reduction of variance | 61% | | 63% | | 50% | | 51% | |

TABLE 4.12

Predictors, coefficients and reduction of variance for 24-hr U and V motion for north-of-ridge category for the North Indian Ocean

| | U | | V | |
|---|---|---|---|---|
| $C_0$ | -624.6672 | | -5654.0409 | |
| $C_1$ | .3538 | $U_{-12}$ | .3653 | $V_{-24}$ |
| $C_2$ | .2334 | $V_{-24}$ | 1.3532 | $H_{5,20}$ |
| $C_3$ | -.2209 | $\Phi_{500NW10v}$ | -16.2332 | $\Delta P_{0,25}$ |
| $C_4$ | 3.3336 | $P_{10,40}$ | 28.7486 | $\Delta P_{5,10}$ |
| $C_5$ | -22.4239 | $\Delta P_{-10,30}$ | -23.9050 | $\Delta P_{-5,0}$ |
| $C_6$ | -.4186 | $\Delta H_{20,35}$ | 1.4433 | $P_{35,-10}$ |
| $C_7$ | 10.1656 | $\Delta P_{0,-20}$ | 7.2717 | $\Delta P_{15,-25}$ |
| $C_8$ | 7.9597 | $\Delta P_{10,40}$ | -.7670 | $\Delta H_{20,30}$ |
| $C_9$ | -7.9171 | $\Delta P_{-5,20}$ | -.8584 | $\Delta H_{5,35}$ |
| $C_{10}$ | -6.1242 | $\Delta P_{10,-5}$ | -.8325 | $H_{5,0}$ |
| $C_{11}$ | .5001 | $H_{5,-15}$ | 15.1203 | $\Delta P_{-5,35}$ |
| $C_{12}$ | -.6807 | $H_{-10,40}$ | .2050 | $H_{25,-20}$ |
| $C_{13}$ | 1.9375 | $\Delta P_{25,-5}$ | -4.5111 | $\Delta P_{15,20}$ |
| $C_{14}$ | 11.8670 | $\Delta P_{-10,0}$ | | |
| $C_{15}$ | -.2813 | $H_{10,25}$ | | |
| Reduction of variance | 72% | | 74% | |

TABLE 4.13

Predictors, coefficients and reduction of variance for 24-hr U and V motion for on-the-ridge category for the North Indian Ocean

| | U | | V | |
|---|---|---|---|---|
| $C_0$ | -12198.8993 | | 60.1728 | |
| $C_1$ | .4841 | $U_{-12}$ | .4757 | $V_{-12}$ |
| $C_2$ | 9.7347 | $P_{-10,-35}$ | 3.0908 | $\Delta P_{30,40}$ |
| $C_3$ | -4.3658 | $\Delta P_{15,-25}$ | -2.7541 | $\Delta P_{25,25}$ |
| $C_4$ | 16.7942 | $\Delta P_{-5,-35}$ | .4747 | $\Delta H_{0,15}$ |
| $C_5$ | -.2266 | $\Delta H_{10,5}$ | .2503 | $\Delta\Phi_{500NW10-5v}$ |
| $C_6$ | -.1340 | $\Phi_{500N15u}$ | 7.3980 | $\Delta P_{-5,30}$ |
| $C_7$ | -.2141 | $\Delta H_{35,-30}$ | -7.0843 | $\Delta P_{10,10}$ |
| $C_8$ | 3.2214 | $\Delta P_{10,40}$ | -1.4414 | $\Phi_{500NW10-5v}$ |
| $C_9$ | -4.7700 | $\Delta P_{15,5}$ | .2748 | $\Delta H_{25,-15}$ |
| $C_{10}$ | -12.3065 | $\Delta P_{-10,20}$ | -.2725 | $\Delta H_{15,30}$ |
| $C_{11}$ | .1666 | $H_{25,-30}$ | 4.6092 | $\Delta P_{5,5}$ |
| $C_{12}$ | .3422 | $\Delta H_{5,20}$ | | |
| $C_{13}$ | 2.8396 | $P_{15,-15}$ | | |
| $C_{14}$ | -6.2172 | $\Delta P_{10,-15}$ | | |
| $C_{15}$ | -1.3645 | $P_{30,-5}$ | | |
| $C_{16}$ | -1.0431 | $\Delta\Phi_{500N5v}$ | | |
| Reduction of variance | 78% | | 64% | |

TABLE 4.14

Predictors, coefficients and reduction of variance for 24-hr U and V motion for south-of-ridge category for the North Indian Ocean

| | U | | V | |
|---|---|---|---|---|
| $C_0$ | 3964.4589 | | -5666.9895 | |
| $C_1$ | .4558 | $U_{-12}$ | .4760 | $V_{-12}$ |
| $C_2$ | -.1678 | $H_{15,-5}$ | .1193 | $H_{15,-35}$ |
| $C_3$ | -2.3967 | $\Delta P_{15,-10}$ | 5.3690 | $P_{-10,15}$ |
| $C_4$ | .2793 | $H_{0,-30}$ | .0677 | $\Phi_{500v}$ |
| $C_5$ | -1.7260 | $\Delta P_{35,-40}$ | -1.0161 | $\Delta P_{25,-25}$ |
| $C_6$ | -.1471 | $H_{10,15}$ | .1604 | $H_{15,40}$ |
| $C_7$ | -2.5425 | $\Delta P_{10,10}$ | -3.8486 | $\Delta P_{5,-5}$ |
| $C_8$ | .1774 | $H_{15,-35}$ | 1.2326 | $\Delta P_{15,20}$ |
| $C_9$ | 7.8780 | $\Delta P_{-10,0}$ | -.1779 | $\Delta H_{5,-30}$ |
| $C_{10}$ | -.1105 | $\Delta H_{25,-30}$ | 4.9715 | $\Delta P_{-10,10}$ |
| $C_{11}$ | -.1317 | $H_{20,40}$ | .0720 | $\Delta H_{25,-5}$ |
| $C_{12}$ | -1.8571 | $P_{5,20}$ | -.1533 | $H_{10,30}$ |
| $C_{13}$ | -.0426 | $\Delta H_{35,35}$ | -.1174 | $H_{5,0}$ |
| $C_{14}$ | .2052 | $\Delta H_{0,-5}$ | -.0525 | $\Delta H_{30,40}$ |
| $C_{15}$ | -2.4812 | $\Delta P_{10,40}$ | .0430 | $H_{30,25}$ |
| $C_{16}$ | 2.8158 | $\Delta P_{0,40}$ | | |
| $C_{17}$ | .0634 | $\Phi_{500u}$ | | |
| $C_{18}$ | -.3391 | $H_{-10,40}$ | | |
| Reduction of variance | 55% | | 47% | |

TABLE 4.15

Predictors, coefficients and reduction of variance for 24-hr U and V motion for the South China Sea

| | U | | V | |
|---|---|---|---|---|
| $C_0$ | 8527.1815 | | -5663.1231 | |
| $C_1$ | .6418 | $U_{-12}$ | .5828 | $V_{-12}$ |
| $C_2$ | -17.7580 | $\Delta P_{5,5}$ | -.7670 | $\Delta H8_{5,-5}$ |
| $C_3$ | -.2903 | $H_{15,10}$ | -.3961 | $H8_{15,-35}$ |
| $C_4$ | -6.3370 | $\Delta P_{5,30}$ | .2340 | $\Delta H_{15,10}$ |
| $C_5$ | -.3097 | $H8_{10,30}$ | -.2470 | $H7_{10,30}$ |
| $C_6$ | -.5059 | $H_{10,-10}$ | -6.6187 | $\Delta P_{-5,5}$ |
| $C_7$ | .3005 | $\Delta H_{15,-25}$ | 1.1260 | $H_{-10,40}$ |
| $C_8$ | -18.2355 | $\Delta P_{-10,40}$ | .0885 | $\Phi_{500v}$ |
| $C_9$ | .1847 | $H7_{30,-40}$ | .7478 | $H7_{-10,-35}$ |
| $C_{10}$ | -.8846 | $\Delta H_{5,5}$ | .2838 | $\Delta H_{30,-25}$ |
| $C_{11}$ | 1.3212 | $\Delta H8_{-5,15}$ | -.2859 | $\Delta H7_{15,40}$ |
| $C_{12}$ | 12.2946 | $\Delta P_{-5,-25}$ | -.3903 | $H_{5,0}$ |
| $C_{13}$ | -1.1634 | $\Delta H_{-10,-15}$ | -.1546 | $\Delta H8_{25,20}$ |
| $C_{14}$ | -.6791 | $H_{-10,20}$ | -.2778 | $\Delta H_{25,-30}$ |
| $C_{15}$ | .2789 | $\Delta H_{20,10}$ | .2429 | $\Delta H_{20,-40}$ |
| $C_{16}$ | -.2503 | $\Delta H8_{25,20}$ | -18.3805 | $\Delta P_{-10,-40}$ |
| $C_{17}$ | .5709 | $\Delta H8_{10,-10}$ | .3540 | $\Delta H8_{5,40}$ |
| $C_{18}$ | -13.3370 | $\Delta P_{-5,-10}$ | -1.2444 | $\Delta P_{25,-10}$ |
| $C_{19}$ | 1.1094 | $\Delta H_{-10,-5}$ | .0619 | $H_{20,5}$ |
| $C_{20}$ | -2.6403 | $\Delta P_{15,-25}$ | | |
| Reduction of variance | 82% | | 64% | |

## 5. VERIFICATION AND RESULTS

### 5.1 Atlantic

For easy reference, Table 5.1 provides a complete list of the various model runs that were made with Atlantic cyclones. The symbolic name for each run was selected to denote the key elements for each particular model run. For example, the first run is deciphered as:

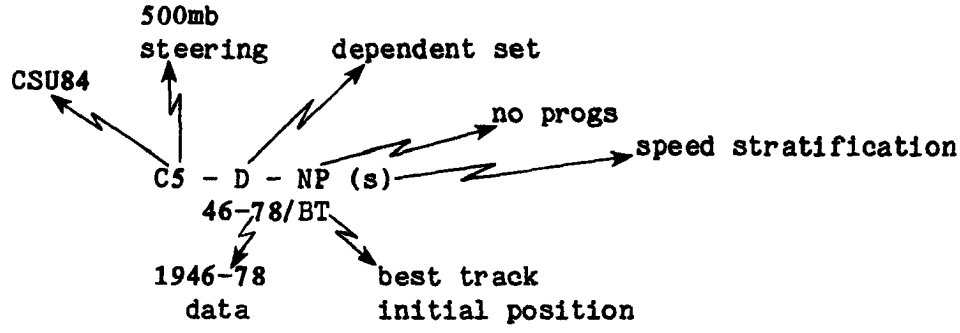


For each run, one or more of the following elements were changed:

1) 500 mb or 200 mb steering level (5 or 2)
2) dependent or independent data set or both combined
3) perfect-prog (PP) (verifying analyses), actual progs (AP) or no progs (NP)
4) speed stratification (s) or no speed stratification (blank)
5) data period of 1946-78, 1962-81, 1968-81, 1973-79, or 1979-81
6) best track (BT) initial positions or perturbed best track (PT) initial positions.

All forecast displacement errors referred to in this paper are in nautical miles (n mi) and this forecast error (great-circle distance between the forecast and the actual location) was computed using the following formula:

$$E = \cos^{-1}[\sin(XLAT)\sin(FLAT) + \cos(XLAT)\cos(FLAT)\cos(XLON - FLON)]60 \text{ n mi}$$

TABLE 5.1

List of the various model runs for the Atlantic. Note that the symbolic name for each run denotes the level of the steering predictors, dependent or independent set, perfect-prog (PP) or actual prog (AP), speed stratification, data period, and best track (BT) initial position or perturbed (PT) best track initial position to simulate a pseudo-warning position.

| CSU84 Model Runs | Steering Level | Dependent (D) or Independent (I) | Perfect-Prog(PP) Actual Prog (AP) No Prog (NP) | Speed Stratification | Data Period | Initial Position |
|---|---|---|---|---|---|---|
| C5-D-NP(s) 46-78/BT | 500 mb | D | NP | YES | 1948-78 | Best Track (BT) |
| C5-D-PP(s) 46-78/BT | 500 mb | D | PP | YES | 1948-78 | BT |
| C5-D-PP(s) 62-81/BT | 500 mb | D | PP | YES | 1962-81 | BT |
| C2-D-PP(s) 62-81/BT | 200 mb | D | PP | YES | 1962-81 | BT |
| C2-D-PP 62-81/BT | 200 mb | D | PP | NO | 1962-81 | BT |
| C5-D-PP 62-81/BT | 500 mb | D | PP | NO | 1962-81 | BT |
| C5-I-PP(s) 62-81/BT | 500 mb | I | PP | YES | 1962-81 | BT |
| C2-I-PP(s) 62-81/BT | 200 mb | I | PP | YES | 1962-81 | BT |
| C5-I-PP 62-81/BT | 500 mb | I | PP | NO | 1962-81 | BT |
| C2-I-PP 62-81/BT | 200 mb | I | PP | NO | 1962-81 | BT |

TABLE 5.1 (cont'd)

| CSU84 Model Runs | Steering Level | Dependent (D) or Independent (I) | Perfect-Prog(PP) Actual Prog (AP) No Prog (NP) | Speed Stratification | Data Period | Initial Position |
|---|---|---|---|---|---|---|
| C2-D-PP 73-79/BT | 200 mb | D | PP | NO | 1973-79 | BT |
| C2-I-PP 73-79/BT | 200 mb | I | PP | NO | 1973-79 | BT |
| C5-DI-PP 68-81/BT | 500 mb | D+I | PP | NO | 1968-81 | BT |
| C5-DI-AP 68-81/BT | 500 mb | D+I | AP | NO | 1968-81 | BT |
| C5-DI-AP 68-81/PBT | 500 mb | D+I | AP | NO | 1968-81 | Perturbed BT(PBT) |
| C5-I-PP 68-81/BT | 500 mb | I | PP | NO | 1968-81 | BT |
| C5-DI-PP 73-79/BT | 500 mb | D+I | PP | NO | 1973-79 | BT |
| C5-DI-AP 73-79/BT | 500 mb | D+I | AP | NO | 1973-79 | BT |
| C5-DI-AP 73-79/PBT | 500 mb | D+I | AP | NO | 1973-79 | PBT |

where XLAT and XLON are the best track latitude and longitude and FLAT and FLON are the forecast latitude and longitude ($^{o}$E). The result of the verification on the dependent data set used to develop the regressions for the Atlantic is shown in Tables 5.2 and 5.3. The three model runs shown in Table 5.2 used 500 mb steering predictors instead of 200 mb steering predictors with the cases categorized with respect to the subtropical ridge and further stratified into fast and slow subsets based on the 500 mb height patterns. C5-D-NP(s)/(46-78/BT) is the traditional or classical approach of applying different regression equations for each of the three cyclone displacements -- 0 to 24, 0 to 48, and 0 to 72. For the synoptic predictors, each of the equations use only the current and 24-hour old analyses with no prognostic data. C5-D-PP(s)/(46-78/BT) used the same data set as C5-D-NP(s)/(46-78/BT) and introduced the new approach of segmenting the forecast motion into three 24-hour steps. It applied the same regression equations three times as the forecast positions were stepped forward. It used perfect prog data to update the synoptic predictors relative to the new cyclone position at the 24-hour and 48-hour forecast positions. C5-D-PP(s)/(62-81/BT) applied the same technique as C5-D-PP(s)/(46-78/BT) to a smaller, more recent data set for the purpose of comparing with a version using 200 mb steering since 200 mb data were available only since 1962. A run similar to C5-D-PP(s)/(62-81/BT) using 200 mb steering predictors instead of 500 mb steering predictors is shown in Table 5.3 as C2-D-PP(s)/(62-81/BT)

The decision to limit the development data to those after 1961 turned out to be very fortuitous because the results indicate that the largest overall decrease in error occurred between model runs

TABLE 5.2

Forecast errors (n mi) using 1946-78 dependent set for the no-prog classical method of regressing from the initial position to the forecast position; i.e., 0-24, 0-48, 0-72 (C5-D-NP(s)/(46-78/BT)), the perfect-prog new method of segmenting the 72-hour forecast period into three 24-hour segments (C5-D-PP(s)/(46-78/BT)), and the perfect-prog new method using a more recent development set (C5-D-PP(s)/(62-81/BT)). The number of verifying cases are in parentheses.

ATLANTIC

| | 24-HR | | | 48-HR | | | 72-HR | | |
|---|---|---|---|---|---|---|---|---|---|
| North | C5-D-NP(s) 46-78/BT | C5-D-PP(s) 46-78/BT | C5-D-PP(s) 62-81/BT | C5-D-NP(s) 46-78/BT | C5-D-PP(s) 46-78/BT | C5-D-PP(s) 62-81/BT | C5-D-NP(s) 46-78/BT | C5-D-PP(s) 46-78/BT | C5-D-PP(s) 62-81/BT |
| Fast | 120(185) | 109(253) | 73( 98) | 250(185) | 217(228) | 139( 84) | 405(185) | 343(227) | 258( 80) |
| Slow | 120(357) | 133(397) | 76(151) | 245(357) | 218(408) | 131(148) | 370(357) | 285(377) | 161(143) |
| Total | 120(542) | 124(650) | 75(249) | 247(542) | 217(636) | 134(262) | 382(542) | 307(604) | 196(223) |
| On | | | | | | | | | |
| Fast | 90(186) | 85(246) | 96( 80) | 197(186) | 167(232) | 166( 79) | 349(186) | 290(223) | 242( 65) |
| Slow | 71(165) | 75(201) | 80( 83) | 164(165) | 184(197) | 145( 66) | 277(165) | 302(187) | 223( 63) |
| Total | 81(351) | 80(447) | 88(163) | 182(351) | 174(429) | 156(145) | 315(351) | 295(410) | 232(128) |
| South | | | | | | | | | |
| Fast | 74(497) | 73(397) | 51(139) | 162(497) | 148(400) | 103(136) | 262(497) | 216(380) | 155(129) |
| Slow | 74(435) | 70(351) | 63(135) | 148(435) | 146(330) | 110(133) | 245(435) | 230(327) | 152(134) |
| Total | 74(932) | 72(748) | 57(274) | 155(932) | 147(730) | 107(269) | 254(932) | 227(707) | 153(263) |
| All | 89(1825) | 92(1845) | 71(686) | 188(1825) | 179(1795) | 127(646) | 304(1825) | 270(1721) | 185(614) |

TABLE 5.3

Speed versus no speed stratification runs. Forecast errors (n mi) for speed stratification run (C2-D-PP(s)/(62-81/BT)) using 200 mb steering is compared to runs without speed stratification using 200 mb steering (C2-D-PP/(62-81/BT)) and 500 mb steering (C5-D-PP/(62-81/BT)) for the years 1962-81. Number of cases are in parentheses.

| | 24-HR | | | 48-HR | | | 72-HR | | |
|---|---|---|---|---|---|---|---|---|---|
| North | C2-D-PP(s) | C2-D-PP | C5-D-PP | C2-D-PP(s) | C2-D-PP | C5-D-PP | C2-D-PP(s) | C2-D-PP | C5-D-PP |
| Fast | 134( 80) | --- | --- | 157( 65) | --- | --- | 249( 58) | --- | --- |
| Slow | 90 (160) | --- | --- | 186(153) | --- | --- | 241(149) | --- | --- |
| Total | 105(240) | 86(242) | 94(312) | 177(218) | 160(219) | 183(291) | 244(207) | 227(206) | 264(280) |
| On | | | | | | | | | |
| Fast | 101( 81) | --- | --- | 176( 74) | --- | --- | 242( 67) | --- | --- |
| Slow | 92( 74) | --- | --- | 141( 61) | --- | --- | 215( 57) | --- | --- |
| Total | 97(155) | 84(159) | 60(170) | 160(135) | 144(139) | 117(145) | 230(124) | 211(124) | 192(124) |
| South | | | | | | | | | |
| Fast | 73(184) | --- | --- | 147(186) | --- | --- | 218(173) | --- | --- |
| Slow | 77( 86) | --- | --- | 132( 77) | --- | --- | 205( 88) | --- | --- |
| Total | 74(270) | 65(274) | 66(284) | 143(263) | 120(267) | 120(277) | 213(261) | 178(261) | 167(269) |
| All | 90(665) | 77(675) | 76(766) | 159(616) | 139(625) | 145(713) | 227(592) | 202(591) | 212(673) |

C5-D-PP(s)/(46-78/BT) and C5-D-PP(s)/(62-81/BT). This surprising result indicates that either the best track cyclone positions or the analysis fields or both for the early pre-satellite years are not up to the quality of those since the early 60's or that the statistical characteristics of the analyses suffered a drastic change somewhere between the early and later years.

A likely source of the difference in the analyses may stem from the implementation of the Cressman (1959) scan analysis method at the National Meteorological Center (NMC) in 1959. Similar data base inhomogeneities may occur on analyses after 1978 due to the replacement of the Cressman scheme with the 'first-guess'/spectral analysis PE hemispheric prognosis package in 1979. Neumann, et al. (1979) cites substantial deterioration in the performance of NHC statistical-synoptic and statistical-dynamical models, particularly NHC73, due to changes in the tropical analysis error characteristics.

Another surprising discovery occurred when the independent set was being verified. Because of the small sample sizes in some of the categories, a version of the model without any speed stratification was developed on the 1962-1981 dependent set. This version, with either 200 mb or 500 mb steering predictors, appears as model runs C2-D-PP/(62-81/BT) and C5-D-PP/(62-81/BT) respectively in Table 5.3. From the results, it is obvious that the speed stratification used in this model failed to enhance its predictive skill in any of the categories. In fact, Table 5.4, which presents the results of the verification on the independent set, reveals the superior skill of the model with no speed stratification. Compare, for example, model runs C5-I-PP(s) with

TABLE 5.4

Speed versus no speed stratification runs. Forecast errors (n mi) with independent data for the speed stratification runs using 500 mb steering (C5-I-PP(s)/(62-81/BT)) and 200 mb steering (C5-I-PP(s)/(62-81/BT)) are compared with runs with no speed stratification using 500 mb steering (C5-I-PP/(62-81/BT)) and 200 mb steering (C2-I-PP/(62-81/BT)). Number of cases are in parentheses. All runs were for the years 1962-81 with the use of Best Track.

| | 24-HR | | | | 48-HR | | | | 72-HR | | | |
|---|---|---|---|---|---|---|---|---|---|---|---|---|
| North | C5-I-PP(s) | C2-I-PP(s) | C5-I-PP | C2-I-PP | C5-I-PP(s) | C2-I-PP(s) | C5-I-PP | C2-I-PP | C5-I-PP(s) | C2-I-PP(s) | C5-I-PP | C2-I-PP |
| Fast | 139(42) | 148(41) | --- | --- | 268(29) | 271(33) | --- | --- | 404(27) | 387(30) | --- | --- |
| Slow | 119(39) | 126(40) | --- | --- | 224(33) | 192(28) | --- | --- | 306(21) | 246(17) | --- | --- |
| Total | 130(81) | 137(81) | 121(81) | 115(81) | 244(62) | 235(61) | 234(61) | 191(60) | 361(48) | 336(47) | 358(45) | 281(44) |
| On | | | | | | | | | | | | |
| Fast | 141(22) | 102(29) | --- | --- | 169(27) | 167(28) | --- | --- | 246(24) | 212(25) | --- | --- |
| Slow | 92(24) | 131(16) | --- | --- | 190(11) | 192(09) | --- | --- | 300(08) | 213(06) | --- | --- |
| Total | 115(46) | 113(45) | 96(46) | 82(45) | 175(38) | 173(37) | 158(38) | 152(37) | 259(32) | 212(31) | 212(32) | 198(30) |
| South | | | | | | | | | | | | |
| Fast | 90(79) | 101(117) | --- | --- | 184(73) | 223(101) | --- | --- | 283(70) | 350(91) | --- | --- |
| Slow | 106(72) | 104(34) | --- | --- | 194(64) | 162(34) | --- | --- | 283(54) | 212(31) | --- | --- |
| Total | 98(151) | 102(151) | 86(151) | 84(151) | 188(137) | 208(135) | 167(137) | 164(136) | 283(124) | 315(122) | 248(124) | 252(123) |
| All | 110(278) | 114(277) | 98(278) | 93(277) | 201(237) | 209(233) | 183(236) | 169(233) | 297(204) | 304(200) | 267(201) | 250(197) |

C5-I-PP and runs C2-I-PP(s) with C2-I-PP. This is especially true for the version with 200 mb steering predictors for the north-of-ridge category.

Possible reasons for the failure of the speed stratification were examined. Table 5.5 presents the number of cases that occurred for a given height pattern and the subsequent 24-hour cyclone speed. As discussed in Chapter 3, the height patterns for the Atlantic were computed according to:

$$H_{15,-40} + H_{15,25} - 2 \times H_{15,-5} \quad \text{for north-of-ridge}$$

$$H_{10,10} - H_{10,-15} - 20 \quad \text{for on-the-ridge}$$

$$2 \times H_{20,5} - H_{20,-25} - H_{20,25} \quad \text{for south-of-ridge}$$

where $H_{i,j}$ is the 500 mb height in meters and the subscripts i and j indicate the degrees of latitude and longitude away from the cyclone center where the heights are to be observed. Latitudes are positive poleward and longitudes are positive eastward from the cyclone center. Recall that if the height pattern indicator HP was greater than or equal to zero, the cyclone was placed in the fast category and if HP was less than zero, the cyclone was placed in the slow category. Although the stratification worked well for the on-the-ridge category, it did poorly for the other two categories. For a given value of the height pattern indicator, there are as many cases that were fast as there were slow. The scheme did a poor job of distinguishing the fast cases from the slow cases for the given height pattern indicator. The results in Table 5.4 bear this out.

Similar speed stratification problems occurred in the NW Pacific as shown in Table 5.6. Although it appears that the height pattern indicator was able to distinguish between the very fast and the very

TABLE 5.5

Number of Atlantic cases that occurred for a given magnitude of 500 mb height pattern indicator (in meters) and subsequent 24-hour cyclone speed (in m/s).

| | $S < 2.5$ | $2.5 \leq S \leq 7.5$ | $S > 7.5$ | |
|---|---|---|---|---|
| North | 78 | 238 | 144 | $100 < HP$ |
| | 15 | 59 | 46 | $50 < HP \leq 100$ |
| | 12 | 95 | 37 | $0 \leq HP \leq 50$ |
| | 24 | 68 | 33 | $-50 \leq HP < 0$ |
| | 22 | 101 | 43 | $-100 \leq HP < -50$ |
| | 175 | 408 | 150 | $HP < -100$ |
| On | 4 | 27 | 17 | $100 < HP$ |
| | 4 | 51 | 18 | $50 < HP \leq 100$ |
| | 26 | 132 | 22 | $0 \leq HP \leq 50$ |
| | 39 | 138 | 2 | $-50 \leq HP < 0$ |
| | 15 | 48 | 1 | $-100 \leq HP < -50$ |
| | 9 | 14 | 0 | $HP < -100$ |
| South | 48 | 242 | 72 | $100 < HP$ |
| | 16 | 112 | 21 | $50 < HP \leq 100$ |
| | 10 | 127 | 41 | $0 \leq HP \leq 50$ |
| | 10 | 84 | 34 | $-50 \leq HP < 0$ |
| | 16 | 140 | 14 | $-100 \leq HP < -50$ |
| | 74 | 288 | 9 | $HP < -100$ |

slow cases based on strongly positive or strongly negative values of HP, this distinction is not as clear as the value of HP approaches zero.

For example, when the height pattern indicator was greater than 100 for the north-of-ridge category, the scheme was able to correctly select almost all of the extremely fast cases. Only 25 cases that actually were slow cases were improperly selected. Similarly, the scheme performed creditably for the on-the-ridge category when the height pattern indicator was greater than 100 and for the south-of-ridge category when a negative height pattern indicator was used to select the extremely slow cases.

The scheme did poorly, however, on all other occasions. The worst examples are for the on-the-ridge and south-of-ridge categories when the height pattern indicator was between zero and 100. More of the cases

TABLE 5.6

Number of NW Pacific cases that occurred for a given magnitude of 500 mb height pattern indicator (in meters) and subsequent 24-hour cyclone speed in (m/s).

| | $S < 2.5$ | $2.5 \leq S \leq 7.5$ | $S > 7.5$ | |
|---|---|---|---|---|
| North | 25 | 244 | 347 | $100 < HP$ |
| | 27 | 141 | 90 | $50 < HP \leq 100$ |
| | 52 | 159 | 73 | $0 \leq HP \leq 50$ |
| | 47 | 174 | 45 | $-50 \leq HP < 0$ |
| | 119 | 357 | 59 | $-100 \leq HP < -50$ |
| | 168 | 453 | 73 | $HP < -100$ |
| On | 17 | 229 | 100 | $100 < HP$ |
| | 58 | 388 | 34 | $50 < HP \leq 100$ |
| | 112 | 504 | 21 | $0 \leq HP \leq 50$ |
| | 27 | 137 | 5 | $-50 \leq HP < 0$ |
| | 127 | 374 | 59 | $-100 \leq HP < -50$ |
| | 170 | 456 | 74 | $HP < -100$ |
| South | 289 | 1930 | 449 | $100 < HP$ |
| | 194 | 1027 | 165 | $50 < HP \leq 100$ |
| | 210 | 971 | 89 | $0 \leq HP \leq 50$ |
| | 157 | 561 | 31 | $-50 \leq HP < 0$ |
| | 93 | 271 | 6 | $-100 \leq HP < -50$ |
| | 134 | 327 | 9 | $HP < -100$ |

selected for the fast set actually turned out to be slow cases. Perhaps, the speed stratification could have been made on very large positive or negative values of HP instead of zero as was done in the stratification here. But this would have resulted in a very small sample size. Further, the fast and slow equations could have been applied to only those cyclone cases with initial speeds greater than 7.5 m/s or less than 2.5 m/s, respectively, as was done in a similar manner for NHC-67. Neither approach was pursued here and the decision was made to use the regression equations without any speed stratification. All further reference to CSU84 for the Atlantic will refer to the version without any speed stratification.

Table 5.7 compares the skill of CSU84 to the official forecast error and the operational error of the best objective technique for a nearly homogeneous sample for the period 1973-1979. Direct comparison between the operational and CSU84 errors are difficult since the CSU84 cases during the period are a combination of dependent and independent cases. For this comparison, just the dependent and independent cases for 1973-1979 from the larger 1962-1981 CSU84 runs were used. The on-the-ridge and north-of-ridge categories were combined to form the north zone. This appeared reasonable since most of the on-the-ridge cases were north of 24.5°N.

These results for CSU84 are based on perfect-prog data, best track initial positions and 200 mb steering predictors and appear to indicate that the accuracy of CSU84 is comparable to the best operational technique at the short forecast period and much better at the longer forecast periods. Relative to the other objective techniques currently used by the National Hurricane Center, CSU84 appears far superior. For example, the 72-hour forecast errors for the north zone range from 401 n mi for NHC72 to 499 n mi for NHC67 and for the south zone, the errors range from 309 n mi for HURRAN to 355 n mi for NHC72.

For the purpose of comparison with a no-skill forecast, Table 5.8 presents 24- and 48-hour forecast errors based only on an extrapolation of the cyclone's past motion using the CSU84 1973-1979 dependent and independent sets combined. The Table reveals that the use of past 12-hour motion for persistence is far better than either the past 24-hour motion or the average of the past 12- and past 24-hour motion. But as the results indicate, pure persistence is a poor indicator of future

TABLE 5.7

Comparison of forecast errors (n mi) on a nearly homogeneous sample of cyclone cases for 1973-1979 between CSU84 usng 200 mb steering and perfect-prog on dependent (C2-D-PP/(73-79/BT)) and independent (C2-I-PP/(73-79/BT)) data and the official NHC forecast (OFF) and the best track (BEST) operational objective technique. The forecast errors for the official and the best objective technique for each category are from Neumann and Pelissier (1981). The north-of-ridge and on-the-ridge categories for CSU84 were combined to form the north zone. Number of cases are in parentheses.

ATLANTIC

| | 24-HR | | | | 48-HR | | | | 72-HR | | | |
|---|---|---|---|---|---|---|---|---|---|---|---|---|
| | C2-D-PP | C2-I-PP | OFF | BEST | C2-D-PP | C2-I-PP | OFF | BEST | C2-D-PP | C2-I-PP | OFF | BEST |
| North (>24.5°N) | 107(104) | 135(38) | 131(156) | 127(156) NHC 67 | 199(89) | 242(19) | 304(102) | 272(102) NHC 73 | 289(80) | 316(10) | 421(60) | 358(60) NHC 73 |
| South (<24.5°N) | 82(67) | 99(114) | 85(129) | 88(129) CLIPER | 151(64) | 159(43) | 179(95) | 180(95) NHC 73 | 194(59) | 253(34) | 317(79) | 298(79) CLIPER |
| All | 97(171) | 108(152) | 110(285) | 113(285) NHC 73 | 179(153) | 184(62) | 244(197) | 228(197) NHC 73 | 249(139) | 267(44) | 362(139) | 344(139) NHC 73 |

TABLE 5.8

Track error (n mi) for a forecast using only persistence for all cyclone cases for the period 1973-79. Forecast based on an extrapolation of the cyclone's past 12-hour motion ($P_{12}$), past 24-hour motion ($P_{24}$), and an average of the past 12- and past 24-hour motion (P12+24) are shown.

| | 24-HR | | | 48-HR | | |
|---|---|---|---|---|---|---|
| | P12 | P24 | P12+24 | P12 | P24 | P12+24 |
| North | 169(102) | 188(102) | 176(102) | 417(102) | 440(102) | 424(102) |
| On | 158(40) | 184(40) | 170(40) | 468(40) | 514(40) | 489(40) |
| South | 88(211) | 97(211) | 91(211) | 216(211) | 230(211) | 220(211) |
| All | 130(323) | 146(323) | 136(323) | 336(323) | 360(323) | 345(323) |

motion outside the deep tropics. Note that forecast errors at 48 hours are well above 400 n mi for the north- and on-the-ridge categories compared to the 48-hour errors of CSU84 that are about half as large.

In the development of this new tropical cyclone prediction model, the emphasis was on improving the track forecast skill at the higher latitudes for the longer forecast periods. These results appear to indicate that this goal has been achieved. Moreover, the equally strong performance of the model at 24 hours was encouraging. On re-examination, there are several reasons for the model's very good performance for both the short- and long-term forecast. These reasons will be amplified later in this chapter.

Operational Simulation. The verification of this new model thus far has used best track data and a perfect-prog approach. In order to simulate more realistic, operational conditions, the sensitivity of the model was evaluated by introducing errors into the initial best track positions. For the seven year period between 1968 and 1974, Neumann (1975) cites an average initial position error of 25 n mi, with the average error decreasing slightly to 22 n mi for cyclones within 500 n mi of the United States (US). With this as a guide and using the model run with 200 mb steering for the data period 1962-81 (C2-D-PP(s)/(62-81/BT)) as the control case, the initial position was perturbed by .3 degrees (18 n mi) for those cyclones west of the 70th meridian and by .5 degrees (30 n mi) for those cyclones east of the 70th meridion.

Since the use of best track information to compute the past 12-hour and 24-hour motion results in perfect persistence predictors, introducing 'erroneous' initial positions can be expected to result in larger forecast errors. However, with the emphasis placed on this model

more accurate long-range position forecasts, it was hoped that the deterioration of skill due to the initial position error would be reduced at the longer time period. The results of the sensitivity test show that this indeed is the case. Compare the results shown in Table 5.9 with those of C2-D-PP(s) in Table 5.3.

As one might expect, displacing the initial position northward by 18 to 30 n mi degrades primarily the 24-hour forecast position and the degradation decreases with time until it is almost negligible at 72 hours.

The degradation is most noticeable for cyclones south of the ridge (40% increase in error at 24 hours) and is most pronounced for a northward displacement of the initial position compared to displacements southward, eastward or westward. This sensitivity test indicates that the use of best track positions rather than warning positions to produce ''perfect'' past-motion predictors does not result in an unrealistically strong reliance on the persistence component of the model beyond 24 hours, particularly for those cylones on and north of the subtropical ridge.

One likely reason for the relatively small increase in error due to initial position error, even for the short-term forecast, is that the model does not use the cyclone's <u>current</u> motion as one of its predictors. Statistical models, such as CLIPER and NHC73 that do use <u>current</u> motion will undoubtedly suffer a large increase in forecast errors at the shorter forecast periods whenever large initial position errors are encountered operationally. Even a relatively small initial position error could be disastrous if the error projects a false change in direction. Use of past 12-hour and past 24-hour motion instead of

TABLE 5.9

Forecast errors (n mi) and percent increase in forecast error (in parentheses) as a result of displacing the best track initial position northward (N), southward (S), westward (W), and eastward (E). Model run C2-D-PP(s)/(62-81/BT)) was used as the control case and the initial position was displaced by .3 degrees (18 n mi) if the initial position was west of the 70th meridian and .5 degrees (30 n mi) if the initial position was east of the 70th meridian.

| | 24-HR | | | | 48-HR | | | | 72-HR | | | |
|---|---|---|---|---|---|---|---|---|---|---|---|---|
| | N | S | W | E | N | S | W | E | N | S | W | E |
| North | | | | | | | | | | | | |
| Fast | 110(29) | 100(18) | 87(02) | 90(06) | 202(14) | 197(11) | 182(03) | 187(06) | 353(06) | 353(06) | 328(-2) | 335(0) |
| Slow | 119(04) | 115(01) | 116(02) | 116(02) | 181(03) | 169(-4) | 174(-1) | 174(-1) | 209(04) | 196(-2) | 204(02) | 200(0) |
| Total | 116(13) | 109(06) | 105(02) | 106(03) | 189(07) | 179(02) | 177(01) | 179(02) | 266(06) | 255(01) | 251(0) | 253(0) |
| On | | | | | | | | | | | | |
| Fast | 91(34) | 73(07) | 74(09) | 83(18) | 158(16) | 138(01) | 140(03) | 143(05) | 224(10) | 203(0) | 215(05) | 205(0) |
| Slow | 84(27) | 74(12) | 71(08) | 79(20) | 154(18) | 133(02) | 148(13) | 133(02) | 277(06) | 272(05) | 284(09) | 260(0) |
| Total | 88(31) | 74(10) | 73(09) | 81(21) | 156(17) | 136(02) | 144(08) | 139(04) | 252(09) | 239(03) | 250(08) | 232(0) |
| South | | | | | | | | | | | | |
| Fast | 92(46) | 85(35) | 79(25) | 81(27) | 161(25) | 144(12) | 138(07) | 141(06) | 255(24) | 212(03) | 221(07) | 224(05) |
| Slow | 81(23) | 78(18) | 72(09) | 77(18) | 148(15) | 139(08) | 137(06) | 143(11) | 216(06) | 218(07) | 213(05) | 212(01) |
| Total | 87(40) | 82(28) | 76(19) | 79(22) | 154(19) | 142(10) | 138(07) | 142(08) | 236(15) | 215(05) | 217(06) | 218(03) |
| All | 99(24) | 91(04) | 87(09) | 90(12) | 168(13) | 155(04) | 154(03) | 156(04) | 251(10) | 236(03) | 237(03) | 235(01) |

current motions could be expected to 'soften' the impact of any initial position error.

However, the use of ''real'' prognostic data in lieu of analysis data, as was done in this perfect-prog approach, will almost certainly degrade the results; just how much is questionable and must be tested in an operational environment. With more sophisticated numerical models and more accurate prognostic fields, the degradation will hopefully be minimal.

Again, because of the new approach taken here of segmenting future 72-hour cyclone motion into three discrete 24-hour time steps, the dependence of the scheme on any one prognostic field is limited to 24 hours of cyclone movement. Thus, the extent of any erroneous track forecast based on a ''bad'' prognostic field should be kept to a minimum and possibly corrected on a subsequent 24-hour forecast. In addition, because the design of this model permits forecaster intervention in providing the input data, if the analysis or prognostic field appears to be obviously in error, the input data required by the model could be easily modified prior to the computation of the forecast position.

Another desirable feature of this model is that it does not use prognostic data to formulate the 24-hour forecast position. Nor does it use the current motion of the cyclone. The synoptic predictors required for calculating the first 24 hours of motion come from the current and 24-hour old analyses. Further, only the 24-hour prog fields are used for computing the 24- to 48-hour motion and likewise, only the 48-hour prog fields are used to compute the 48- to 72-hour motion. This may explain some of the degradation in skill experienced by traditional statistical-dynamical prediction models that apply 24-, 36-, and 48-hour

forecast fields for each and every forecast period in transitioning from a perfect-prog approach used in development to an operational setting that uses real progs.

Figure 5.1, taken from Neumann and Lawrence (1973), is presented as an example of the predictors selected by the NHC73 screening program for zonal and meridional motion for zone 22 which is centered near the eastern tip of Cuba. Their H0010 refers to the current 1000 mb height, H2405 refers to the 24-hour forecast height of the 500 mb surface, H4805 refers to the 48-hour forecast height of the 500 mb surface, and so on. Note that their short range 12- and 24-hour forecasts are heavily dependent on forecast fields. Specifically, 10 of the 12 predictors for 24-hour zonal motion come from forecast fields while 7 of the 12 predictors for 24-hour meridional motion come from forecast fields. A fair number of these predictors come from the 48-hour forecast field as well. Since forecast fields for the tropics are known to be rather poor and zone 22 can be considered to lie in the tropics, the use of forecast fields, particularly extended forecasts for 36 and 48 hours, can be expected to play a significant role in the degradation of statistical forecast models when actual forecast fields are used operationally.

Model Runs Using Operational Data. To determine the amount of degradation that might occur in using this newly developed model operationally, the model was tested with actual forecast fields from a numerical model. This was accomplished by using prognostic fields archived at the Fleet Numerical Oceanography Center (FNOC) for the period 1968-1981. Twenty-four- and 48-hour forecast fields of sea level pressures and 500 mb D-values on a 63x63 hemispheric grid provided the

Table 10 Variance analysis of zonal motion predicted by equation set number 22 (22N, 75W)

| Predictor Selection Order | 12 HOUR FCST (k=1) Predictor | RV | 24 HOUR FCST (k=2) Predictor | RV | 36 HOUR FCST (k=3) Predictor | RV | 48 HOUR FCST (k=4) Predictor | RV | 72 HOUR FCST (k=5) Predictor | RV |
|---|---|---|---|---|---|---|---|---|---|---|
| J=1 | H0005( 37) | 0.626 | H2405( 37) | 0.643 | H2405( 37) | 0.665 | H2405( 37) | 0.659 | H2405( 37) | 0.515 |
| 2 | H0005( 52) | 0.043 | H0005( 37) | 0.064 | H0010( 74) | 0.052 | H0005( 88) | 0.073 | H0005( 88) | 0.132 |
| 3 | H0010( 75) | 0.055 | H0010( 75) | 0.042 | H0005( 37) | 0.044 | HL805( 65) | 0.042 | HL805( 80) | 0.047 |
| 4 | H3605( 54) | 0.031 | H2405( 22) | 0.038 | H0005(103) | 0.034 | H3605( 54) | 0.040 | H0005( 46) | 0.052 |
| 5 | HL805( 50) | 0.031 | HL805( 42) | 0.021 | H3605( 54) | 0.020 | H3605( 56) | 0.034 | HL805( 37) | 0.035 |
| 6 | HL805( 40) | 0.020 | H3605( 38) | 0.023 | HL805( 41) | 0.024 | H0010( 74) | 0.017 | H0005( 37) | 0.030 |
| 7 | H0005( 88) | 0.014 | H3605( 65) | 0.016 | HL805( 65) | 0.022 | H2405( 94) | 0.017 | H3605( 54) | 0.019 |
| 8 | H0010( 52) | 0.013 | HL805( 01) | 0.015 | H0007( 22) | 0.022 | H3605( 01) | 0.010 | H0010( 75) | 0.022 |
| 9 | HL805( 13) | 0.012 | H3605( 64) | 0.011 | H3605( 01) | 0.009 | H0005( 37) | 0.007 | HL805( 01) | 0.015 |
| 10 | H2405( 54) | 0.012 | HL805( 80) | 0.009 | H0005( 03) | 0.011 | H2405( 31) | 0.011 | H3605( 03) | 0.013 |
| 11 | HL805( 80) | 0.012 | H3605( 54) | 0.009 | HL805( 37) | 0.007 | H2405( 77) | 0.005 | H3605( 80) | 0.006 |
| 12 | H2405( 57) | 0.008 | H3605( 50) | 0.009 | H2405( 77) | 0.006 | H3605( 98) | 0.005 | H3605( 79) | 0.011 |
| Total Reduction | | 0.879 | | 0.900 | | 0.917 | | 0.922 | | 0.897 |

Table 8 Variance analysis of meridional motion predicted by equation set number 22 (22N, 75W)

| Predictor Selection Order | 12 HOUR FCST (k=1) Predictor | RV | 24 HOUR FCST (k=2) Predictor | RV | 36 HOUR FCST (k=3) Predictor | RV | 48 HOUR FCST (k=4) Predictor | RV | 72 HOUR FCST (k=5) Predictor | RV |
|---|---|---|---|---|---|---|---|---|---|---|
| J=1 | HL805( 65) | 0.167 | H2405( 50) | 0.183 | H2405( 50) | 0.241 | H2405( 50) | 0.254 | H2405( 50) | 0.237 |
| 2 | H0005( 65) | 0.145 | HL805( 80) | 0.208 | HL805( 80) | 0.196 | HL805( 80) | 0.175 | H2405( 47) | 0.148 |
| 3 | H0007( 84) | 0.188 | H2405( 84) | 0.098 | H2405( 84) | 0.073 | H0007( 61) | 0.076 | H3605( 73) | 0.091 |
| 4 | H0005( 30) | 0.046 | H0005( 65) | 0.058 | H0007( 61) | 0.049 | H0010( 61) | 0.046 | H0005( 85) | 0.042 |
| 5 | H2405( 56) | 0.038 | H0007( 61) | 0.054 | H0005( 65) | 0.047 | H0005( 88) | 0.047 | H0010( 80) | 0.061 |
| 6 | H2405( 50) | 0.028 | H0007( 84) | 0.029 | H0005( 64) | 0.026 | H0010( 80) | 0.057 | HL805( 37) | 0.031 |
| 7 | H0010( 63) | 0.022 | H0005( 14) | 0.026 | HL805( 37) | 0.027 | H0007( 95) | 0.029 | H2405( 22) | 0.030 |
| 8 | H2405( 97) | 0.019 | H0005( 94) | 0.022 | H3605( 96) | 0.026 | HL805(102) | 0.025 | H2405( 37) | 0.028 |
| 9 | H2405( 13) | 0.017 | HL805( 30) | 0.020 | H3605( 22) | 0.023 | H0005( 19) | 0.023 | HL805( 99) | 0.029 |
| 10 | HL805( 38) | 0.014 | H3605( 36) | 0.021 | HL805( 30) | 0.015 | H0007( 63) | 0.010 | HL805( 76) | 0.025 |
| 11 | H2405( 2) | 0.018 | H3605( 96) | 0.017 | H0005( 14) | 0.013 | HL805( 35) | 0.009 | H0010( 58) | 0.015 |
| 12 | H0007( 30) | 0.015 | H2405( 86) | 0.016 | H3605( 36) | 0.011 | H3605( 21) | 0.016 | H3605( 50) | 0.018 |
| Total Reduction | | 0.737 | | 0.751 | | 0.747 | | 0.767 | | 0.756 |

Fig. 5.1. Predictors selected by the NHC73 screening program for zonal and meridional motion for zone 22. H0005 refers to the current 500 mb height, H3605 refers to the 36-hour forecast height of the 500 mb surface, H0007 refers to the current 700 mb height, H0010 refers to the current 1000 mb height and so on. The tables are taken from Neumann and Lawrence (1973).

synoptic predictors. A standard height of 5574 m was used to convert the 500 mb D-values to geopotential heights.

Unfortunately, 200 mb prognostic height fields are not archived by the FNOC. Comparative testing is thus limited to the version of the model using 500 mb steering predictors instead of 200 mb steering predictors. Although comparing the independent set results of model run C5-I-PP/(62-81/BT)) and C2-I-PP/(62-81/BT)) in Table 5.4 would indicate that the version with 500 mb steering is not as accurate as the version with 200 mb steering, the verification runs using actual forecast fields should be able to indicate the amount of degradation in forecast accuracy that the model would suffer.

Table 5.10A presents a comparison of the model using perfect-prog data (C5-DI-PP/(68-81/BT)) and actual forecast fields (C5-DI-AP/(68-81/BT)). Verification of the model using both actual forecast fields and perturbation of the initial position (C5-DI-AP/(68-81/PBT)) is also shown. To simulate warning positions, the best track initial positions were randomly perturbed by an amount equal to warning position errors observed operationally (Neumann, 1975). The relatively small amount of degradation resulting from the use of actual forecast fields and pseudo-warning positions is comforting. As expected, the largest increases in error using real progs occur for the south-of-ridge and on-the ridge categories. The poor quality of forecast fields in the tropics is well-known. This is precisely where statistical schemes that do not rely on synoptic data perform well. Yet, the results indicate that the skill of this model compares very favorably with these analog techniques that use just climatology and persistence and, as will be

TABLE 5.10A

Verification of the model for Atlantic using perfect-progs (C5-D-PP/(68-81/BT)); actual progs (C5-D-AP/(68-81/BT)); actual progs and pseudo-warning positions (C5-D-AP/(68-81/PBT)) for the Atlantic for 1968-1981. The model uses 500 mb steering instead of 200 mb steering. Number of cases are in parentheses and they differ beyond 24 hours due to missing forecast fields.

| | 24-HR | | | 48-HR | | | 72-HR | | |
|---|---|---|---|---|---|---|---|---|---|
| | C5-DI-PP 68-81/BT | C5-DI-AP 68-81/BT | C5-DI-AP 68-81/PBT | C5-DI-PP 68-81/BT | C5-DI-AP 68-81/BT | C5-DI-AP 68-81/PBT | C5-DI-PP 68-81/BT | C5-DI-AP 68-81/BT | C5-DI-AP 68-81/PBT |
| North | 106(329) | 106(329) | 111(329) | 207(294) | 219(157) | 216(157) | 297(273) | 321(150) | 319(150) |
| On | 84(118) | 84(118) | 91(118) | 139(96) | 167(96) | 164(94) | 222(81) | 303(87) | 294(85) |
| South | 85(397) | 85(397) | 91(397) | 148(330) | 172(358) | 176(358) | 211(296) | 259(348) | 261(348) |
| All | 93(844) | 93(844) | 99(844) | 171(720) | 184(611) | 184(609) | 248(650) | 282(585) | 281(583) |

TABLE 5.10B

Verification of the model for Atlantic on independent set using perfect progs for 1968-1981.

| | 24-HR | 48-HR | 72-HR |
|---|---|---|---|
| | C5-I-PP 68-81/BT | C5-I-PP 68-81/BT | C5-I-PP 68-81/BT |
| North | 122(94) | 242(73) | 358(59) |
| On | 102(53) | 160(39) | 263(32) |
| South | 96(228) | 166(166) | 242(138) |
| All | 103(375) | 185(278) | 275(229) |

shown later, outperforms them at the longer forecast periods for the south zone. At higher latitudes, this model appears superior.

The forecast errors for the on-the-ridge category are the key to whether the model is capable of discerning a major track change from one with a westward component to one with an eastward component. Although there appears to be a sizeable degradation in skill by introducing actual forecast fields, bear in mind that model run C5-DI-PP was an attempt to compare homogeneous cyclone cases for the period 1968-1981.

By keeping the sample cases homogeneous, however, both dependent and independent cases from the perfect-prog approach were combined. Table 5.10B shows the results from the model run (C5-I-PP) on just the independent set using perfect-progs for the period 1968-1981. Using these forecast errors for comparison, the degradation from using actual prognostic fields is relatively small. A truly homogeneous sample would probably have resulted in forecast errors somewhere between the two model runs of C5-DI-PP shown in Table 5.10A and model run C5-I-PP shown in Table 5.10B. Be aware that although the 1968-1981 data set is a mixture of dependent and independent data for the perfect-prog case, it can be considered totally independent beyond 24 hours for the actual prog case. From these results, it would appear safe to assume that the use of this model in an operational setting would not degrade its forecast skill as much as the deterioration suffered by the other statistical-dynamical models. Possible explanations why the approach used in the development of CSU84 limits the normal operational degradation suffered by statistical models will be offered in the summary to this chapter.

## 5.2 NW Pacific and South China Sea

The development of regression equations for the NW Pacific and South China Sea followed along the same line taken for the Atlantic. As was shown in Table 5.6, speed stratification was not beneficial for the Pacific; thus, only the versions of the model with no speed stratification will be discussed from here on. Table 5.11 summarizes the various model runs for the NW Pacific for easy reference. Table 5.12 presents verification results for the dependent and independent sets using either the 500 mb steering predictors or 200 mb steering predictors. Unlike the Atlantic where the version of the model using 200 mb steering was more accurate overall, the version with 500 mb steering was more accurate overall in the NW Pacific, except for intense cyclones which are accelerating north of the subtropical ridge. The reason for this is unclear although a likely explanation is the difference in the percent of cases in the north-of-ridge category compared to the cases in the south-of-ridge category for the two ocean basins. As will be shown later, even for the NW Pacific, the version using 200 mb steering was more accurate for those strong cyclone cases undergoing recurvature north of the ridge. But since the number of these cases is small compared to the other cases for the Pacific, the accuracy of the version with 500 mb steering appears better overall.

The model's better performance on strong cyclones undergoing recurvature when 200 mb steering is used instead of 500 mb steering appears to support recent findings correlating the recurvature phenomenon with upper tropospheric winds. A number of these studies were reviewed earlier in Chapter 2.

TABLE 5.11

List of the various model runs for the NW Pacific. Note that the symbolic name for each run denotes the level of the steering predictors, dependent or independent set, perfect-prog or actual prog, speed stratification, data period, and best track initial position or perturbed best track initial position to simulate a pseudo-warning position.

| CSU84 Model Runs | Steering Level | Dependent (D) or Independent (I) | Perfect-Prog(PP) Actual Prog (AP) No Prog (NP) | Speed Stratification | Data Period | Initial Position |
|---|---|---|---|---|---|---|
| C5-D-PP 62-81/BT | 500 mb | D | PP | NO | 1962-81 | Best Track (BT) |
| C5-I-PP 62-81/BT | 500 mb | I | PP | NO | 1962-81 | BT |
| C2-D-PP 62-81/BT | 200 mb | D | PP | NO | 1962-81 | BT |
| C2-I-PP 62-81/BT | 200 mb | I | PP | NO | 1962-81 | BT |
| C5-D-PP 79-81/BT | 500 mb | D | PP | NO | 1979-81 | BT |
| C5-I-PP 79-81/BT | 500 mb | I | PP | NO | 1979-81 | BT |
| C5-I-PP 62-81/PBT | 500 mb | I | PP | NO | 1962-81 | Perturbed BT(PBT) |
| C5-DI-PP 68-81/BT | 500 mb | D+I | PP | NO | 1968-81 | BT |
| C5-DI-AP 68-81/BT | 500 mb | D+I | AP | NO | 1968-81 | BT |

TABLE 5.11 (cont'd)

| CSU84 Model Runs | Steering Level | Dependent (D) or Independent (I) | Perfect-Prog(PP) Actual Prog (AP) No Prog (NP) | Speed Stratification | Data Period | Initial Position |
|---|---|---|---|---|---|---|
| C5-DI-AP 68-81/PBT | 500 mb | D+I | AP | NO | 1968-81 | PBT |
| C5-I-PP 68-81/BT | 500 mb | I | PP | NO | 1968-81 | BT |
| C5-DI-AP 79-81/PBT | 500 mb | D+I | AP | NO | 1979-81 | PBT |

TABLE 5.12

Comparison of forecast errors (n mi) between model runs using 500 mb steering on dependent (C5-D-PP) and independent (C5-I-PP) data and 200 mb steering on dependent (C2-D-PP) and independent (C2-I-PP) data for the NW Pacific for 1962-81. Number of cases are in parentheses.

NW PACIFIC

| | 24-HR | | | | 48-HR | | | | 72-HR | | | |
|---|---|---|---|---|---|---|---|---|---|---|---|---|
| | C5-D-PP | C5-I-PP | C2-D-PP | C2-I-PP | C5-D-PP | C5-I-PP | C2-D-PP | C2-I-PP | C5-D-PP | C5-I-PP | C2-D-PP | C2-I-PP |
| North | 77(122) | 95(75) | 73(120) | 111(75) | 135(89) | 171(57) | 134(88) | 205(57) | 188(71) | 242(42) | 204(71) | 282(42) |
| On | 60(256) | 81(131) | 59(240) | 82(127) | 121(215) | 161(105) | 118(196) | 171(102) | 199(172) | 252(91) | 194(154) | 248(87) |
| South | 76(1322) | 80(667) | 76(1322) | 81(667) | 144(1243) | 155(617) | 144(1236) | 159(615) | 198(1167) | 215(570) | 200(1156) | 224(568) |
| All | 74(1700) | 81(873) | 74(1682) | 84(869) | 141(1547) | 157(779) | 140(1520) | 164(774) | 197(1410) | 221(703) | 199(1381) | 231(697) |

TABLE 5.12 (cont'd)

SOUTH CHINA SEA

Comparison of forecast errors (n mi) for South China Sea (SCS) cyclones using the regression equations developed on SCS cyclones (dependent) and using the regression equations developed on NW Pacific cyclones (independent).

| | 24-HR | 48-HR | 72-HR |
|---|---|---|---|
| ALL (Dependent) | 74(395) | 146(376) | 223(361) |
| North (Independent) | 83(47) | 181(43) | 275(40) |
| On (Independent) | 68(35) | 108(32) | 195(31) |
| South (Independent) | 68(359) | 138(337) | 210(321) |
| All (Independent) | 70(441) | 140(412) | 215(392) |

In the Atlantic, however, the percent of cases in the north-of-ridge category is rather high compared to the number of cases in the other categories. Thus, the skill of the model with 200 mb steering for the north-of-ridge category translates to better skill overall.

Table 5.12 also shows the verification results for the South China Sea. The verification for the dependent set uses the regression equations that were developed using the surface pressure, 850 mb heights, 700 mb heights, and 500 mb heights with no ridge or speed stratification. The independent set is comprised of the same cyclone cases but uses the regression equations developed for the NW Pacific cyclones. Note that comparable results are obtained using the NW Pacific regression equations. Thus, unless it is impossible to select the proper ridge category, it is suggested that the regression equations developed for the NW Pacific be used for the South China Sea.

Table 5.13 presents a comparison between the CSU84 version with 500 mb steering and perfect-prog data and the official forecast and the best objective technique for the period 1979-1981. These operational errors were compiled from the Annual Tropical Cyclone Report (1979-1981). Over the last few years, the best objective technique has been the One-Way Interactive Tropical Cyclone Model (OTCM). Although one of the objectives in the development of a new prediction model was the improvement at the longer forecast periods, sizeable reduction in forecast error is also evident at the shorter period.

Analogous to the Atlantic, the sensitivity of the model was evaluated by perturbing the initial cyclone position as a way of simulating operational conditions. Using the mean deviation of satellite-derived cyclone positions from the JTWC best track positions

TABLE 5.13

Forecast errors (n mi) of CSU84 using 500 mb steering and perfect-prog data on dependent (C5-D-PP) and independent (C5-I-PP) sets for the NW Pacific compared to the official (JTWC) forecast errors and the operational errors of the best objective technique (OTCM). The comparison is based on a nearly homogeneous sample of cyclone cases for the years 1979-1981. The forecast errors for the official (JTWC) and the best operational technique (OTCM) were compiled from the Annual Typhoon/Tropical Cyclone Reports (1979-1981). The number of cases appear in parentheses.

| | 24-HR | | | | 48-HR | | | | 72-HR | | | |
|---|---|---|---|---|---|---|---|---|---|---|---|---|
| | C5-D-PP | C5-I-PP | JTWC | BEST | C5-D-PP | C5-I-PP | JTWC | BEST | C5-D-PP | C5-I-PP | JTWC | BEST |
| North | 77(122) | 95(75) | --- | --- | 135(89) | 171(57) | --- | --- | 188(71) | 242(42) | --- | --- |
| On | 60(256) | 81(131) | --- | --- | 121(215) | 161(105) | --- | --- | 199(172) | 252(91) | --- | --- |
| South | 76(1322) | 80(667) | --- | --- | 144(1243) | 155(617) | --- | --- | 198(1167) | 215(570) | --- | --- |
| ALL | 74(1700) | 81(873) | 121(2570) | 122(1204) | 141(1547) | 157(779) | 237(1984) | 185(969) | 197(1410) | 221(703) | 357(1499) | 345(727) |

for 1974-1983 (calculated from figures in Table 2-3 of the 1983 Annual Tropical Cyclone Report of 13.3 n mi for cyclones possessing a well-defined eye, 19.3 n mi for cyclones possessing a well-defined circulation center and 35.8 n mi for all others), the following adjustments to the initial best track positions were made:

1) if the intensity of the cyclone was greater than 69 kts, the initial position was altered by .2 degrees (12 n mi);

2) if the intensity of the cyclone was between 35 and 69 kts, the initial position was altered by .3 degrees (18 n mi);

3) otherwise, the initial position was altered by .5 degrees (30 n mi);

Based on the sensitivity test done on the Atlantic cases indicating that initial position errors increase the forecast errors the most when the estimated initial position is in error to the north of the actual position, all of the best track initial latitudes were increased northward by the adjustments cited above. Model run C5-I-PP/(62-81/BT) using 500 mb steering on the 1962-1981 independent set was used as the control run. The results shown in Table 5.14, therefore, represent the worst case situation. In addition, since cyclone intensities were not recorded on every forecast situation prior to 1977, and since these cases appear with an intensity of zero in the best track file, the initial positions were altered by an amount greater than necessary on many of the cases. Also, with the 1983 typhoon season, JTWC no longer extrapolates forward 2-3 hours to estimate a warning position. Instead, the reconnaissance fix is made at the synoptic time of the warning and no extrapolation of the initial warning position is necessary. Thus,

TABLE 5.14

Forecast errors (n mi) in the NW Pacific and the percent increase in error as a result of displacing the best track initial position northward (PBT) either 12, 18 or 30 n mi depending on cyclone intensity. Model run C5-I-PP/(62-81/BT) was used as the control case and appears as BT in the table.

| | 24-HR | | | 48-HR | | | 72-HR | | |
|---|---|---|---|---|---|---|---|---|---|
| | BT | PBT | % | BT | PBT | % | BT | PBT | % |
| North | 95(75) | 113(75) | 19% | 171(57) | 192(57) | 12% | 242(42) | 269(42) | 11% |
| On | 81(131) | 97(131) | 20% | 161(105) | 185(105) | 15% | 252(91) | 279(91) | 11% |
| South | 80(667) | 95(667) | 19% | 155(617) | 167(617) | 8% | 215(570) | 224(570) | 4% |
| All | 81(873) | 97(873) | 20% | 157(779) | 171(779) | 9% | 221(703) | 234(703) | 6% |

initial position error now can be expected to be reduced somewhat from those prior to 1983.

As with the Atlantic sensitivity test, Table 5.14 indicates that the impact of a poor initial position is greatest at 24 hours and decreases steadily to about an 11% increase in error at the higher latitude at 72 hours. Unlike the Atlantic, however, the effect of displacing the initial position northward was smallest south of the ridge.

Model Runs Using Operational Data. The model was tested on NW Pacific cyclones using actual forecast fields produced by the Fleet Numerical Oceanography Center (FNOC) hemispheric primitive equation model. Again, because 200 mb prognostic heights are not archived, the version of the model with 500 mb steering was used. For the NW Pacific, this presented no problems since this version was more accurate overall than the version of the model with 200 mb steering. Table 5.15A

TABLE 5.15A

Verification of the model for 1968-1981 using perfect-progs with both dependent and independent sets (C5-DI-PP/(68-81)/BT); actual progs (C5-DI-AP/(68-81)/BT); actual progs and pseudo-warning positions (C5-DI-AP/(68-81)/PBT) for the NW Pacific. The model uses 500 mb steering. Number of cases are in parentheses and they differ beyond 24 hours due to missing forecast fields.

| | 24-HR | | | 48-HR | | | 72-HR | | |
|---|---|---|---|---|---|---|---|---|---|
| | C5-DI-PP 68-81/BT | C5-DI-AP 68-81/BT | C5-DI-AP 68-81/PBT | C5-DI-PP 68-81/BT | C5-DI-AP 68-81/BT | C5-DI-AP 68-81/PBT | C5-DI-PP 68-81/BT | C5-DI-AP 68-81/BT | C5-DI-AP 68-81/PBT |
| North | 80(104) | 80(104) | 88(104) | 141(74) | 150(51) | 153(51) | 190(58) | 265(41) | 274(41) |
| On | 69(291) | 69(291) | 76(291) | 132(238) | 136(219) | 142(219) | 216(195) | 256(187) | 260(187) |
| South | 78(1509) | 78(1509) | 85(1509) | 149(1403) | 163(1380) | 168(1380) | 204(1310) | 251(1339) | 256(1339) |
| All | 77(1904) | 77(1904) | 84(1904) | 146(1715) | 159(1650) | 164(1650) | 205(1563) | 252(1567) | 257(1567) |

TABLE 5.15B

Verification of the model on independent set using perfect-progs for 1968-1981.

| | 24-HR | 48-HR | 72-HR |
|---|---|---|---|
| | C5-I-PP 68-81/BT | C5-I-PP 68-81/BT | C5-I-PP 68-81/BT |
| North | 96(46) | 164(36) | 214(29) |
| On | 83(100) | 160(81) | 253(71) |
| South | 81(527) | 157(490) | 219(453) |
| All | 82(673) | 158(607) | 223(553) |

presents the verfication of the model using actual forecast fields and pseudo-warning positions (C5-DI-AP/(68-81/PBT)) along with the perfect-prog version (C5-DI-PP/(68-81/BT)) and the atual prog version using best track initial positions (C5-DI-AP/(68-81/BT)). To simulate warning positions, pseudo-warning positions were computed by randomly perturbing the best track initial cyclone positions by an amount equal to warning position errors encountered operationally. Thus, if the cyclone intensity was greater than 69 kts, the initial position was perturbed by 0.2 degrees (12 n mi), for intensities of 35 kts to 69 kts, the initial position was perturbed by 0.3 degrees (18 n mi), for intensities less than 35 kts, the initial position was perturbed by 0.5 degrees (30 n mi).

As in the Atlantic simulation, model run C5-DI-PP was an attempt to compare homogeneous cyclone cases for the period 1968-1981 and as a result, both dependent and independent cases from the perfect-prog approach were combined. Table 5.15B presents the forecast errors using just the independent cases for this time period. A fair comparison between the perfect-prog and real prog verification should lie somewhere between the two runs. Based on this comparison, the increase in forecast error using actual forecast fields ranges from approximately 37% at 72 hours for the north-of-ridge category to approximately 13% at 72 hours for the on-the-ridge category.

A homogeneous comparison of selected techniques for 1979-1981 accomplished by T. Tsui (NEPRF, personal communication) is shown in Table 5.16. For comparison, the forecast errors for CSU84 for the same years with actual forecast fields and with the best track initial

TABLE 5.16

A nearly homogeneous comparison of forecast errors (n mi) between CSU84 using 500 mb steering with actual forecast fields and perturbed initial position (C5-DI-AP) and selected dynamical and climatological operational objective techniques for 1979–81 in the NW Pacific (provided by Tsui, NEPRF). In each case, the corresponding official forecast error is indicated in parentheses for a homogeneous sample. HPAC - half persistence and climatology; CLMW - climatology based on warming position; OTCM - one-way interactive dynamical model; NTCM - nested two-way interactive dynamical model.

| | 24h | 48h | 72h |
|---|---|---|---|
| OTCM | 126(124) | 229(233) | 320(348) |
| HPAC | 137(126) | 231(229) | 320(339) |
| CLMW | 157(126) | 247(229) | 327(343) |
| NTCM | 143(124) | 248(235) | 354(368) |
| C5-DI-AP | 80(129) | 152(235) | 235(330) |

positions randomly perturbed (C5-DI-AP/(79-81/PBT)) are also included. Note the very substantial reduction in the forecast error.

Since the largest forecast errors are normally associated with recurving cyclones, an in-depth analysis of the forecast errors for all recurving cyclones during the period 1978–1981 was performed. Table 5.17 and Table 5.18 list all of the cyclones that comprise this set along with their respective official forecast errors. Note that with the exception of 1981, the average error for recurving cyclones was significantly greater at 72 hours than the average error for non-recurving cyclones.

The skill of any objective technique and the confidence a forecaster places on a particular technique is based on its ability to forecast a change in the track, either in direction or speed. As mentioned earlier, any simple technique based on persistence and climatology performs satisfactorily on straight-line climatological tracks. Obviously, these objective aids will do poorly on cyclones that

deviate from their previous course or from climatology. Thus, many objective techniques are least useful in those particular non-climatological situations when the forecaster needs objective guidance the most.

To evaluate how the new model performed on those difficult cases when the forecaster really needed to rely on objective guidance, the 00Z and 12Z forecast situations that resulted in abnormally high forecast errors (greater than 500 n mi. at 72 hours) were selected from the 1978-1981 set of recurving cyclones presented in Tables 5.17 and 5.18. These forecast situations, along with their subsequent forecast verification are presented in Tables 5.19 through 5.22. The tables also inlude a homogeneous comparison of all forecasts made for each cyclone. In comparing the official forecast errors and this model's forecast errors, several points should be kept in mind. The official forecast is highly subjective and is heavily biased towards the previous forecasts. In contrast, all prediction models, including this model, are objective techniques with little bias from one forecast to the next. In these respects, the official forecast tends to lag the objective techniques when a large change in direction becomes necessary and thus is at a disadvantage whenever forecast errors are compared. In addition, prior to the 1983 tropical cyclone season, the initial warning position was extrapolated forward approximately three hours from the latest reconnaissance fix position. As a result, the ensuing initial position error could be expected to have an impact on the subsequent forecast positions.

TABLE 5.17

List of official forecast errors for NW Pacific recurving cyclones for 1978 and 1979. Number of forecasts are in parentheses. TY indicates typhoon; TS indicates tropical storm.

| 1978 | 24-HR Error | 48-HR Error | 72-HR Error |
|---|---|---|---|
| #1 TS Nadine | 185(16) | 568(12) | 980(08) |
| #2 TY Olive | 100(32) | 224(28) | 328(20) |
| #3 TS Polly | 93(12) | 139(08) | 208(02) |
| #7 TY Virginia | 112(39) | 231(35) | 399(31) |
| #15 TY Faye | 158(40) | 360(36) | 514(29) |
| #18 TY Irma | 92(12) | 134(08) | 154(04) |
| #19 TY Judy | 127(14) | 242(10) | 346(06) |
| #22 TY Mamie | 182(14) | 386(10) | 722(06) |
| #24 TY Ora | 124(17) | 314(11) | 460(05) |
| #27 TY Phyllis | 132(24) | 263(20) | 436(15) |
| #29 TS Tess | 108(16) | 194(12) | 367(08) |
| #31 TY Viola | 96(25) | 269(21) | 434(17) |
| #32 TS Winnie | 238(08) | 614(04) | ------- |
| Avg. for recurvers | 129(269) | 287(215) | 451(151) |
| Avg. for non-recurvers | 125(305) | 255(220) | 370(153) |
| 1979 | | | |
| #2 TY Bess | 114(17) | 265(13) | 348(09) |
| #3 TY Cecil | 87(37) | 191(33) | 320(29) |
| #4 TS Dot | 130(23) | 244(20) | 315(16) |
| #12 TY Irving | 163(34) | 286(30) | 441(28) |
| #13 TY Judy | 105(36) | 173(27) | 277(23) |
| #15 TS Ken | 116(10) | 278(07) | 415(03) |
| #16 TY Lola | 88(21) | 172(19) | 287(14) |
| #19 TY Owen | 146(33) | 250(29) | 327(25) |
| #21 TS Roger | 195(13) | 251(09) | 303(04) |
| #23 TY Tip | 135(56) | 259(52) | 345(48) |
| #27 TY Abby | 164(48) | 286(39) | 338(26) |
| Avg. for recurvers | 132(328) | 242(278) | 338(223) |
| Avg. for non-recurvers | 114(263) | 203(193) | 282(145) |

TABLE 5.18

List of official forecast errors for NW Pacific recurving cyclones for 1980 and 1981. Number of forecasts are in parentheses. TY indicates typhoon; TS indicates tropical storm.

| 1980 | 24-HR Error | 48-HR Error | 72-HR Error |
|---|---|---|---|
| #2 TS Carmen | 154(09) | 266(07) | 250(05) |
| #3 TY Dom | 137(39) | 191(27) | 324(23) |
| #4 TY Ellen | 130(31) | 300(27) | 484(23) |
| #12 TY Lex | 137(32) | 314(24) | 499(20) |
| #13 TY Marge | 114(26) | 276(20) | 506(12) |
| #17 TY Orchid | 95(16) | 175(12) | 284(08) |
| #20 TY Sperry | 176(19) | 324(10) | 571(08) |
| #21 TS Thelma | 145(11) | 358(07) | 978(04) |
| #22 TY Vernon | 145(21) | 216(17) | 248(13) |
| #23 TY Wynne | 119(41) | 248(36) | 370(30) |
| #25 TY Betty | 131(36) | 306(29) | 524(28) |
| #27 TY Dinah | 145(13) | 304(09) | 673(05) |
| Avg. for recurvers | 133(294) | 268(225) | 442(179) |
| Avg. for non-recurvers | 116(188) | 205(139) | 283(87) |

| 1981 | | | |
|---|---|---|---|
| #1 TY Freda | 106(19) | 222(14) | 369(09) |
| #2 TS Gerald | 161(15) | 289(11) | 426(07) |
| #5 TY June | 119(18) | 227(13) | 196(05) |
| #18 TY Agnes | 104(21) | 167(17) | 244(12) |
| #21 TY Doyle | 149(10) | 269(06) | 494(02) |
| #22 TY Elsie | 97(27) | 213(23) | 377(19) |
| #24 TY Gay | 163(32) | 275(27) | 410(24) |
| #25 TY Hazen | 130(33) | 263(30) | 361(26) |
| #26 TY Irma | 76(29) | 118(25) | 141(21) |
| Avg. for recurvers | 120(204) | 222(166) | 324(125) |
| Avg. for non-recurvers | 122(254) | 216(177) | 342(122) |

TABLE 5.19

Difficult forecast situations that resulted in 72-hour official forecast errors greater than 500 n mi. A homogeneous comparison for each cyclone is made. The number in parentheses is the number of homogeneous forecast situations. JTWC is the official forecast; C5-I-PP is the model version using 500 mb steering with perfect progs; C2-I-PP is the model version using 200 mb steering with perfect-prog; C5-I-AP is the model version using 500 mb steering with actual prognostic fields and perturbation of the initial position. At 24 hours, results for C5-I-AP are identical to results for C5-I-PP.

| | | 24-HR | | | 48-HR | | | | 72-HR | | | |
|---|---|---|---|---|---|---|---|---|---|---|---|---|
| 1978 | | JTWC | C5-I-PP | C2-I-PP | JTWC | C5-I-PP | C2-I-PP | C5-I-AP | JTWC | C5-I-PP | C2-I-PP | C5-I-AP |
| 1 | TS Nadine | 130(4) | 74(2) | 48(2) | 414(4) | 121(2) | 92(2) | 352(2) | 672(2) | 89(2) | 241(2) | 459(2) |
| | 010812 | 19 | 77 | 54 | 186 | 104 | 104 | 305 | 564 | 100 | 242 | 348 |
| | 010900 | 21 | 71 | 42 | 280 | 137 | 80 | 398 | 779 | 77 | 239 | 569 |
| 2 | TY Olive | 43(4) | 46(4) | 54(4) | 84(4) | 92(4) | 123(4) | 76(4) | 75(4) | 95(4) | 157(4) | 91(4) |
| 3 | TS Polly | 116(2) | 72(2) | 57(2) | 205(2) | 157(2) | 153(2) | 221(2) | 378(1) | 176(1) | 181(1) | 341(1) |
| 7 | TY Virginia | 108(14) | 61(14) | 70(14) | 222(14) | 127(14) | 154(14) | 119(14) | 398(14) | 164(14) | 208(14) | 221(14) |
| | 073000 | 121 | 99 | 125 | 284 | 167 | 187 | 198 | 699 | 63 | 20 | 240 |
| | 073012 | 151 | 75 | 25 | 389 | 127 | 138 | 78 | 842 | 174 | 274 | 146 |
| 15 | Faye | 177(11) | 140(11) | 135(11) | 428(9) | 311(9) | 308(9) | 335(9) | 587(7) | 458(7) | 467(7) | 537(7) |
| | 082900 | 181 | 149 | 136 | 522 | 409 | 376 | 483 | 754 | 491 | 414 | 672 |
| | 082912 | 248 | 211 | 201 | 546 | 399 | 381 | 470 | 682 | 403 | 363 | 587 |
| | 083012 | 196 | 145 | 137 | 511 | 219 | 252 | 250 | 719 | 203 | 348 | 134 |
| 22 | Mamie | 117(3) | 173(3) | 163(3) | 270(3) | 198(3) | 227(3) | 212(3) | 714(3) | 210(3) | 227(3) | 435(3) |
| | 093012 | 229 | 163 | 125 | 413 | 300 | 262 | 333 | 758 | 200 | 113 | 394 |
| | 100100 | 117 | 229 | 247 | 162 | 214 | 299 | 278 | 661 | 144 | 236 | 478 |
| | 100112 | 5 | 126 | 116 | 234 | 80 | 119 | 25 | 722 | 285 | 331 | 434 |

TABLE 5.19 (cont'd)

| 1978 | 24-HR | | | 48-HR | | | | 72-HR | | | |
|---|---|---|---|---|---|---|---|---|---|---|---|
| | JTWC | C5-I-PP | C2-I-PP | JTWC | C5-I-PP | C2-I-PP | C5-I-AP | JTWC | C5-I-PP | C2-I-PP | C5-I-AP |
| 24 TY Ora | 98(4) | 107(4) | 100(4) | 255(4) | 144(4) | 122(4) | 140(4) | 497(3) | 178(3) | 162(3) | 206(3) |
| 101000 | 115 | 102 | 100 | 347 | 138 | 140 | 117 | 591 | 87 | 70 | 184 |
| 101012 | 126 | 110 | 97 | 394 | 146 | 114 | 192 | 507 | 239 | 187 | 260 |
| 27 TY Phyllis | 100(8) | 39(8) | 45(8) | 261(8) | 64(8) | 84(8) | 109(8) | 448(8) | 96(8) | 118(8) | 193(8) |
| 101712 | 119 | 28 | 41 | 365 | 45 | 64 | 18 | 569 | 69 | 93 | 118 |
| 101800 | 181 | 26 | 52 | 412 | 69 | 67 | 133 | 637 | 92 | 93 | 276 |
| 101812 | 98 | 79 | 78 | 327 | 130 | 152 | 200 | 554 | 271 | 252 | 175 |
| 29 TS Tess | 191(1) | 72(1) | 75(1) | 397(1) | 163(1) | 102(1) | 94(1) | 638(1) | 258(1) | 266(1) | 242(1) |
| 31 TY Viola | 69(8) | 57(8) | 66(8) | 207(8) | 127(8) | 114(8) | 141(8) | 426(8) | 170(8) | 179(8) | 259(8) |
| 111912 | 150 | 73 | 74 | 334 | 122 | 146 | 124 | 500 | 245 | 252 | 309 |
| 112000 | 135 | 38 | 58 | 266 | 123 | 131 | 119 | 603 | 199 | 187 | 315 |
| 112012 | 11 | 7 | 35 | 155 | 201 | 80 | 192 | 526 | 172 | 149 | 255 |
| 112100 | 30 | 103 | 104 | 242 | 176 | 132 | 216 | 741 | 190 | 250 | 335 |
| TOTAL | 113(59) | 79(59) | 80(59) | 269(57) | 147(57) | 154(57) | 165(57) | 450(51) | 192(51) | 221(51) | 280(51) |

TABLE 5.20

Same as Table 5.19 but for 1979.

| 1979 | 24-HR | | | 48-HR | | | | 72-HR | | | |
|---|---|---|---|---|---|---|---|---|---|---|---|
| | JTWC | C5-D-PP | C2-D-PP | JTWC | C5-D-PP | C2-D-PP | C5-I-AP | JTWC | C5-D-PP | C2-D-PP | C5-I-AP |
| 2 TY Bess | 95(5) | 59(5) | 71(5) | 196(5) | 135(5) | 125(5) | 199(5) | 392(5) | 267(5) | 178(5) | 384(5) |
| 032012 | 128 | 88 | 80 | 309 | 201 | 208 | 226 | 664 | 367 | 329 | 481 |
| 032100 | 109 | 46 | 40 | 250 | 57 | 13 | 271 | 592 | 164 | 28 | 392 |
| 3 TY Cecil | 60(13) | 41(13) | 57(13) | 140(13) | 68(13) | 88(13) | 81(10) | 252(13) | 93(13) | 107(13) | 119(10) |
| 041512 | 33 | 49 | 110 | 257 | 151 | 143 | 163 | 536 | 233 | 191 | 212 |
| 041700 | 138 | 10 | 69 | 339 | 18 | 125 | --- | 514 | 67 | 245 | --- |
| 4 TS Dot | 94(2) | 41(2) | 47(2) | 134(2) | 107(2) | 114(2) | 89(2) | 183(2) | 176(2) | 215(2) | 186(2) |
| 12 TY Irving | 145(13) | 90(13) | 83(13) | 267(12) | 138(12) | 134(12) | 138(12) | 430(10) | 172(10) | 161(10) | 175(10) |
| 081100 | 187 | 194 | 129 | 365 | 277 | 197 | 275 | 572 | 248 | 212 | 329 |
| 081112 | 88 | 73 | 65 | 341 | 123 | 124 | 175 | 521 | 134 | 142 | 189 |
| 081200 | 103 | 66 | 56 | 321 | 32 | 55 | 41 | 535 | 49 | 42 | 97 |
| 13 TY Judy | 89(14) | 74(14) | 64(14) | 166(13) | 164(13) | 149(13) | 160(13) | 281(11) | 258(11) | 223(11) | 273(11) |
| 082000 | 89 | 63 | 62 | 329 | 210 | 196 | 166 | 649 | 309 | 285 | 255 |
| 082012 | 139 | 81 | 67 | 340 | 260 | 234 | 208 | 616 | 268 | 217 | 180 |
| 15 TS Ken | 143(2) | 53(2) | 43(2) | 241(2) | 129(2) | 132(2) | 193(2) | 562(1) | 290(1) | 426(1) | 750(1) |
| 16 TY Lola | 88(5) | 53(5) | 48(5) | 179(3) | 96(3) | 97(3) | 146(3) | 195(1) | 74(1) | 160(1) | 305(1) |
| 19 TY Owen | 133(7) | 91(7) | 84(7) | 233(6) | 182(6) | 190(6) | 228(6) | 290(5) | 254(5) | 321(5) | 236(5) |
| 092312 | 309 | 170 | 153 | 445 | 260 | 236 | 264 | 506 | 246 | 228 | 232 |

TABLE 5.20 (cont'd)

| 1979 | 24-HR | | | 48-HR | | | | 72-HR | | | |
|---|---|---|---|---|---|---|---|---|---|---|---|
| | JTWC | C5-D-PP | C2-D-PP | JTWC | C5-D-PP | C2-D-PP | C5-I-AP | JTWC | C5-D-PP | C2-D-PP | C5-I-AP |
| 21 TS Roger | 268(2) | 175(2) | 201(2) | 322(2) | 329(2) | 361(2) | 370(2) | 350(2) | 429(2) | 406(2) | 561(2) |
| 100400 | 365 | 248 | 277 | 515 | 387 | 419 | 431 | 586 | 482 | 430 | 627 |
| 23 TY Tip | 107(24) | 100(24) | 98(24) | 196(23) | 176(23) | 180(23) | 182(23) | 281(22) | 203(22) | 203(22) | 220(22) |
| 27 TY Abbey | 183(19) | 90(19) | 91(17) | 339(17) | 138(17) | 135(15) | 152(17) | 371(9) | 151(9) | 140(9) | 152(9) |
| 121000 | 129 | 123 | 127 | 412 | 128 | 153 | 186 | 999 | 272 | 224 | 403 |
| 121012 | 108 | 72 | 51 | 512 | 96 | 82 | 119 | 1145 | 88 | 160 | 142 |
| TOTAL | 121(106) | 81(106) | 81(104) | 222(98) | 145(98) | 147(96) | 162(95) | 314(81) | 195(81) | 191(81) | 220(81) |

TABLE 5.21

Same as Table 5.19 but for 1980.

| 1980 | 24-HR | | | 48-HR | | | | 72-HR | | | |
|---|---|---|---|---|---|---|---|---|---|---|---|
| | JTWC | C5-D-PP | C2-D-PP | JTWC | C5-D-PP | C2-D-PP | C5-I-AP | JTWC | C5-D-PP | C2-D-PP | C5-I-AP |
| 2 TS Carmen | 125(3) | 109(3) | 112(3) | 105(2) | 148(2) | 133(2) | 81(2) | 187(3) | 133(3) | 190(2) | 77(2) |
| 3 TY Dom | 86(13) | 63(13) | 60(13) | 175(10) | 129(10) | 123(10) | 170(10) | 324(8) | 171(8) | 185(8) | 280(8) |
| 4 TY Ellen | 111(9) | 69(9) | 69(9) | 278(7) | 137(7) | 124(7) | 118(7) | 502(5) | 175(5) | 143(5) | 119(5) |
| 051312 | 202 | 70 | 73 | 398 | 128 | 147 | 148 | 574 | 153 | 136 | 212 |
| 051412 | 154 | 52 | 89 | 314 | 87 | 89 | 72 | 538 | 155 | 92 | 125 |
| 5 TY Forrest | 117(4) | 83(4) | 86(4) | 198(3) | 177(3) | 163(3) | 181(3) | 309(3) | 243(3) | 236(3) | 310(3) |
| 12 TY Lex | 145(12) | 79(12) | 82(12) | 326(3) | 122(3) | 163(3) | 138(3) | 650(2) | 146(2) | 207(2) | 229(2) |
| 080212 | 220 | 36 | 64 | 444 | 127 | 179 | 150 | 775 | 215 | 263 | 265 |
| 080300 | 160 | 48 | 76 | 338 | 76 | 134 | 117 | 524 | 77 | 150 | 192 |
| 17 TY Orchid | 89(3) | 103(3) | 94(3) | 133(3) | 186(3) | 164(3) | 191(3) | 202(2) | 139(2) | 155(2) | 328(2) |
| 20 TY Sperry | 160(5) | 68(5) | 59(5) | 279(3) | 164(3) | 145(2) | 232(3) | 500(2) | 245(2) | 214(2) | 382(2) |
| 091600 | 116 | 102 | 90 | 384 | 221 | 215 | 240 | 653 | 270 | 221 | 385 |
| 21 TS Thelma | 193(1) | 89(1) | 86(1) | 490(1) | 95(1) | 115(1) | 320(1) | 850(1) | 120(1) | 152(1) | 644(1) |
| 22 TY Vernon | 116(5) | 69(5) | 47(5) | 169(5) | 123(5) | 93(5) | 104(5) | 180(5) | 177(5) | 163(5) | 255(5) |

TABLE 5.21 (cont'd)

| 1980 | 24-HR | | | 48-HR | | | | 72-HR | | | |
|---|---|---|---|---|---|---|---|---|---|---|---|
| | JTWC | C5-D-PP | C2-D-PP | JTWC | C5-D-PP | C2-D-PP | C5-I-AP | JTWC | C5-D-PP | C2-D-PP | C5-I-AP |
| 23 TY Wynne | 108(17) | 62(17) | 63(17) | 230(17) | 129(17) | 132(17) | 141(17) | 366(15) | 189(15) | 190(15) | 217(5) |
| 100600 | 177 | 105 | 115 | 380 | 224 | 236 | 164 | 510 | 240 | 239 | 211 |
| 100700 | 142 | 96 | 75 | 289 | 104 | 57 | 149 | 618 | 84 | 10 | 182 |
| 100712 | 119 | 31 | 16 | 305 | 45 | 53 | 39 | 711 | 86 | 116 | 55 |
| 100800 | 190 | 47 | 60 | 395 | 91 | 118 | 74 | 692 | 135 | 165 | 89 |
| 100812 | 59 | 10 | 26 | 276 | 62 | 83 | 53 | 554 | 79 | 114 | 102 |
| 100900 | 104 | 18 | 38 | 332 | 74 | 83 | 60 | 679 | 110 | 119 | 161 |
| 25 TY Betty | 139(13) | 76(13) | 79(13) | 304(13) | 139(13) | 142(13) | 141(13) | 549(13) | 175(13) | 182(13) | 185(13) |
| 102912 | 130 | 241 | 249 | 401 | 499 | 517 | 516 | 554 | 630 | 662 | 645 |
| 103100 | 79 | 36 | 50 | 222 | 66 | 67 | 91 | 558 | 140 | 156 | 182 |
| 103112 | 181 | 24 | 35 | 431 | 54 | 55 | 36 | 902 | 120 | 141 | 116 |
| 110100 | 100 | 18 | 15 | 344 | 80 | 84 | 95 | 527 | 67 | 95 | 77 |
| 110112 | 192 | 62 | 62 | 388 | 131 | 148 | 123 | 780 | 61 | 100 | 65 |
| 110200 | 221 | 77 | 78 | 438 | 62 | 59 | 118 | 1056 | 101 | 53 | 166 |
| 110212 | 146 | 41 | 49 | 223 | 71 | 31 | 55 | 504 | 145 | 113 | 175 |
| 110400 | 54 | 19 | 11 | 260 | 76 | 68 | 80 | 560 | 123 | 167 | 150 |
| 110412 | 141 | 62 | 67 | 447 | 38 | 89 | 116 | 918 | 118 | 148 | 192 |
| TOTAL | 120(89) | 72(89) | 68(89) | 235(69) | 136(69) | 129(68) | 145(69) | 397(60) | 177(60) | 180(59) | 223(60) |

TABLE 5.22

Same as Table 5.19 but for 1981.

| 1981 | 24-HR | | | 48-HR | | | | 72-HR | | | |
|---|---|---|---|---|---|---|---|---|---|---|---|
| | JTWC | C5-I-PP | C2-I-PP | JTWC | C5-I-PP | C2-I-PP | C5-I-AP | JTWC | C5-I-PP | C2-I-PP | C5-I-AP |
| 1 TY Freda | 113(4) | 81(4) | 101(3) | 252(3) | 184(3) | 195(2) | 234(2) | 461(2) | 290(2) | 319(2) | 445(2) |
| 2 TS Gerald | 235(3) | 121(3) | 117(3) | 394(3) | 166(3) | 192(3) | 180(3) | 451(3) | 191(3) | 207(3) | 258(3) |
| 041612 | 213 | 198 | 197 | 478 | 297 | 332 | 247 | 532 | 283 | 355 | 312 |
| 5 TY June | 130(3) | 50(3) | 56(3) | 255(3) | 107(3) | 97(3) | 92(3) | 182(1) | 148(1) | 155(1) | 173(1) |
| 18 TY Agnes | 65(6) | 42(6) | 29(6) | 112(6) | 63(6) | 42(6) | 108(6) | 256(6) | 70(6) | 80(6) | 151(6) |
| 082992 | 44 | 60 | 34 | 91 | 27 | 44 | 72 | 529 | 53 | 164 | 123 |
| 21 Doyle | 58(1) | 82(1) | --- | 299(1) | 57(1) | --- | 91(1) | 390(1) | 294(1) | --- | 458(1) |
| 22 TY Elsie | 79(8) | 74(8) | 66(5) | 173(7) | 117(7) | 89(5) | 128(7) | 352(6) | 143(6) | 112(4) | 185(6) |
| 092612 | 225 | 94 | 92 | 421 | 49 | 60 | 111 | 531 | 88 | 63 | 178 |
| 24 TY Gay | 141(11) | 68(11) | 62(11) | 231(11) | 123(11) | 100(11) | 153(11) | 391(11) | 191(11) | 119(11) | 266(11) |
| 101512 | 374 | 73 | 66 | 535 | 133 | 114 | 182 | 929 | 110 | 67 | 189 |
| 102000 | 99 | 41 | 24 | 274 | 130 | 31 | 209 | 650 | 532 | 240 | 747 |
| 25 TY Hazen | 128(8) | 62(8) | 69(8) | 262(8) | 160(8) | 179(8) | 159(8) | 377(8) | 266(8) | 286(8) | 235(8) |
| 111400 | 156 | 23 | 42 | 467 | 146 | 205 | 195 | 852 | 262 | 371 | 221 |
| 111500 | 249 | 95 | 100 | 453 | 181 | 206 | 174 | 592 | 268 | 311 | 200 |
| 26 TY Irma | 39(10) | 88(10) | 76(10) | 103(10) | 196(10) | 182(10) | 190(10) | 128(9) | 280(9) | 288(10) | 249(9) |
| TOTAL | 104(53) | 72(53) | 65(51) | 201(51) | 140(51) | 131(48) | 152(51) | 317(46) | 204(46) | 196(45) | 245(46) |
| TOTAL (1978-1981) | 116(307) | 76(307) | 74(303) | 231(275) | 142(275) | 141(269) | 156(272) | 365(238) | 192(238) | 196(236) | 238(238) |

However, as discussed earlier, sensitivity tests with the model reveal that initial position errors affect the short-term forecast positions to a much larger degree than the longer-range forecasts.

Note that with the exception of TS Roger in 1979 and one forecast for TY Betty in 1980, both versions of CSU84 using perfect-progs and 500 mb steering/200 mb steering consistently produced forecast errors that were much lower than those of the official forecasts. Although the forecast errors for C5-I-AP (that simulates operational conditions) were usually greater than the perfect-prog versions, the errors were consistently less than the official forecast errors. These results appear to indicate that this new prediction model is able to accurately predict cyclone motion even during very difficult situations that resulted in official forecast "busts".

The only instances where the model did poorly (but still much better than the official forecasts) were on TY Faye in 1978 and on the last few forecasts for TY Gay in 1981. Based on the total forecast errors for the period 1978-1981, CSU84 - using actual forecast fields and pseudo-warning positions - was able to decrease the forecast error of this homogeneous sample by more than 30% for all three forecast periods.

5.3 North Indian Ocean

The verification results for the North Indian Ocean with the perfect-prog method are presented in Table 5.23. Although the comparison between the model and the operational forecast is on an inhomogeneous sample, the amount of improvement is very substantial.

TABLE 5.23

Verification results for the dependent (C5-D-PP) and independent (C5-I-PP) sets for the North Indian Ocean for 1946-1981 using 500 mb steering and perfect-prog and the official (JTWC) and operational error of the best objective technique (BEST) for 1979-1983.

| | 24-HR | | | | 48-HR | | | | 72-HR | | | |
|---|---|---|---|---|---|---|---|---|---|---|---|---|
| | C5-D-PP | C5-I-PP | JTWC | BEST | C5-D-PP | C5-I-PP | JTWC | BEST | C5-D-PP | C5-I-PP | JTWC | BEST |
| North | 62(52) | 99(33) | --- | --- | 115(50) | 166(20) | --- | --- | 160(47) | 237(18) | --- | --- |
| On | 43(48) | 75(21) | --- | --- | 96(48) | 144(18) | --- | --- | 158(48) | 223(17) | --- | --- |
| South | 68(527) | 72(182) | --- | --- | 123(506) | 145(168) | --- | --- | 165(491) | 214(161) | --- | --- |
| ALL | 66(627) | 76(236) | 135(146) | 131(137) HPAC | 121(604) | 147(206) | 265(77) | 258(78) HPAC | 164(586) | 217(195) | 464(30) | 564(12) CLIM |

The model was not run for this ocean basin using real progs. However, assuming the decrease in accuracy using actual forecast fields would be on the same order as the Atlantic and the NW Pacific -- 20% at 48 hours and 30% at 72 hours - errors of 176 n mi at 48 hours and 282 n mi at 72 hours can be projected for all cases. Compared to the best operational techniques, these forecast errors translate to an improvement of 32% at 48 hours and 50% at 72 hours! At 24 hours, there is no degradation due to the use of actual forecast fields since they do not enter into the computation of the 24-hour forecast position. However, as shown for the Atlantic and NW Pacific, perturbing the best-track initial position to simulate warning position errors does have a strong impact on the 24-hour forecast position. Even using the worst case scenario of a northward track perturbation for all cases (which results in a 25% decrease in accuracy), the resulting improvement in the forecast error at 24 hours compared to HPAC is a very creditable 27%.

5.4 Synopsis and Summary

As mentioned earlier, a universal problem of previous statistical-dynamical prediction models is the use of a perfect-prog approach to introducing prognostic data into the development of regression equations. Degradation in skill is commonly observed in operations when actual forecast fields are used. In fact, other than NHC73, they do not attempt to forecast beyond 48 hours. Table 5.24 illustrates the amount of degradation that statistical-dynamical models suffer when they use actual forecast fields.

TABLE 5.24

A comparison of development and operational errors for selected statistical techniques. The developmental errors for NHC73, NHC72, and CLIPER are from Neumann and Lawrence (1973). The operational errors for NHC73, NHC72 and CLIPER are the entire sample errors from Neumann and Pelissier (1981). The errors for SNT are from Nomoto et al. (1976) and the errors for Keenan are from Keenan (1984).

| | 24-HR | | | 48-HR | | | 72-HR | | |
|---|---|---|---|---|---|---|---|---|---|
| | DEV | OP | (OP-DEV) | DEV | OP | (OP-DEV) | DEV | OP | (OP-DEV) |
| NHC73 | 42 | 113 | 71 | 78 | 228 | 150 | 142 | 344 | 202 |
| NHC72 | 68 | 113 | 45 | 175 | 257 | 82 | 308 | 375 | 67 |
| CSU84A*** | 93 | 99 | 6 | 171 | 184 | 13 | 248 | 281 | 33 |
| CSU84P**** | 77 | 84 | 7 | 146 | 164 | 18 | 205 | 257 | 52 |
| SNT* | 141 | 149 | 8 | 234 | 388 | 154 | --- | --- | --- |
| Keenan** | 83 | 99 | 16 | 135 | 222 | 87 | --- | --- | --- |

* SNT is statistical-dynamical model developed by Nomoto et al. (1976) for the NW Pacific in the vicinity of Japan.

** Keenan is statistical-dynamical model developed by Keenan (1984) for the Australian region.

***CSU84A is the Atlantic version of the new model using 500 mb steering. The errors were on a homogeneous sample for the period 1968-1981 and taken from Table 5.10A.

****CSU84P is the NW Pacific version of the new model using 500 mb steering. The errors were on a homogeneous sample for the period 1968-1981 and taken from Table 5.15A.

Note the relatively small amount of deterioration associated with CSU84. Although the degradation suffered by NHC72 is also comparatively small, NHC72 does not use prog data.

This large degradation in skill associated with statistical-dynamical schemes is in large part due to the over-reliance or overweighing of the "perfect" prognostic data at the expense of the analysis data. This problem was vividly shown earlier with the NHC73

predictor selection process that chose predictors from 36- and 48-hour forecast fields for the short-range 12- and 24-hour cyclone motion. As a result, although the model may produce very impressive results in development, when actual forecast fields obviously not as accurate as the verifying analysis fields are used operationally, the accuracy tends to deteriorate. In certain instances where prognostic data are notoriously poor, as in the ocean region to the west of Australia, regression technique using just the analysis data outperforms one using prognostic data (T. Keenan, 1984).

The approach developed here attempts to circumvent this problem by discretizing 72 hours of cyclone motion into three shorter 24-hour time steps. This permits:

(1) the introduction of a revised persistence predictor after each 24 hours of motion

(2) the opportunity to change the category relative to the ridge after each 24 hours of motion

(3) the limiting of the reliance of the model on any one prognostic field to 24 hours of motion

(4) the absence of any degradation for the 24-hour forecast since the first 24 hours of motion is based only on analysis fields

(5) the updating of prognostic data relative to a new cyclone position — not the initial cyclone position.

The advantages of this method over the customary method of applying prognostic data are obvious. If the prognostic fields are in error, there will be no impact on the 24-hour forecast position. In addition, since CSU84 does not use current motion as a predictor, an initial position error will have a much smaller effect on the 24-hour forecast

position than it will with, for example, NHC73 that does use current motion as a predictor. If the 24-hour forecast position is accurate, the updated persistence predictor as well as the ridge category in which to place the cyclone should be accurate. Then, even if the 24-hour forecast field is in error, the resulting 48-hour forecast position certainly will be more accurate than if the motion over 48 hours was calculated from the initial position. Also recall that half of the data needed to compute the height and pressure tendencies at the 24-hour forecast position to determine the 48-hour forecast position come from the analysis field. Thus, a solid forecast track for the early portion of the forecast period has been created on which to build the final 24 hours of motion to determine the 72-hour forecast position.

Comparable Skill of Model. In order to show skill in forecasting cyclone motion, a model's forecast accuracy must exceed that achieved by basic methods such as climatology and persistence. Neumann and Pelissier (1981) have proposed using the CLIPER model as a normalizer or no-skill model to provide a benchmark on which to judge the skills of other models. They compute the percentage improvement or deterioration of a forecast as to how well the CLIPER forecast has done. This percentage is given by:

$$\% = 100\ (E_c - E_m)\ /\ E_c,$$

where % is the percent improvement or deterioration over CLIPER forecast error, $E_c$ is CLIPER forecast error and $E_m$ is the model forecast error. Positive % indicates the model performed better than CLIPER, whereas negative % indicates the model performed poorer than CLIPER.

Figure 5.2 shows the relative skill of NHC73, which was the best overall performer among the operational models at the US National Hurricane Center, and CSU84. The north-of-ridge and on-the-ridge categories for CSU84 were combined to form the north zone since a cursory examination of those cases in the on-the-ridge category revealed that nearly all of the cases were north of 24.5°N. This version of the model used actual forecast fields with random perturbation of the initial position to simulate operational conditions as closely as possible for cyclone cases during 1973-1979.

Panel a presents the ''all'' cyclone category. It appears that relative to CLIPER, CSU84 possesses six times as much skill as NHC73 at 24 and 72 hours. It is also able to beat the official forecast by a wide margin at all forecast periods.

The most significant feature is shown on panel b where CSU84 is clearly superior to climatology and persistence at the longer forecast periods even in the south zone. While NHC73 is degrading rapidly between 48 and 72 hours, CSU84 is improving in performance.

Finally, panel c compares the relative performance on cyclones in the northern zone. The strength of any statistical-dynamical model should emerge in this category and indeed NHC73 and CSU84 performed better than CLIPER by the largest margin in this zone. The relative skill of CSU84 appears to be nearly twice that of NHC73 for this category.

Figures 5.3 through 5.5 offered a graphic comparison of the relative skill of CSU84 and NHC73 for the three categories in the Atlantic. As shown in panel a of Fig. 5.2 and again in Fig. 5.3, CSU84

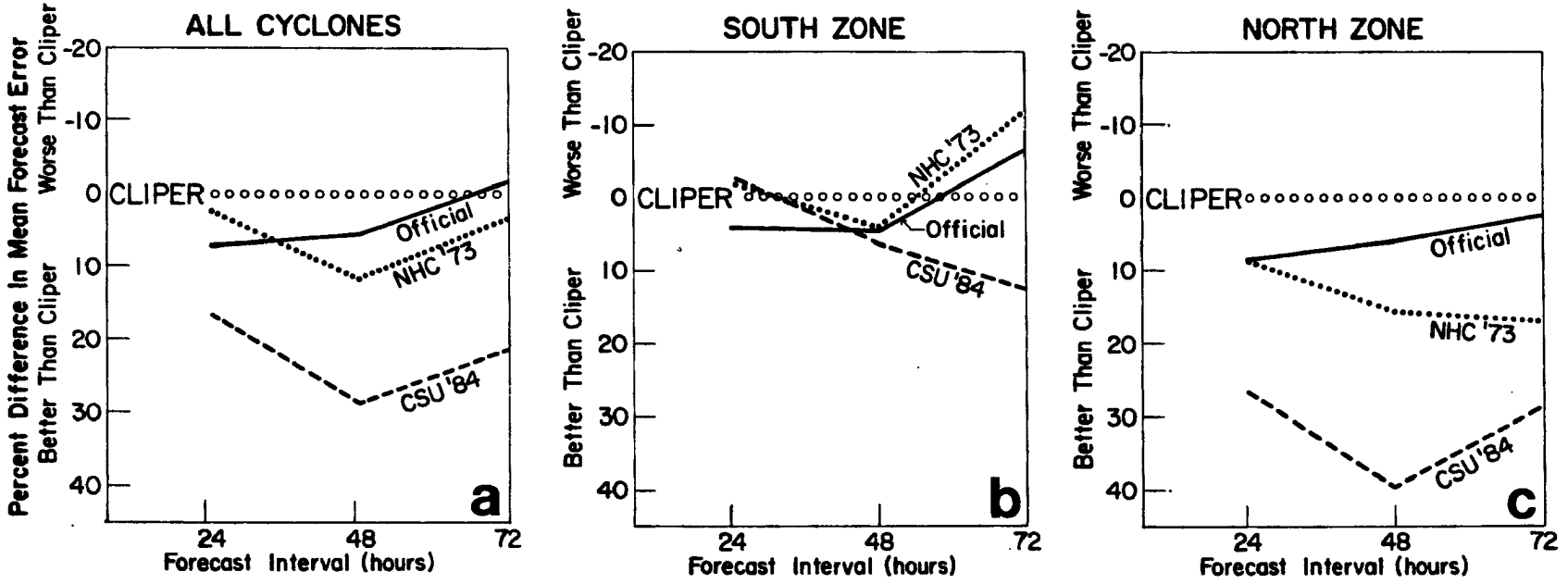


Fig. 5.2. Performance of specified models relative to performance of CLIPER model on (a) entire sample of cyclones, (b) south zone cyclones and (c) north zone cyclones. Sample is nearly homogeneous over years 1973-1979. Forecast errors for CLIPER, NHC73 and official are from Neumann and Pelissier (1981).

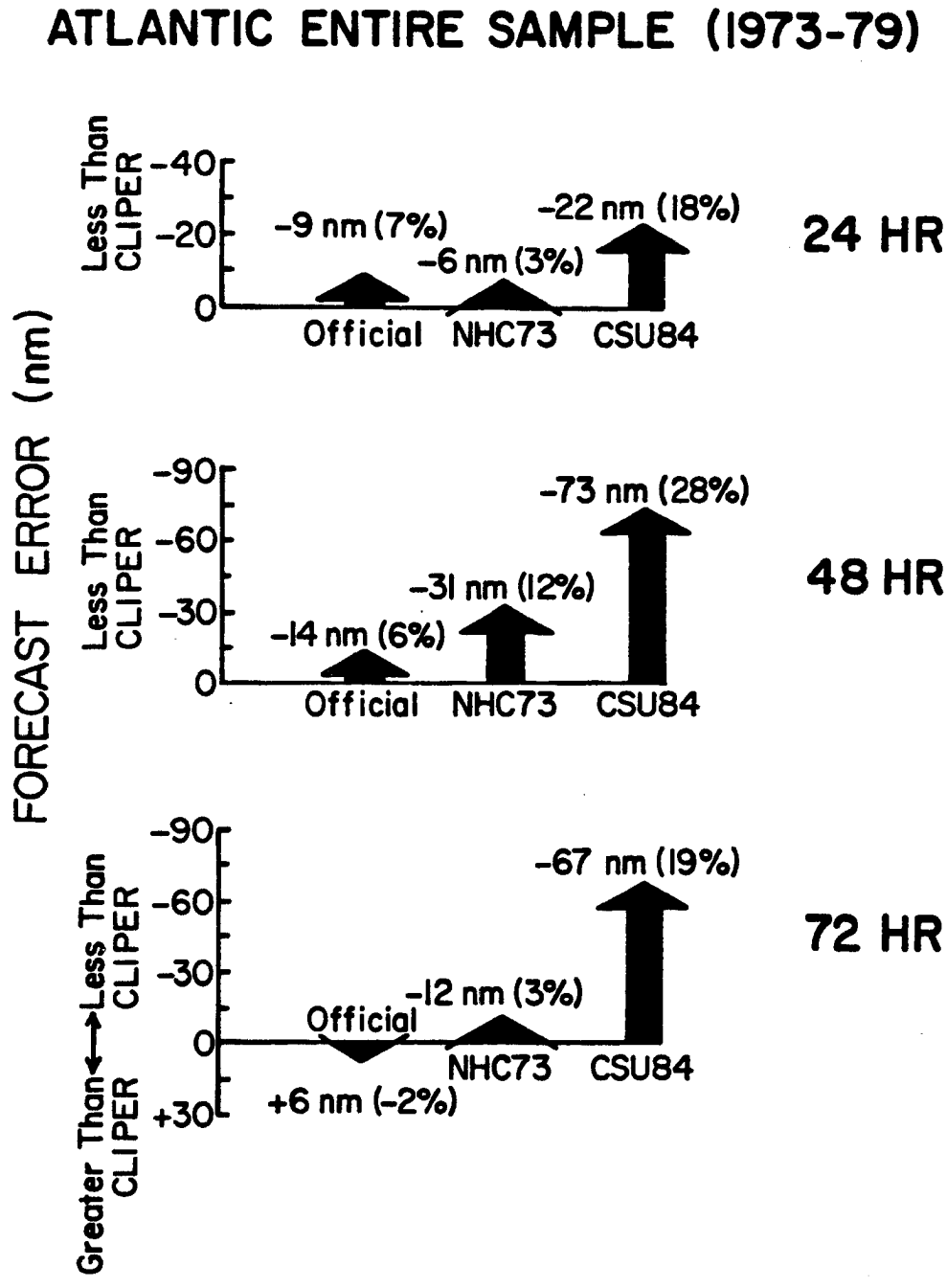


Fig. 5.3. Relative skill of CSU84 compared to NH73 using CLIPER as a no-skill model to provide a benchmark. Decrease or increase in the forecast error over CLIPER is shown with the percent improvement in parentheses for Atlantic entire sample. Errors for NHC73 and official are from Neumann and Pelissier (1981).

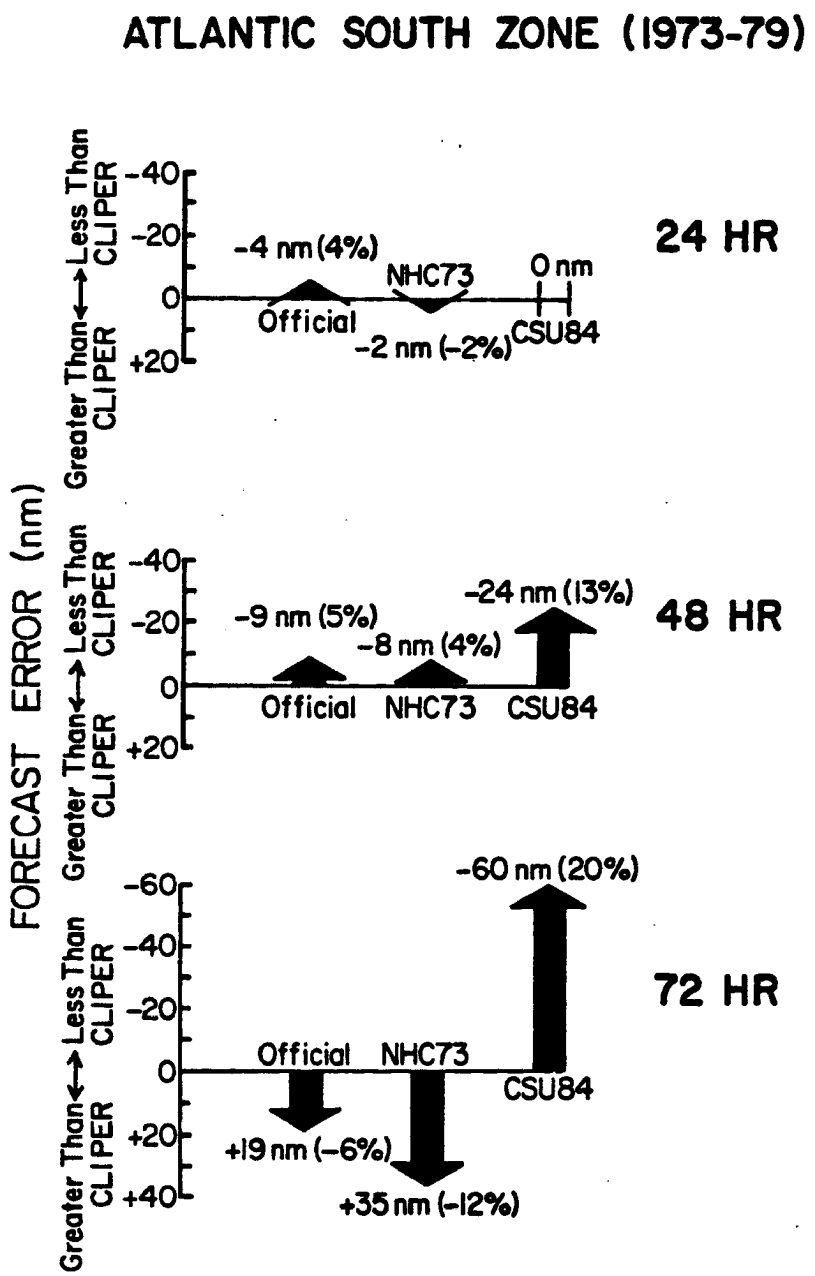


Fig. 5.4. Same as Fig. 5.3 except for Atlantic south zone.

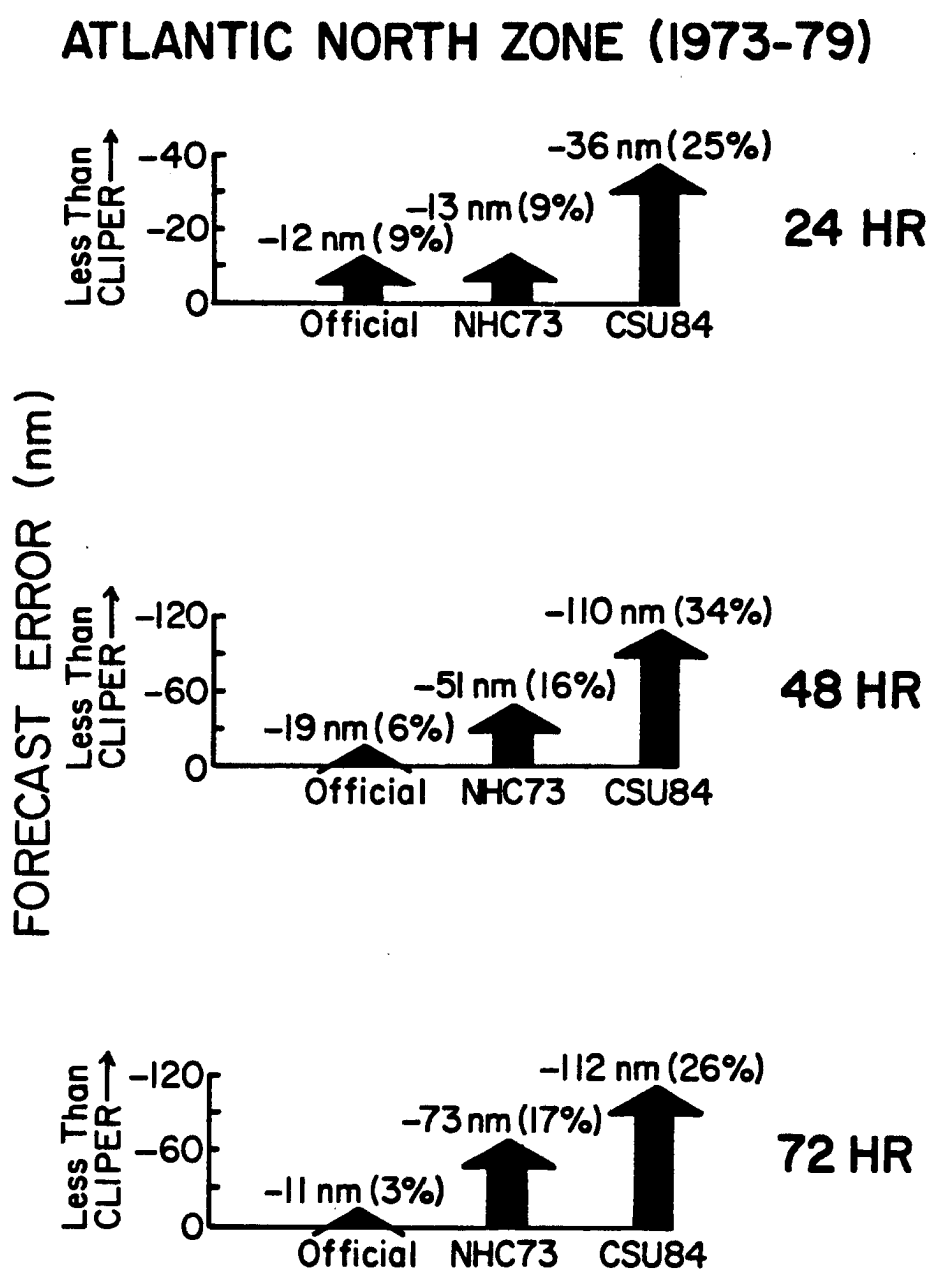


Fig. 5.5. Same as Fig. 5.3 except for Atlantic north zone.

is six times as skillful as NHC73 relative to CLIPER at both the 24- and 72-hour foreast periods for the entire sample. CSU84's high skill at the 24-hour period comes primarily from its strong performance on north zone cyclones (see Fig. 5.5) while the skill at 72 hours comes largely from its performance on south zone cyclones (see Fig. 5.4).

The model's encouraging performance on north zone cyclones appears to be related to its ability to accurately depict and anticipate changes in the synoptic and steering forcings as a result of the ridge stratification and the 24-hour time steps. The short time steps permit the category the cyclone is placed relative to the ridge to change as it becomes necessary. The model's ability to provide accurate position forecasts at the longer periods for the south zone is similarly related to the segmented 24-hour time steps which permits the reintroduction of updated persistence at each step.

A similar comparison for the NW Pacific was done using HPAC as the normalizer or no-skill model to provide the benchmark for comparison. The forecast error data used for this comparison are from NEPRF (T. Tsui, personal communication) and appear in Fig. 5.6 and 5.7.

The relative skill of CSU84 compared to the two best overall performers in the NW Pacific (OTCM and NTCM) is considerable and the apparent improvement in forecast error provided by CSU84 is encouraging. The model was at least four times as skillful as the best operational technique (OTCM) at all forecast periods. As in the Atlantic, the ridge stratification and the 24-hour time steps are believed to provide a method for the model to optimumly formulate the current synoptic state and its changes that affect cyclone movement over a 24-hour time span.

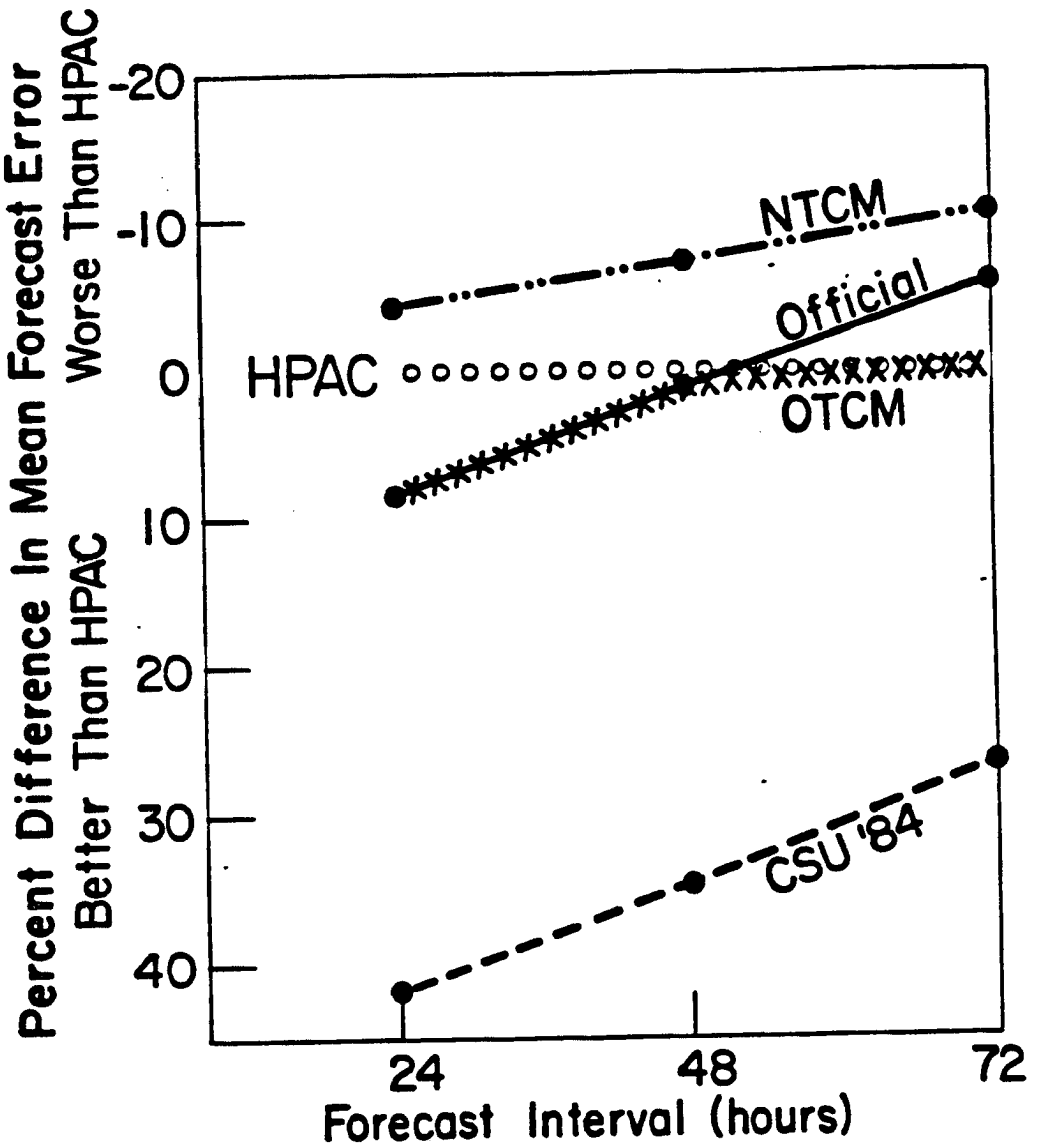


Fig. 5.6. Performance of specified models relative to performance of HPAC on NW Pacific cyclones. Sample is nearly homogeneous over years 1979-1981. Forecast errors for official, HPAC, NTCM and OTCM are from Tsui (personal communication).

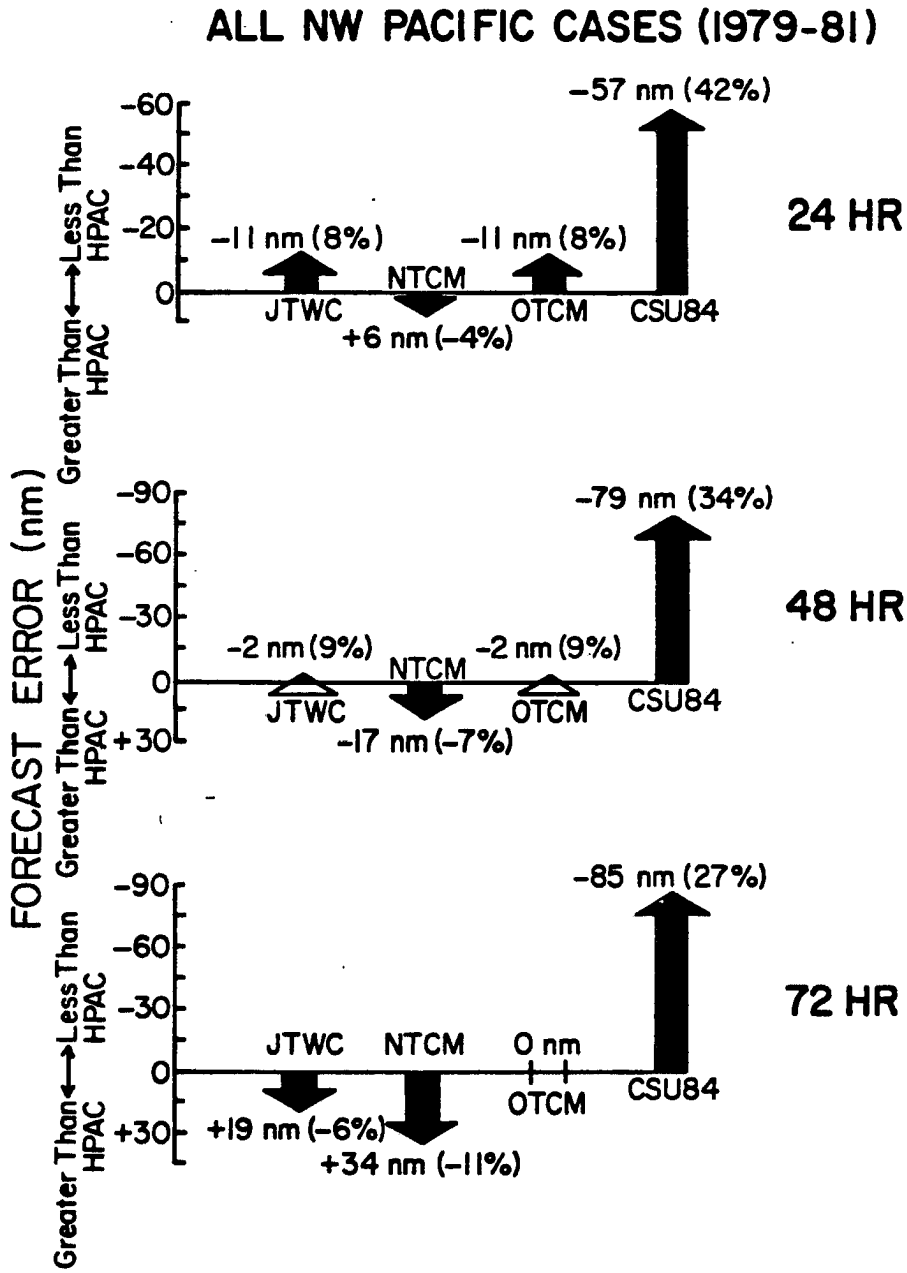


Fig. 5.7. Relative skill of CSU84 for the NW Pacific compared to OTCM and NTCM using HPAC as a no-skill model to provide a benchmark. Decrease or increase in the forecast error over HPAC is shown with the percent improvement in parentheses. Errors for OTCM, NTCM and JTWC are from NEPRF (T. Tsui, personal communication).

Figures 5.8 and 5.9 for the Atlantic and NW Pacific, summarize the results of the various attempts to simulate operational conditions in comparison with operational forecast models. The perfect-prog runs for CSU84 are shown along with the runs using actual progs as well as the runs with both actual progs and pseudo-warning positions. Note that the CSU84 forecast errors from the operational simulation runs lie closer to the perfect-progs than to those of the other operational models. This appears to strongly indicate that CSU84 is capable of improving one- to three-day track predictions in the operational arena.

Based on the CSU84 forecast errors for the Atlantic and NW Pacific, it would appear that cyclones in the Atlantic basin are more difficult to forecast. A cursory examination of the number of forecast situations in each of the three categories relative to the ridge indicates that in the NW Pacific, the south-of-ridge cases dominate with a sizeable number in the on-the-ridge category. Relatively few cases occur north of the ridge. For the Atlantic, the situation is reversed. The number of cases north of the ridge is nearly the same as the number to the south with relatively few cases on the ridge.

The reason for the observed difference in cyclone tracks for the two ocean basins is due to differences in climatology. Majority of cyclones in the NW Pacific form at a lower latitude than those in the Atlantic. Hence, Pacific cyclones have a tendency to track poleward for greater distances prior to recurving eastward than cylones in the Atlantic. Following recurvature, shearing or extratropical transition follows rather quickly. Atlantic cylones, on the other hand, come under

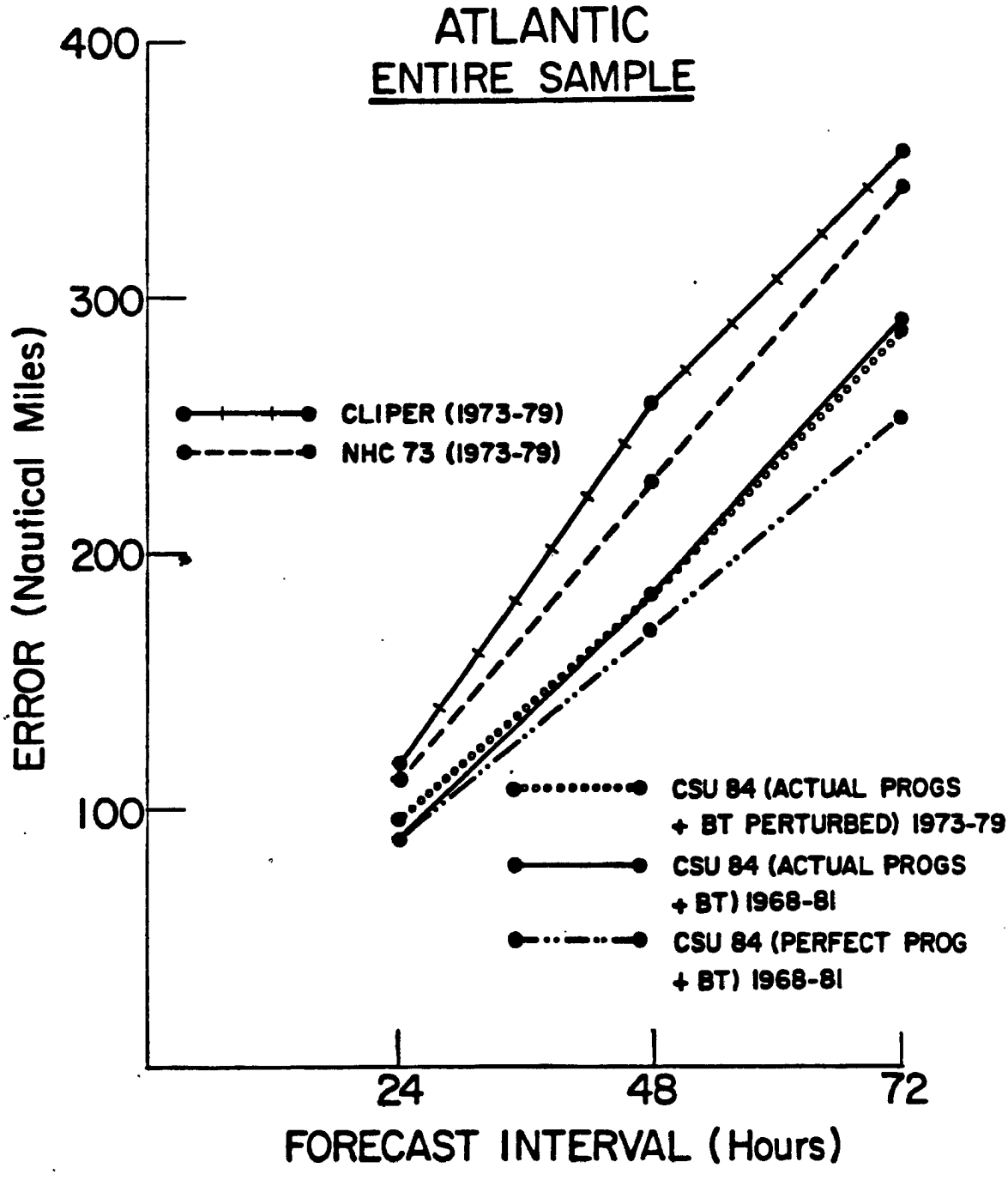


Fig. 5.8. Mean Atlantic forecast error (n mi) for the various CSU84 runs compared to CLIPER and NHC73 at 24, 48 and 72 hours. Errors for CLIPER and NHC73 are for 1973-1979 entire sample and are taken from Neumann and Pelissier (1981). One of the CSU84 runs denoted by oooooooooo is for 1973-1979. The other runs are for 1968-1981.

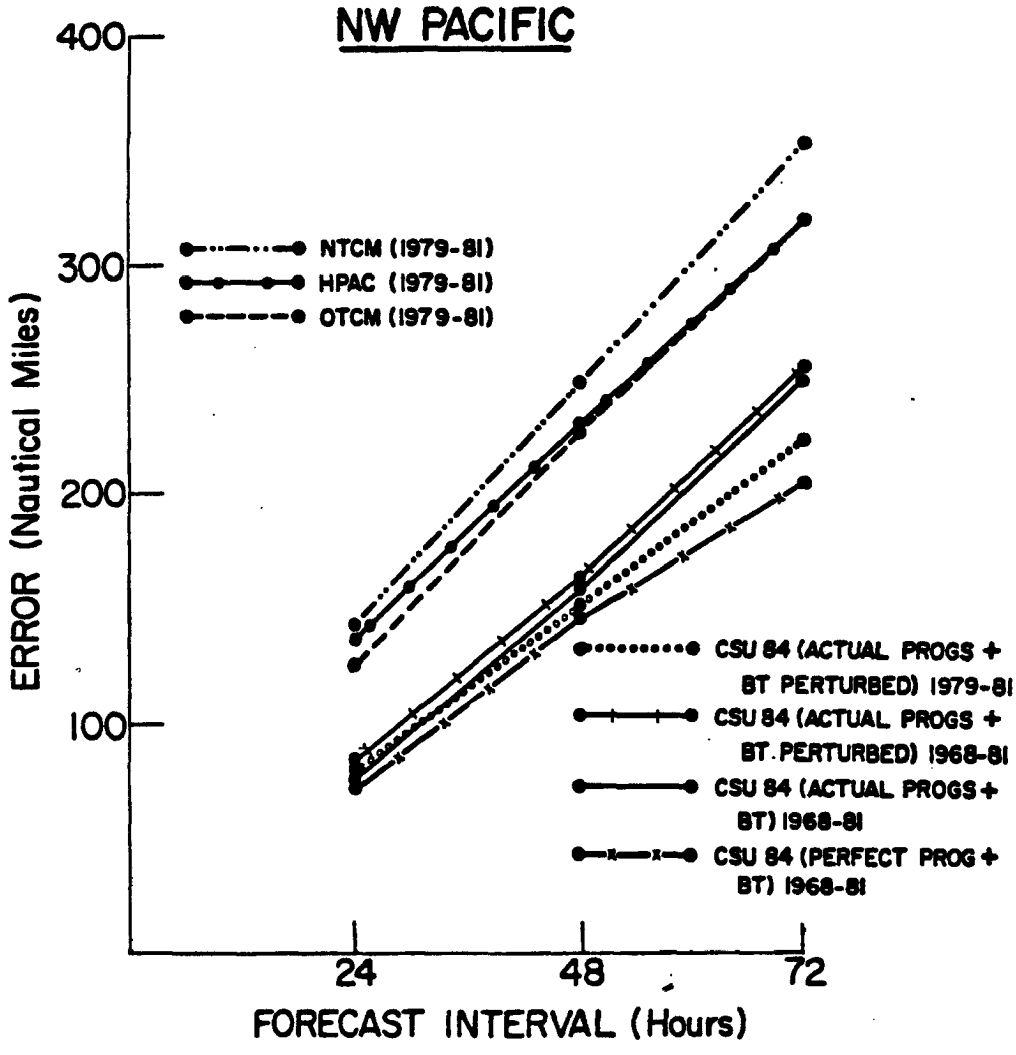


Fig. 5.9. Mean NW Pacific forecast error (n mi) for the various CSU84 runs compared to HPAC, OTCM and NTCM at 24, 48 and 72 hours. Errors for HPAC, OTCM and NTCM are for 1979–1981 and were provided by NEPRF (T. Tsui, personal communication). One of the CSU84 runs denoted by oooooooooo is for 1979–1981. The other runs are for 1968-1981.

the influence of mid-latitude westerlies before tracking very far poleward and the portion of their track that would fall into the on-ridge category is relatively small.

In addition, as shown by Xu and Gray (1982) the percentage of cyclones undergoing fast (> 7.5 m/s), slow (< 2.5 m/s) or looping motion is much higher overall in the Atlantic than in the NW Pacific. Figure 5.10 is taken from the work of Xu and Gray (1982) to illustrate the difference. Due to the large number of fast-moving cyclones at low latitudes and the large number of slow-moving and looping cyclones at higher latitudes, along with the relatively small number of cases, the average forecast errors become inflated by these difficult forecast situations.

In view of these difficult forecast cases, the quite skillful performance of CSU84 in the Atlantic is particularly noteworthy. In the NW Pacific and North Indian Oceans where a statistical-dynamical model is not available, the potential for a large improvement in track forecast accuracy looks very promising.

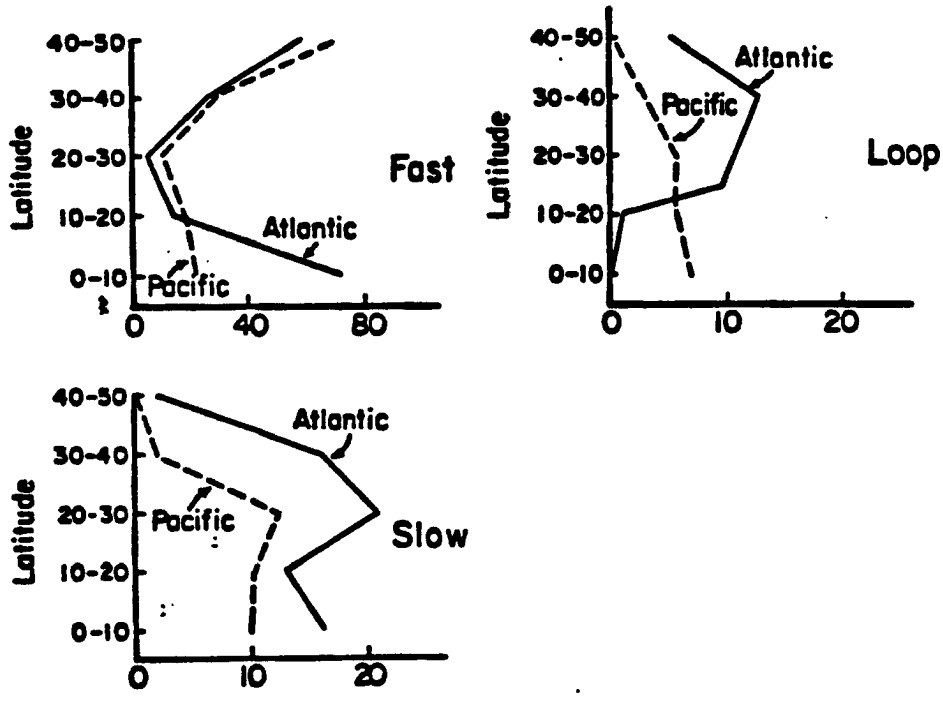


Fig. 5.10. Percentage of storms in the Atlantic and western North Pacific which are fast (> 7.5 m/s), slow (<2.5 m/s) or looping vs. latitude. (From Xu and Gray, 1982).

## 6. CONCLUSION

Although significant progress has been made in developing statistical and dynamical models for forecasting the tracks of tropical cyclones, the forecast errors over the past decade have shown little improvement. The lack of observations over the data-sparse regions of the tropical oceans, and the resulting difficulty of accurately specifying the initial state of the atmosphere for both the dynamical tropical cyclone models and the global PE models, have most often been cited for the lack of improvement. "Give me more observations and better analyses and I'll give you better track forecasts" has been the motto for the last few years.

This adage of requiring better analyses is certainly true, but another important consideration to improving the accuracy of statistical track prediction models is the proper application of the existing data. The need for synoptic data, especially in a prognostic sense, to be able to forecast cyclone motion at the longer forecast periods and to predict anomalous motion is well known. However, the statistical-dynamical models in existence that incorporate the output from a numerical model as one set of predictors apply the prognostic data always from the initial position of the cyclone to the desired forecast projection of 12, 24, 36, 48, or 72 hours. The inherent weakness of using prognostic data in such a manner was shown by comparison with the results from this newly developed model using an approach of introducing prognostic

data relative to each new cyclone position as if they were analysis data.

The suggested new method of applying the various climatological, persistence and synoptic predictors is patterned after the normal procedure followed by operational forecasters as they subjectively formulate the forecast track. This process usually begins with an examination of the current and 24-hour old analysis fields relative to the initial position of the cyclone. Synthesis of the synoptic information with motion persistence produces a short-range 24-hour forecast motion. The 24-hour forecast field is introduced at this point in the cycle to provide the updated environmental influence on the cyclone relative to the new position. The cyclone is then projected forward another 24 hours. Likewise, the 48-hour forecast field provides the environmental forcings to project the cyclone from the 48-hour forecast position to the 72-hour position. Persistence information is also formulated relative the latest cyclone position.

Although the scheme proposed here was developed with an emphasis on improving the forecast accuracy for cyclones at the higher latitudes and at the longer forecast periods, it performed at the lower latitudes and at shorter forecast periods with "significant" skill. As shown in Chapter 5, the degradation in skill resulting from the use of actual forecast fields was minimal compared to that suffered by the other discussed statistical-dynamical models.

The increase in forecast errors between the perfect-prog and the actual prog cases for the three other statistical-dynamical models that were examined ranged from 87 n mi to 154 n mi at 48 hours compared to

less than 20 n mi for CSU84. Further, two of the previous models do not forecast beyond 48 hours.

A comparison of the model under a simulated operational setting on a nearly homogeneous sample in comparison with the best operational techniques in the Atlantic and NW Pacific using climatology and persistence as a normalizer to indicate the relative skill of the models as compared to a no-skill forecast was presented in Chapter 5. The comparison indicated the strength of the new scheme at both the shorter 24-hour foreast period and the longer 72-hour forecast period. For the entire Atlantic sample, CSU84 is <u>six</u> times as skillful as NHC73 relative to CLIPER at both the short and long forecast times. CSU84's relatively high skill at the 24-hour period comes primarily from its strong performance on north zone cyclones while the skill at 72 hours comes largely from its performance on south zone cyclones.

The model's encouraging performance on north zone cyclones appears to be related to its ability to acurrately depict and anticipate changes in the synoptic and steering forcings as a result of the ridge stratification and the 24-hour time steps. Its ability to provide accurate position forecasts at the longer periods for the south zone is similarly related to the segmented 24-hour time steps which permits the reintroduction of persistence at each step.

Equally strong performance of CSU84 in the NW Pacific was evident. The model was at least <u>four</u> times as skillful as the best operational technique (OTCM) at all forecast periods. Again, the ridge stratification and the 24-hour time steps are believed to provide a method for the model to formulate the current synoptic state and its changes that affect cyclone movement over a 24-hour time span.

The key to this large improvement in accuracy lies in the unique application of the predictors normally used in statistical prediction models. Climatology is incorporated via a stratification scheme based on the position of the cyclone relative to the 500 mb subtropical ridge. Each cyclone forecast situation is initially stratified by one of three categories relative to the 500 mb ridge -- south-of-ridge, on-the-ridge, or north-of-ridge -- and the appropriate regression equations are used to calculate the 24-hour displacement. The 72-hour forecast period is segmented into three 24-hour time steps and the 24-hour displacements are stepped off until the desired multi-day forecast projection is reached. This permits the introduction of updated persistence and synoptic predictors relative to the new cyclone position as well as the opportunity to change the stratification category as necessary based either on the past direction of motion or on the judgment of the forecaster. Two hundred millibar geostrophic winds $5^{o}$ to $20^{o}$ northwest and north of the cyclone were used as key steering predictors in the Atlantic and in recurvature situations for strong typhoons in the NW Pacific. Five hundred millibar steering predictors proved to be more accurate for all other situations in the NW Pacific, however.

An additional advantage of a prediction model such as this is the ease with which it can be applied directly at operational locations and aboard ships without a link to a large computer data base. The initial analyses and the 24- and 48-hour forecast fields of sea level pressure and 500 mb and 200 mb geopotential heights are all that is required. Further, since the model permits forecaster intervention in computing the forecast positions, the operational forecaster could easily modify the synoptic predictors required for input if the analysis or prognostic

field appears to be in error. The forecaster could also make his own forecast fields based on subjective extrapolation of large-scale synoptic patterns in the areas where predictors are required.

This discretized forecast method revealed the significant contribution to the forecast of the steering predictors on 24-hour motion at the higher latitude in the Atlantic. For the NW Pacific, steering predictors had a strong impact only for east-west motion north of the ridge and only at the 200 mb level. The motion of south-of-ridge cyclones was dominated by persistence whereas the motion of on-the-ridge category cyclones was strongly influenced by the synoptic predictors, primarily the current 500 mb heights. For the North Indian Ocean, cyclone motion south of the ridge was dominated by persistence. However, cyclone motion on or north of the ridge was strongly dependent on synoptic predictors, primarily the 24-hour tendency of surface pressure.

Incremental improvement in the accuracy of this model can likely be made by several smaller modifications. It is felt, however, that the major improvement was gained by the special methodological approach developed in this paper.

One obvious source of improvement is to redevelop the regression equations for use in the NW Pacific and North Indian Oceans using synoptic data from the Navy FNOC rather than the NMC data used to develop the CSU84 equations. Fiorino, et al., (1982), while comparing the NTCM and MFM, discovered considerably degraded performance for the NTCM when it was initialized with NMC analysis rather than FNOC tropical analysis. An initialization procedure that resulted in much smaller

amplitude of the zonal wind features in the NMC data (greatest in the lower 1000-850 mb levels) was suspected as the primary reason. Redevelopment of the regression equations usng the FNOC data was the projected plan if the degradation using the Navy prognostic fields had been severe. Since it was not, the plan to redevelop the equations was abandoned. However, since the statistical characteristics of the two data sources differ, one would expect better model performance if it used the same data source in operational use that it used in development. The fact that the deterioration in the accuracy of the model was as small as it was is certainly encouraging.

The ideal method of developing the regression equations, as alluded to in Chapter 2, is to use the MOS approach and use the actual forecast fields instead of analysis fields. This would certainly be possible for the NW Pacific since there are adequate cyclone cases and the forecast fields for the surface and 500 mb level are available since 1968. The degradation in skill from the development to the operational fields then primarily would be eliminated. This may now be more difficult, however, since the Navy has abandoned its hemispheric PE model and is now using a global PE model.

A second source of possible improvement to this scheme would be the substratification of the development set to separate those cyclones with very fast motion (>7.5 m/s) from those with very slow (<2.5 m/s) motion. An attempt along this line was made and alluded to in Chapter 3. However, the method of separating these two classes of cyclones was poor and the results were discouraging. Better results could probably be achieved if, as mentioned in Chapter 5, a larger threshhold value of positive or negative 500 mb height pattern indicator was used and the

resulting fast and slow equations were used on only those cyclones that exhibited fast or slow motion based on, for example, their past 12-hour motion. Instead, in the aborted method attempted here, all cyclones used either the fast or slow equations and this is probably where the scheme failed. The only problem with the suggested substratification is the small sample size that might result for the very fast and very slow subsets.

Other improvements may be possible by changing the grid for computing the geostrophic winds from the geopotential height gradients. This model used a diamond grid with grid points north, south, east, and west $5^{o}$ away from the point where the steering wind was being computed. Patterns other than a diamond or distances greater than $5^{o}$ could be tested. The use of actual observed winds rather than height gradients should be tested although the use of wind field data did not seem to produce any signficant impact on forecast errors when compared to the use of height field data for Southern Hemisphere statistical-synoptic schemes (Keenan, personal communication).

In any event, CSU84 - as developed and detailed in this paper - appears to offer very encouraging verification results and appears to produce significant improvement in forecast skill. The amount of reduction in forecast position errors suggested by these results should, hopefully, hasten the testing of the model in an operational environment.

ACKNOWLEDGEMENTS

The author is indebted to Professor William M. Gray for his support and encouragement of this operationally oriented research topic. The author also profited from extensive discussion with Jianmin Xu of the China Central Meteorological Agency, Beijing. Jianmin Xu was a visiting scientist on Professor Gray's research project from 1980 to 1982. Thanks go to Robert Merrill, Roger Edson and Mike Fiorino for their manuscript review. Gratitude is also expressed to Ms. Barbara Brumit, Patti Nimmo, and Cindy Schrandt for their invaluable help in manuscript preparation and drafting. And, of course, none of this would have been possible without the patience and understanding of my wife, Frances.

This research was performed while the author was a graduate student with the support of the U.S. Air Force. The research was primarily supported by the Naval Environmental Prediction Research Facility Grant No. N00014-83-K-0002 with supplementary computing resources from the National Center for Atmospheric Research which is sponsored by the National Science Foundation Grant No. ATM-8214041.

## REFERENCES

Allen, R. L., 1984: COSMOS: CYCLOPS objective steering model output statistics. Postprints, 15th Conf. on Hurricanes and Tropical Meteorology. Miami, FL, Jan 9-13, 1984, 14-20.

38th Annual Interdepartmental Hurricane Conference, 1984: Minutes. Federal Coordinator for Meteorological Services and Supporting Research, US Dept. of Commerce, NOAA, Rockville, MD, Jan. 24-26, 4-4.

Arakawa, H., 1961: Prediction of movements and surface pressures of typhoon centers in the Far East by statistical methods. National Hurricane Research Project Report No. 43, 18 pp.

Arakawa, H., 1964: Statistical method to forecast the movement and the central pressure of typhoons in the western North Pacific. J. Appl. Meteor., Vol. 3, No. 5, 524-528.

Bao, C. L. and J. C. Sadler, 1982: On the speed of recurving typhoons over the western North Pacific Ocean. NEPRF CR 82-05, 57 pp.

Burroughs, L. D. and S. Brand, 1973: Speed of tropical storm and typhoons after recurvature in the western Pacific Oceans. J. Appl. Meteor., 12, 452-458.

Chan, J. C. L., 1982: On the physical processes responsible for tropical cyclone motion. Dept. Atmos. Sci. Paper 358, Colo. State Univ., Fort Collins, CO, 200 pp.

Cressman, G. P., 1959: An operational objective analysis system. Mon. Wea. Rev., 87, 367-374.

Fiorino, M., E. J., Harrison, Jr., and D. G. Marks, 1982: A comparison of the performance of two operational dynamic tropical cyclone models. Mon. Wea. Rev., 110, 651-656.

Gentry, R. C., 1983: Forecasting cyclone recurvature with upper tropospheric winds. NASA Tech. Memo 85114, 23 pp.

George, J. E., 1975: Tropical cyclone motion and surrounding parameter relationships. Dept. Atmos. Sci. Paper No. 241, Colo. State Univ., Ft. Collins, CO, 105 pp.

George, J. E. and W. M. Gray, 1977: Tropical cyclone recurvature and non-recurvature as related to surrounding wind-height fields. J. Appl. Meteor., 16, 34-42.

Gray, W. M., 1977: Tropical cyclone motion and steering flow relationships in the western Atlantic and in the western Pacific. Preprints, 11th Tech. Conf. on Hurricanes and Tropical Meteorology, Dec. 13-16, Miami Beach, FL, 472-477.

Harrison, E. J., Jr., 1973: Three-dimensional numerical simulation of tropical systems utilizing nested finite grids. J. Atmos. Sci., 30, 1528-1543.

Harrison, E. J., Jr., 1981: Initial results from the Navy two-way interactive nested tropical cyclone model. Mon. Wea. Rev., 109, 173-177.

Hodge, W. T. and G. F. McKay, 1970: A computer program to select typhoon analogs and printout their descriptions, including subsequent changes. First Progress Report, NAVWEA RSCHFAC Project Order PO-9003, ESSA, Nat. Wea. Rev. Center, Asheville, NC 40 pp.

Hodur, R. M. and S. D. Burk, 1978: The Fleet Numerical Weather Central tropical cyclone model: Comparison of cyclonic and one-way interactive boundary conditions. Mon. Wea. Rev., 106, 1665-1671.

Holland, G. J., 1983: Tropical cyclone motion: Environmental interaction plus a beta effect. J. Atmos. Sci., 40, 2, 328-342.

Hope, J. R. and C. J. Neumann, 1970: An operational technique for relating the movement of existing tropical cyclones to past tracks. Mon. Wea. Rev., 98, 925-933.

Hovermale, J. B. and R. E. Livezey, 1977: Three-year performance characteristics of the NMC hurricane model. Preprints 11th Tech. Conf. on Hurricanes and Tropical Meteorology, AMS, Miami Beach, FL, 122-125.

IMSL Library Reference Manual, Ed. 9, 1982: 6th Floor-NBC Bldg., 7500 Bellaire Blvd., Houston, TX 77036.

Jordan, E., 1952: An observational study of the upper wind circulation around tropical storms. J. Meteor., 9, 340-346.

Jarrell, J. D., S. Brand, and D. S. Nicklin, 1978: An analysis of western North Pacific tropical cyclone forecast errors. Mon. Wea. Rev., 106, 925-937.

Jarrell, J. D. and Somerville, 1970: A computer technique for using typhoon analogs as a forecast aid. Technical Paper No. 6-70. U.S. Weather Research Facility, Norfolk, VA, 39 pp.

Joint Typhoon Warning Center, 1962-1983: Annual Typhoon/Tropical Cyclone Reports. NAVOCEANCOMCEN/JTWC Guam.

Keenan, T. D., 1984: Recent development in the statistical prediction of tropical cyclone movement in Australia. Postprints 15th Conference on Hurricane and Tropical Meteorology, Miami, FL, January 9-13.

Kumar, S. and K. Prasad, 1973: An objective method for the prediction of tropical storm movement in Indian seas. Indian J. Met. Geophys., 24, pp. 31-34.

Lund, I. A., 1971: An application of stagewise and stepwise regression procedures to a problem of estimating precipitation in California. J. Appl. Meteor., 10, 892-902.

Miller, B. I., 1958: The use of mean layer winds as a hurricane steering mechanism. National Hurricane Res. Proj. Rept., No. 18, 24 pp.

Miller, B. I. and P. L. Moore, 1960: A comparison of hurricane steering levels. Bull. Amer. Meteor. Soc., 41, 2, 59-63.

Miller, B. I. and P. P. Chase, 1966: Prediction of hurricane motion by statistical methods. Mon. Wea. Rev., 94, 6, 399-406.

Miller, B. I., E. C. Hill, and P. P. Chase, 1968: A revised technique for forecasting hurricane movement by statistical methods. Mon. Wea. Rev., 96, 540-548.

National Hurricane Center Staff, 1976: Annual data and verification tabulation Atlantic tropical cyclones, 1974. NOAA Tech. Memo. NWS NHC 1, 54 pp.

National Hurricane Center Staff, 1977: Annual data and verification tabulation Atlantic tropical cyclones, 1975. NOAA Tech. Memo. NWS NHC 2, 63 pp.

National Hurricane Center Staff, 1977: Annual data and verification tabulation Atlantic tropical cyclones, 1976. NOAA Tech. Memo. NWS NHC 4, 66 pp.

National Hurricane Center Staff, 1979: Annual data and verification tabulation Atlantic tropical cyclones, 1977. NOAA Tech. Memo. NWS NHC 8, 46 pp.

National Hurricane Center Staff, 1979: Annual data and verification tabulation Atlantic tropical cyclones, 1978. NOAA Tech. Memo. NWS NHC 9, 61 pp.

National Hurricane Center Staff, 1980: Annual data and verification tabulation Atlantic tropical cyclones, 1979. NOAA Tech. Memo. NWS NHC 13, 77 pp.

National Hurricane Center Staff, 1981: Annual data and verification tabulation Atlantic tropical cyclones, 1980. NOAA Tech. Memo. NWS NHC 15, 78 pp.

National Hurricane Center Staff, 1982: Annual data and verification tabulation Atlantic tropical cyclones, 1981. NOAA Tech. Memo. NWS NHC 17, 84 pp.

National Hurricane Center Staff, 1983: Annual data and verification tabulation Atlantic tropical cyclones, 1982. NOAA Tech. Memo. NWS NHC 19, 68 pp.

Neumann, C. J., 1972: An alternate to the HURRAN tropical cyclone forecast system. NOAA Tech. Memo., NWS SR-62, 32 pp.

Neumann, C. J., 1975: A statistical study of tropical cyclone positioning errors with economic applications. NOAA Tech. Memo. NWS SR-82, 21 pp.

Neumann, C. J., 1979: Operational techniques for forecasting tropical cyclone intensity and movement. World Weather Watch WMO Tropical Cyclone Project #6, II. 4-3 - II. 4-26.

Neumann, C. J., and J. R. Hope, 1972: A performance analysis of the HURRAN tropical cyclone forecast system: Mon. Wea. Rev., 100, 245-255.

Neumann, C. J., J. R. Hope and B. I. Miller, 1972: A statistical method of combining synoptic and empirical tropical cyclone prediction systems. NOAA Tech. Memo NWS Sr-63, 32 pp.

Neumann, C. J. and M. B. Lawrence, 1973: Statistical-dynamical prediction of tropical cyclone motion. NOAA Tech. Memo NWS SR-69, 34 pp.

Neumann, C. J., M. B. Lawrence and P. W. Leftwich, 1979: NMC numerical model errors and their impact on tropical cyclone track forecasting. Preprints Fourth Conference on Numerical Weather Prediction, Silver Spring, MD, October 29-November 1.

Neumann, C. J. and J. M. Pelissier, 1981: Models for the prediction of tropical cyclone motion over the North Atlantic: An operational evaluation. Mon. Wea. Rev., 109, 522-538.

Nomoto, S., K. Takenaga, M. Shimamura, and T. Hara, 1976: A statistical prediction for typhoon movement using numerically forecasted data as predictors. J. Meteor. Soc. Japan, Vol. 54, 99-104.

Pike, A. C., 1972: Improved barotropic hurricane track prediction by adjustment of the initial wind field. NOAA Tech. Memo. NWS SR-66, 16 pp.

Renard, R. J., 1968: Forecasting the motion of tropical cyclones using a numerially derived steering current and its bias. Mon. Wea. Rev., Vol. 96, No. 7, 453-469.

Renard, R. J., S. G. Calgon, M. J. Daley, and S. K. Rinard, 1973: Forecasting the motion of North Atlantic tropical cyclones by the objective MOHATT scheme. Mon. Wea. Rev., Vol. 101, No. 3, 206-214.

Riehl, H., W. H. Haggard, and R. W. Sanborn, 1956: On the prediction of 24 hour hurricane motion. J. Meteor., 13, 415-420.

Sanders, F. and R. W. Burpee, 1968: Experiments in barotropic hurriane track forecasting. J. Appl. Meteor., 7, 313-323.

Shewchuk, J. D. and R. L. Elsberry, 1978: Improvement of a baroclinic typhoon motion prediction system by adjustment of the initial wind field. Mon. Wea. Rev., 106, 713-718.

Tropical Cyclones of the North Atlantic Ocean, 1871-1981, U.S. Dept. of Commerce, NOAA.

Tse, S. Y. W., 1966: A new method for the prediction of typhoon movement using the 700 mb chart. Quart. J. Roy. Met. Soc., 92, 239-253.

Tsui, T., 1984: Postprints from 15th Conference on Hurricanes and Tropical Meteorology, AMS, 40-44.

Veigas, K. W., 1961: Prediction of twelve, twenty-four, and thirty-six hour development of hurricanes by statistical methods. Final Report, The Travelers Research Center, Hartford, CT, 39 pp.

Veigas, K. W., R. B. Miller, and G. H. Howe, 1959: Probabilistic prediction of hurricane movements by synoptic climatology. Travelers Weather Research Center, Occasional Papers in Meteorology, No. 2, Hartford, CT, 54 pp.

Wang, G., 1960: A method in regression equations for forecasting the movement of typhoons. Bull. Amer. Meteor. Soc., Vol. 41, No. 3, 115-124.

Weir, R. C., 1982: Predicting the acceleration of northward-moving tropical cyclones using upper-tropospheric winds. NOCC/JTWC Tech. Note 82-2, 40 pp.

Woodcock, F., 1980: On the use of analogues to improve regression forecasts. Mon. Wea. Rev., 108, 292-297.

Xu, J. M. and W. M. Gray, 1982: Environmental circulations associated with tropical cyclone experiencing fast, slow and looping motion. Dept. Atmos. Sci. Paper No. 346, Colo. State Univ., Ft. Collins, Co, 111 pp.

## APPENDIX A

### List Of All Objective Techniques Currently In Operational Use

Atlantic

HURRAN - HURRicane ANalog system uses analog cyclones in a time and space window similar to the current cyclone to generate forecast track. (Hope and Neumann, 1970)

CLIPER - CLImatology and PERsistence system is a purely statistical technique that uses climatology and persistence information as predictors to generate regression equations using essentially the same predictors used in the analog sense by HURRAN. (Neumann, 1972)

NHC67 - statistical-synoptic system that uses linear combinations of observed height and height change fields at the 1000, 700, and 500 mb surfaces as predictors for zonal and meridional components of cyclone motion. Persistence is also used for the early forecast periods. (Miller, et al., 1968)

NHC72 - combines output from HURRAN, CLIPER and NHC67 into one forecast using a modified stepwise screening technique. (Neumann, et al., 1972)

NHC73 - combines output from CLIPER, a steering subset using height gradients and thicknesses and a synoptic subset that introduces 24-, 36-, and 48-hour 500 mb prognostic height data into one forecast using an optimized geographical stratification system. (Neumann and Lawrence, 1973)

SANBAR - SANders BARotropic model is a filtered barotropic model using observed 1000 to 100 mb pressure weighted winds. The wind field near the cyclone is modified to conform to the observed cyclone motion. (Sanders and Burpee, 1968)

MFM - Moveable Fine Mesh baroclinic model has 10 vertical levels and 60 km horizontal grid spacing. (Hovermale and Livezey, 1977)

NW Pacific, South China Sea, and N Indian Oceans

TYAN - TYphoon ANalog system uses analog cyclones with similar time and space characteristics to generate 24, 48, and 72 hour forecast positions. (Jarrell and Somerville, 1970)

CY50 - CYclops 500 is an updated HATTRACK/MOHATT steering program that provides geostrophic steering forecasts at the 500 mb level using prognostic fields and a 12-hour persistence bias. (Renard, 1968; Renard, et al., 1973)

CLIM - CLIMatology aid that provides forecast positions based upon the month and position of the current cyclone.

HPAC - Half Persistence And Climatology provides 24- and 48-hour forecast positions that are the mid-points of straight lines connecting the 24- and 48-hour forecast points on the XTRP and CLIM tracks.

XTRP - EXTRaPolation forecast that extropolates a straight line from the 12-hour old position to the current position.

BPAC - Blended Persistence And Climatology provides 24-, 48-, and 72-hour forecast positions with less weight being given to persistence at each succeeding forecast interval.

NTCM - Nested Tropical Cyclone Model is a primitive equation model with 3 vertical levels and a 41 km grid centered on the cyclone that moves within a coarser grid. (Harrison, 1981)

OTCM - One-way Tropical Cyclone Model is a three-layer primitive equation model with a 205 km horizontal grid. Navy hemispheric prog fields are used at 12-hour intervals to update the model's boundaries. (Hodur and Burk, 1978)

# APPENDIX B

Correlation coefficients fields for the Atlantic on-the-ridge and south-of-ridge categories.

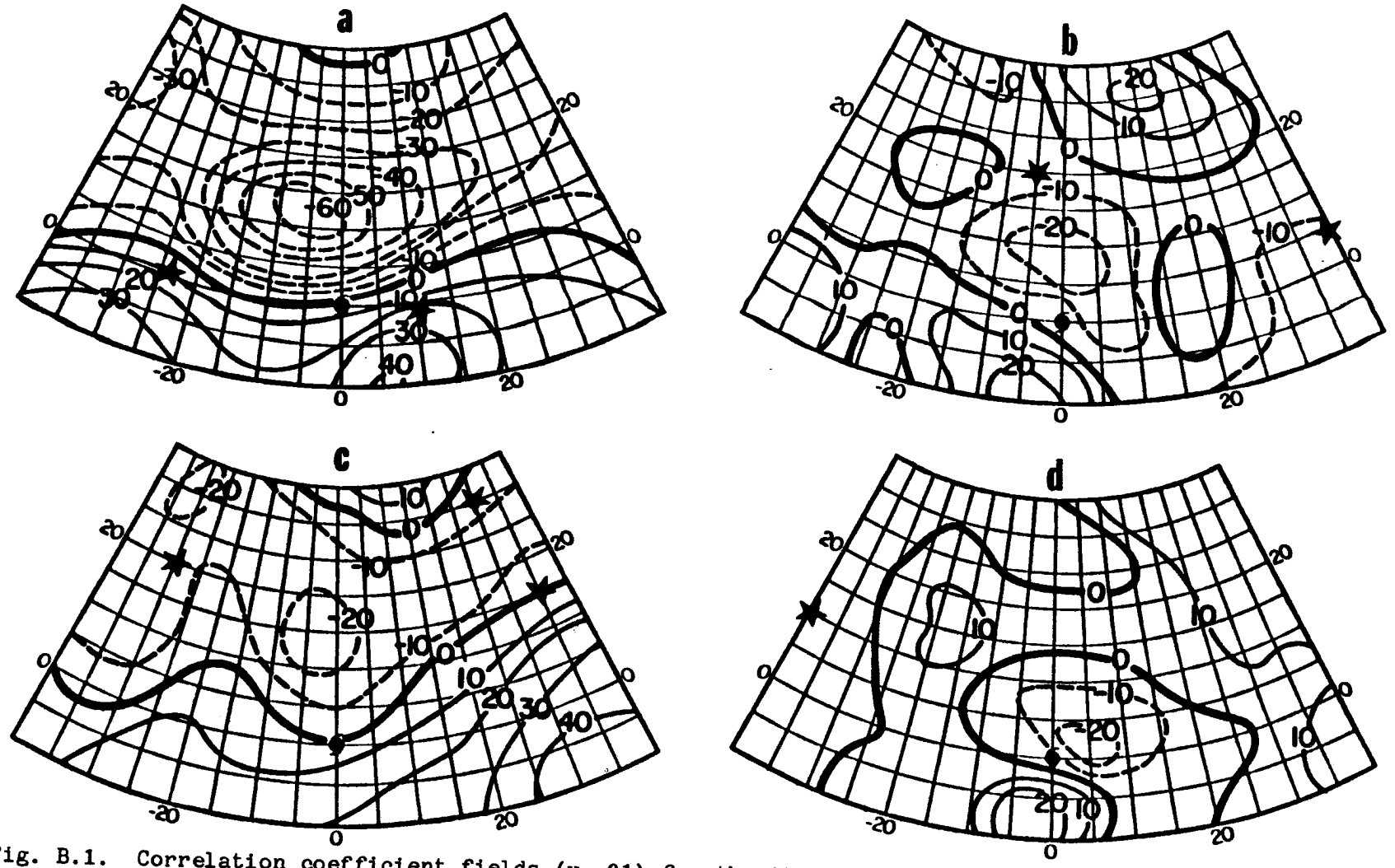


Fig. B.1. Correlation coefficient fields (x .01) for the Atlantic on-the-ridge fast U motion. The four panels present the correlation between cyclone motion and (a) 500 mb height; (b) 24-hour change of the 500 mb height; (c) sea level pressure; and (d) 24-hour change of sea level pressure. Northward and eastward cyclone motions are positive. The position of the cyclone is denoted by (6) and the stars indicate the gridpoints at which predictors were selected.

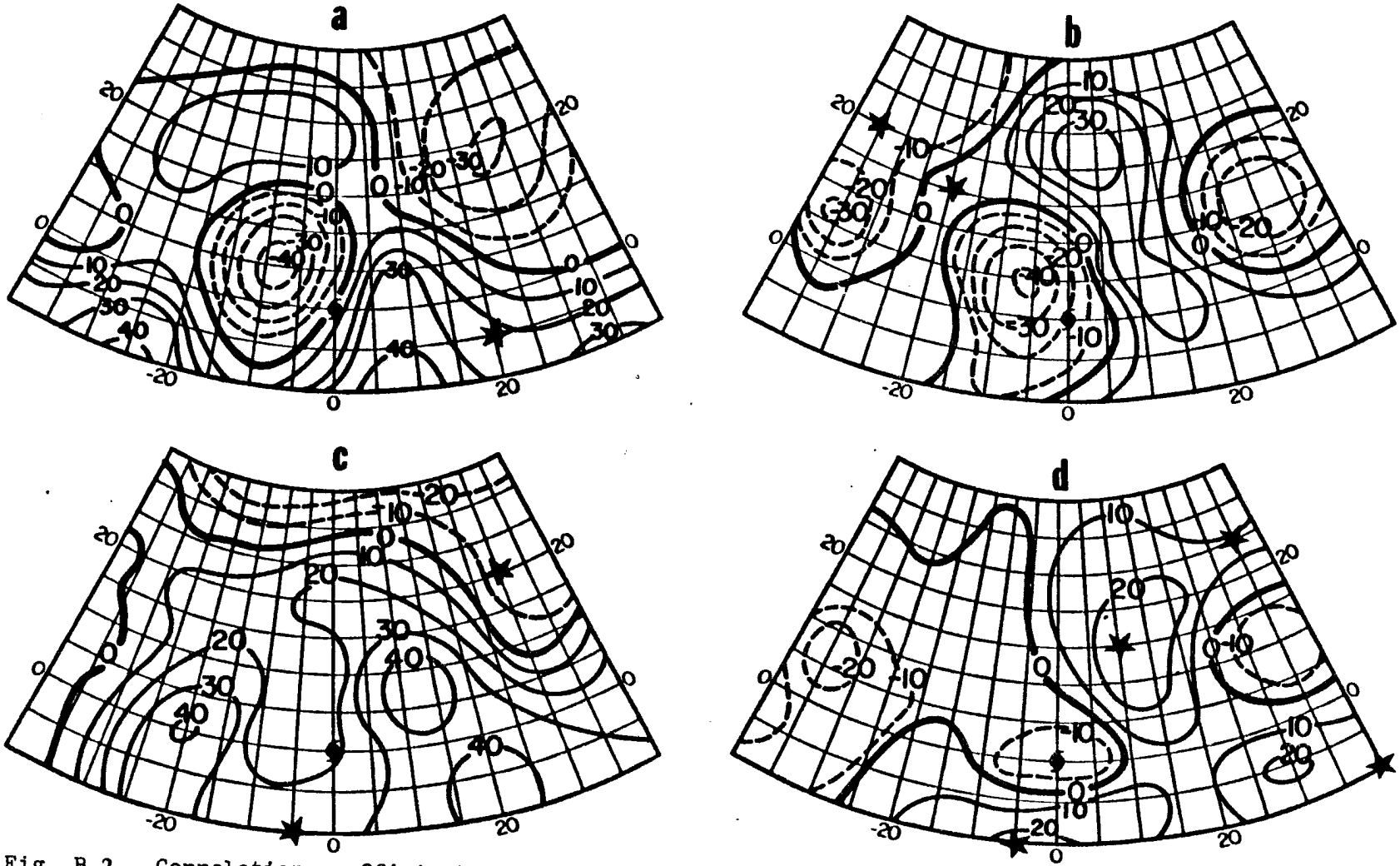


Fig. B.2. Correlation coefficient fields (x .01) for the Atlantic on-the-ridge fast V motion. The four panels present the correlation between cyclone motion and (a) 500 mb height; (b) 24-hour change of the 500 mb height; (c) sea level pressure; and (d) 24-hour change of sea level pressure. Northward and eastward cyclone motions are positive. The position of the cyclone is denoted by (🌀) and the stars indicate the gridpoints at which predictors were selected.

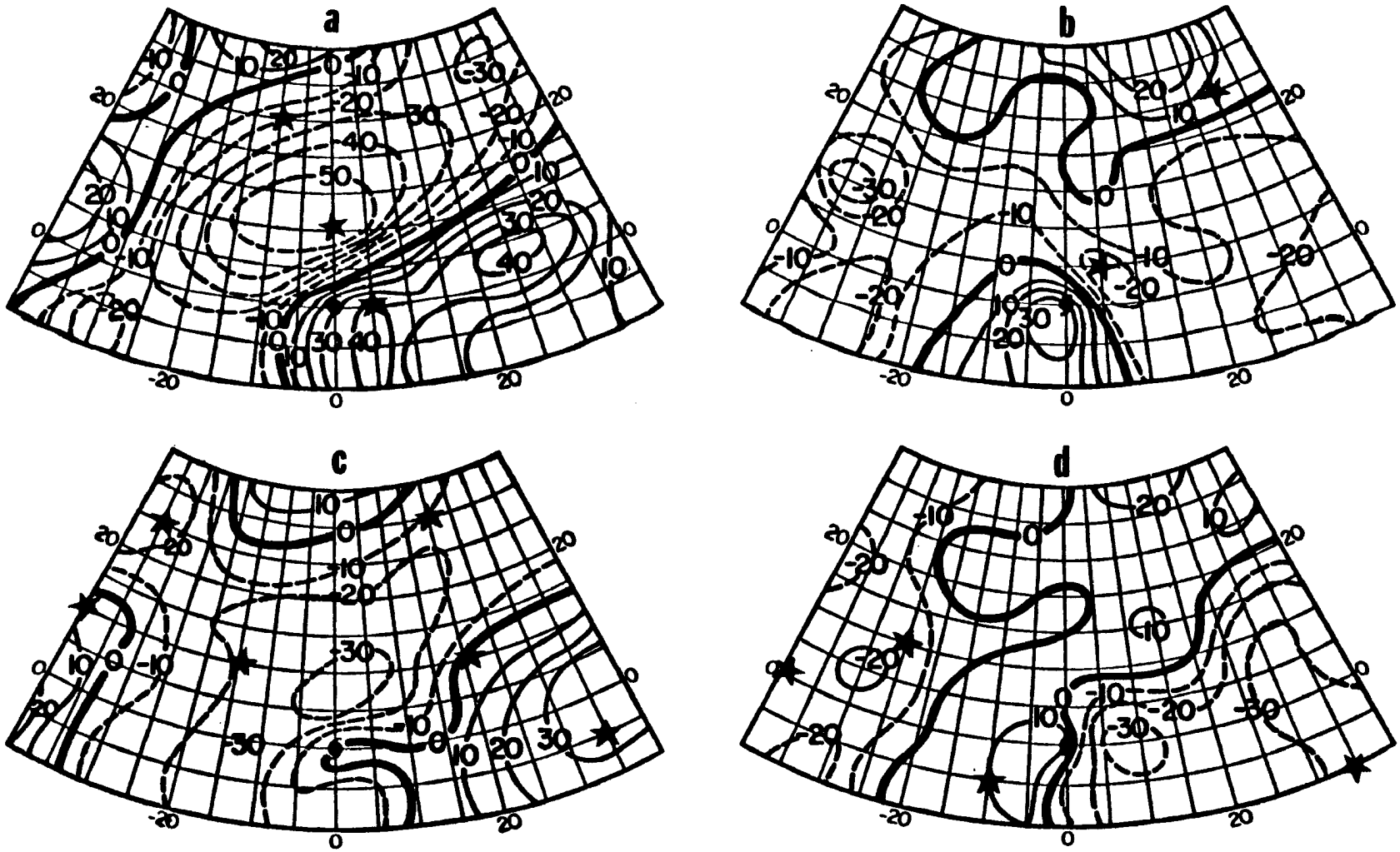


Fig. B.3. Correlation coefficient fields (x .01) for the Atlantic on-the-ridge slow U motion. The four panels present the correlation between cyclone motion and (a) 500 mb height; (b) 24-hour change of the 500 mb height; (c) sea level pressure; and (d) 24-hour change of sea level pressure. Northward and eastward cyclone motions are positive. The position of the cyclone is denoted by (◖) and the stars indicate the gridpoints at which predictors were selected.

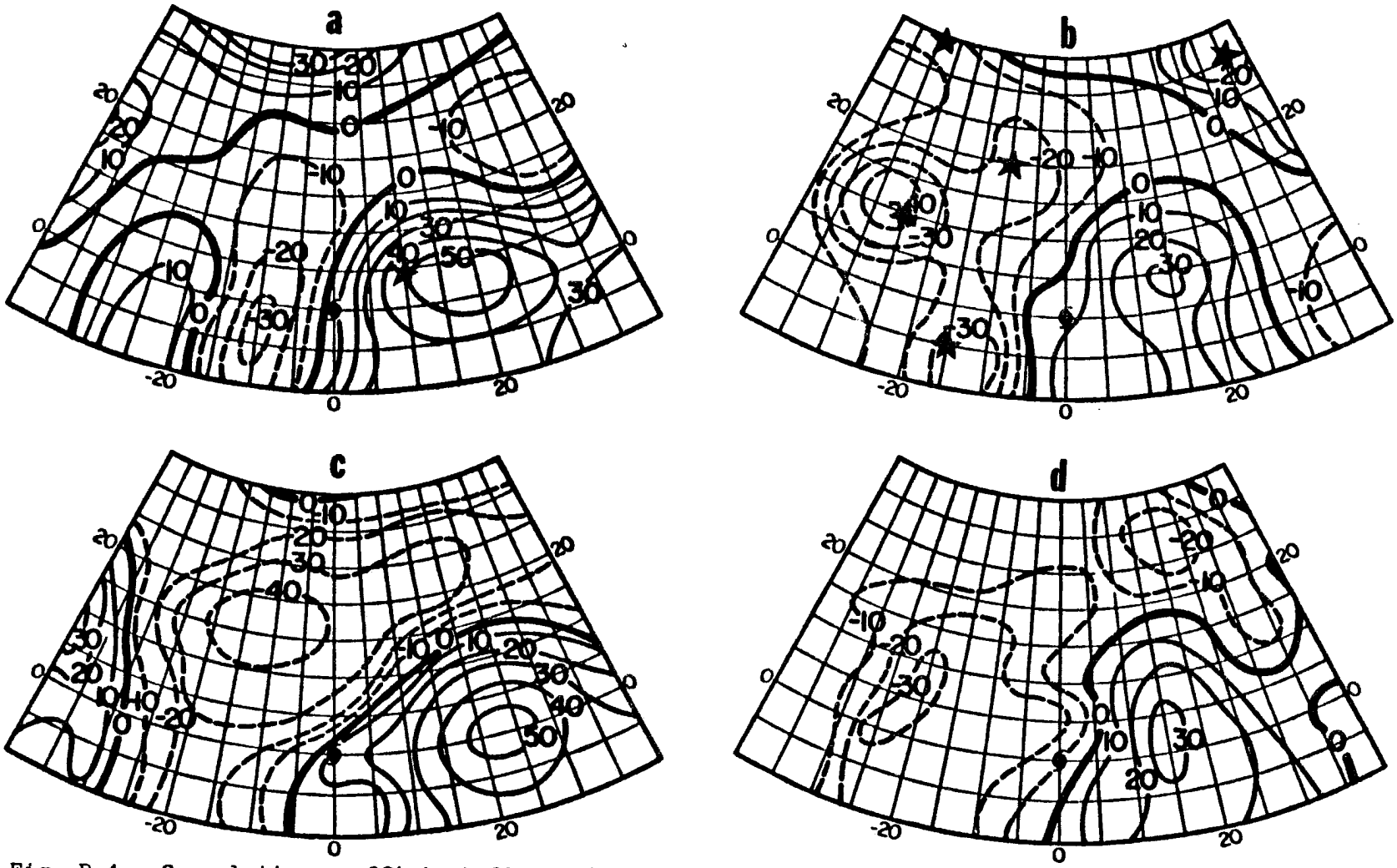


Fig. B.4. Correlation coefficient fields (x .01) for the Atlantic on-the-ridge slow V motion. The four panels present the correlation between cyclone motion and (a) 500 mb height; (b) 24-hour change of the 500 mb height; (c) sea level pressure; and (d) 24-hour change of sea level pressure. Northward and eastward cyclone motions are positive. The position of the cyclone is denoted by (6) and the stars indicate the gridpoints at which predictors were selected.

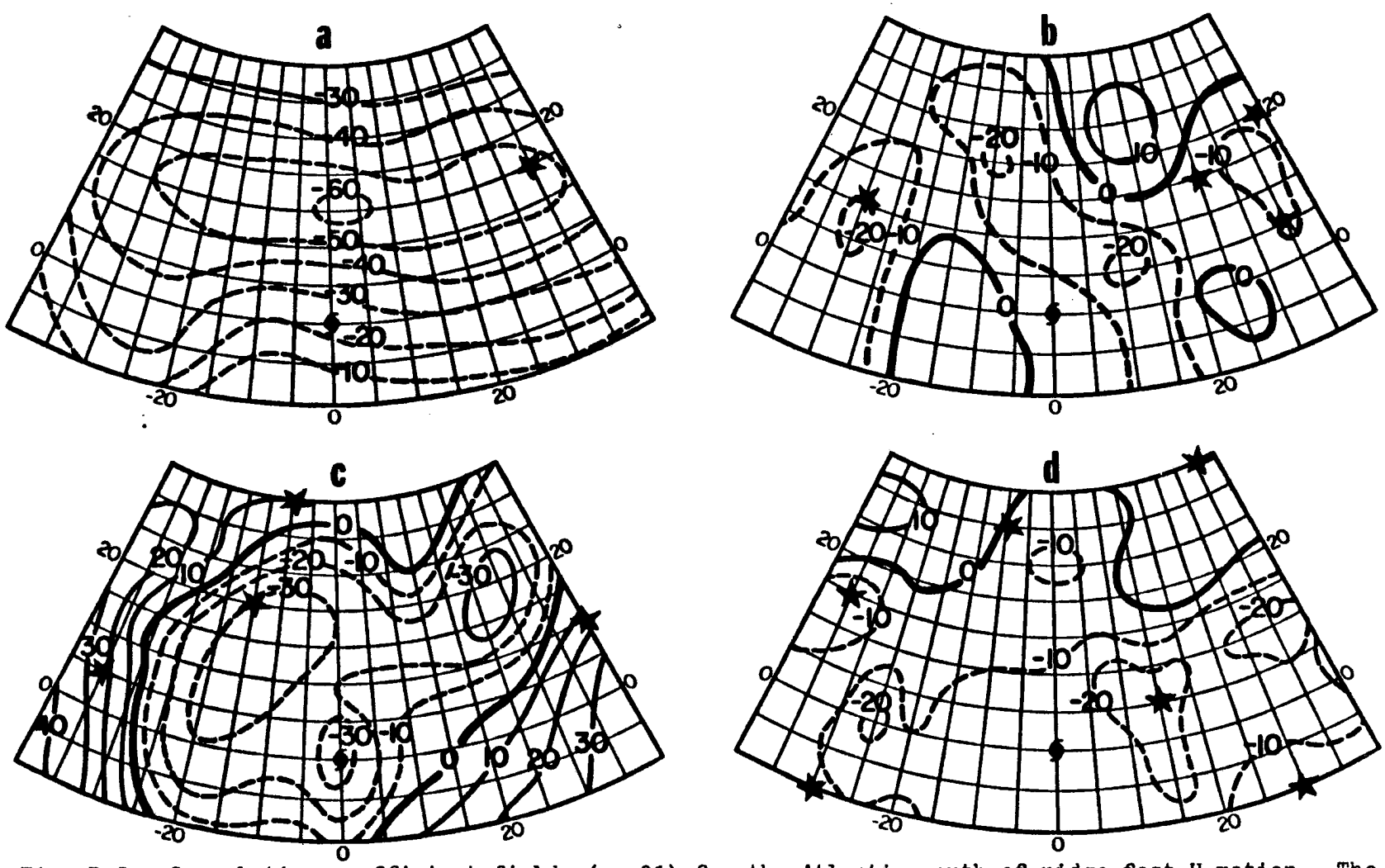


Fig. B.5. Correlation coefficient fields (x .01) for the Atlantic south-of-ridge fast U motion. The four panels present the correlation between cyclone motion and (a) 500 mb height; (b) 24-hour change of the 500 mb height; (c) sea level pressure; and (d) 24-hour change of sea level pressure. Northward and eastward cyclone motions are positive. The position of the cyclone is denoted by (6) and the stars indicate the gridpoints at which predictors were selected.

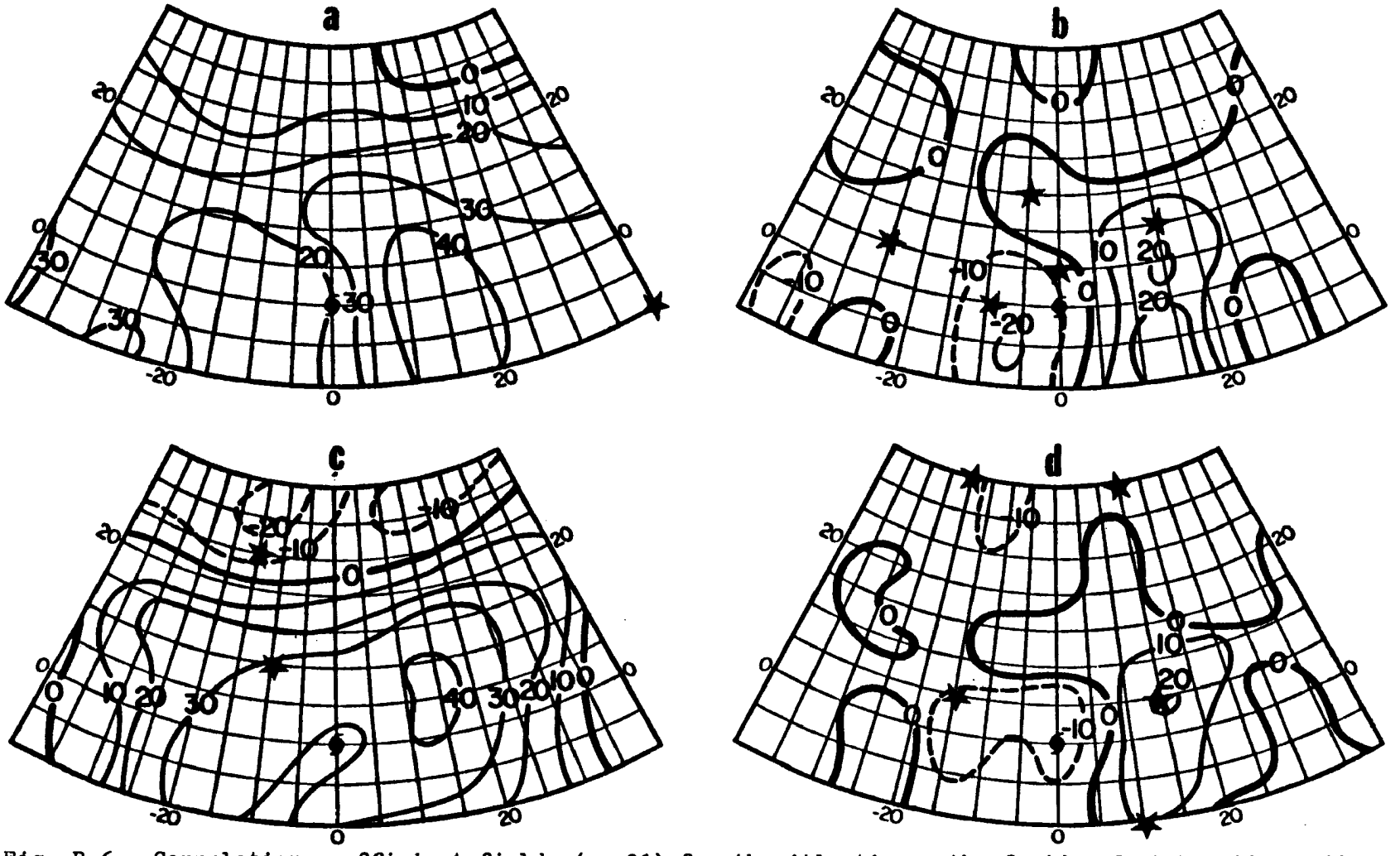


Fig. B.6. Correlation coefficient fields (x .01) for the Atlantic south-of-ridge fast V motion. The four panels present the correlation between cyclone motion and (a) 500 mb height; (b) 24-hour change of the 500 mb height; (c) sea level pressure; and (d) 24-hour change of sea level pressure. Northward and eastward cyclone motions are positive. The position of the cyclone is denoted by (§) and the stars indicate the gridpoints at which predictors were selected.

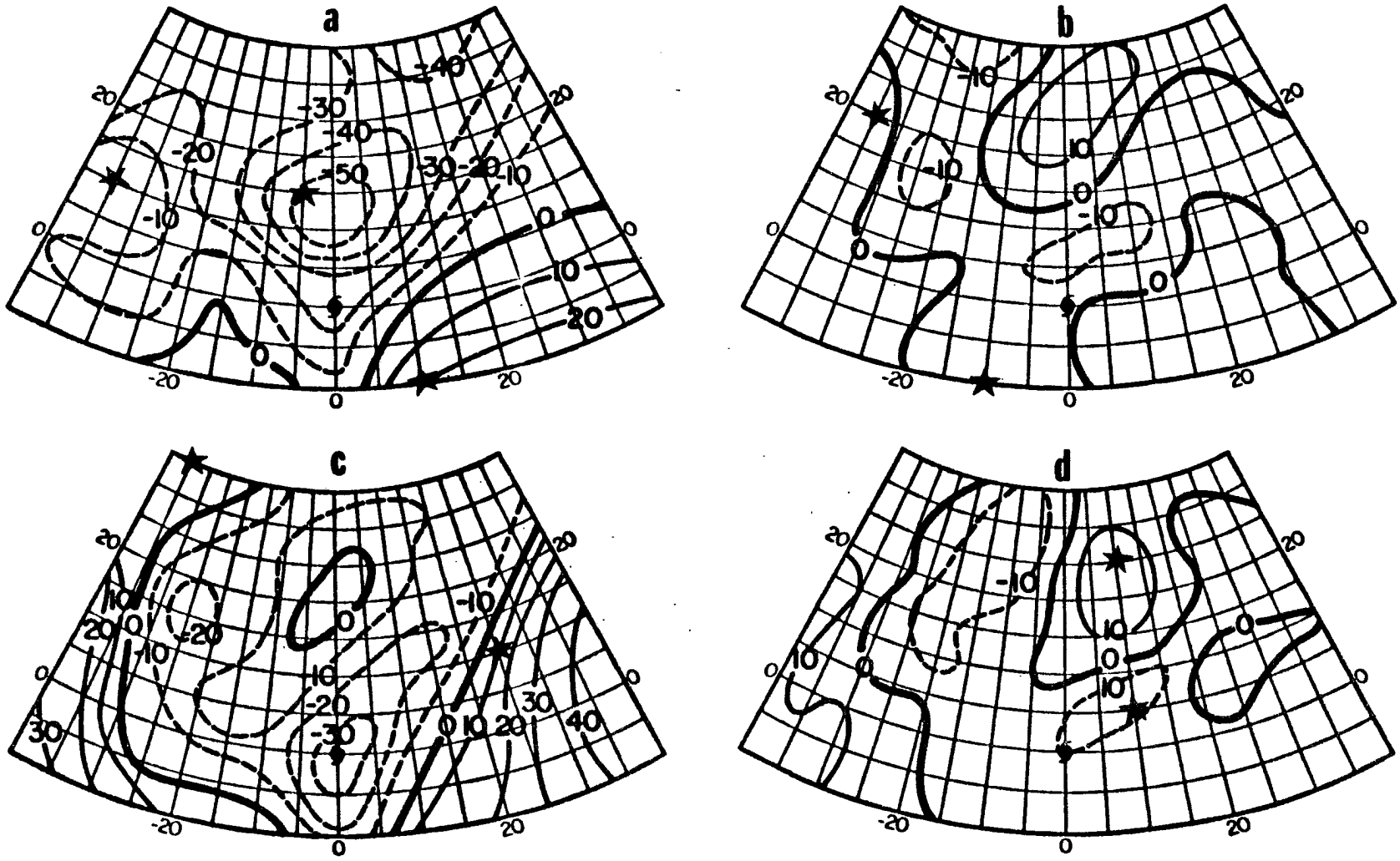


Fig. B.7. Correlation coefficient fields (x .01) for the Atlantic south-of-ridge slow U motion. The four panels present the correlation between cyclone motion and (a) 500 mb height; (b) 24-hour change of the 500 mb height; (c) sea level pressure; and (d) 24-hour change of sea level pressure. Northward and eastward cyclone motions are positive. The position of the cyclone is denoted by (6) and the stars indicate the gridpoints at which predictors were selected.

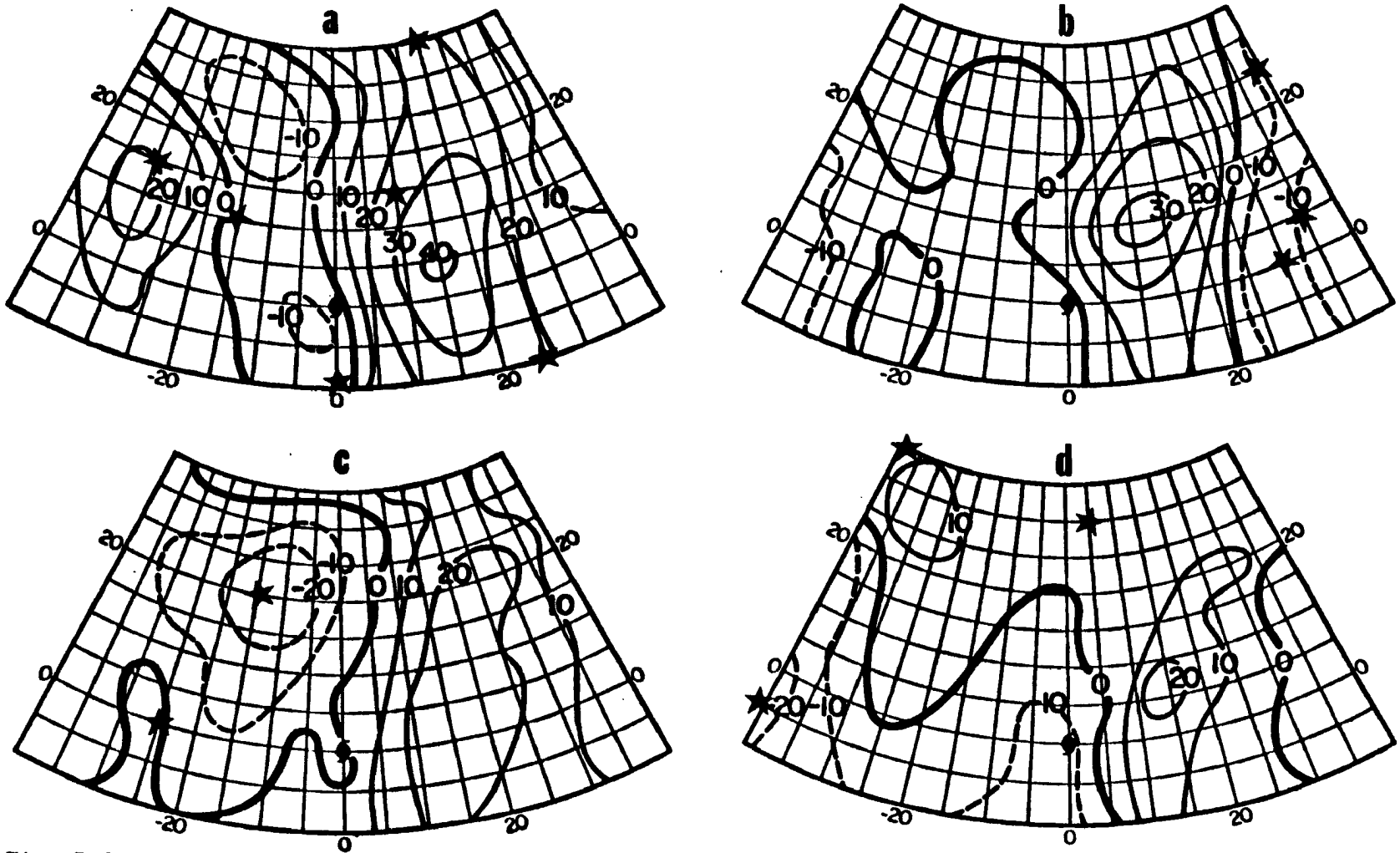


Fig. B.8. Correlation coefficient fields (x .01) for the Atlantic south-of-ridge slow V motion. The four panels present the correlation between cyclone motion and (a) 500 mb height; (b) 24-hour change of the 500 mb height; (c) sea level pressure; and (d) 24-hour change of sea level pressure. Northward and eastward cyclone motions are positive. The position of the cyclone is denoted by (§) and the stars indicate the gridpoints at which predictors were selected.

# APPENDIX C

Correlation coefficients fields for the NW Pacific on-the-ridge and south-of-ridge categories.

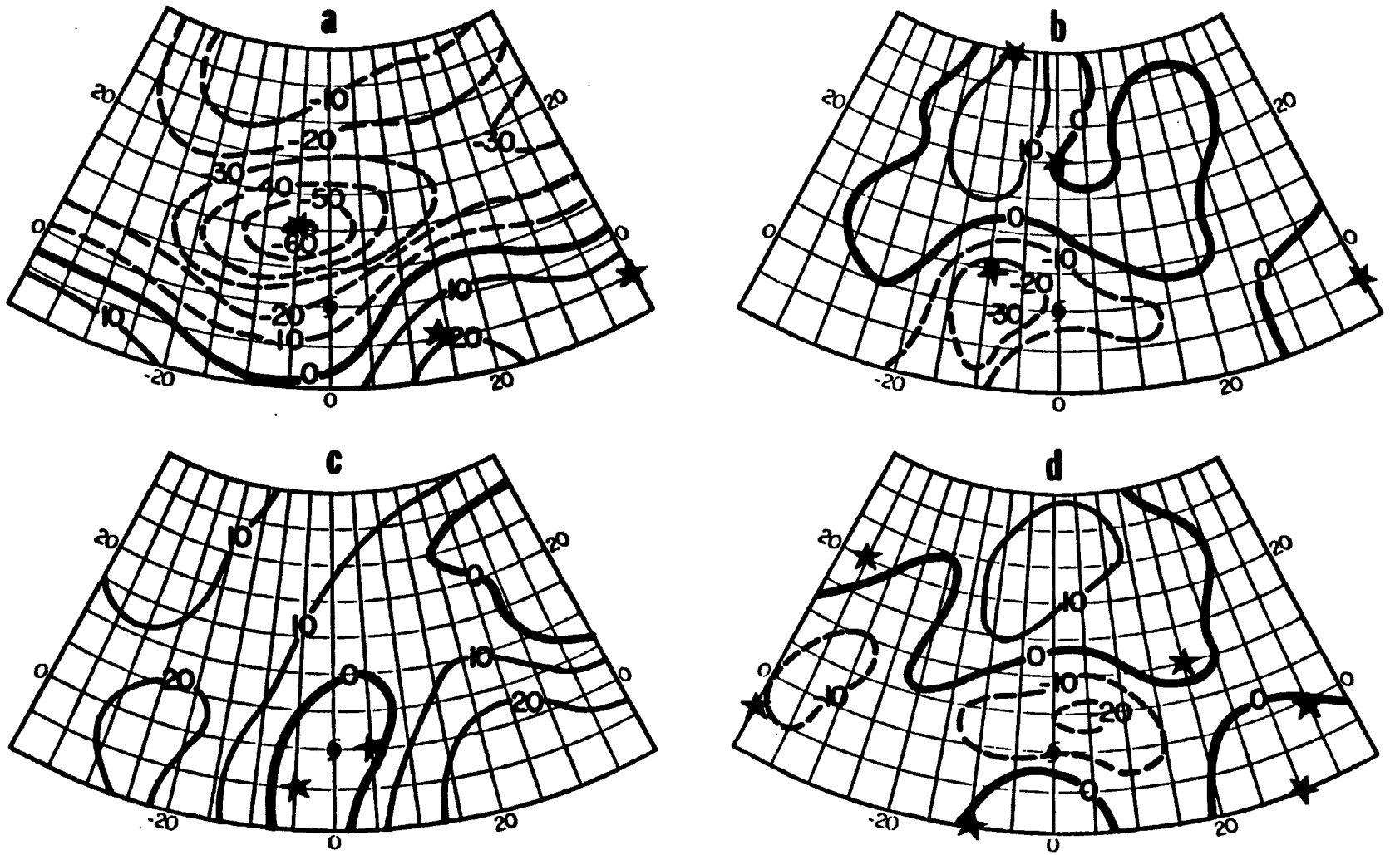


Fig. C.1. Correlation coefficient fields (x .01) for the NW Pacific on-the-ridge fast U motion. The four panels present the correlation between cyclone motion and (a) 500 mb height; (b) 24-hour change of the 500 mb height; (c) sea level pressure; and (d) 24-hour change of sea level pressure. Northward and eastward cyclone motions are positive. The position of the cyclone is denoted by (§) and the stars indicate the gridpoints at which predictors were selected.

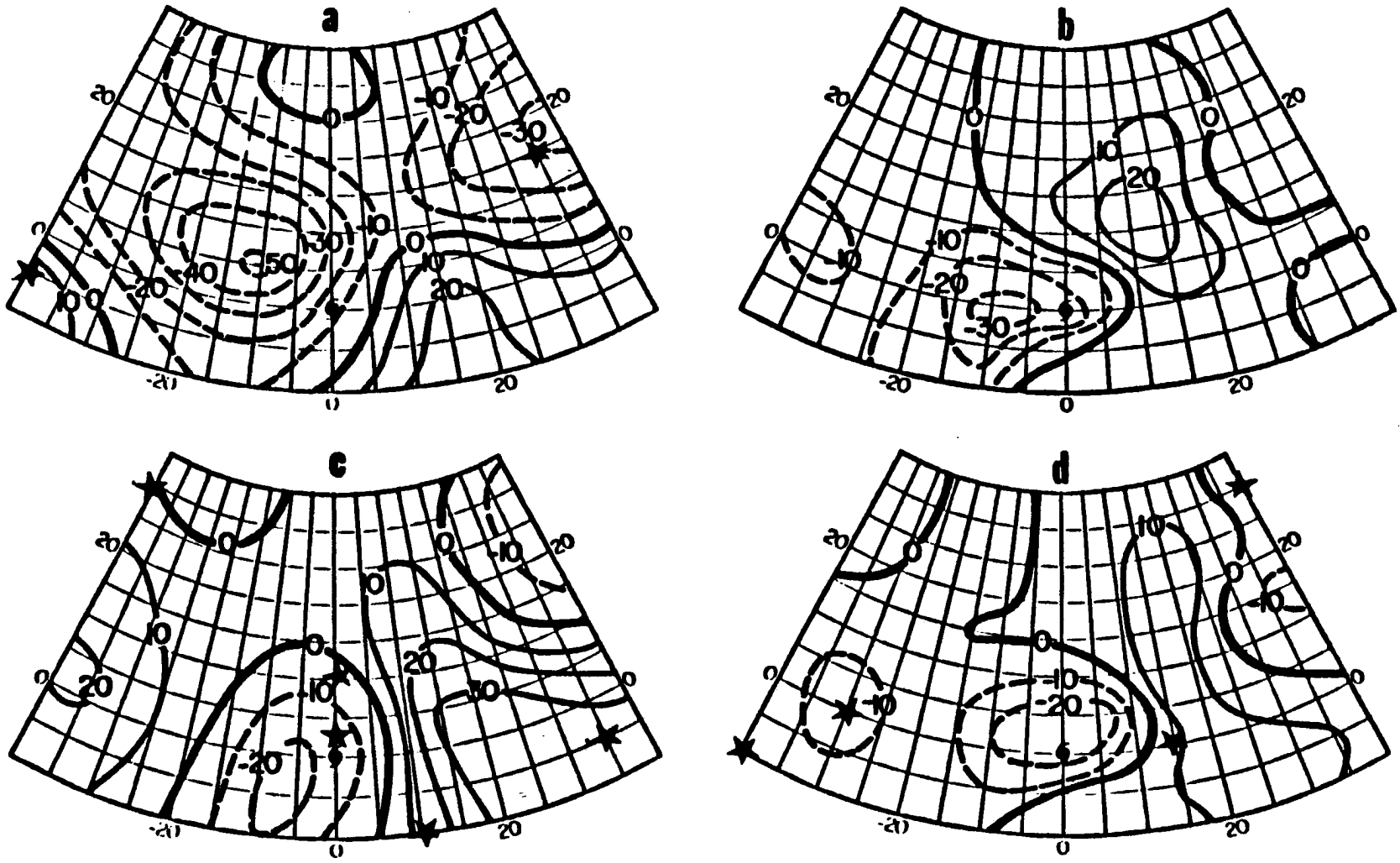


Fig. C.2. Correlation coefficient fields (x .01) for the NW Pacific on-the-ridge fast V motion. The four panels present the correlation between cyclone motion and (a) 500 mb height; (b) 24-hour change of the 500 mb height; (c) sea level pressure; and (d) 24-hour change of sea level pressure. Northward and eastward cyclone motions are positive. The position of the cyclone is denoted by (🌀) and the stars indicate the gridpoints at which predictors were selected.

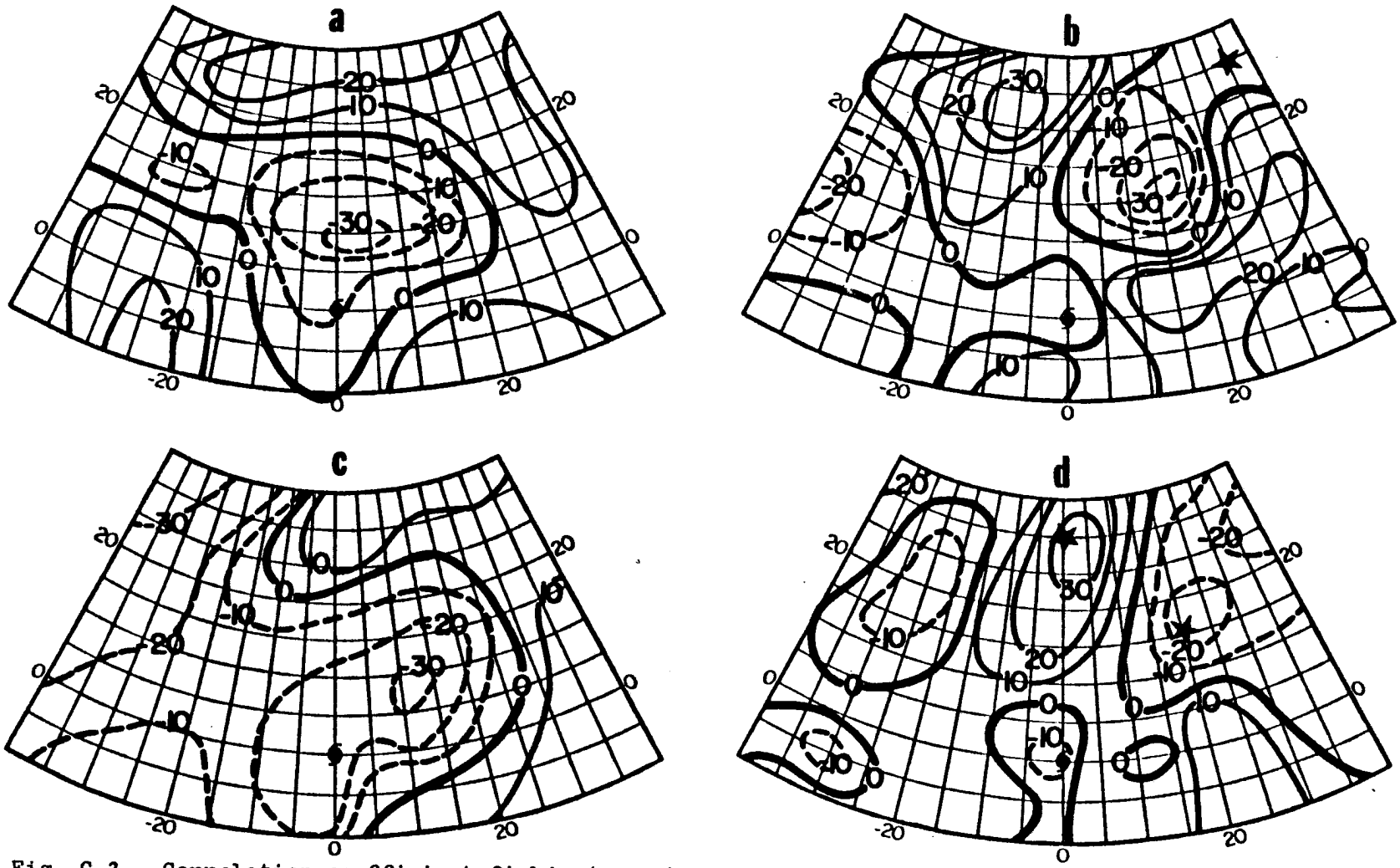


Fig. C.3. Correlation coefficient fields (x .01) for the NW Pacific on-the-ridge slow U motion. The four panels present the correlation between cyclone motion and (a) 500 mb height; (b) 24-hour change of the 500 mb height; (c) sea level pressure; and (d) 24-hour change of sea level pressure. Northward and eastward cyclone motions are positive. The position of the cyclone is denoted by (§) and the stars indicate the gridpoints at which predictors were selected.

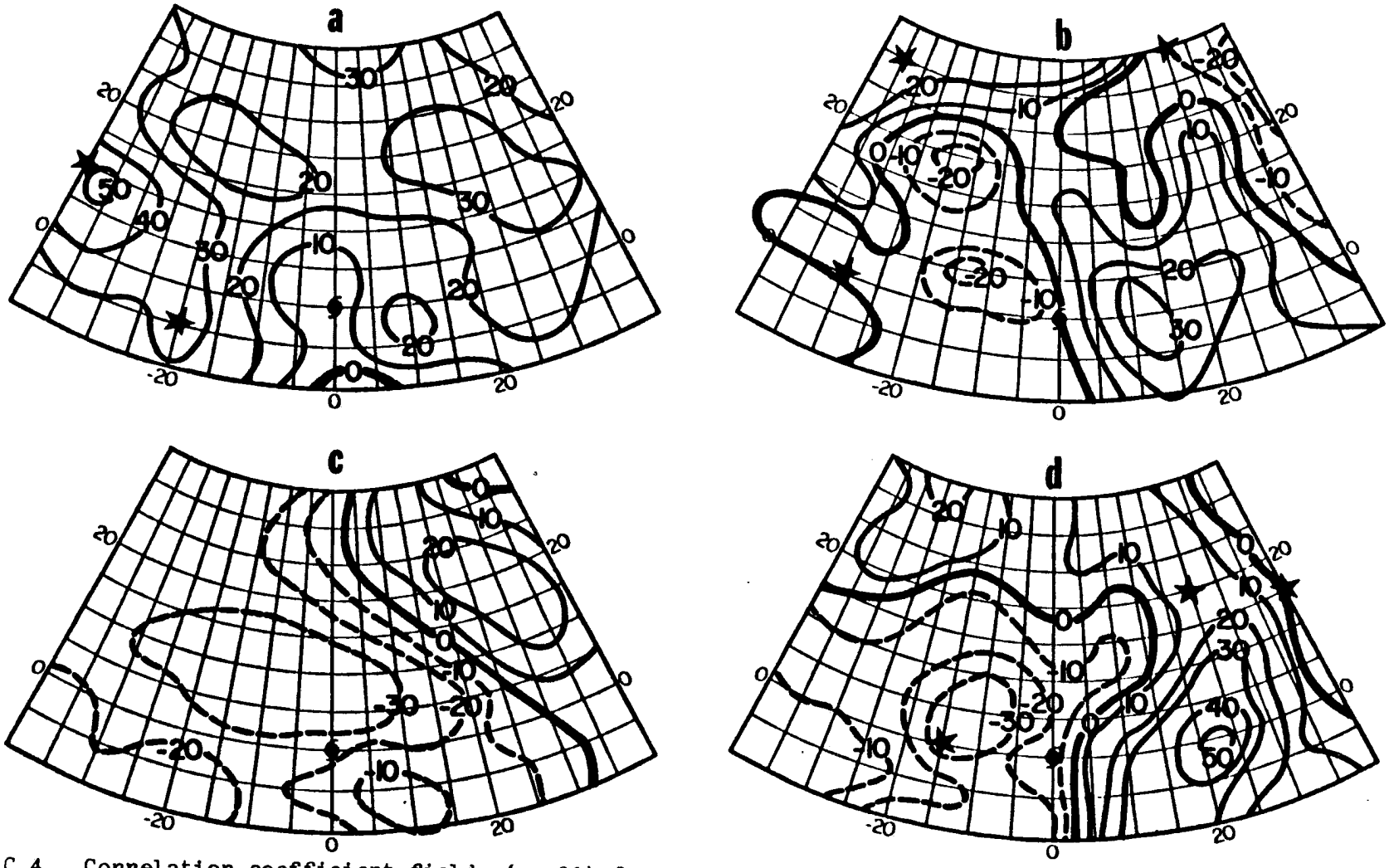


Fig. C.4. Correlation coefficient fields (x .01) for the NW Pacific on-the-ridge slow V motion. The four panels present the correlation between cyclone motion and (a) 500 mb height; (b) 24-hour change of the 500 mb height; (c) sea level pressure; and (d) 24-hour change of sea level pressure. Northward and eastward cyclone motions are positive. The position of the cyclone is denoted by (§) and the stars indicate the gridpoints at which predictors were selected.

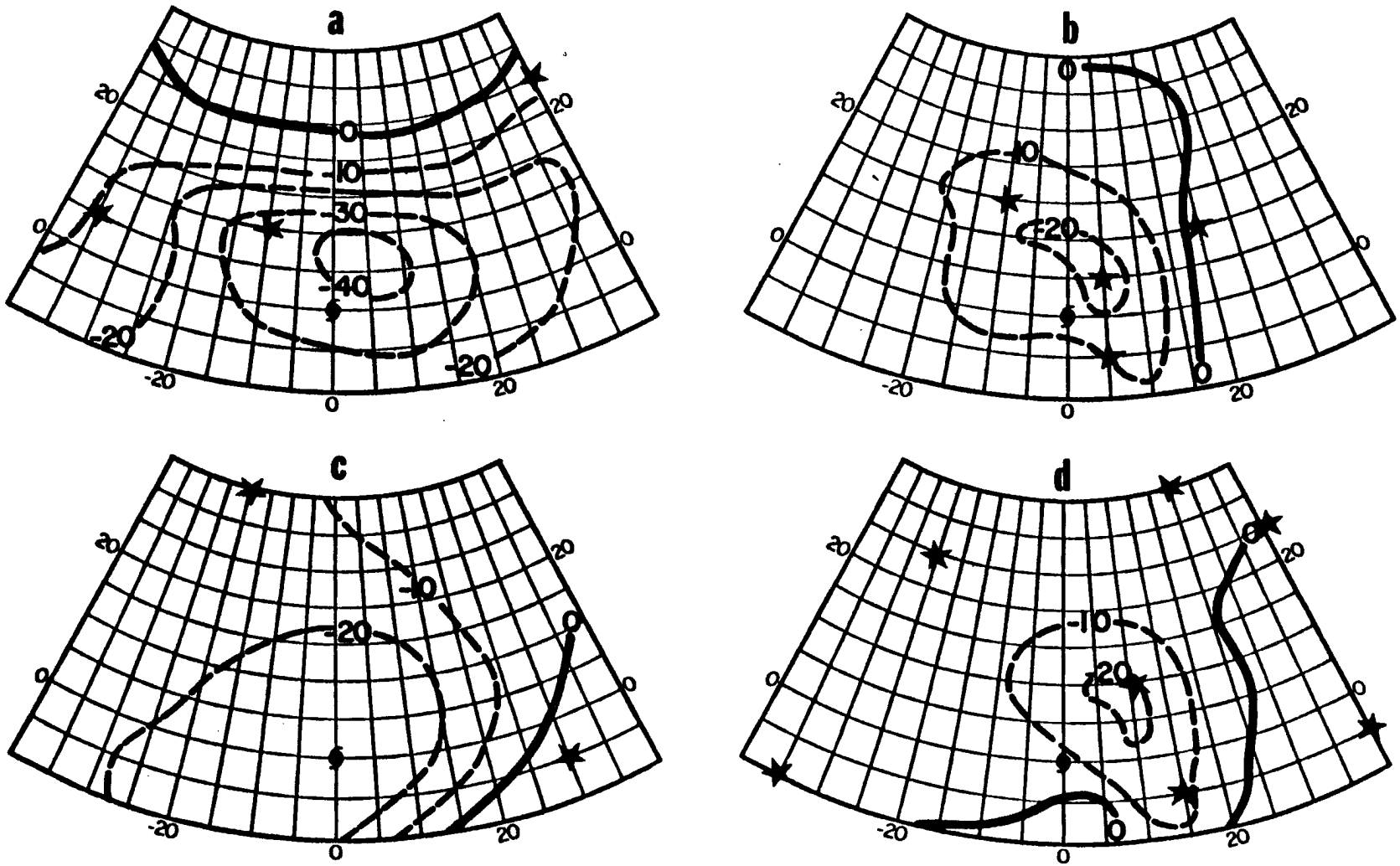


Fig. C.5. Correlation coefficient fields (x .01) for the NW Pacific south-of-ridge fast U motion. The four panels present the correlation between cyclone motion and (a) 500 mb height; (b) 24-hour change of the 500 mb height; (c) sea level pressure; and (d) 24-hour change of sea level pressure. Northward and eastward cyclone motions are positive. The position of the cyclone is denoted by (§) and the stars indicate the gridpoints at which predictors were selected.

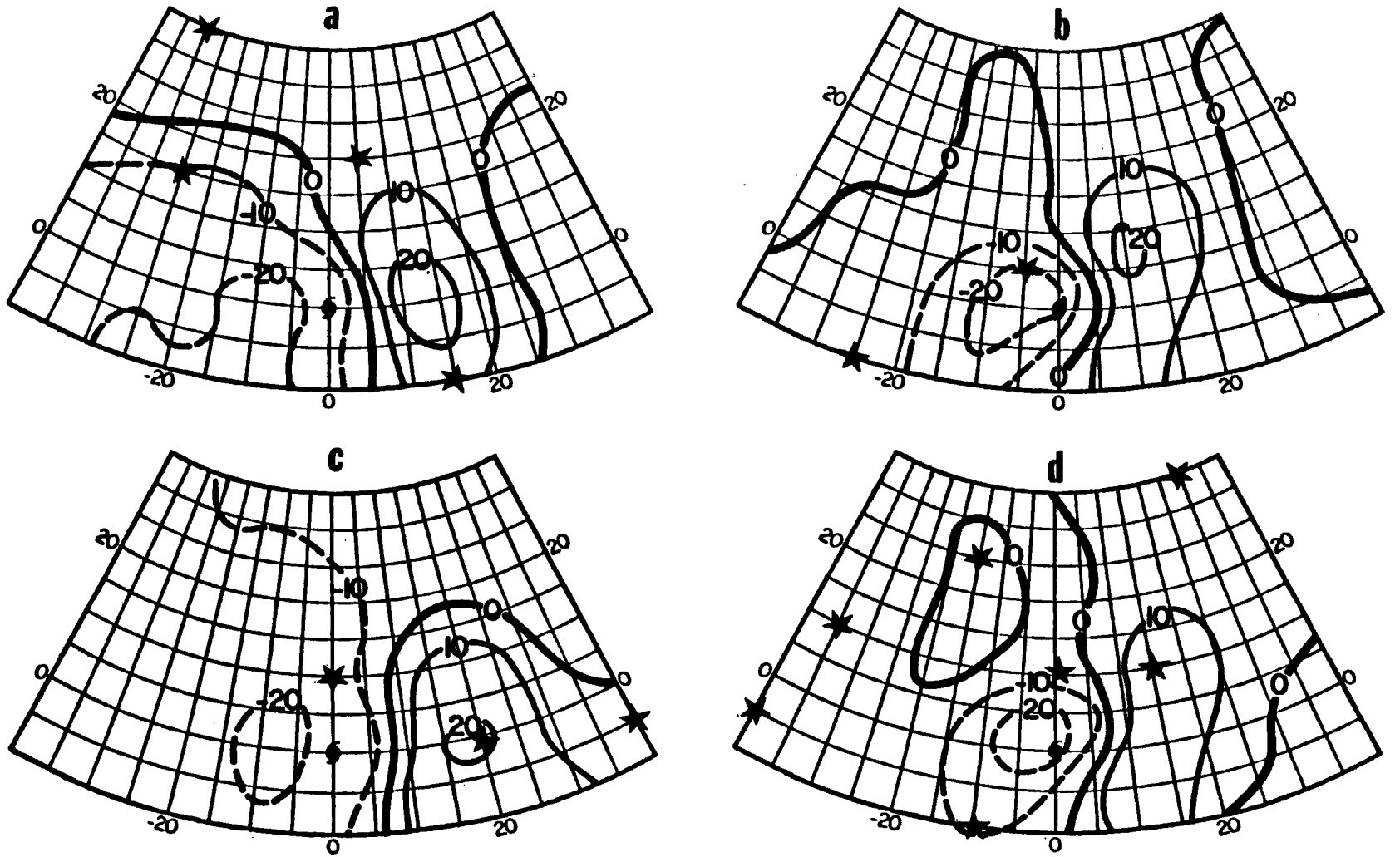


Fig. C.6. Correlation coefficient fields (x .01) for the NW Pacific south-of-ridge fast V motion. The four panels present the correlation between cyclone motion and (a) 500 mb height; (b) 24-hour change of the 500 mb height; (c) sea level pressure; and (d) 24-hour change of sea level pressure. Northward and eastward cyclone motions are positive. The position of the cyclone is denoted by (🌀) and the stars indicate the gridpoints at which predictors were selected.

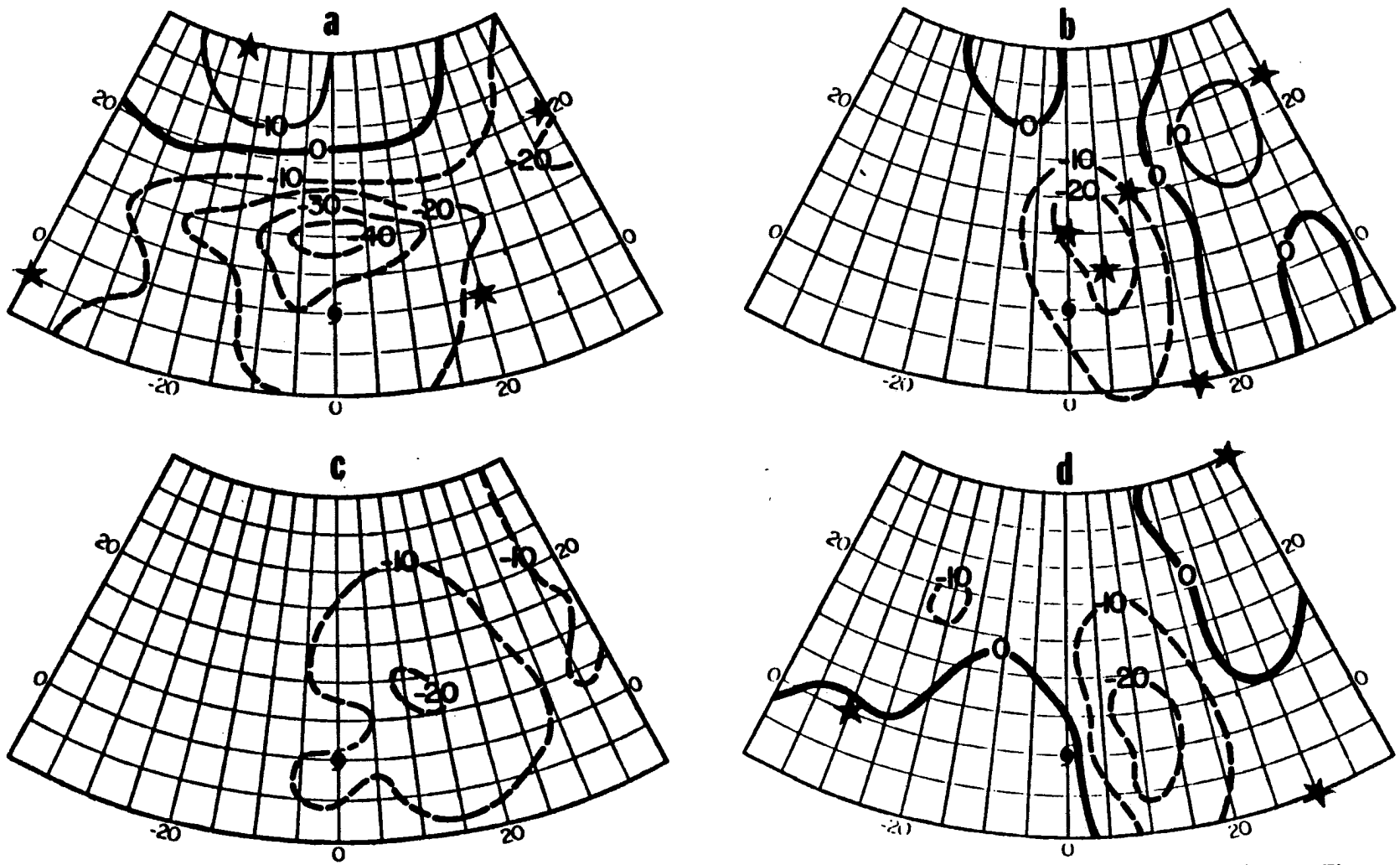


Fig. C.7. Correlation coefficient fields (x .01) for the NW Pacific south-of-ridge slow U motion. The four panels present the correlation between cyclone motion and (a) 500 mb height; (b) 24-hour change of the 500 mb height; (c) sea level pressure; and (d) 24-hour change of sea level pressure. Northward and eastward cyclone motions are positive. The position of the cyclone is denoted by (●) and the stars indicate the gridpoints at which predictors were selected.

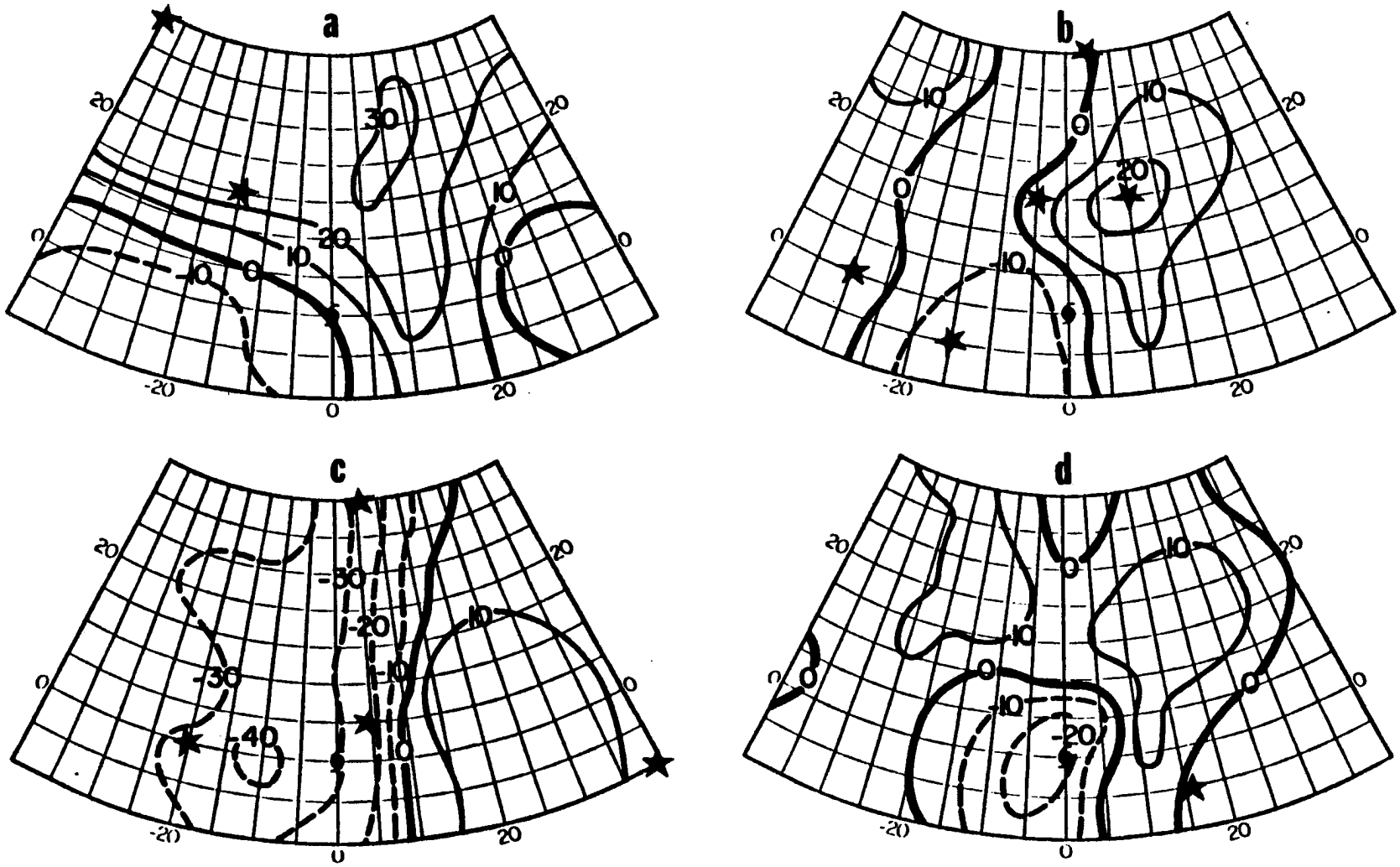


Fig. C.8. Correlation coefficient fields (x .01) for the NW Pacific south-of-ridge slow V motion. The four panels present the correlation between cyclone motion and (a) 500 mb height; (b) 24-hour change of the 500 mb height; (c) sea level pressure; and (d) 24-hour change of sea level pressure. Northward and eastward cyclone motions are positive. The position of the cyclone is denoted by (6) and the stars indicate the gridpoints at which predictors were selected.

# APPENDIX D

Correlation coefficients fields for the North Indian Ocean on-the-ridge and south-of-ridge categories.

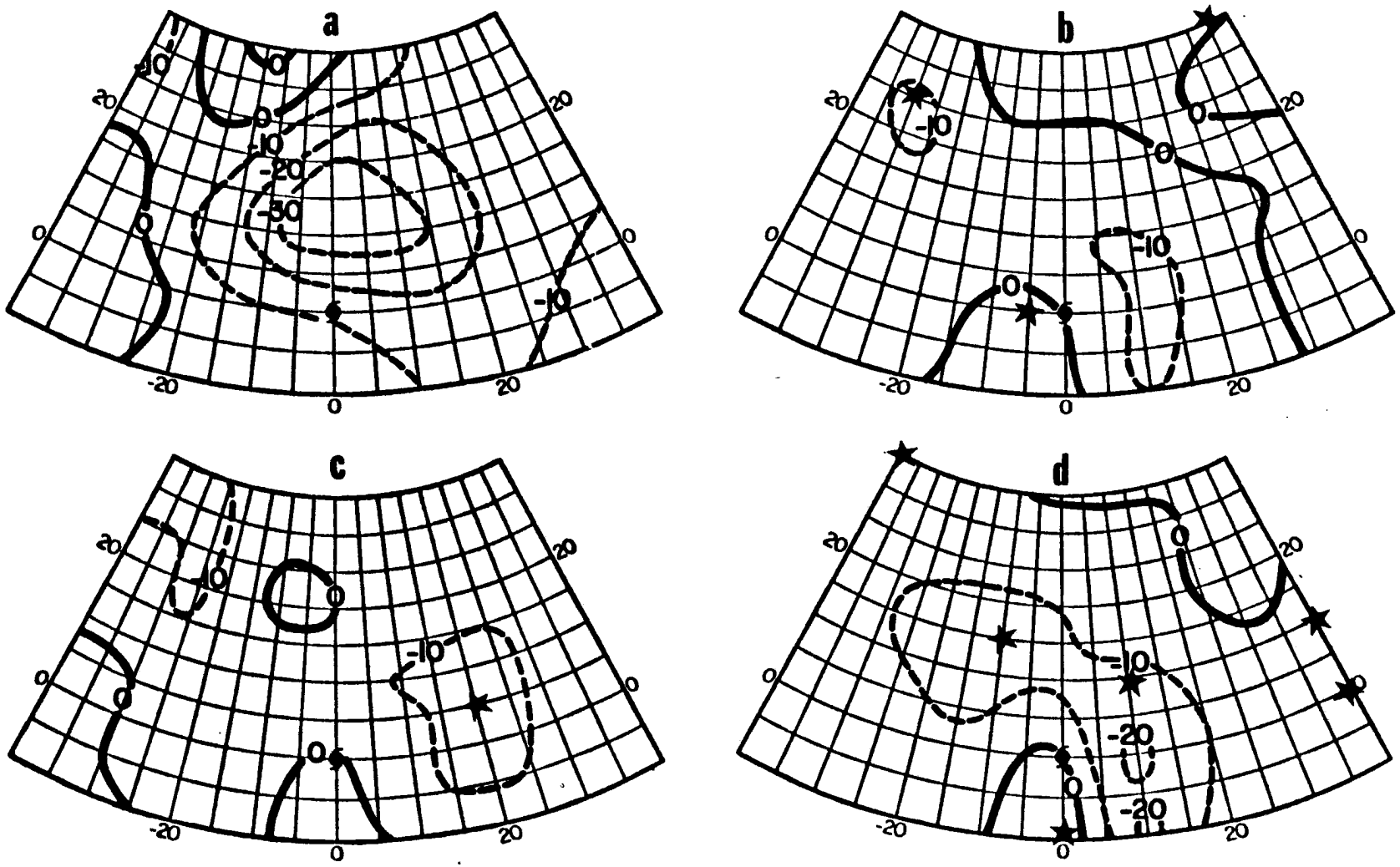


Fig. D.3. Correlation coefficient fields (x .01) for the North Indian Ocean south-of-ridge U motion. The four panels present the correlation between cyclone motion and (a) 500 mb height; (b) 24-hour change of the 500 mb height; (c) sea level pressure; and (d) 24-hour change of sea level pressure. Northward and eastward cyclone motions are positive. The position of the cyclone is denoted by (●) and the stars indicate the gridpoints at which predictors were selected.

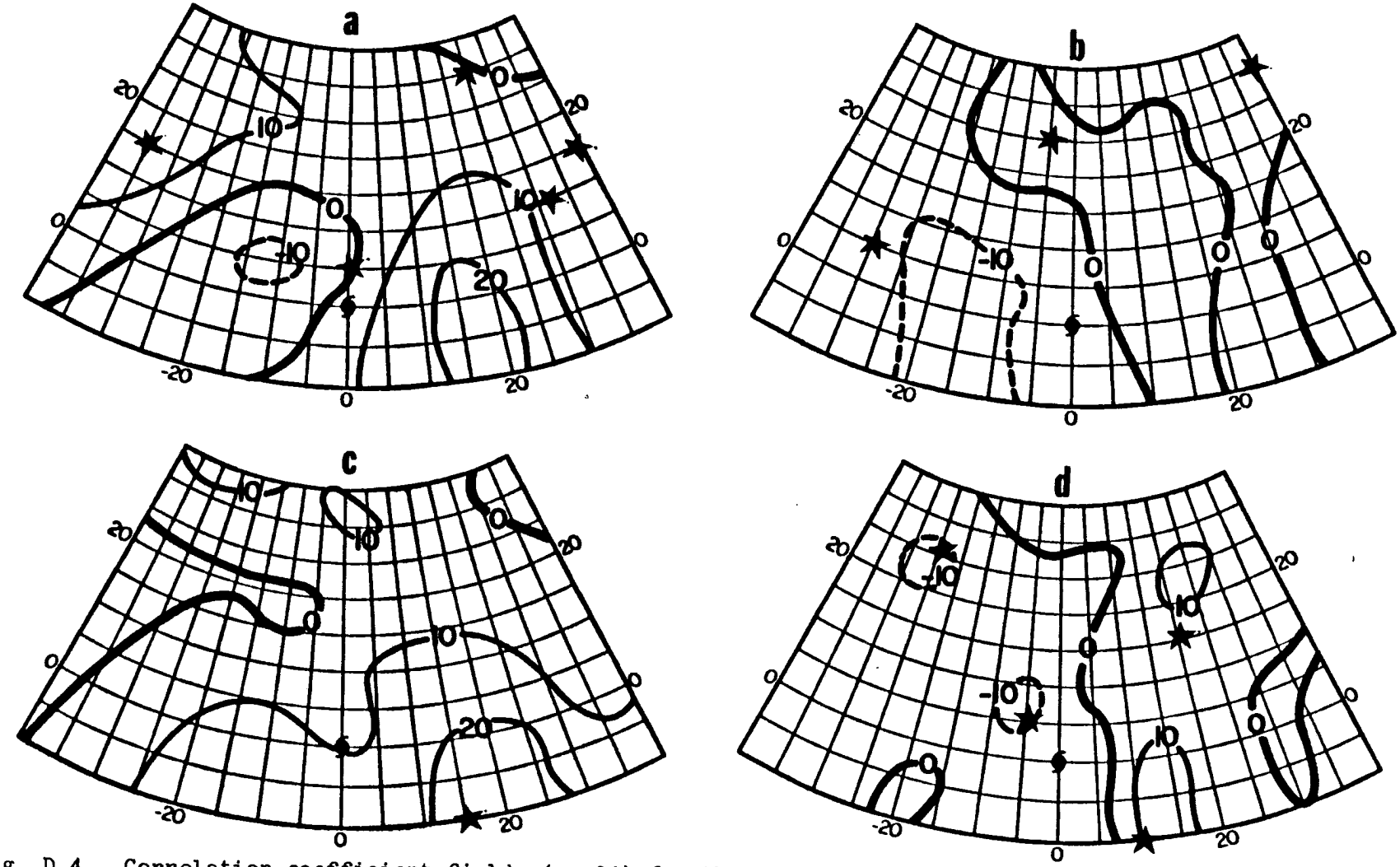


Fig. D.4. Correlation coefficient fields (x .01) for the North Indian Ocean south-of-ridge V motion. The four panels present the correlation between cyclone motion and (a) 500 mb height; (b) 24-hour change of the 500 mb height; (c) sea level pressure; and (d) 24-hour change of sea level pressure. Northward and eastward cyclone motions are positive. The position of the cyclone is denoted by (◖) and the stars indicate the gridpoints at which predictors were selected.

## APPENDIX E

## OPERATIONAL IMPLEMENTATION

The attractiveness of a statistical-dynamical prediction model such as this is the ease with which it can be applied directly at operational locations and aboard ships without a link to a large computer data base.

The basic design concept of the new model is simple enough such that a forecaster could generate the 24-, 48-, and 72-hour forecast positions with the use of a desk-top calculator.

The only information required as input for the model are the current, past 12-hour and past 24-hour positions of the cyclone and the current surface, 500 mb and 200 mb charts plus the 24- and 48-hour surface, 500 mb and 200 mb forecast fields. These forecast fields could be subjectively made by the forecaster for the specific areas where predictor values are required.

For the NW Pacific, South China Sea, and North Indian Oceans, the regression equations with 500 mb steering and no speed stratification should be used. The regression equations with 200 mb steering should only be used for strong typhoons ($\geq$ 90 kts) undergoing recurvature in the NW Pacific. For the Atlantic, the regression equations with 200 mb steering and no speed stratification should be used.

Basically, one always starts with the 500 mb height field to determine the position of the cyclone relative to the subtropical ridge (south, on, or north). Then select the appropriate regression equations (one for north-south displacement, a second for east-west displacement)

and determine the predictors required. If one or more of the predictors is past motion, compute it as follows:

north-south displacement Y is given by

$1111.949 * (LAT_o - LAT_p)/HOUR$

where $LAT_o$ is the current latitude

$LAT_p$ is the previous latitude either 12 or 24 hours earlier

HOUR is 12 or 24 depending on whether a 12-hour past motion or 24-hour past motion is being computed;

east-west displacement X is given by:

$1111.949 * COS\ [(LAT_o + LAT_p)/2] \times (LON_o - LON_p)/HOUR$

where $LAT_o$ is the current latitude

$LAT_p$ is the previous latitude either 12 or 24 hours earlier

$LON_o$ is the current longitude

$LON_p$ is the previous longitude either 12 or 24 hours earlier

HOUR is 12 or 24 depending on whether a 12-hour or 24-hour past motion is being computed

In computing the past 12-hour motion at the 24- and 48-hour forecast positions, a position halfway between the forecast position and the position 24 hours earlier is used as the 12-hour old position.

If the required predictor is 500 mb height or sea level pressure, go to the appropriate chart and estimate the value at the proper gridpoint from the cyclone. If the forecast process is at the initial position, the chart to use would be the current analysis. If the process is at the 24-hour forecast position, the chart to use is the 24-hour prognostic field valid at the time of the 24-hour position. If the forecast process is at the 48-hour forecast position, the chart to use is the 48-hour prog field valid at the time of the 48-hour position.

If the required predictor is the tendency of the 500 mb height or sea level pressure, i.e., the 24-hour change in the height or pressure, two charts are required. If the forecast process is at the initial position, the charts to use are the current analysis and the 24-hour old analysis. If the process is at the 24-hour forecast position, the charts to use are the 24-hour prog field valid at the time of the 24-hour position and the initial analysis. If the process is at the 48-hour forecast position, the charts to use are the 48-hour prog field valid at the time of the 48-hour position and the 24-hour prog valid at the time of the 24-hour position. In this way, one is only using "current" analysis and previous 24-hour changes, never looking ahead at any "prog" fields.

The synoptic and steering predictors are always computed relative to the "current" cyclone position. The steering predictors are computed differently depending on whether the steering is being computed over the cyclone or away from the cyclone center. For steering over the cyclone, the five nearest gridpoints $10^{o}$ away from the center on either side are averaged and then subtracted to provide a gradient across the cyclone. For steering away from the cyclone, a single gridpoint $5^{o}$ either side of the point for which the steering is being computed is used. For the exact gridpoints, refer to Chapter 3.

In the development of the regression equations, geostrophic winds were computed from the gradient of geopotential heights for the steering predictors rather than using actual observed winds. If, in an operational setting, it is preferable to use the observed winds rather than computing the winds from the height gradient, the only conversion required is to multiply the U and V components (in m/s) by 33 $s^{-1}$. This

conversion is required because the $2\Omega$ and the $\Delta X$, $\Delta Y$ terms from the geostrophic wind equation were not used to compute the regression coefficients for the steering predictors.

Following each of the first two 24-hour displacements, a category change relative to the subtropical ridge may be required. This can be done either objectively by noting the direction of motion (DOM) between the new forecast position and the position 24 hours earlier or subjectively by noting if the forecast position is approaching the subtropical ridge axis. If the objective method is used, for cyclones in the south-of-ridge category, a change to on-the-ridge category should be made if the DOM is between $330^{\circ}$ and $30^{\circ}$ and a change to north-of-ridge category should be made if the DOM is greater than $30^{\circ}$. Likewise, for cyclones in the on-the-ridge category, a change to north-of-ridge category should be made if the DOM is greater than $30^{\circ}$. For cyclones north of the ridge, no category change is necessary. Although the use of a blend zone was never tested, for cases with DOM between $310^{\circ}$ and $330^{\circ}$ or if the choice between two categories is not clear-cut, both the south-of-ridge equation and on-the-ridge equation may be used to compute an average position between the two.

The formula for computing the 24-hour displacement to determine the forecast position is given by:

$$\text{NEWLAT} = ((C_o + \sum_n C_n P_n)24)/1111.949 + \text{OLDLAT}$$

$$\text{NEWLON} = ((C_o + \sum_n C_n P_n)24)/ (1111.949\cos(\text{NEWLAT}+\text{OLDLAT})+\text{OLDLON})$$

where NEWLAT is the forecast latitude

OLDLAT is the forecast minus 24-hour latitude

NEWLON is the forecast longitude

OLDLON is the forecast minus 24-hour longitude

$C_o$ is the intercept

$C_n$ are the n regression coefficient

$P_n$ are the n predictor values

The actual procedure for computing one 24-hour segment of a 72-hour forecast will be presented as an example. The example is the forecast situation for Supertyphoon Wynne on October 11, 1980 at 1200 GMT. The track for Wynne is shown in Fig. E.1. Table E.1 contains the 500 mb geopotential heights at the 17 x 10 gridpoints at warning time $T_o$ and at $T_o$ minus 24 hours. Similarly, Tables E.2 and E.3 contain the sea level pressures and the 200 mb heights, respectively. Figure E.2 is the JTWC hand-drawn streamline analysis at the 500 mb level for 1200 GMT on October 11. Based on the 1200 GMT analysis, the cyclone should be placed in the on-the-ridge category. Applying the regression equation for the north-south displacement for on-the-ridge category, the first predictor is the past 12-hour north-south motion. The initial cyclone position is 23.8°N 127.2°E. The past 12-hour position is 22.6°N 128.8°E. The past 12-hour north-south displacement is computed as:

$$Y = 1111.949 \times (23.8-22.6)/12$$
$$= 111.1949$$

Multiplying this displacement by its coefficient 0.533 results in a contribution of 59.2669.

The second predictor is the 500 mb height 5° north and 10° west of the cyclone center. From Table E.1, this height is 5861 m. Multiplying this height by its coefficient - .8972 results in a contribution of -5258.4892.

Similarly, predictors (3) through (2) results in:

(3) pressure 40° east of cyclone = 1015 x 3.9989 = 4058.8835

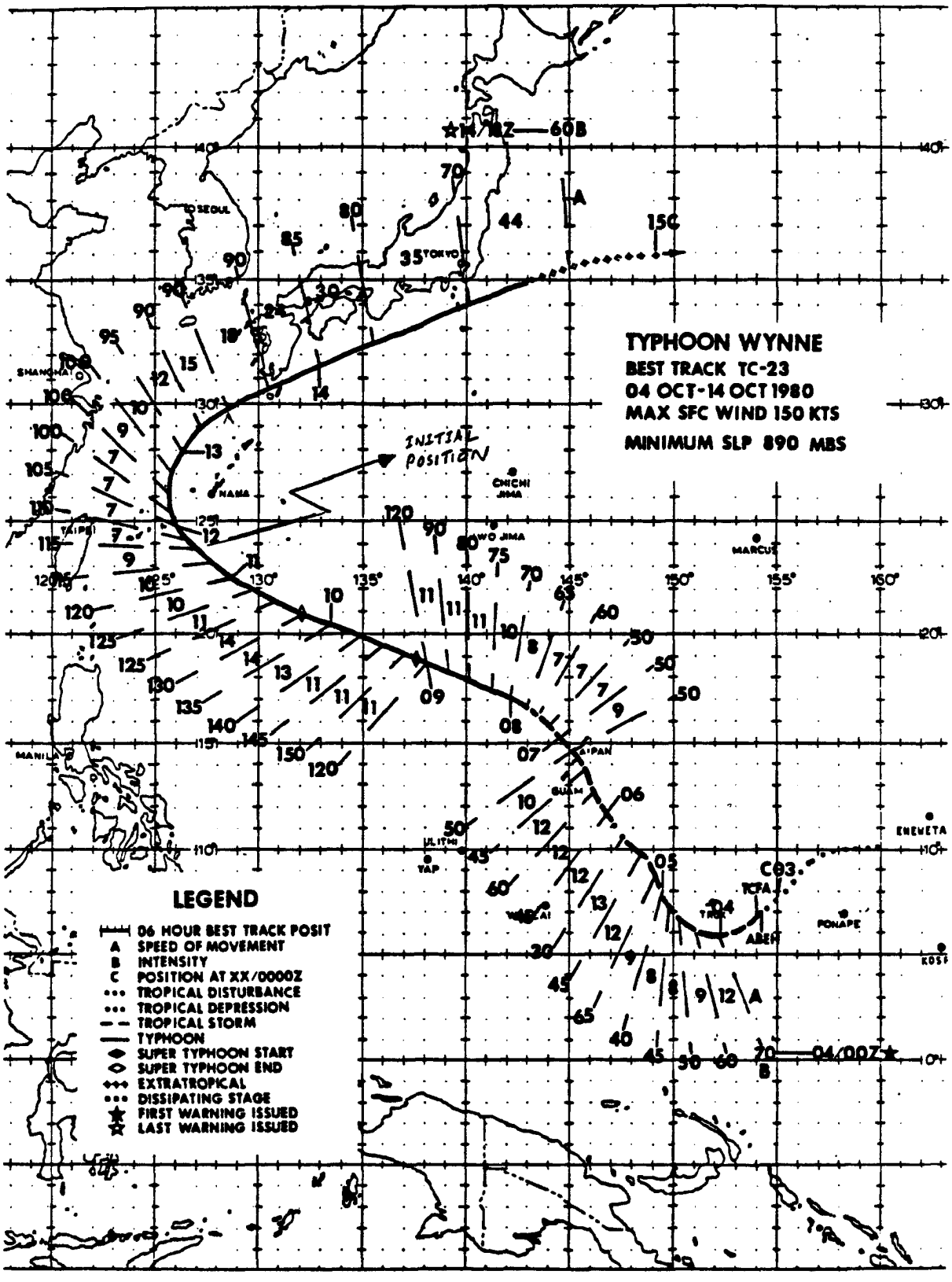


Fig. E.1. The track for Supertyphoon Wynne (from JTWC Annual Tropical Cyclone Report, 1980).

TABLE E.1

Panel A contains the current (October 11 1200GMT) 500 mb geopotential heights (m) at the 17 x 10 gridpoints relative to the cyclone center. The cyclone is located at the gridpoint indicated by a box. Panel B contains the 24-hour old (October 10 1200GMT) 500 mb geopotential heights at the 17 x 10 gridpoints relative to the cyclone center. The grid is $5^{o}$ x $5^{o}$.

**A**

| | | | | | | | | | | | | | | | | |
|---|---|---|---|---|---|---|---|---|---|---|---|---|---|---|---|---|
| 5564. | 5501. | 5471. | 5464. | 5471. | 5470. | 5458. | 5429. | 5377. | 5314. | 5283. | 5239. | 5225. | 5207. | 5186. | 5170. | 5179. |
| 5611. | 5539. | 5492. | 5472. | 5468. | 5474. | 5485. | 5407. | 5422. | 5363. | 5306. | 5275. | 5261. | 5248. | 5238. | 5232. | 5260. |
| 5657. | 5589. | 5532. | 5498. | 5489. | 5508. | 5533. | 5534. | 5504. | 5480. | 5415. | 5387. | 5376. | 5378. | 5383. | 5402. | 5436. |
| 5719. | 5673. | 5628. | 5806. | 5610. | 5628. | 5643. | 5654. | 5638. | 5609. | 5588. | 5580. | 5577. | 5585. | 5600. | 5619. | 5650. |
| 5798. | 5782. | 5755. | 5742. | 5740. | 5743. | 5754. | 5786. | 5768. | 5761. | 5757. | 5758. | 5763. | 5769. | 5774. | 5784. | 5806. |
| 5823. | 5830. | 5820. | 5805. | 5802. | 5809. | 5823. | 5842. | 5855. | 5863. | 5869. | 5871. | 5870. | 5873. | 5878. | 5879. | 5882. |
| 5826. | 5835. | 5838. | 5836. | 5840. | 5850. | 5861. | 5863. | 5860. | 5879. | 5903. | 5905. | 5898. | 5896. | 5902. | 5908. | 5901. |
| 5847. | 5849. | 5856. | 5863. | 5866. | 5874. | 5873. | 5837. | [5814] | 5848. | 5887. | 5884. | 5869. | 5872. | 5883. | 5892. | 5882. |
| 5846. | 5847. | 5852. | 5858. | 5861. | 5867. | 5866. | 5837. | 5819. | 5846. | 5878. | 5875. | 5863. | 5865. | 5874. | 5881. | 5873. |
| 5844. | 5845. | 5849. | 5858. | 5855. | 5860. | 5859. | 5836. | 5825. | 5845. | 5866. | 5865. | 5857. | 5858. | 5865. | 5870. | 5865. |

**B**

| | | | | | | | | | | | | | | | | |
|---|---|---|---|---|---|---|---|---|---|---|---|---|---|---|---|---|
| 5598. | 5531. | 5488. | 5468. | 5467. | 5464. | 5446. | 5410. | 5355. | 5292. | 5243. | 5219. | 5210. | 5188. | 5161. | 5133. | 5189. |
| 5607. | 5543. | 5494. | 5479. | 5494. | 5511. | 5502. | 5459. | 5396. | 5329. | 5265. | 5242. | 5235. | 5231. | 5223. | 5213. | 5231. |
| 5629. | 5681. | 5530. | 5510. | 5535. | 5564. | 5560. | 5535. | 5506. | 5476. | 5437. | 5408. | 5379. | 5371. | 5373. | 5389. | 5420. |
| 5669. | 5651. | 5637. | 5631. | 5641. | 5651. | 5646. | 5634. | 5633. | 5636. | 5632. | 5628. | 5618. | 5603. | 5602. | 5618. | 5646. |
| 5744. | 5743. | 5748. | 5754. | 5764. | 5752. | 5750. | 5743. | 5739. | 5745. | 5749. | 5758. | 5777. | 5795. | 5805. | 5817. | 5827. |
| 5786. | 5792. | 5795. | 5796. | 5806. | 5822. | 5838. | 5836. | 5846. | 5860. | 5866. | 5870. | 5879. | 5889. | 5896. | 5894. | 5894. |
| 5810. | 5820. | 5823. | 5824. | 5842. | 5864. | 5874. | 5887. | 5898. | 5908. | 5916. | 5921. | 5917. | 5910. | 5910. | 5907. | 5904. |
| 5845. | 5852. | 5856. | 5863. | 5860. | 5889. | 5892. | 5887. | [5863] | 5852. | 5879. | 5899. | 5884. | 5867. | 5871. | 5883. | 5880. |
| 5844. | 5850. | 5857. | 5868. | 5871. | 5879. | 5881. | 5877. | 5858. | 5849. | 5871. | 5887. | 5875. | 5862. | 5865. | 5874. | 5871. |
| 5843. | 5847. | 5849. | 5853. | 5863. | 5869. | 5870. | 5867. | 5859. | 5847. | 5863. | 5874. | 5865. | 5856. | 5858. | 5865. | 5863. |

TABLE E.2

Panel A contains the current (October 11 1200GMT) sea level pressures (mb) at the 17 x 10 gridpoints relative to the cyclone center. The cyclone is located at the gridpoint indicated by a box. Panel B contains the 24-hour old (October 10 1200GMT) sea level pressures at the 17 x 10 gridpoints relative to the cyclone center. The grid is $5^{o}$ x $5^{o}$.

**A**

| | | | | | | | | | | | | | | | | |
|---|---|---|---|---|---|---|---|---|---|---|---|---|---|---|---|---|
| 1029. | 1029. | 1029. | 1027. | 1026. | 1025. | 1024. | 1023. | 1021. | 1017. | 1012. | 1006. | 1001. | 997. | 993. | 990. | 988. |
| 1033. | 1031. | 1030. | 1030. | 1028. | 1025. | 1024. | 1025. | 1023. | 1019. | 1012. | 1006. | 1002. | 1000. | 998. | 997. | 998. |
| 1027. | 1029. | 1030. | 1029. | 1027. | 1024. | 1025. | 1026. | 1025. | 1021. | 1017. | 1014. | 1012. | 1010. | 1008. | 1008. | 1011. |
| 1026. | 1024. | 1025. | 1028. | 1028. | 1025. | 1025. | 1027. | 1024. | 1022. | 1018. | 1016. | 1014. | 1012. | 1013. | 1017. | 1019. |
| 1018. | 1020. | 1022. | 1024. | 1022. | 1022. | 1023. | 1022. | 1020. | 1019. | 1017. | 1016. | 1015. | 1016. | 1018. | 1018. | 1020. |
| 1014. | 1016. | 1017. | 1017. | 1017. | 1019. | 1020. | 1018. | 1016. | 1015. | 1015. | 1016. | 1017. | 1017. | 1017. | 1017. | 1020. |
| 1009. | 1009. | 1009. | 1010. | 1013. | 1015. | 1015. | 1015. | 1010. | 1011. | 1015. | 1016. | 1015. | 1014. | 1015. | 1017. | 1019. |
| 1007. | 1006. | 1007. | 1008. | 1009. | 1010. | 1010. | 1005. | [1003.] | 1009. | 1012. | 1013. | 1011. | 1011. | 1013. | 1015. | 1015. |
| 1007. | 1007. | 1007. | 1008. | 1009. | 1010. | 1010. | 1006. | 1005. | 1009. | 1012. | 1012. | 1010. | 1011. | 1012. | 1013. | 1014. |
| 1008. | 1007. | 1007. | 1008. | 1009. | 1009. | 1009. | 1006. | 1006. | 1008. | 1011. | 1011. | 1010. | 1010. | 1011. | 1012. | 1012. |

**B**

| | | | | | | | | | | | | | | | | |
|---|---|---|---|---|---|---|---|---|---|---|---|---|---|---|---|---|
| 1035. | 1032. | 1030. | 1029. | 1027. | 1027. | 1025. | 1024. | 1021. | 1017. | 1009. | 998. | 992. | 986. | 981. | 978. | 978. |
| 1033. | 1032. | 1032. | 1030. | 1028. | 1027. | 1026. | 1026. | 1022. | 1016. | 1009. | 1002. | 998. | 995. | 992. | 990. | 992. |
| 1030. | 1032. | 1030. | 1024. | 1022. | 1024. | 1027. | 1026. | 1023. | 1018. | 1013. | 1011. | 1009. | 1007. | 1007. | 1008. | 1010. |
| 1025. | 1023. | 1018. | 1018. | 1020. | 1024. | 1024. | 1024. | 1020. | 1017. | 1015. | 1016. | 1016. | 1017. | 1018. | 1021. | 1022. |
| 1018. | 1018. | 1019. | 1018. | 1018. | 1019. | 1020. | 1018. | 1015. | 1016. | 1019. | 1020. | 1022. | 1023. | 1024. | 1025. | 1025. |
| 1014. | 1015. | 1014. | 1014. | 1013. | 1017. | 1016. | 1014. | 1014. | 1017. | 1019. | 1020. | 1022. | 1022. | 1021. | 1022. | 1023. |
| 1010. | 1010. | 1010. | 1010. | 1012. | 1014. | 1014. | 1013. | 1014. | 1014. | 1016. | 1017. | 1018. | 1017. | 1017. | 1018. | 1020. |
| 1008. | 1008. | 1008. | 1008. | 1010. | 1011. | 1011. | 1011. | [1010.] | 1009. | 1013. | 1015. | 1014. | 1012. | 1013. | 1014. | 1015. |
| 1008. | 1008. | 1008. | 1008. | 1009. | 1010. | 1011. | 1010. | 1009. | 1008. | 1012. | 1013. | 1012. | 1011. | 1012. | 1013. | 1014. |
| 1008. | 1008. | 1008. | 1008. | 1009. | 1010. | 1010. | 1010. | 1009. | 1008. | 1011. | 1012. | 1011. | 1011. | 1011. | 1012. | 1012. |

## TABLE E.3

Panel A contains the current (October 11 1200GMT) 200 mb geopotential heights (m) at the 17 x 10 gridpoints relative to the cyclone center. The cyclone is located at the gridpoint indicated by a box. Panel B contains the 24-hour old (October 10 1200GMT) 200 mb geopotential heights at the 17 x 10 gridpoints relative to the cyclone center. The grid is $5^{o}$ x $5^{o}$.

**A**

| | | | | | | | | | | | | | | | | |
|---|---|---|---|---|---|---|---|---|---|---|---|---|---|---|---|---|
| 11727. | 11626. | 11558. | 11520. | 11508. | 11507. | 11496. | 11487. | 11412. | 11357. | 11321. | 11318. | 11322. | 11316. | 11309. | 11310. | 11333. |
| 11744. | 11642. | 11551. | 11494. | 11476. | 11485. | 11507. | 11498. | 11452. | 11405. | 11369. | 11365. | 11363. | 11359. | 11371. | 11392. | 11441. |
| 11780. | 11693. | 11606. | 11563. | 11565. | 11593. | 11620. | 11635. | 11605. | 11553. | 11524. | 11510. | 11512. | 11524. | 11543. | 11585. | 11643. |
| 11889. | 11812. | 11761. | 11758. | 11768. | 11834. | 11881. | 11902. | 11893. | 11862. | 11838. | 11831. | 11840. | 11851. | 11862. | 11886. | 11922. |
| 12062. | 12021. | 11998. | 12011. | 12059. | 12118. | 12161. | 12190. | 12208. | 12207. | 12194. | 12189. | 12193. | 12189. | 12186. | 12192. | 12196. |
| 12208. | 12208. | 12721. | 12253. | 12296. | 12339. | 12372. | 12393. | 12411. | 12415. | 12407. | 12402. | 12399. | 12390. | 12379. | 12361. | 12340. |
| 12321. | 12350. | 12377. | 12400. | 12420. | 12440. | 12454. | 12471. | 12483. | 12489. | 12489. | 12478. | 12462. | 12450. | 12435. | 12406. | 12367. |
| 12418. | 12441. | 12452. | 12458. | 12466. | 12469. | 12468. | 12472. | [12486] | 12500. | 12499. | 12482. | 12467. | 12462. | 12447. | 12406. | 12357. |
| 12424. | 12443. | 12452. | 12456. | 12463. | 12465. | 12464. | 12467. | 12479. | 12490. | 12489. | 12476. | 12463. | 12460. | 12447. | 12415. | 12376. |
| 12431. | 12445. | 12451. | 12454. | 12460. | 12461. | 12460. | 12463. | 12471. | 12479. | 12479. | 12469. | 12460. | 12457. | 12448. | 12424. | 12396. |

**B**

| | | | | | | | | | | | | | | | | |
|---|---|---|---|---|---|---|---|---|---|---|---|---|---|---|---|---|
| 11675. | 11586. | 11530. | 11502. | 11492. | 11474. | 11458. | 11435. | 11403. | 11358. | 11326. | 11320. | 11319. | 11315. | 11318. | 11330. | 11367. |
| 11646. | 11574. | 11529. | 11517. | 11527. | 11538. | 11545. | 11534. | 11490. | 11435. | 11383. | 11368. | 11348. | 11338. | 11346. | 11363. | 11420. |
| 11706. | 11661. | 11622. | 11604. | 11622. | 11649. | 11659. | 11660. | 11656. | 11640. | 11622. | 11602. | 11557. | 11525. | 11520. | 11551. | 11612. |
| 11826. | 11815. | 11807. | 11802. | 11824. | 11860. | 11882. | 11888. | 11902. | 11926. | 11944. | 11939. | 11904. | 11869. | 11857. | 11871. | 11914. |
| 11998. | 12021. | 12047. | 12072. | 12104. | 12138. | 12165. | 12178. | 12187. | 12211. | 12236. | 12228. | 12199. | 12178. | 12167. | 12167. | 12187. |
| 12184. | 12222. | 12259. | 12295. | 12325. | 12349. | 12376. | 12392. | 12404. | 12419. | 12423. | 12405. | 12380. | 12354. | 12323. | 12318. | 12343. |
| 12334. | 12362. | 12393. | 12420. | 12438. | 12451. | 12462. | 12474. | 12479. | 12488. | 12487. | 12471. | 12455. | 12439. | 12422. | 12415. | 12418. |
| 12420. | 12443. | 12459. | 12467. | 12472. | 12475. | 12476. | 12474. | [12484] | 12500. | 12503. | 12484. | 12465. | 12460. | 12461. | 12449. | 12408. |
| 12427. | 12445. | 12457. | 12464. | 12468. | 12470. | 12470. | 12469. | 12477. | 12490. | 12491. | 12477. | 12462. | 12458. | 12459. | 12449. | 12417. |
| 12433. | 12446. | 12455. | 12460. | 12463. | 12465. | 12465. | 12464. | 12470. | 12479. | 12480. | 12470. | 12459. | 12456. | 12457. | 12450. | 12426. |

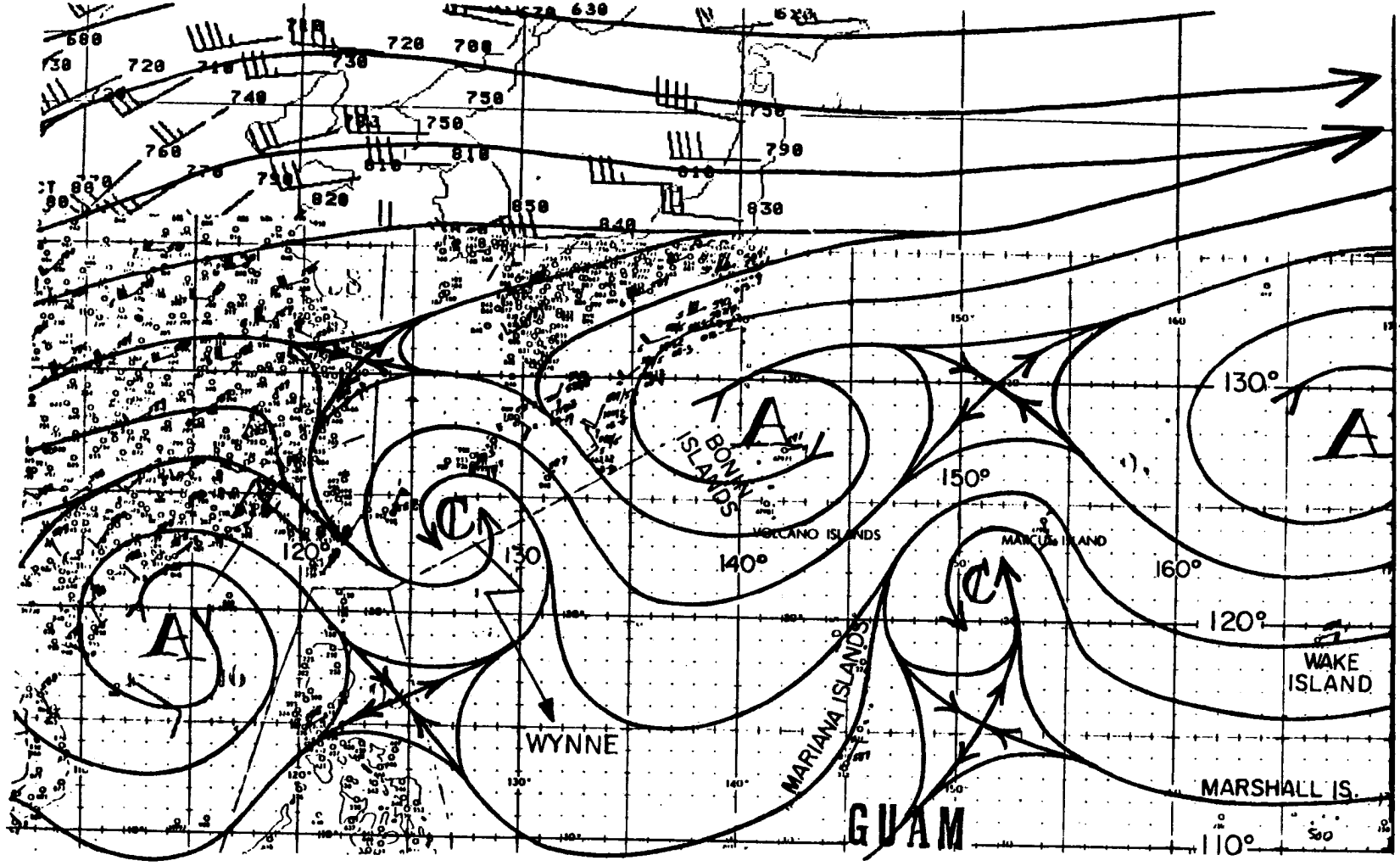


Fig. E.2. JTWC hand-drawn 500 mb streamline analysis for 1200 GMT on October 11. Typhoon Wynne is located at 23.8°N 127.2°E or approximately 300 n mi. east of Taiwan at this time.

(4) 24-hour pressure change $10^{o}$ south $10^{o}$ west of cyclone =
(1009-1010) x -8.2569 = 8.2569

(5) pressure $10^{o}$ south of cyclone = 1006 x 3.4909 = 3511.8454

(6) 24-hour pressure change $20^{o}$ north $5^{o}$ west of cyclone =
(1027-1024) x -1.4298 = -4.2894

(7) 24-hour height change $15^{o}$ north $25^{o}$ west of cyclone =
(5742-5754) x -.2148 = 2.5776

(8) 24-hour pressure change $5^{o}$ north $15^{o}$ east of cyclone =
(1016-1017) x 4.6907 = -4.6907

(9) pressure $5^{o}$ north $5^{o}$ west of cyclone = 1015 x -3.9711 =
-4030.6665

(10) height $10^{o}$ south $40^{o}$ west of cyclone = 5844 x .2906 =
1698.2664

(11) past 24-hour east-west motion = 1111.949 x cos [21.5 +23.8)/2] x
(127.2-130.8)/24 = -153.9284 x -.1238 = 19.0563

(12) 24-hour height change $30^{o}$ north $5^{o}$ east of cyclone =
(5363-5329) x -.1294 = -4.3996

(13) pressure $20^{o}$ east of cyclone = 1011 x 4.7028 = 4654.5308

(14) 24-hour pressure change $15^{o}$ north $40^{o}$ west of cyclone =
(1018-1018) x 1.6751 = 0

(15) 24-hour height change $15^{o}$ north $20^{o}$ east of cyclone =
(5763-5777) x -.1196 = 1.6744

(16) 24-hour height change $35^{o}$ north $30^{o}$ east of cyclone =
(5186-5161) x -.0761 = -1.9025

(17) 24-hour change of the north-south component of the 200 mb steering over the cyclone =

{[(12407+12489+12499+12489+12479)/5 - (12372+12454+12468+12464+12460)/5] / [sin(23.8) x cos(23.8)] - [(12423+12487+12503+12491+12480)/5 - (12376+12462+12476+12470+12465)/5] / [sin(23.8) x cos(23.8)]} x .0498

= (78.5423 - 73.1256) x .0498 = .2698

(18) 24-hour height change 35° north 30° west of cyclone =

(5471-5488) x -.0844 = -1.4348

(19) 24-hour change of the east-west component of the 200 mb steering 10° north of cyclone =

[(12483-12208)/sin(33.8)] - [(12479-12187)/sin(33.8)] x -.0353 = 1.0787

(20) 24-hour pressure change 10° south 10° east of cyclone =

(1011-1011) x -3.98 = 0

(21) Intercept = -4706.5091

Summing all of the contributions (103.3249) and adding it to the initial latitude results in a 24-hour forecast latitude of

[(103.3249 x 24) / 1111.949] + 23.8 = 26.0

Applying the regression equation for the east-west displacement for the on-the-ridge category, the first predictor is the 500 mb height 10° north and 5° west of the cyclone center. From Table E.1, this height is 5842 m. Multiplying this height by its coefficient -.464 results in a contribution of -2710.688. The second predictor is the past 12-hour east-west motion. The initial cyclone position is 23.8°N 127.2°E. The past 12-hour position is 22.6°N 128.8°E. The past 12-hour east-west displacement is computed as:

$$X = 1111.949 \times \cos[(22.6 + 23.8)/2] \times (1272-128.8)/12$$

$$= -136.3$$

Multiplying this displacement by its coefficient .302 results in a contribution of -41.163. Similarly, predictors (3) through (20) results in:

(3) pressure $10^{\circ}$ south of cyclone = 1006 x 4.497 = 4523.982

(4) height $10^{\circ}$ north $15^{\circ}$ east of cyclone = 5871 x -.261 = -1532.331

(5) 24-hour height change $5^{\circ}$ north $10^{\circ}$ west of cyclone = (5861-5874) x -.628 = 8.164

(6) 24-hour pressure change $25^{\circ}$ north $35^{\circ}$ west of cyclone = (1029-1032) x 1.53 = -4.59

(7) pressure $5^{\circ}$ south $25^{\circ}$ east of cyclone = 1011 x 3.031 = 3064.341

(8) 24-hour pressure change $10^{\circ}$ south $30^{\circ}$ west of cyclone = (1007-1008) x 8.773 = -8.773

(9) height $40^{\circ}$ east of cyclone = 5882 x .349 = 2052.818

(10) 24-hour height change $10^{\circ}$ south $10^{\circ}$ west of cyclone = (5859-5870) x -.892 = 9.812

(11) 24-hour height change $30^{\circ}$ north $15^{\circ}$ west of cyclone = (5474-5511) x .114 = -4.218

(12) 24-hour pressure change $10^{\circ}$ north $20^{\circ}$ east of cyclone = (1017-1022) x -2.928 = 14.64

(13) pressure $30^{\circ}$ north $25^{\circ}$ east of cyclone = 1000 x 1.92 = 1920

(14) past 24-hour north-south motion = [1111.949 x (23.8-21.5)/24] x .183 = 19.5

(15) east-west component of the 200 mb steering over the cyclone =

[(12460+12463+12471+12479)/5 - (12372+12393+12411+12415+12407)/5] / sin(23.8) x .062 = 10.85

(16) 24-hour pressure change $35^{\circ}$ north $25^{\circ}$ east of cyclone = (997-986) x -1.332 = -14.652

(17) height $35^{\circ}$ west of cyclone = 5849 x -.319 = -1865.831

(18) height $5^{\circ}$ south $10^{\circ}$ west of cyclone = 5866 x -.369 = 2164.554

(19) 24-hour height change 25° north 35° east of cyclone = (5402-5389) x -.059 = -.767

(20) 24-hour height change 35° north 25° west of cyclone = (5464-5468) x -.091 = .364

(21) Intercept = -7662.345

Summing all the contributions (-56.333) and adding it to the initial longitude results in a 24-hour forecast longitude of

$$(-56.333 \times 24) / 1111.949 \times \cos[(23.8 + 26.0)/2] + 127.2 = 125.9$$

In a manual mode, gridpoint data would not be available to the forecaster. Instead, he must use the available observations and estimate heights and pressures at the required gridpoints. To test the sensitivity of the regression equations, all of the required heights were either increased or decreased by 30 m from those that appear in Table E.1. Similarly, all of the pressures were either increased or decreased by 5 mb from those that appear in Table E.2. Neither the tendencies nor the steering predictors were altered since it was felt that 24-hour changes and height gradients are easier to estimate than the absolute values.

For the case of increasing all of the heights and pressures, the forecast latitude was half a degree further north and the forecast longitude nearly a degree further east, i.e., 26.5°N and 126.8°E. For the case of decreasing all of the heights and pressures, the forecast latitude was half a degree further south and the forecast longitude was one degree further west, i.e., 25.5°N and 125.0°E. Thus, the worst case situation of all the heights and pressures being too high or too low would 'add' approximately 60 n mi to the forecast position. Assuming that 30 m for the 500 mb height and 5 mb for the surface pressure are a

realistic range of values that a subjective analysis could vary from the gridpoint analysis, a 60 n mi difference in the forecast position would result.

Two points should be emphasized. The first is that relative to the verifying best track position, there is no way of knowing which forecast position is more accurate. The second is that the sensitivity test examined the worst case situation. In reality, some of the subjective estimation of synoptic values at specific gridpoints will be greater and some will be less than the gridpoint data. Hopefully, when all of them are summed, many of the erroneous high and the low values will cancel. The test was to provide a degree of 'slop' one could expect in the forecast position if subjective estimates for gridpoint values were used.

Obviously, in an automatic mode, no subjective estimation would be required. But again, one of the desirable features of a relatively simple model such as this is the opportunity for the forecaster to input the data with subjective quality control. If the synoptic values at gridpoints required by the model appear questionable, the forecaster could easily modify them to more realistic values. With the aid of a desk-top calculator, he/she could rerun the model several times with different predictor values to see the effect of the changes. Until the output from the global PE model improves, subjective modification of the forecast fields such as outlined here will probably be necessary.

A statistical-dynamical track prediction model is not currently available for use in the NW Pacific/South China Sea and North Indian

Oceans. As shown by the verificiation of the model in Chapter 5, the potential for significant improvement exists with the use of this model.

PROJECT REPORTS, PUBLICATIONS, and CONFERENCE PROCEEDINGS TO DATE

Summary of W. M. Gray's CSU research project reports, publications and conference proceedings since 1965. A majority of these reports and publications have made use of the rawinsonde compositing techniques here being advocated.

a) Project Reports
b) Publications
c) Conference Proceedings

W. M. GRAY'S FEDERALLY SUPPORTED RESEARCH PROJECT REPORTS SINCE 1967

| CSU Dept. of Atmos. Sci. Report No. | Report Title, Author, Date, Agency Support |
|---|---|
| 104 | The Mutual Variation of Wind, Shear and Baroclinicity in the Cumulus Convective Atmosphere of the Hurricane (69 pp.). W. M. Gray. February 1967. NSF Support. |
| 114 | Global View of the Origin of Tropical Disturbances and Storms (105 pp.). W. M. Gray. October 1967. NSF Support. |
| 116 | A Statistical Study of the Frictional Wind Veering in the Planetary Boundary Layer (57 pp.). B. Mendenhall. December 1967. NSF and ESSA Support. |
| 124 | Investigation of the Importance of Cumulus Convection and Ventilation in Early Tropical Storm Development (88 pp.). R. Lopez. June 1968. ESSA Satellite Lab. Support. |
| Unnumbered | Role of Angular Momentum Transports in Tropical Storm Dissipation over Tropical Oceans (46 pp.). R. F. Wachtmann. December 1968. NSF and ESSA Support. |
| Unnumbered | Monthly Climatological Wind Fields Associated with Tropical Storm Genesis in the West Indies (34 pp.). J. W. Sartor. December 1968. NSF Support. |
| 140 | Characteristics of the Tornado Environment as Deduced from Proximity Soundings (55 pp.). T. G. Wills. June 1969. NOAA and NSF Support. |
| 161 | Statistical Analysis of Trade Wind Cloud Clusters in the Western North Pacific (80 pp.). K. Williams. June 1970. ESSA Satellite Lab. Support. |
| --- | A Climatology of Tropical Cyclones and Disturbances of the Western Pacific with a Suggested Theory for Their Genesis/ Maintenance (225 pp.). W. M. Gray. NAVWEARSCHFAC Tech. Paper No. 19-70. November 1970. (Available from US Navy, Monterey, CA). US Navy Support. |
| 179 | A diagnostic Study of the Planetary Boundary Layer over the Oceans (95 pp.). W. M. Gray. February 1972. Navy and NSF Support. |
| 182 | The Structure and Dynamics of the Hurricane's Inner Core Area (105 pp.). D. J. Shea. April 1972. NOAA and NSF Support. |

| CSU Dept. of Atmos. Sci. Report No. | Report Title, Author, Date, Agency Support |
|---|---|
| 188 | Cumulus Convection and Larger-scale Circulations, Part I: A Parametric Model of Cumulus Convection (100 pp.). R. E. Lopez. June 1972. NSF Support. |
| 189 | Cumulus Convection and Larger-scale Circulations, Part II: Cumulus and Meso-scale Interactions (63 pp.). R. E. Lopez. June 1972. NSF Support. |
| 190 | Cumulus Convection and Larger-scale Circulations, Part III: Broadscale and Meso-scale Considerations (80 pp.). W. M. Gray. July 1972. NOAA-NESS Support. |
| 195 | Characteristics of Carbon Black Dust as a Tropospheric Heat Source for Weather Modification (55 pp.). W. M. Frank. January 1973. NSF Support. |
| 196 | Feasibility of Beneficial Hurricane Modification by Carbon Black Seeding (130 pp.). W. M. Gray. April 1973. NOAA Support. |
| 199 | Variability of Planetary Boundary Layer Winds (157 pp.). L. R. Hoxit. May 1973. NSF Support. |
| 200 | Hurricane Spawned Tornadoes (57 pp.). D. J. Novlan. May 1973. NOAA and NSF Support. |
| 212 | A Study of Tornado Proximity Data and an Observationally Derived Model of Tornado Genesis (101 pp.). R. Maddox. November 1973. NOAA Support. |
| 219 | Analysis of Satellite Observed Tropical Cloud Clusters (91 pp.). E. Ruprecht and W. M. Gray. May 1974. NOAA/ NESS Support. |
| 224 | Precipitation Characteristics in the Northeast Brazil Dry Region (56 pp.). R. P. L. Ramos. May 1974. NSF Support. |
| 225 | Weather Modification through Carbon Dust Absorption of Solar Energy (190 pp.). W. M. Gray, W. M. Frank, M. L. Corrin, and C. A. Stokes. July 1974. |
| 234 | Tropical Cyclone Genesis (121 pp.). W. M. Gray. March 1975. NSF Support. |

| CSU Dept. of Atmos. Sci. Report No. | Report Title, Author, Date, Agency Support |
|---|---|
| --- | Tropical Cyclone Genesis in the Western North Pacific (66 pp.). W. M. Gray. March 1975. US Navy Environmental Prediction Research Facility Report. Tech. Paper No. 16-75. (Available from the US Navy, Monterey, CA). Navy Support. |
| 241 | Tropical Cyclone Motion and Surrounding Parameter Relationships (105 pp.). J. E. George. December 1975. NOAA Support. |
| 243 | Diurnal Variation of Oceanic Deep Cumulus Convection. Paper I: Observational Evidence, Paper II: Physical Hypothesis (106 pp.). R. W. Jacobson, Jr. and W. M. Gray. February 1976. NOAA-NESS Support. |
| 257 | Data Summary of NOAA's Hurricanes Inner-Core Radial Leg Flight Penetrations 1957-1967, and 1969 (245 pp.). W. M. Gray and D. J. Shea. October 1976. NSF and NOAA Support. |
| 258 | The Structure and Energetics of the Tropical Cyclone (180 pp.). W. M. Frank. October 1976. NOAA-NHEML, NOAA-NESS and NSF Support. |
| 259 | Typhoon Genesis and Pre-typhoon Cloud Clusters (79 pp.). R. M. Zehr. November 1976. NSF Support. |
| Unnumbered | Severe Thunderstorm Wind Gusts (81 pp.). G. W. Walters. December 1976. NSF Support. |
| 262 | Diurnal Variation of the Tropospheric Energy Budget (141 pp.). G. S. Foltz. November 1976. NSF Support. |
| 274 | Comparison of Developing and Non-developing Tropical Disturbances (81 pp.). S. L. Erickson. July 1977. US Army Support. |
| --- | Tropical Cyclone Research by Data Compositing (79 pp.). W. M. Gray and W. M. Frank. July 1977. US Navy Environmental Prediction Research Facility Report. Tech. Paper No. 77-01. (Available from the US Navy, Monterey, CA). Navy Support. |
| 277 | Tropical Cyclone Cloud and Intensity Relationships (154 pp.). C. P. Arnold. November 1977. US Army and NHEML Support. |
| 297 | Diagnostic Analyses of the GATE A/B-scale Area at Individual Time Periods (102 pp.). W. M. Frank. November 1978. NSF Support. |

| CSU Dept. of Atmos. Sci. Report No. | Report Title, Author, Date, Agency Support |
|---|---|
| 298 | Diurnal Variability in the GATE Region (80 pp.). J. M. Dewart. November 1978. NSF Support. |
| 299 | Mass Divergence in Tropical Weather Systems, Paper I: Diurnal Variation; Paper II: Large-scale Controls on Convection (109 pp.). J. L. McBride and W. M. Gray. November 1978. NOAA-NHEML Support. |
| --- | New Results of Tropical Cyclone Research from Observational Analysis (108 pp.). W. M. Gray and W. M. Frank. June 1978. US Navy Environmental Prediction Research Facility Report. Tech. Paper No. 78-01. (Available from the US Navy, Monterey, CA). Navy Support. |
| 305 | Convection Induced Temperature Change in GATE (128 pp.). P. G. Grube. February 1979. NSF Support. |
| 308 | Observational Analysis of Tropical Cyclone Formation (230 pp.). J. L. McBride. April 1979. NOAA-NHEML, NSF and NEPRF Support. |
| --- | Tropical Cyclone Origin, Movement and Intensity Characteristics Based on Data Compositing Techniques (124 pp.). W. M. Gray. August 1979. US Navy Environmental Prediction Research Facility Report. Tech. Paper No. CR-79-06. (Available from the US Navy, Monterey, CA). Navy Support. |
| --- | Further Analysis of Tropical Cyclone Characteristics from Rawinsonde Compositing Techniques (129 pp.). W. M. Gray. March 1981. US Navy Environmental Prediction Research Facility Report. Tech. Paper No. CR-81-02. (Available from the US Navy, Monterey, CA). Navy Support. |
| 333 | Tropical Cyclone Intensity Change - A Quantitative Forecasting Scheme. K. M. Dropco. May 1981. NOAA Support. |
| --- | Recent Advances in Tropical Cyclone Research from Rawinsonde Composite Analysis (407 pp.). WMO Publication. W. M. Gray. 1981. |
| 340 | The Role of the General Circulation in Tropical Cyclone Genesis (230 pp.). G. Love. April 1982. NSF Support. |
| 341 | Cumulus Momentum Transports in Tropical Cyclones (78 pp.). C. S. Lee. May 1982. ONR Support. |

| CSU Dept. of Atmos. Sci. Report No. | Report Title, Author, Date, Agency Support |
|---|---|
| 343 | Tropical Cyclone Movement and Surrounding Flow Relationships (68 pp.). J. C. L. Chan and W. M. Gray. May 1982. ONR Support. |
| 346 | Environmental Circulations Associated with Tropical Cyclones Experiencing Fast, Slow and Looping Motions (273 pp.). J. Xu and W. M. Gray. May 1982. NOAA and NSF Support. |
| 348 | Tropical Cyclone Motion: Environmental Interaction Plus a Beta Effect (47 pp.). G. J. Holland. May 1982. ONR Support. |
| --- | Tropical Cyclone and Related Meteorological Data Sets Available at CSU and Their Utilization (186 pp.). W. M. Gray, E. Buzzell, G. Burton and Other Project Personnel. February 1982. NSF, ONR, NOAA, and NEPRF Support. |
| 352 | A Comparison of Large and Small Tropical Cyclones (75 pp.). R. T. Merrill. July 1982. NOAA and NSF Support. |
| 358 | On the Physical Processes Responsible for Tropical Cyclone Motion (200 pp.). Johnny C. L. Chan. November 1982. NSF, NOAA/NHRL and NEPRF Support. |
| 363 | Tropical Cyclones in the Australian/Southwest Pacific Region (264 pp.). Greg J. Holland. March 1983. NSF, NOAA/NHRL and Australian Government Support. |
| 370 | Atlantic Seasonal Hurricane Frequency, Part I: El Nino and 30 mb QBO Influences; Part II: Forecasting Its Variability (105 pp.). W. M. Gray. July 1983. NSF Support. |
| 379 | A Statistical Method for One- to Three-Day Tropical Cyclone Track Prediction (201 pp). Clifford R. Matsumoto. December, 1984. NSF/NOAA and NEPRF support. |
| | Tropical cyclone structure and intensity change (290 pp.). Edwin Nunez. NSF Support. |
| | Global view of the upper level flow patterns associated with tropical cyclone intensity change during FGGE. Lianshou Chen. |

| BIBLIOGRAPHIC DATA SHEET | 1. Report No. ATS-379 | 2. | 3. Recipient's Accession No. |
|---|---|---|---|
| 4. Title and Subtitle<br>A STATISTICAL METHOD FOR ONE- TO THREE-DAY TROPICAL CYCLONE TRACK PREDICTION | | | 5. Report Date December, 1984<br>6. |
| 7. Author(s)<br>Clifford R. Matsumoto | | | 8. Performing Organization Rept. No. ATS-379 |
| 9. Performing Organization Name and Address<br>Colorado State University, Department of Atmospheric Science<br>Fort Collins, CO 80523 | | | 10. Project/Task/Work Unit No.<br>11. Contract/Grant No. ATM-8214041 & N00014-83-K-0002 |
| 12. Sponsoring Organization Name and Address<br>NSF/NOAA<br>18th and G Streets, N.W.<br>Washington, DC 20550<br>NEPRF<br>Monterey, CA 93940 | | | 13. Type of Report & Period Covered<br>Project Report<br>14. |

15. Supplementary Notes

16. Abstracts The problem of forecasting the movement of tropical cyclones is crucial in many parts of the world. Progress on improving the accuracy of track prediction has been slow to come and the need for further research on statistical-synoptic approaches exists. This newly developed method of forecasting one- to three-day cyclone motion is an improvement over existing forecast schemes for the following reasons: (1) cyclones are stratified based on their positions relative to the 500 mb subtropical ridge to better define the environmental influences on the cyclones; (2) the 72-hour forecast track is segmented into three 24-hour time steps to permit the application of updated persistence and synoptic data relative to each new cyclone position as the 24-hour displacements are stepped forward to the desired forecast projection; and (3) the prognostic synoptic data are introduced only at their valid times and relative to the cyclone position at the valid time such that they are treated like analysis data.

17. Key Words and Document Analysis. 17a. Descriptors

Tropical Cyclones
Track Prediction
Cyclone Motion

17b. Identifiers/Open-Ended Terms

17c. COSATI Field/Group

| 18. Availability Statement | 19. Security Class (This Report) UNCLASSIFIED | 21. No. of Pages 201 pp. |
|---|---|---|
| | 20. Security Class (This Page) UNCLASSIFIED | 22. Price |

FORM NTIS-35 (Rev. 3-72)